Imperial College London
Department of Physics

Group Symmetries and the Moduli Space Structures of SUSY Quiver Gauge Theories

Rudolph John Kalveks

Supervised by Professor Amihay Hanany

Submitted in part fulfilment of the requirements for the degree of
Doctor of Philosophy in Physics of Imperial College London
and the Diploma of Imperial College London

Acknowledgements

I would like to thank my supervisor, Amihay Hanany for his expert guidance in the development of this thesis, along with the theory group faculty at Imperial College, who have informed and grounded my understanding of the broader context. I am also indebted to my colleagues, Andrew Thomson, Marcus Sperling, Santiago Cabrera and Giulia Ferlito, amongst others, who have helped me grapple with the many puzzles encountered in this exploration of quiver theories and their group theoretic connections. Last but not least, I am grateful to my family for their encouragement and steadfast support throughout.

Declaration

This thesis draws upon work that was published in the following papers:

- A. Hanany and R. Kalveks, Highest Weight Generating Functions for Hilbert Series, JHEP 10 (2014) 152, arXiv:1408.4690 [hep-th].
- A. Hanany and R. Kalveks, Construction and Deconstruction of Single Instanton Hilbert Series, JHEP 12 (2015) 118, arXiv:1509.01294 [hep-th].
- A. Hanany and R. Kalveks, Quiver Theories for Moduli Spaces of Classical Group Nilpotent Orbits, JHEP 06 (2016) 130, arXiv:1601.04020 [hep-th].

The work above has not been submitted by me for any other degree, diploma or similar qualification. Furthermore, I herewith certify that, to the best of my knowledge, all of the material in this thesis which is not my own work has been properly acknowledged.

Rudolph John Kalveks

The copyright of this thesis rests with the author and is made available under a Creative Commons Attribution Non-Commercial No Derivatives licence. Researchers are free to copy, distribute or transmit the thesis on the condition that they attribute it, that they do not use it for commercial purposes and that they do not alter, transform or build upon it. For any reuse or redistribution, researchers must make clear to others the licence terms of this work.

Abstract

This thesis takes steps towards the development of a systematic account of the relationships between SUSY quiver gauge theories and the structures of their moduli spaces. Highest Weight Generating functions ("HWGs"), which concisely encode the field content of a moduli space, are introduced and developed to augment the established plethystic techniques for the construction and analysis of Hilbert series ("HS"). HWGs are shown to provide a faithful means of decoding and describing HS in terms of their component fields, which transform in representations of Classical and/or Exceptional symmetry groups. These techniques are illustrated in the context of Higgs branch quiver theories for SQCD and instanton moduli spaces, as a prelude to an account of the quiver theory constructions for the canonical class of moduli spaces represented by the nilpotent orbits of Classical and Exceptional symmetry groups. The known Higgs and/or Coulomb branch quiver theory constructions for nilpotent orbits are systematically extended to give a complete set of Higgs branch quiver theories for Classical group nilpotent orbits and a set of Coulomb branch constructions for near to minimal orbits of Classical and Exceptional groups. A localisation formula ("NOL Formula") for the normal nilpotent orbits of Classical and Exceptional groups based on their Characteristics is proposed and deployed. Dualities and other relationships between quiver theories, including A series $3d$ mirror symmetry, are analysed and discussed. The use of nilpotent orbits, for example in the form of $T(G)$ quiver theories, as building blocks for the systematic (de)construction of moduli spaces is illustrated. The roles of orthogonal bases, such as characters and Hall Littlewood polynomials, in providing canonical structures for the the analysis of quiver theories is demonstrated, along with their potential use as building blocks for more general families of quiver theories.

Contents

List of Tables

List of Figures

1. Introduction

1.1. Perspective

This study intertwines a number of streams of research that are relevant to the structures of the moduli spaces of gauge theories set within supersymmetric ("SUSY") and string theoretic or supergravity ("SUGRA") backgrounds. The central physical questions that this study seeks to address are those of how to characterise, determine and understand the possible field content, or "moduli space", of a field theory whose underlying structure is determined by the interplay of gauge groups.

Observable fields are, by definition, invariant under gauge group transformations. So, although gauge fields have isometries (or isotropies) under continuous Lie group transformations, they always occur contracted as singlets, and are not directly observable. Gauge fields manifest themselves indirectly through their invariants and their imprint on observable fields. Gauge groups can be semi-simple, or reductive, with Abelian elements. Discrete symmetries associated with finite groups also have a bearing. In the case of the SUSY quiver gauge theories that form the subject matter of this study, the moduli spaces typically describe the field content of the SUSY vacuum.

The characterisation of field content is perhaps the simplest aspect. Representation theory provides us with lattice structures in the form of Dynkin labels that can be used both to describe the irreducible representations ("irreps") within which fields transform and also to label the states within irreps. In effect, Dynkin labels provide consistent and complete quantum mechanical descriptions, from simple $U(1)$ R-charges and $SU(2)$ spins, through to high rank Classical or Exceptional groups. It is, of course, possible to translate between field descriptions in terms of Dynkin labels and those in terms of tensors and indices. The merits of using Dynkin labels, besides their ubiquity, include their bijective correspondence with the eigenvalues of

a commuting system of Casimir and Cartan subalgebra ("CSA") operators, which together comprise the observables of a given field theory. Equally importantly, the Dynkin labels of the states within an irrep uniquely specify its trace or character, which provides a faithful encoding of its symmetry properties. Furthermore, the character algebra of the tensor products of representations, which is given by polynomial multiplication and addition, is often more tractable than the alternative of working with explicit representation matrices, with the attendant complications of composing tensor indices and imposing symmetry and trace conditions.

The determination of the field content of a theory is more involved. Given some underlying structure, one approach is to identify the relevant symmetry groups, their basic irreps and their combinatorics. Bosonic fields naturally form symmetric representations and fermionic fields naturally form antisymmetric representations. However, fields transforming in product groups exhibit much richer combinatoric behaviour. Often the field combinations of interest are gauge invariant (i.e. singlets) under one or more symmetry group(s) and this places restrictions on the resulting field content. As an alternative to combining basic field representations, field theories can result from symmetry breaking, where representations of some parent group split to those of its subgroups as a result of some perturbation. Either way, the moduli spaces of possible field representations can in principle be decomposed into irreps and enumerated by their Dynkin labels. A non-trivial amount of representation theory may, however, need to be applied to effect such decompositions and the development of the generating functions and custom *Mathematica* routines necessary to carry out such transformations in an efficient manner has been a major practical exercise within this study.

The most interesting aspect is the development of an understanding of why particular gauge and flavour group structures, typically described by quiver theories, give rise to moduli spaces with canonical group theoretic significance, and of the reasons for highly non-trivial identities between the moduli spaces of superficially different structures. Much of this study is devoted to the vacuum moduli spaces of the Higgs branches and Coulomb branches of SUSY quiver gauge theories. Remarkably, different branches of different theories can have identical moduli spaces, leading to many dualities, including three dimensional ("3d") mirror symmetry [1], amongst others. Mappings between these theories can be facilitated by their string

theoretic interpretation in terms of brane systems [2]. Exploration of the group theory underlying these relationships leads intriguingly to the mathematical topic of nilpotent orbits (or, to be more precise, the closures of nilpotent orbits). These are canonical combinatoric objects that live in the root spaces of Classical and Exceptional groups, and which match the moduli spaces of the Higgs branches and/or Coulomb branches of particular quiver theories. The understanding of all the mechanisms behind these relationships remains an open task, but one with which this study would claim to make interesting progress. Indeed, it would appear that the physics motivated exploration of SUSY quiver theories may shed new light upon matters that are opaque, when approached from the mathematical Literature.

1.2. Antecedents

This project falls under the broad auspices of the Plethystics Program, which has its origins in the application of Hilbert series ("HS") to analyse the moduli spaces of field theories.

An early use of Hilbert series (also referred to as partition functions or indices) in the context of SUSY theories, was to describe the moduli spaces of Classical group instantons and pure spinors [3, 4, 5]. These Hilbert series were calculated from Higgs branch constructions, by using Weyl integration[1] and HyperKähler quotients to impose SUSY vacuum conditions [3].

Interestingly, while the use of quiver theories to define such constructions is a relatively recent development within SUSY, it has roots in the prior study of moment maps and HyperKähler quotients. Thus, the foundations for Higgs branch calculations based on quiver theories were laid by geometric and algebraic analyses in the mathematical Literature [6, 7], well before the linkage to the vacuum moduli spaces of SUSY quiver theories was made in [8, 9].

A systematic and streamlined treatment of plethystic methods, embracing symmetrisation, anti-symmetrisation and Molien sums, is given in [10] and [11]. The motivation there was to study the moduli spaces given by the chiral rings of mesonic single-trace and multi-trace BPS operators that arise when $D3$ branes probe singular Calabi-Yau ("CY") manifolds. The CY

[1] This procedure implements averaging over a continuous Lie group to find gauge invariant field or operator combinations, as summarised in Appendix A.2.

manifolds analysed include $\mathbb{C}^2$ orbifolds under finite symmetry groups of ADE type, and also $\mathbb{C}^3$ orbifolds. For such orbifolds, with discrete gauge groups, their Hilbert series, which count invariant polynomials of a given degree, are constructed by taking gauge group averages using Molien sums.

Importantly, the Plethystics Program approach can in principle be generalised to any type of gauge theory. As noted in [11]:

> "... the applicability of the plethystic programme is not limited to world-volume theories of D-brane probes on Calabi-Yau singularities. Indeed, if we knew the geometry of the classical moduli space of a gauge theory, ... we could obtain the Hilbert series and thenceforth use the plethystic exponential to find the gauge invariants."

In such early papers, the Hilbert series analysis of continuous symmetry groups was limited to the prolific $U(1)$ groups implicated in the CY manifolds of toric, $Y^{p,q}$ and delPezzo hypersurfaces. The Hilbert series of non-Abelian gauge groups $SU(2)$, $SU(2) \otimes SU(2)$ and $SU(3)$ appear in [12], which makes the important observations that, for a Lie group G, (i) a Hilbert series can always be collected into a series in irreps of G and (ii) group averaging over G can be implemented by Weyl integration in place of Molien summation.

Subsequent developments within the Plethystics Program include the calculation of Hilbert series, on the Higgs branches of quiver theories of many different types, without and with superpotentials, but involving continuous Lie gauge groups. These include, inter alia, (i) $\mathcal{N} = 1$ SQCD theories, where the moduli spaces of gauge invariant operators are found to be affine CY cones with palindromic Hilbert series [13, 14, 15] and (ii) constructions for the moduli spaces of instantons [16, 17, 18, 19]. The former yield, as by-products, methods for identifying the invariant tensors of symmetry groups, which in turn illuminate the structure of the latter.

In parallel with more recent Higgs branch work, and following on from impetus provided by [20], the Coulomb branches of the vacuum moduli spaces of quiver theories and their Hilbert series have come in for considerable study. Relationships between these quiver theories and Dynkin diagrams have been known since [9]. Much subsequent progress has been made in developing the precise formulae for Coulomb branch quiver theory

constructions and analysing the Hilbert series of (i) the instanton moduli spaces of simply laced ADE and non-simply laced $BCFG$ series [21, 22], (ii) $T(SU(N))$ type quiver theories [23], and (iii) some other types of nilpotent orbit [24].

These studies have in turn opened up avenues for confirming and exploiting the relationships between Higgs branch and Coulomb branch constructions and their quiver theories. For example, in [25], the Coulomb branch Hilbert series of $T(SU(N))$ quiver theories were calculated from their Higgs branch mirror theories; and, in [23] and [26], the correspondence between the Higgs branch Hilbert series of three dimensional Sicilian (star shaped) quiver theories and the Coulomb branch Hilbert series of their mirrors was confirmed, via their building blocks in $T(SU(N))$ quiver theories (or A series modified Hall Littlewood polynomials).

Traditional Hilbert series analysis revolves around the unrefined Hilbert series, which effectively grades a moduli space, by projecting it onto a lattice defined by the charges assigned to a "fugacity" or "counting variable", and enumerates its field content at each level of charge (typically R-charge). A Hilbert series is generated by a rational function that is a quotient of polynomials, and this can be described, using the language of algebraic geometry and varieties, in terms of dimensions, generators and relations, amongst other properties. For some purposes, counting of operators or invariants suffices, for example, [27] uses Hilbert series with multi-graded fugacities (termed "spurions") to count invariants of basic fields corresponding to scattering vertices.

More generally, however, issues can arise from birational equivalence and other ambiguities inherent in unrefined Hilbert series. Thus, different moduli spaces can have the same unrefined HS, or identical moduli spaces can appear to have different unrefined HS, all depending on the counting and field grading methods chosen. Such limitations can be avoided, in principle, by working with character valued (or "refined") Hilbert series, which faithfully track the representation content of a field theory; however, the use of refined Hilbert series to describe field content (rather than as an intermediate stage in calculations) has been hampered by their cumbersome nature.

The development of Highest Weight Generating functions ("HWGs"), which encode refined Hilbert series in a concise form, using fugacities for the

highest weights of irreps, rather than their full characters, was a significant early milestone in the course of this study [28]. HWGs give an efficient and unambiguous description of a moduli space in terms of its representation content. If all the quantum fields in a system can be included in a moduli space, then a complete enumeration of their quantum numbers gives a unique and precise description of the quantum system, and this is what HWGs are, in principle, able to achieve.

HWGs describe moduli spaces concisely, resolving questions of identity. While their use requires an orthogonal basis for class functions, such bases are not limited to the characters of a Lie group G and, indeed, it is feasible (at some expense in algebraic computation) to define HWGs in in terms of Hall Littlewood polynomials of G (or their modifications), in an analogous manner to characters of irreps of G. These HWG approaches were applied to the study of the Hilbert series of SQCD in [28] and to instanton constructions in [29].

Much of this work revolves around the investigation of relationships between SUSY quiver gauge theories and the closures of nilpotent orbits ("nilpotent orbits" or "orbits") of compact Lie groups. This intriguing avenue of research was opened up by recent papers, such as [20, 30, 31]. In the first of these [20], the S-duality of boundary conditions on four-dimensional $\mathcal{N} = 4$ superconformal field theories is related to the action of mirror symmetry on three-dimensional gauge theories, which can exchange the Higgs and Coulomb branches of different theories. In many cases, as will be discussed, the moduli spaces of these Higgs and Coulomb branches are described in terms of nilpotent orbits. It is known that $\mathcal{N} = 4$ SUSY theories have finite beta functions to all orders [32] and such constructions therefore generate a large class of candidates, parameterised by nilpotent orbits, for UV-finite theories.

The theory of nilpotent orbits [33] provides a language for classifying and describing equivalence classes constructed from the nilpotent Lie algebra matrices or generators of a Classical or Exceptional group.[2]

Nilpotent orbits are increasingly being recognised for their relevance to theoretical physics. Topics range from SUGRA theories involving G/H coset

[2]Recall that the nilpotent matrices of a group are nilpotent linear combinations of its raising and lowering operators, each of which corresponds to one of its roots, relative to some chosen basis of Cartan operators.

manifolds, whose field content can be characterised by nilpotent orbits [34], to the counting of massive vacua in $\mathcal{N} = 1$ Super Yang-Mills ("SYM") theory [35], where the number of vacua is derived from the structure of the nilpotent orbits of the Yang-Mills group. In [36], the normalised vacuum states in $\mathcal{N} = 4$ SUSY theories are counted, based on the number of distinguished nilpotent orbits in the Yang-Mills group, which is shown to equal the Witten index for the theory. In [37], nilpotent orbits are used as building blocks in the construction of $3d$ Sicilian theories and their mirrors. In a series of papers including [30, 38, 39], nilpotent orbits are used to label punctures on Riemann spheres, which are used as building blocks (or "fixtures") for $6d$ $\mathcal{N} = (2, 0)$ theories. The status of nilpotent orbits, as a class of canonical representation theoretic objects, underlies this appearance in many different contexts; and this in turn motivates the case for developing a systematic understanding of their constructions, along with their properties and relationships. The approach herein constructs nilpotent orbits as moduli spaces of SUSY quiver gauge theories and studies them through their Hilbert series.

Nilpotent orbits generalise the moduli spaces of (single) G-instantons, which provide their simplest non-trivial examples. Instantons have attracted considerable interest since their proposal as self-dual solutions of Yang-Mills field equations in 1975 [40]. They have also been studied in general relativity in the form of self-dual ("SD") and anti-self-dual ("ASD") Weyl or Riemann tensors in 4 dimensions [41], where they are related to Einstein Manifolds [42, 43, 44, 45]. Turning to Yang-Mills theories, the ADHM [46] construction for instanton fields with classical Yang-Mills groups G has been a foundation for the study of instanton moduli spaces using SUSY constructions [4]. The Hilbert series of the moduli spaces of one and two G-instanton theories have been calculated on the Higgs branches of $\mathcal{N} = 2$ SUSY theories, for classical G [16, 19], and on the Coulomb branches of $\mathcal{N} = 4$ SUSY theories [22] in 3 dimensions. All these theories contain 8 SUSY supercharges. Some other constructions have also been given for exceptional G-instantons [17, 18, 26, 21, 29].

An instanton field is defined as a field that is SD or ASD under the action of the Hodge star dualisation operator. On a real manifold $\mathcal{M}$ of dimension $2n$, the epsilon tensor has length $2n$ and the dual of an $n-$form is also an $n-$form. This limits the possibilities for instanton fields to Riemannian

$\mathcal{M}$ of even dimension, including Lorentzian and Euclidean manifolds as special cases. The instanton fields on a real Euclidean $\mathcal{M}$ of fundamental dimension $2r$ are associated with pairs of symmetrised $SO(2r)$ spinor irreps, with one symmetrised spinor irrep being ASD and the other being SD. The representation structure generalises to Lorentzian $\mathcal{M}$.

Different approaches to the study of manifolds involving instantonic fields have been followed in the Literature. One school of thought identifies instantons based on symmetries of the Riemann tensor [47, 48, 44, 45]. If $\mathcal{M}$ is four dimensional, the Riemann tensor has two pairs of antisymmetric indices and can be dualised on one or both pairs. It then follows from Riemann tensor identities, that if the Riemann tensor is SD under dualisation on both pairs of indices, then $\mathcal{M}$ is an Einstein manifold [49] of constant curvature, with non-vanishing Ricci tensor $R_{\mu\nu} = \frac{1}{4} R g_{\mu\nu}$. Since $\mathcal{M}$ is four dimensional, this essentially limits the possibilities for non Ricci-flat $\mathcal{M}$ to four dimensional de Sitter and Anti de Sitter space-times and their counterparts with Euclidean signature.

If, however, the Riemann tensor is either (i) SD or ASD under dualisation of a single pair of indices, or (ii) ASD under dualisation on both pairs, then $\mathcal{M}$ is Ricci flat with $R_{\mu\nu} = 0$; such instantons are termed *gravitational instantons*. These Ricci-flat manifolds include Fubini-Study and Eguchi-Hanson metrics [47]. In [45] it is shown how gravitational instantons from singly SD or singly ASD Riemann tensors, when viewed in local inertial frame coordinates, can be interpreted as self-gravitating SD or ASD Yang-Mills fields.

The possibilities for Yang-Mills constructions extend beyond the class of gravitational instantons. Yang-Mills fields are described by a connection $D = d + A$ and field strength $F = D \wedge D$. A Yang-Mills field F has the action $\mathcal{S}_{YM} = \int vol\ Tr\,(F \wedge *F)$ and an (anti-)self dual field F satisfies the relationship $F = \pm * F$, so a self dual Yang-Mills field could be expected to have the action $\mathcal{S}_{SD} = \int vol\ Tr\,(F \wedge F)$. However, as discussed in [50], the variation of such an action is trivially zero for *any* Yang-Mills field strength, so the construction of an action for an inherently self-dual field is problematic.

Nonetheless, an algebraic construction of a connection with a SD field strength was provided in [40]. BPST use the Euclidean manifold R^4, with its $SO(4)$ symmetry. The Yang-Mills connection can be expanded [51, 52]

as:

$$\begin{aligned} D^{BPST}_{\mu} &= \partial_{\mu} + A^{BPST}_{\mu}, \\ A^{BPST}_{\mu} &= \frac{-x^{\nu}}{4\left(r^2+\lambda^2\right)} \underbrace{[\gamma_{\mu},\gamma_{\nu}]}_{\text{left}} \\ &= \frac{-ix^{\nu}}{r^2+\lambda^2} \eta^{i}_{\mu\nu\, SD} \sigma_i, \end{aligned} \tag{1.1}$$

where r is a radial coordinate orthogonal to the $SO(4)$ symmetry and λ is a scale parameter.

Unlike the Christoffel connection, which acts on the tangent vectors of $\mathcal{M}$, the BPST connection contains a fibre over one only of the Weyl spinors of $\mathcal{M}$. This is seen most clearly in the gamma matrix notation, where the SD construction selects a single diagonal block from $[\gamma_{\mu},\gamma_{\nu}]$, intertwining the spatial coordinates with the left Weyl spinors only. (An ASD connection results from selecting the other diagonal block).

The BPST construction lends itself to generalisation, by splitting the anti-symmetrised gamma matrices into the contraction of t'Hooft matrices ${\eta_{\mu\nu}}^{i}_{SD/ASD}$ with Pauli matrices σ_i, and by making the physical assumption that the $SU(2)$ subalgebra acting on the left or SD Weyl spinor is embedded in the Lie algebra of some larger symmetry group G. Anticipating the discussion in section 2.6, there are many ways of embedding $SU(2)$ into a larger group and this leads to the concept of a G-instanton.

Although it was pointed out in [53] that the different possible embeddings of $SU(2)$ into G correspond to the nilpotent orbits of G, the ensuing physics Literature, such as [4], has largely confined itself to a restricted interpretation of G-instanton, based on the minimal nilpotent orbit of G.

The subject of nilpotent orbits is well covered in the mathematical Literature, which builds on early work by Dynkin [54], and has a valuable reference provided by [33]. These mathematical treatments do not, however, describe nilpotent orbits in the explicit language of Hilbert series, as would be helpful for a physics interpretation. While steps have been taken in this direction within the Plethystics Program [22, 31, 55], the systematic translation of the mathematical treatment of nilpotent orbits into equivalent descriptions in terms of refined Hilbert series forms a key aspect of this study. Certainly, it is an essential ingredient in the process of defining the relationships between SUSY quiver theories and nilpotent orbits.

Viewed as moduli spaces, nilpotent orbits can be constructed by a variety of methods, including Higgs and Coulomb branch quiver theories [24], as well as localisation techniques. This is a rich area, which draws on many strands of the Plethystics Program, including Hilbert series, HWGs, Higgs branch and Coulomb branch SUSY quivers theories, and localisation methods, all set against a background of representation and group theory.

1.3. Outline

As a necessary preliminary, Chapter 2 is pedagogical in nature. Its aims are to lay the theoretical foundations that are common across this study, to summarise relevant aspects of established theory, to introducing some new techniques and to set up common frameworks and notation.

The areas of established theory include the use of Hilbert series to describe moduli spaces, plethystic tools for symmetrisation and anti-symmetrisation, and aspects of the representation theory of compact Lie group characters and their branching to subgroups.

The new techniques primarily revolve around the methodology of Highest Weight Generating functions. These can be used to decode, encode and/or transform refined (character valued) Hilbert series. The methodology encompasses: (i) HWG notation, based around Dynkin labels, which uses $U(1)^{\text{rank}[G]}$ fugacities for the highest weights of irreps to give a compact notation for character valued Hilbert series; (ii) development (from the Weyl character formula and its generalisations) of generating functions for characters, Hall Littlewood polynomials and their modifications, which together provide alternative or complementary orthogonal bases for decomposing class functions; (iii) the combination of Weyl integration with the appropriate Haar measures and generating functions to transform refined Hilbert series to HWGs, and vice versa, and; (iv) the use of Weyl group summation techniques to transform HWGs back to refined Hilbert series.

The supporting materials to Chapter 2, contained in Appendices A.1, A.2 and A.3, cover plethystic functions, Weyl/Molien integration, and the relationship between Dynkin diagrams and affine or twisted affine Lie algebras.

As a set of warm up exercises, Chapter 3 deals with the moduli spaces associated with invariant tensors, and with the gauge invariant operators ("GIOs") on the Higgs branches of some SUSY quiver theories, including

SQCD and $SU(N)$-instanton theories. HWGs are used to decode how gauge groups are imprinted onto flavour groups through their invariant tensors, shedding light on the interplay of group invariants behind the logic of Higgs and Coulomb branch constructions. The use of HWGs makes it possible to identify and give a simple description of generalised SQCD for Classical gauge groups of any rank. Section 3.3 summarises the established Higgs branch constructions for the moduli spaces of $SU(N)$-instantons and introduces reduced single instanton moduli spaces ("RSIMS"), which correspond to minimal nilpotent orbits, as a stepping stone to subsequent Chapters.

Chapter 4 provides an introduction to the topic of nilpotent orbits, touching on the different approaches in the mathematical Literature, as well as the various methods of classifying the orbits of a group. A consistent narrative is set out, starting from an enumeration of the possible $SU(2)$ homomorphisms (or embeddings) into a group G, described in terms of Characteristics or partitions, that define a nilpotent element of G, and relating these to the nilpotent orbit dimensions and partitions that supply the parameters for their Higgs and Coulomb branch quiver theory constructions.

The generalisation of the Higgs branch RSIMS construction to the wider class of moduli spaces represented by nilpotent orbits is discussed in detail in Chapter 5. This Chapter reviews the known Higgs branch constructions for minimal, maximal and A series nilpotent orbits and, following [24], sets out a consistent methodology, starting from Characteristics or character maps, for identifying quiver theories whose Higgs branch moduli spaces match each nilpotent orbit of any Classical group G. Key developments include the incorporation into the Higgs branch formula of group averaging over the $\mathbb{Z}_2$ components of orthogonal gauge groups, in order to obtain nilpotent orbits (rather than their extensions) of BCD series groups. This is followed by a complete analysis of the nilpotent orbits of low rank Classical groups - in terms of Hilbert series, character and mHL HWGs, the identification of some generalisations regarding their structures, and a discussion of quiver dualities.

Coulomb branch constructions for RSIMS and other nilpotent orbits are covered in depth in Chapter 6. This Chapter reviews the known Coulomb branch constructions for minimal and A series nilpotent orbits and, drawing on [24], sets out a methodology, starting from Characteristics and/or twisted affine Dynkin diagrams, for identifying quiver theories whose Coulomb branch

moduli spaces match near to minimal nilpotent orbits of Classical and Exceptional groups. The implicit roles played in Coulomb branch constructions by Dynkin diagrams, the Cartan matrix and the Weyl group, are identified and discussed. The consistency between Higgs branch and Coulomb branch constructions of normal Classical nilpotent orbits is verified, and apparent differences between these constructions for non-normal orbits are reconciled.

Chapter 7 develops a plethystic formula ("Nilpotent Orbit Localisation" or "NOL") formula for constructing the normal nilpotent orbits of any group G, directly from their Characteristics, by drawing on Weyl group symmetries and localisation techniques. This method of constructing nilpotent orbits is reconciled to the Higgs branch and Coulomb branch constructions. The NOL formula extends the range of nilpotent orbits of Exceptional groups that can be constructed as explicit moduli spaces (subject to practical computation constraints). Their Hilbert series are analysed in terms of unrefined HS and, where practicable, character and mHL HWGs. The results of this (as yet incomplete) moduli space analysis of Exceptional group nilpotent orbits are largely consistent with the findings and claims encountered in the mathematical Literature; however, some differences emerge and these are discussed.

Chapter 8 outlines some of the ways in which nilpotent orbits can be related to, or used as building blocks for, other quiver theories. The topics examined include (i) the deconstruction of star shaped quiver families into $T(S(UN))$ quivers, using A series mHL functions, (which correspond to maximal nilpotent orbits dressed by background charges), and (ii) the branching of nilpotent orbits, under symmetry breaking and/or Hyper Kähler quotients, into the moduli spaces of subgroups.

The concluding Chapter draws together these various threads and findings and outlines potential avenues for future investigation in this nascent field.

2. Highest Weight Generating Functions

2.1. Hilbert Series

The Hilbert series ("HS") has its origins as a means of enumerating algebraic varieties and provides a powerful tool in the study of moduli spaces. In its simplest form, a Hilbert series is constructed by grading a lattice of monomials in the coordinates describing a variety, according to their projection onto a counting fugacity, often taken as t. The grading is chosen such that negative exponents of t do not appear and this yields a power series in t, with coefficients determined by the multiplicities in the projection. In this study we designate this an *unrefined* Hilbert series, although the distinction between unrefined and refined HS (to be defined) is not always made in the Literature.

Following [11], we can arrange such a Hilbert series $g_{HS}(t)$ as a quotient of polynomials $P(t)$ and $Q(t)$, in the form:

$$g_{HS}(t) = \sum_{n=0}^{\infty} a_n t^n = \frac{P(t)}{Q(t)}, \tag{2.1}$$

where the a_n are integers.

Clearly, the polynomials $P(t)$ and $Q(t)$ can be multiplied or divided by a common factor without changing $g_{HS}(t)$ and this permits the quotient to be rearranged into a canonical form. It is useful to distinguish certain types:

A *freely generated* HS has $P(t)$=1 and $Q(t) = \prod_{i=1}^{|HS|} \left(1 - t^{k_i}\right)$, which gives a product of geometric series. Its Plethystic Logarithm (see Appendix A.1) is finite and contains positive coefficients only.

A *complete intersection* HS is a quotient of geometric series defined by

$P(t) = \prod_{i=1}^{|R|}\left(1-t^{j_i}\right)$ and $Q(t) = \prod_{i=1}^{|HS|+|R|}\left(1-t^{k_i}\right)$. This rearrangement is sometimes termed the Euler form [10]. Its Plethystic Logarithm is finite and contains both positive and negative coefficients. A freely generated series is trivially a complete intersection.

A *non-complete intersection* HS. Any quotient of non-trivial polynomials $P(t)$ and $Q(t)$, that is neither a complete intersection nor freely generated. Its Plethystic Logarithm is not a finite series.

An *(anti-)palindromic* HS is one where the numerator, $P(t) = \sum_{k=0}^{n} b_k t^k$, is palindromic (or anti-palindromic). A palindromic (or anti-palindromic) numerator $P(t)$ of degree n, is one for which $\forall k : b_k = +$ (or $-$) b_{n-k}. The significance of an (anti-)palindromic HS follows from a theorem by Stanley; the numerator of an HS is (anti-)palindromic if and only if the moduli space is an affine Calabi-Yau variety [13]. Freely generated series and complete intersections are always (anti-)palindromic and therefore Calabi-Yau.

The *dimension* of a moduli space, denoted $|HS|$, counts the order of the pole at $t = 1$ in its Hilbert series. Generally, $|HS|$ equals the order of the poles contributed by $Q(t)$ less $|R|$, the number of relations contributed by $P(t)$. For a complete intersection or freely generated series $g(t)$ the dimension equals $PL[g(1)]$. By an extension of terminology, this study may refer to the order of the poles of a HS, HWG (or other quotient of polynomials) as its *dimension*.

Examples of Hilbert series for simple algebraic varieties, such as the complex plane $\mathbb{C}$ and conifold $\mathbb{C}^2/\mathbb{Z}_2$, are given by $g^{\mathbb{C}}(t) = \frac{1}{1-t}$ and $g^{\mathbb{C}^2/\mathbb{Z}_2}(t) = \frac{1-t^2}{(1-t)^3}$, respectively. The complex plane is freely generated of dimension 1 and the conifold is a complete intersection of dimension 2.

Whilst the unrefined Hilbert series gives the overall dimension of a moduli space and can be a powerful analytic tool, it has an inherent limitation steming from the grading of the underlying variety in terms of a single counting fugacity. Clearly, whenever the number of fugacities is less than the number of independent coordinate degrees of freedom, some information must be lost, and, moreover, the properties of a Hilbert series can depend upon the grading method chosen.

The Hilbert series can, however, be generalised to work with multiple fugacites, whereupon it is termed a *refined* Hilbert series. By working with a refined Hilbert series, it is possible to mitigate the limitations of an unrefined Hilbert series. For a toric manifold of rank r, it is a straightforward refinement to use counting fugacities $t_1 \dots t_r$ to track the $U(1)^r$ coordinate degrees of freedom, for example as in [56, 57]. For manifolds with non-Abelian symmetries, the HS can also be refined, in a powerful manner, by choosing counting fugacities that track the weight space (or root space) lattice of G. Specifically, the monomial elements within the character of a representation of G can be constructed from a set of weight space fugacities $x \equiv x_1 \dots x_r$, or root space fugacities $z \equiv z_1 \dots z_r$, as described further in section 2.2. For compact groups, these CSA coordinates are all unimodular, with complex modulus 1, and can be combined with counting fugacities, as desired. Such a refined Hilbert series can also be described as a *character valued* Hilbert series.

Hilbert series can be constructed in different ways. Many of these involve symmetrisations or antisymmetrisations of class functions of characters and can be carried out using plethystic functions. These are described in Appendix A.1.

2.2. Characters of Representations

The character of a representation of a Classical group G is defined by the trace of its representation matrix and possesses a number of important combinatoric properties. Each character (i) is unique to its representation, (ii) is invariant, both under the action of G and of the Weyl group of inner automorphisms W_G, (iii) decomposes under addition into the characters of its constituent irreps, and (iv) combines under multiplication into the characters of tensor products of representations. Also, in accordance with the Peter Weyl Theorem, the characters of a group yield an orthonormal basis for its *class functions*, i.e. functions that are invariant under the action of the group [58]. Taken together, these properties make characters highly effective for studying the combinatorics of Lie group representations.

The canonical classification of the representations of a Lie group is carried out using Dynkin labels. These label the states or weights within an irrep by their charges under the maximal torus of Cartan subalgebra operators;

each irrep has a unique highest weight and this can also be identified by its Dynkin labels, properly termed *highest weight Dynkin labels*. It is naturally useful to parameterise characters in a way that incorporates a simple relationship with Dynkin labels. Different approaches are possible.

Starting from first principles, one method is to diagonalise a representation matrix and to find its eigenvalues; analysis of the relations between the eigenvalues yields information about the weights and hence the Dynkin labels of the field states in the representation.

For most cases, however, we can draw on the representation theory of compact groups and use the canonical CSA or weight space coordinates $x \equiv x_1 \dots x_r$, or alternatively root space coordinates $z \equiv z_1 \dots z_r$, to parameterise the characters a G with rank r. These coordinates are related by coordinate transformations derived from the Cartan matrix A_{ij} of G, as $z_i = \prod_j x_j^{A_{ij}}$ and $x_i = \prod_j z_j^{{A^{-1}}_{ij}}$. The character $\chi^G_{[n]}$ for an irrep with highest weight Dynkin labels $[n] \equiv [n_1, \dots, n_r]$ expands in terms of coordinate monomials as:

$$\chi^G_{[n]}(x) = \sum_{[n'] \in irrep[n]} a_{[n][n']} x_1^{{n'}_1} \dots x_r^{{n'}_r} \equiv \sum_{[n'] \in irrep[n]} a_{[n][n']} x^{[n']}, \qquad (2.2)$$

where $a_{[n][n']}$ are the integer multiplicities of the weights $[n']$ in $[n]$.

It is possible to identify all the weights $[n']$ in a character, by starting from the highest weight in the positive weight space $[n]$, subtracting the weights of simple roots until all positive Dynkin labels are exhausted, and then using the Freudenthal multiplicity formula to assign multiplicities [58].

The main method used for obtaining characters in this study, however, draws on the Weyl character formula [58], which can be stated in two equivalent forms:

$$\chi^G_{[n]}(x,t) = \sum_{w \in W_G} w \cdot \left(x^{[n]} \prod_{\alpha \in \Phi+} \frac{1}{1 - z^{-\alpha}} \right), \qquad (2.3)$$

or

$$\chi^G_{[n]}(x,t) = x^{-\rho} \prod_{\alpha \in \Phi+} \frac{1}{1 - z^{-\alpha}} \sum_{w \in W_G} |w|\, w \cdot \left(x^{[n]} x^{\rho} \right), \qquad (2.4)$$

where the product is taken over all roots α in the positive root space Φ^+,

G	$\|G\|$	W	$\|W\|$
$U(N)$	N^2	S_N	$N!$
A_n	$n(n+2)$	S_{n+1}	$(n+1)!$
B_n	$n(2n+1)$	$S_n \otimes {\mathbb{Z}_2}^n$	$2^n n!$
C_n	$n(2n+1)$	$S_n \otimes {\mathbb{Z}_2}^n$	$2^n n!$
D_n	$n(2n-1)$	$S_n \otimes {\mathbb{Z}_2}^{n-1}$	$2^{n-1} n!$
E_6	78		72.6!
E_7	133		8.9!
E_8	248		192.10!
F_4	52		48.4!
G_2	14		2.3!

Table 2.1.: Weyl Group Dimensions

$x^\rho \equiv \prod_{i=1}^{r} x_i$ is the Weyl vector and $|w|$ denotes the sign (i.e. determinant) of a Weyl group matrix w. The Weyl group W_G acts on all functions of x and z inside the summation, as $w : (f[x], g[z]) \to (f[w \cdot x], g[w \cdot z])$.

Recalling that $x^\rho = \prod_{\alpha \in \Phi+} z^{\alpha/2}$, the equivalence of 2.3 and 2.4 follows from the fact that the product of root differences $\prod_{\alpha \in \Phi+} \frac{1}{z^{\alpha/2} - z^{-\alpha/2}}$ transforms in the alternating representation of the Weyl group, and can be moved through the summation if balanced by the sign of the Weyl group matrix.

The Weyl character formula has various features, including generalisability to all Classical and Exceptional groups, convertibility to a generating function form and the explicit treatment of Weyl group symmetries, which fit naturally with subgroup branching relationships and permit various simplifying rearrangements. Table 2.1 sets out the dimensions of the Weyl groups, from which such subgroup relations follow.

To make the fullest use of Highest Weight Generating functions, introduced in the next section, we require a generating function for characters. First, we map highest weight Dynkin labels $[n]$ onto the complex manifold $\mathbb{C}^r$ by introducing the $U(1)^r$ Dynkin label counting fugacities $m \equiv m_1 \dots m_r$ and establish the correspondence:

$$\chi^G_{[n]} \Leftrightarrow \prod_{i=1}^{r} m_i^{n_i} = m_1^{n_1} \dots m_r^{n_r} \equiv m^n. \tag{2.5}$$

If we choose the fugacities $\{m_1, \dots, m_r\}$ each to have absolute values less

than unity, then each point on the infinite lattice of Dynkin labels corresponds to a unique point lying inside the unit complex disk on $\mathbb{C}^r$. This lattice is freely generated since the Dynkin labels can be chosen independently of each other.

To formalise the correspondence, we require the generating function that yields the infinite series:

$$g^G_\chi(x,m) \equiv \sum_{[n]} \chi^G_{[n]}(x) m^n, \tag{2.6}$$

We obtain this function by combining 2.3 and 2.6:

$$\begin{aligned} g^G_\chi(x,m) &= \sum_{[n]} \sum_{w\in W_G} m^n (w\cdot x)^n \prod_{\alpha\in\Phi+} \frac{1}{1-(w\cdot z)^{-\alpha}} \\ &= \sum_{w\in W_G} \left(\prod_{i=1}^{r} \frac{1}{1-m_i(w\cdot x)_i} \right) \prod_{\alpha\in\Phi+} \frac{1}{1-(w\cdot z)^{-\alpha}}, \end{aligned} \tag{2.7}$$

where the Weyl group acts on x and z within the summands. An alternative form can be obtained from 2.4 as:

$$g^G_\chi(x,m) = x^{-\rho} \prod_{\alpha\in\Phi+} \frac{1}{1-z^{-\alpha}} \sum_{w\in W_G} |w| (w\cdot x)^\rho \prod_{i=1}^{r} \frac{1}{1-m_i(w\cdot x_i)}. \tag{2.8}$$

The character generating function 2.7 can also be written using plethystic notation:

$$g^G_\chi(x,m,) = \sum_{w\in W_G} PE\left[\sum_{i=1}^{r} m_i (w\cdot x_i)\right] PE\left[\sum_{\alpha\in\Phi+} (w\cdot z)^{-\alpha}\right]. \tag{2.9}$$

This plethystic form highlights the contributions to the character generating function from (i) Weyl group averaging to give class functions of G, (ii) symmetrisations of the root system of G and (iii) fugacities for the *basic* irreps of G, which we define to be those containing a single non-zero unit Dynkin label in the i^{th} slot.[1]

For low rank G, the evaluation of 2.9 is relatively straightforward; W_G can be generated from the simple reflection matrices $\{w_1,\ldots,w_r\}$ of G, which

[1]The basic irreps of G are in turn related by anti-symmetrisations, using the PEF, to the fundamental/vector/spinor irreps of G.

follow from the Cartan matrix of G. The CSA coordinate transformation from the simple Weyl reflection w_k is:

$$w_k \cdot x_i = x_i \prod_{j=1}^{r} x_j^{-\delta_{ik} A_{ij}} \tag{2.10}$$

Following evaluation, the character generating functions all take the form:

$$g_\chi^G(x,m) = PE\left[\sum_{i=1}^{r} \chi^G_{[0,\ldots 1_i \ldots,0]}(x)\ m_i\right]\ P^G(\chi(x),m), \tag{2.11}$$

where the denominator symmetrises the characters of the basic irreps of G, using the highest weight fugacities m, and the numerator $P^G(\chi(x),m)$ is some polynomial class function of χ^G and m. By way of example, $P^G(\chi(x),m)$ is shown for some low rank simple groups in Table 2.2.[2]

Group	$P^G(\chi,m)$
$A_1 \cong B_1 \cong C_1$	1
A_2	$(1-m_1m_2)$
B_2	$\left(1-m_1^2+m_1m_2^2-m_1^3m_2^2\right)+m_1m_2(m_1-1)[0,1]$
C_2	As B_2 with $m_1 \Leftrightarrow m_2$ and $[1,0] \Leftrightarrow [0,1]$
$D_2 \cong A_1 \otimes A_1$	1
A_3	$\left(1-m_2^2\right)\left(1-m_1m_3+m_2m_3^2+m_1^2m_2-m_1m_2^2m_3+m_1^2m_2^2m_3^2\right)[0,0,0]$ $+m_2\left(-m_3+m_1m_2-m_1^2m_2m_3+m_1m_2^2m_3^2\right)[1,0,0]$ $+m_2\left(-m_1+m_2m_3-m_1m_2m_3^2+m_1^2m_2^2m_3\right)[0,0,1]$ $+m_1m_2m_3\left(1-m_2^2\right)[0,1,0]$
D_3	As A_3 with $m_1 \Leftrightarrow m_2$ and $[1,0,0] \Leftrightarrow [0,1,0]$

Table 2.2.: P^G for Low Rank Classical Groups

The characters $\chi^G_{[n]}(x)$ can be extracted from $g_\chi^G(x,m)$ by Taylor expansion in m, followed by identification of the coefficient of m^n. Alternatively, the character generating function can be used in further analytic procedures or specialised in some way.

Specialisation is possible when the characters sought do not span the entire lattice of Dynkin labels, such that x^n takes a simpler form, for example, if $n_i = 0$ for some i, or $n_i = n_j$ for some $\{i,j\}$. In such cases, the highest weights of the characters have an invariance group that is a non-trivial subgroup H of G and we can take advantage of this to simplify

[2] $P^G(\chi(x),m)$ for G_2 and A_4 are tabulated in [28].

the Weyl group summation in 2.7. We introduce the quotient group partition, $W_G = W_{G/H} \otimes W_H$, where W_H is a normal subgroup of W_G and $W_{G/H}$ is a set of coset representatives [59], and apply the Weyl identity $\sum_{w \in W_H} \prod_{\alpha \in \Phi_H^+} \frac{1}{1-(w \cdot z)^{-\alpha}} = 1$ to obtain:

$$g_\chi^G(x,m) = \sum_{w \in W_{G/H}} w \cdot \underbrace{\sum_{[n]} m^n x^n}_{f^{G/H}(x,m)} \prod_{\alpha \in \Phi_{G/H}^+} \frac{1}{1-(w \cdot z)^{-\alpha}}, \tag{2.12}$$

where $f^{G/H}(x,m)$ is a generating function that interleaves the sub-lattice of weights x with the highest weight Dynkin label fugacities m. This category of specialised character generating functions includes, as an example, the construction for reduced single instanton moduli spaces given in [17]. The subject of Weyl group rearrangements is revisited in section 7.1.

Other simplifications of character generating functions can also be useful. For example, unrefining the character generating function, by setting the weight space coordinates to unity, yields a generating function $g_\chi^G(1,m)$ for the dimensions of irreps of G, as elaborated further in [28].

2.3. HWGs and Transformations

Suppose we are given some refined Hilbert series $g_{HS}^G(x,t)$, expressed as a generating function in terms of weight space coordinates x and counting fugacity t. This is a class function of G and, by the Peter Weyl Theorem, has a character expansion with coefficients that are functions of t. The expansion takes the form of a series, which may be infinite in length:

$$g_{HS}^G(x,t) = \sum_{[n]} a_{[n]}(t)\, \chi_{[n]}^G(x) \tag{2.13}$$

We can find the coefficients $a_{[n]}(t)$ by using Weyl integration, as described in Appendix A.2, to project $g_{HS}^G(x,t)$ onto a character generating function $g_\chi^G(x^*,m)$ for the conjugate characters $\chi_{[n']}^G(x^*)$ of G, and then using character orthogonality. This yields a generating function $g_{HWG}^G(m,t)$ in the

highest weight Dynkin label fugacities m for the coefficients $a_{[n]}(t)$:

$$\begin{aligned} g^G_{HWG}(m,t) &\equiv \oint_G d\mu \; g^G_\chi(x^*,m) \; g^G_{HS}(x,t) \\ &= \oint_G d\mu \; \sum_{[n']} \chi^G_{[n']}(x^*)\, m^{n'} \; \sum_{[n]} a_{[n]}(t)\, \chi^G_{[n]}(x) \\ &= \sum_{[n'][n]} m^{n'} a_{[n]}(t)\, \delta_{[n'][n]} \\ &= \sum_{[n]} a_{[n]}(t)\, m^n \end{aligned} \tag{2.14}$$

The function $g^G_{HWG}(m,t)$ is termed a Highest Weight Generating function for the Hilbert series $g^G_{HS}(x,t)$. In this case, $g^G_{HWG}(m,t)$ lives on the lattice $\mathbb{C}^{r+1}$. Since an HWG identifies each irrep by its highest weight only, this provides a compact notation, compared with a refined Hilbert series, which includes the full character for each irrep. The approach generalises naturally to Hilbert series that incorporate multiple counting fugacities.

Importantly, this transformation is faithful, and we can recover the original Hilbert series, either by acting on the HWG with the Weyl group, as in 2.15, or, alternatively, by *gluing* the HWG to a character generating function, as in 2.16:

$$g^G_{HS}(x,t) = \sum_{w\in W_G} w\cdot\left(g^G_{HWG}(m,t)\big|_{m->x} \prod_{\alpha\in\Phi+} \frac{1}{1-z^{-\alpha}} \right) \tag{2.15}$$

$$g^G_{HS}(x,t) = \oint_{U(1)^r} d\mu^{U(1)^r}(q) \; g^G_\chi(x,m)\big|_{m\to q^{-1}} \; g^G_{HWG}(m,t)\big|_{m\to q} \tag{2.16}$$

The transformation 2.15 follows from the fact that the Weyl character formula 2.3 takes the highest weight of the character as an argument. The gluing transformation 2.16 is implemented by mapping the fugacities m of the two generating functions to conjugate $U(1)^r$ charges and then gauging to select $U(1)^r$ singlets by Weyl integration. Having recovered $g^G_{HS}(x,t)$, this can, if required, be unrefined as $g^G_{HS}(1,t)$.

The Hilbert series of a theory can thus be presented in various ways; in

refined or unrefined form, or as an HWG. Importantly, the HWG captures all the group theoretic content of the class functions of the theory; if we encode the information as a HWG series, we can always recover a refined or unrefined HS, as desired.

2.4. Hall Littlewood Polynomials

While characters provide a basis for the decomposition of any class function of G, many of the Hilbert series that are generated by quiver theories are graded by $U(1)$ counting fugacities, such as those tracking R-charges, and this invites the question as to whether it is possible to find families of functions, other than characters, that incorporate such additional parameters to provide more concise decompositions. Such families of functions are indeed provided by Hall Littlewood ("HL") polynomials and the related modified Hall Littlewood ("mHL") polynomials (or, strictly speaking, functions) [60]. These have proved a useful tool for describing the Hilbert series of certain SUSY gauge theories [26, 55]. The aim in this section is to develop a generating function methodology that enables the deployment of HL and mHL functions in a systematic manner, comparable to the use of character decompositions elaborated above.

HL and mHL functions of G are plethystic class functions in weight space/root space coordinates that are additionally parameterised by a counting fugacity, (say) t. They can be identified conveniently by Dynkin labels, although other methods, such as partitions, are also used [55]. They are most helpfully defined to give an orthogonal basis under Weyl integration using an explicit measure, as in [26]. There are various choices of normalisation possible: [26] chooses a normalisation under which the Hall Littlewood polynomials are strictly orthonormal; [60] chooses a normalisation under which the Hall Littlewood polynomials for $U(N)$ become symmetric monomial functions for $t = 1$; we shall use a third normalisation scheme, as in [55], that yields natural generating functions for orthogonal polynomials.

Table 2.3 compares the HL and mHL measures. These are the products of the usual Haar measure for G with an additional plethystic function, parameterised by t, on its root space.

The families of orthogonal Hall Littlewood polynomials HL^G and modified Hall Littlewood functions mHL^G of a group G, having rank r, root

Group and Basis	Notation	Measure
χ^G	$d\mu^G(x)$	$\frac{1}{\lvert W_G\rvert}\frac{dx}{x}\prod_{\alpha\in\Phi}(1-z^\alpha)$
HL^G	$d\mu^G_{HL}(x,t)$	$\frac{1}{\lvert W_G\rvert}\frac{dx}{x}\prod_{\alpha\in\Phi}\frac{1-z^\alpha}{1-z^\alpha t}$
mHL^G	$d\mu^G_{mHL}(x,t)$	$\frac{1}{\lvert W_G\rvert}\frac{dx}{x}\prod_{\alpha\in\Phi}(1-z^\alpha)(1-z^\alpha t)$

Table 2.3.: Measures for Orthogonal Bases of G

space Φ, weight space coordinates x, roots $\{z^\alpha : \alpha \in \Phi\}$ and Dynkin labels $[n]$, can be defined as:

$$HL^G_{[n]}(x,t) = \sum_{w\in W_G} w\cdot\left(x^{[n]}\prod_{\alpha\in\Phi+}\frac{1-z^{-\alpha}t}{1-z^{-\alpha}}\right), \tag{2.17}$$

and

$$mHL^G_{[n]}(x,t) = \sum_{w\in W_G} w\cdot\left(x^{[n]}\prod_{\alpha\in\Phi+}\frac{1}{(1-z^{\alpha}t)(1-z^{-\alpha})}\right), \tag{2.18}$$

The orthogonality between the $(m)HL_{[n]}$ and their complex conjugates, under an inner product incorporating the (modified) Hall Littlewood measure $d\mu^G{}_{(m)HL}$, is given by:

$$\oint_G d\mu^G_{HL}\ HL^G_{[n]}(x^*,t)\ HL^G_{[n']}(x,t) = \delta_{[n][n']}\ v^G_{[n]}(t), \tag{2.19}$$

and

$$\oint_G d\mu^G_{mHL}\ mHL^G_{[n]}(x^*,t)\ mHL^G_{[n']}(x,t) = \delta_{[n][n']}\ v^G_{[n]}(t). \tag{2.20}$$

The factors $v^G_{[n]}(t)$ relate to the symmetric Casimirs of G and its subgroups, and are determined by any zero Dynkin labels in the irrep $[n]$:

$$v^G_{[n]}(t) = \prod_{C\in\text{Casimirs}(G/[n])}\left(\frac{1-t^{\text{degree}(C)}}{1-t}\right). \tag{2.21}$$

The subgroup $G/[n]$ is defined by the Dynkin diagram that remains after eliminating from the Dynkin diagram of G any nodes that correspond to

non-zero Dynkin labels of $[n]$. Thus, $v^G_{[n]}(t)$ incorporates all the Casimirs of G if the Dynkin labels of $[n]$ are all zero, and reduces to unity if the Dynkin labels are all non-zero. For example, $v^{D_4}_{[0,0,0,0]}(t) = \frac{\left(1-t^2\right)\left(1-t^4\right)^2\left(1-t^6\right)}{(1-t)^4}$, while $v^{D_4}_{[0,1,0,0]}(t) = \frac{\left(1-t^2\right)^3}{(1-t)^3}$ and $v^{D_4}_{[1,1,1,1]}(t) = 1$.

In the limit $t \to 0$, the (modified) Hall Littlewood polynomials reduce to the characters of G, the (modified) Hall Littlewood measure reduces to the Haar measure for G, and the factors $v^G_{[n]}(0)$ reduce to unity. In the limit where $t \to 1$, the Hall Littlewood polynomials reduce to the characters of $U(1)^{\text{rank}[G]}$,

We now introduce the fugacities $h \equiv \{h_1, \ldots, h_r\}$ for the highest weight Dynkin labels of the (modified) Hall Littlewood polynomials and define and construct their generating functions in a similar manner to characters:

$$\begin{aligned} g^G_{HL}(x,h,t) &\equiv \sum_{[n]} HL^G_{[n]}(x,t)\, h^n \\ &= \sum_{w\in W_G} w\cdot\left(\left(\prod_{i=1}^{r}\frac{1}{1-x_i h_i}\right)\prod_{\alpha\in\Phi+}\frac{1-z^{-\alpha}t}{1-z^{-\alpha}}\right) \end{aligned} \tag{2.22}$$

and

$$\begin{aligned} g^G_{mHL}(x,h,t) &\equiv \sum_{[n]} mHL^G_{[n]}(x,t)\, h^n \\ &= \sum_{w\in W_G} w\cdot\left(\left(\prod_{i=1}^{r}\frac{1}{1-x_i h_i}\right)\prod_{\alpha\in\Phi+}\frac{1}{(1-z^{\alpha}t)(1-z^{-\alpha})}\right) \\ &= \left(\prod_{\alpha\in\Phi}\frac{1}{1-z^{\alpha}t}\right) g^G_{HL}(x,h,t)\,, \end{aligned} \tag{2.23}$$

where we have defined $h^n \equiv \prod_{i=1}^{r} h_i^{n_i}$.

From 2.19 and 2.20, it follows that the generating functions $g^G_{(m)HL}(x,t,h)$ have the orthogonality property with the $(m)HL^G_{[n]}$:

$$\oint_G d\mu^G_{(m)HL}\; g^G_{(m)HL}(x^*,h,t)\;\; (m)HL^G_{[n]}(x,t) = v^G_{[n]}(t)\, h^n. \tag{2.24}$$

We can obtain more useful contragredient generating functions $\overline{g^G_{(m)HL}}(x,h,t)$, which generate polynomials $\overline{(m)HL^G}(x,h,t)$ that are orthonormal (rather than just orthogonal) to the $(m)HL^G_{[n]}$, by gluing together the $g^G_{(m)HL}(x^*,t,h)$ with generating functions for the $1/v^G_{[n]}(t)$, as described in [29]. These have the orthonormality:

$$\oint_G d\mu_{(m)HL}\ \overline{g^G_{(m)HL}}(x,h,t)\ \ (m)HL^G_{[n]}(x,t) = h^n, \tag{2.25}$$

Since the (modified) Hall Littlewood polynomials provide a complete basis for class functions that combine the characters of a group G with coefficients given by polynomials in the fugacity t, we can use these generating functions and orthonormality relationships to decompose a Hilbert series $g^G_{HS}(x,t)$ into (modified) Hall Littlewood polynomials. We first define the decomposition coefficients $C_{[n]}(t)$ from:

$$g^G_{HS}(x,t) \equiv \sum_{[n]} C_{[n]}(t)\,(m)HL^G_{[n]}(x,t). \tag{2.26}$$

We can then find a HWG for the $C_{[n]}(t)$, using the contragredient generating functions:

$$\begin{aligned} g^G_{HWG}(h,t) &\equiv \sum_{[n]} C_{[n]}(t)\,h^n \\ &= \oint_G d\mu^G_{(m)HL}\ \overline{g^G_{(m)HL}}(x,h,t)\ \ g^G_{HS}(x,t)\,. \end{aligned} \tag{2.27}$$

Individual $C_{[n]}(t)$ can be extracted from $g^G_{HWG}(h,t)$ by Taylor expansion, followed by selecting the coefficients of the monomials h^n.

This study mostly works with mHL functions, rather than HL polynomials, since the former typically provide more concise HWGs for the decomposition coefficients of Plethystic Exponentials on the root space of G.

2.5. Generating Function Notation

It is helpful to consolidate the notational conventions developed in this section and in Appendix A.1. For our purposes, the PE and PEF functions can be summarised as:

$$\begin{aligned} PE\left[\sum_{i=1}^{d} A_i t\right] &\equiv \prod_{i=1}^{d} \frac{1}{(1-A_i t)}, \\ PE\left[\sum_{i=1}^{d} -A_i t, t\right] &\equiv \prod_{i=1}^{d} (1-A_i t), \\ PE\left[\sum_{i=1}^{d} A_i t, -t\right] &\equiv \prod_{i=1}^{d} \frac{1}{(1+A_i t)}, \\ PEF\left[\sum_{i=1}^{d} A_i t\right] \equiv PE\left[-\sum_{i=1}^{d} A_i, -t\right] &\equiv \prod_{i=1}^{d} (1+A_i t), \end{aligned} \tag{2.28}$$

where A_i are monomials in weight and/or root coordinates.

The characters of G can be presented either in the generic form $\chi^G(x)$, or as $[irrep]_G$, or, using Dynkin labels, as $[n]_G \equiv [n_1, \ldots, n_r]_G$, where r is rank.

CSA or weight space coordinates are typically labelled by $x \equiv (x_1 \ldots x_r)$ and root space coordinates by $z \equiv (z_1 \ldots z_r)$, dropping subscripts if no ambiguities arise. The Cartan matrix A_{ij} is used to define the canonical relationships between simple roots and CSA coordinates as $z_i = \prod_j x_j^{A_{ij}}$ and $x_i = \prod_j z_j^{A^{-1}{}_{ij}}$. The CSA and root space coordinates are all unimodular.

Field counting variables are generally labelled by t, adding subscripts when necessary. In the case of Higgs branch constructions of RSIMS or nilpotent orbits, these naturally have their non-trivial terms at powers of t^2, whereas in the Coulomb branch and NOL constructions, these terms naturally arise at integer powers of t, reflecting half integer vs integer conventions for counting R-charges in the Literature. Such conventions do not affect the dimensions or structure of Hilbert series.

Dynkin label counting variables are typically denoted by $m \equiv (m_1 \ldots m_r)$ for functions based on characters and by $h \equiv (h_1 \ldots h_r)$ for functions based on (modified) Hall Littlewood polynomials, although other letters may also be used, where this is helpful. All these counting variables are defined to

have a complex modulus of less than unity and are referred to as "fugacities", along with the monomials formed from CSA or root coordinates.

Series, such as $1 + f + f^2 + \ldots$, may be referred to by their generating functions, $1/(1-f)$. Distinct variables are used, as above, to help distinguish the many different types of generating function shown in Table 2.4.

Generating Function	Notation	Definition
Refined HS (Weight coordinates)	$g^G_{HS}(x,t)$	$\sum_{n=0}^{\infty} a_n(x)t^n$
Refined HS (Root coordinates)	$g^G_{HS}(z,t)$	$\sum_{n=0}^{\infty} a_n(z)t^n$
Unrefined HS	$g^G_{HS}(t)$	$\sum_{n=0}^{\infty} a_n t^n \equiv \sum_{n=0}^{\infty} a_n(1)t^n$
HWG (Character) for HS	$g^G_{HWG}(m,t)$	$\sum_{[n]} a_{[n]}(t)m^n$
HWG (mHL) for HS	$g^G_{HWG}(h,t)$	$\sum_{[n]} a_{[n]}(t)h^n$
Character	$g^G_{\chi}(x,m)$	$\sum_{[n]} \chi^G_{[n]}(x)m^n$
(modified) Hall Littlewood	$g^G_{(m)HL}(x,h,t)$	$\sum_{[n]} (m)HL^G_{[n]}(x,t)\,h^n$

Table 2.4.: Types of Generating Function

2.6. Subgroups and Branching

Many parts of this study draw upon the theory surrounding Dynkin diagrams and/or branching (or symmetry breaking) relationships; these include the theory of nilpotent orbits in Chapter 4, the identification of quivers whose Coulomb branches correspond to nilpotent orbits in Chapter 6, the analysis of quotient group constructions for nilpotent orbits in Chapter 7, the deconstruction of RSIMS in Chapter 8, and the identification of HyperKähler quotients between nilpotent orbits in Chapter 8.

From a group theoretic perspective, symmetry breaking occurs when some factor (such as a perturbation) causes a parent group G to split into a product group. This can be described by a branching map $G \to G_1 \otimes \ldots G_k$, which determines a map from the weight space and root space coordinates of G to those of $G_1 \otimes \ldots G_k$.

Branchings of the form:

$$[adjoint]_G \to \sum_{i=1}^{k} [adjoint]_{G_i} \oplus \sum [irreps]_{G_1 \otimes \ldots G_k}, \tag{2.29}$$

where the adjoint representation of G splits to the adjoint representations of $\{G_1, \ldots, G_k\}$, with each root of G_i being mapped to a distinct root of G, are termed *regular* [58]. Subgroup mappings that are not regular are termed *special* [58]. Special embeddings involve rank reduction, such that rank$[G_1 \otimes \ldots G_k] <$ rank$[G]$. Special $SU(2)$ subgroups arise in the classification of nilpotent orbits, as discussed in Chapter 4. Other than these, most of the branching relationships dealt with herein are regular.

The Haar measure (i.e. volume form) of G similarly decomposes to the Haar measure of the product group, plus some non-trivial field content that is a signature of the branching map. Understanding patterns of symmetry breaking requires the enumeration of the possible subgroup branchings, $G \to G_1 \otimes \ldots G_k$, and this non-trivial task was first tackled in a systematic manner by Dynkin in [61] and [54].

A group G has many possible *regular* subgroup branchings, including semi-simple branchings and those with one or more Abelian components. However, as identified in [61] and [54], these can be generated by repeated application of a small set of regular branching transformations. These basic transformations can be described and classified most effectively in terms of their action on the Dynkin diagram of G, by drawing on the correspondence between nodes, simple roots and weights. These comprise:

1. The *elementary transformation* of a simple group G into a semi-simple subgroup, $G_1 \otimes \ldots G_k$, by the elimination of a single node from the extended (or affine) Dynkin diagram of G. Each simple root of $G_1 \otimes \ldots G_k$ maps either to a distinct simple root $\{z_1, \ldots, z_r\}$ of G or to the extended (i.e. lowest) root z_0 of G. Rank is preserved, but group dimension is reduced. The subgroup is termed *maximal* if it is not possible to interpose a proper subgroup between it and G.

2. The *Abelian transformation* of a simple root k in a Dynkin diagram to a $U(1) \cong SO(2)$ root. The group splits to the Levi subgroup $U(1) \otimes \tilde{G}$, where $\tilde{G}$ is defined by the Dynkin diagram remaining after node k is

excluded. The fugacity map,

$$\{x_1, \ldots, x_k, \ldots x_r\} \;\rightarrow\; \{x_1 q^{\nu_{1,k}}, \ldots, q^{\nu_{k,k}}, \ldots x_r q^{\nu_{r,k}}\}\,, \tag{2.30}$$

replaces x_k by a $U(1)$ fugacity $q^{\nu_{k,k}}$ and shifts the other weight space coordinates such that $\{x_1, \ldots, x_{k-1}, x_{k+1}, \ldots x_r\}$ become canonical weight space coordinates for $\tilde{G}$. The $U(1)$ charges can be obtained from the Cartan matrix as $\nu_{i,k} = \left(A^{-1}\right)_{ik}$. Rank is preserved, but group dimension is reduced.

3. *Folding* of the Dynkin diagram of type A_{2r-1}, D_{r+1} or E_6 to give C_r, B_r or F_4, respectively, by identifying the nodes related by outer-automorphism, and their fugacities. This gives the non-simply laced simple group defined by the folded Dynkin diagram. Both rank and group dimension are reduced.

4. *Rank reduction*, by the elimination of a node k in the Dynkin diagram for G, to obtain $\tilde{G}$, as defined above. This is a special case of unitary transformation with $q \to 1$. Both rank and group dimension are reduced.

The elementary transformations of simple groups are determined by their affine Dynkin diagrams [58], which are shown in Figures 2.1 and 2.2.[3] The elimination of a node from the affine diagram yields a regular Dynkin diagram and this defines the subgroup obtained. The result depends on the node eliminated, with the possibilities summarised in Table 2.5.

Elementary transformations can be chained by acting on one or more parts of each subgroup. These chains terminate in A series (product) groups, which are invariant under elementary transformations.

A general regular subgroup mapping can be obtained by compounding such a chain of elementary transformations with other basic transformations (rank reducing, folding, and/or $U(1)$). Each such mapping defines a *CSA coordinate map* $\mathcal{M}$ between the weight space $\{x_1, \ldots, x_r\}$ of the parent group G and the weight space $\{x'_1, \ldots, x'_{r'}\}$ of its subgroup $G_1 \otimes \ldots G_k$. $\mathcal{M}$ is injective and provides a decomposition of the representations of G in terms of the irreps of $G_1 \otimes \ldots G_k$. However, other than for the usual

[3] Additional background information on affine Lie algebras is contained in Appendix A.3.

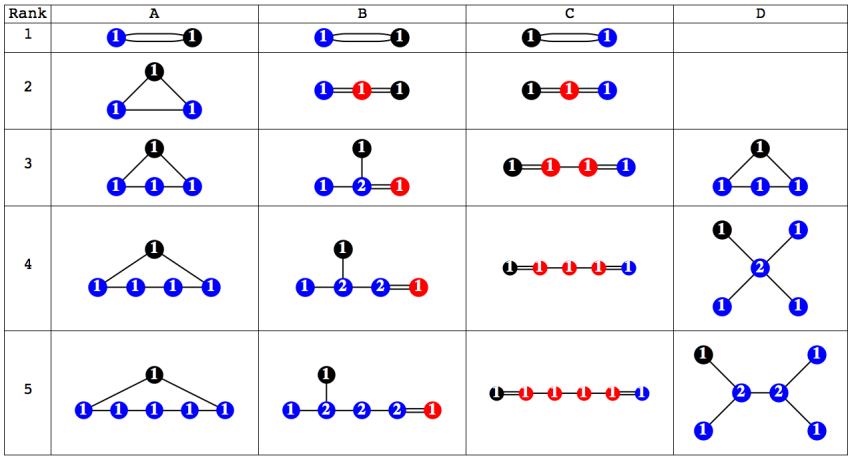

Figure 2.1.: Extended Dynkin diagrams for simple Classical groups up to rank 5. Blue nodes denote long roots with length 2. Red nodes denote short roots. A black node denotes the long root added in the affine construction. The dual Coxeter labels giving the $U(N)$ symmetry for each node are also shown.

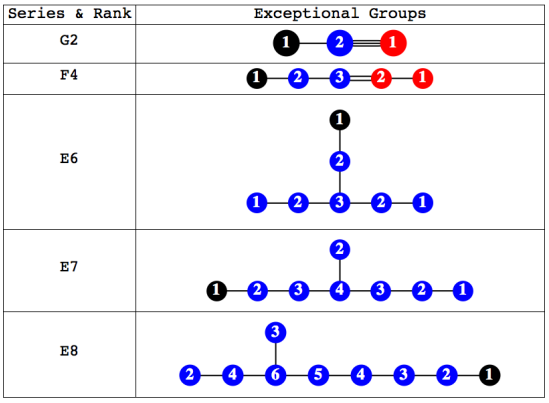

Figure 2.2.: Extended Dynkin diagrams for Exceptional groups. Blue nodes denote long roots with length 2. Red nodes denote short roots. A black node denotes the long root added in the affine construction. The dual Coxeter labels giving the $U(N)$ symmetry for each node are also shown.

Group	Proper Semi-Simple Subgroups	Type
A_r		
$B_{r\geq 2}$	$B_{r-2} \otimes D_2, \ldots, B_1 \otimes D_{r-1}, D_r$	$Maximal$
$C_{r\geq 2}$	$C_{r-1} \otimes C_1, \ldots, C_{\lceil r/2 \rceil} \otimes C_{\lfloor r/2 \rfloor}$	$Maximal$
$D_{r\geq 4}$	$D_{r-2} \otimes D_2, \ldots, D_{\lceil r/2 \rceil} \otimes D_{\lfloor r/2 \rfloor}$	$Maximal$
E_6	$A_5 \otimes A_1,\ A_2 \otimes A_2 \otimes A_2$	$Maximal$
E_7	$D_6 \otimes A_1,\ A_5 \otimes A_2,\ A_7$	$Maximal$
E_7	$A_3 \otimes A_3 \otimes A_1$	$Non-maximal$
E_8	$E_7 \otimes A_1,\ E_6 \otimes A_2,\ A_4 \otimes A_4,\ A_8,\ D_8$	$Maximal$
E_8	$A_7 \otimes A_1,\ A_5 \otimes A_2 \otimes A_1,\ D_5 \otimes A_3$	$Non-maximal$
F_4	$C_3 \otimes A_1,\ A_2 \otimes A_2,\ B_4$	$Maximal$
F_4	$A_3 \otimes A_1$	$Non-maximal$
G_2	$A_1 \otimes A_1,\ A_2$	$Maximal$

Table 2.5.: Subgroups from Single Elementary Transformations

isomorphisms, $\mathcal{M}$ is not bijective, even if no rank reduction occurs, since the subgroup has lower group dimension than G, so that not all irreps of $G_1 \otimes \ldots G_k$ can be mapped to representations of G.

Armed with a CSA coordinate map $\mathcal{M}$, we can transform any Hilbert series from G to one of its subgroups, $g^G_{HS}(t,x) \overset{\mathcal{M}}{\to} g^{G_1 \otimes \ldots G_k}_{HS}(t,x')$, and apply any of the analytical tools outlined in this section. This permits the investigation of relationships between the Hilbert series and HWGs of quiver theories with related symmetry group structures.

3. HWGs of Simple Moduli Spaces

3.1. Hilbert Series and HWGs for Invariant Tensors

One interesting set of moduli spaces to study is that of the invariant tensors of simple groups. These are illuminating, since we shall be symmetrising and/or anti-symmetrising representations of many groups in the course of this study, and the resulting combinatorics is determined by the symmetry properties and structure of invariant tensors. A group has numerous invariant tensors, such as delta or epsilon tensors, structure constants, sigma and gamma matrices, or other intertwiners, and these act to contract fields to create fields transforming in other irreps. All these invariants can be described using the language of tensor algebra, in terms of their indices and symmetry. The plethystic method complements this approach by identifying such tensors as singlets within the tensor products of the irreps in which they transform.

An invariant tensor of a group G occurs whenever the decomposition of a tensor product of representations (i.e. product of characters of representations) contains a singlet. This permits a simple plethystic method to generate the Hilbert series that enumerate the degrees of totally symmetric or totally antisymmetric invariants of a chosen representation. These series can be found by using Weyl integration to project out singlets from characters that have been symmetrised using the PE, or anti-symmetrised using the PEF. This is a straightforward generalisation to Lie groups of Molien summation over finite groups [10].

$$g_{HS:Sym}^{\chi^G}(t) = \oint_G d\mu^G \; PE\left[\chi \; t\right] \tag{3.1}$$

and

$$g^{\chi^G}_{HS:\Lambda}(t) = \oint_G d\mu^G \; PEF\left[\chi \; t\right]. \tag{3.2}$$

A HS for the degrees of symmetric invariants is freely generated, and can be treated with the Plethystic Logarithm to find its generators $t^{d_i^S}$. The exponents of the counting fugacity t in these generators correspond to the degrees d_i^S of the primitive symmetric invariants of χ^G.

$$\sum_i t^{d_i^S} = PL\left[g^{\chi^G}_{HS:Sym}(t)\right]. \tag{3.3}$$

The degrees of antisymmetric tensors are given by the exponents d_i^Λ from 3.2:

$$1 + \sum_i t^{d_i^\Lambda} = g^{\chi^G}_{HS:\Lambda}(t). \tag{3.4}$$

If $g^{\chi^G}_{HS:\Lambda}(t)$ factorises, the degrees d_i^Λ of the AS invariants can also be written in terms of the degrees $d_i^{\Lambda_P}$ of primitive AS invariants:

$$\prod_i \left(1 + t^{d_i^{\Lambda_P}}\right) = 1 + \sum_i t^{d_i^\Lambda} \tag{3.5}$$

The totally symmetric and totally antisymmetric invariant tensors of the defining (fundamental/vector) and adjoint representations of Classical and Exceptional Lie groups are summarised in Tables 3.1 and 3.2.

As can be seen from Table 3.1, each Classical and Exceptional group has a unique signature in terms of the invariant tensors of its defining representation [62]. Within these, there is a minimal set of tensors in terms of which the other invariant tensors can be expressed, termed *primitive* invariant tensors. If these primitive tensors are symmetric, they can be symmetrised into symmetric tensors of higher degree. If the primitive tensors are antisymmetric, they can be anti-symmetrised, up to the degree of the overall volume form associated with the defining representation. This degree is determined by the dimension of the defining irrep, which consequently equals the sum of the degrees of the primitive invariant AS tensors.

A similar analysis applies to the adjoint representation. In this case, the primitive symmetric tensors are equal in number to the rank of G and their degrees match those of the Casimirs of G, since each invariant tensor contracts with the Lie algebra generators of G to give a distinct symmetric

Group	Defining Representation χ	$PL\left[g^{\chi^G}_{HS:Sym}(t)\right]$	$g^{\chi^G}_{HS:\Lambda}(t)$	Degrees of primitive Sym tensors	Degrees of primitive$^{(*)}$ AS tensors
A_r	$[1,0,\ldots,0]$	0	$1+t^{r+1}$	$-$	$r+1$
B_r	$\begin{cases}[2]: r=1\\ [1,0,\ldots,0]: r>1\end{cases}$	t^2	$1+t^{2r+1}$	2	$2r+1$
C_r	$[1,0,\ldots,0]$	0	$1+t^2+t^4+\ldots t^{2r}$	$-$	$2,4,\ldots,2r^{(*)}$
D_r	$\begin{cases}[1,1]: r=2\\ [1,0,\ldots,0]: r>2\end{cases}$	t^2	$1+t^{2r}$	2	$2r$
G_2	$[0,1]$	t^2	$\left(1+t^3\right)\left(1+t^4\right)$	2	$3,4$
f_4	$[0,0,0,1]$	t^2+t^3	$\left(1+t^9\right)\left(1+t^{17}\right)$	$2,3$	$9,17$
E_6	$[0,0,0,0,1,0]$	t^3	$1+t^{27}$	3	27
E_7	$[0,0,0,0,0,1,0]$	t^4	$1+t^2+t^4\ldots+t^{56}$	4	$2,4,\ldots,56^{(*)}$
E_8	$[0,0,0,0,0,0,1,0]$	$t^2+t^8+t^{12}+t^{14}$ $+t^{18}+t^{20}+t^{24}+t^{30}$	$\left(1+t^3\right)\left(1+t^{15}\right)\left(1+t^{23}\right)$ $\times\left(1+t^{27}\right)\left(1+t^{35}\right)\left(1+t^{39}\right)$ $\times\left(1+t^{47}\right)\left(1+t^{59}\right)$	$2,8,12,14,$ $18,20,24,30$	$3,15,23,27,$ $35,39,47,59$

$^{(*)}$ Full lists of AS tensors are given for C_r and E_7.

Table 3.1.: Sym/AS Invariants of Defining Irreps of Lie Groups

Group	Adjoint Representation χ	$PL\left[g^{\chi^G}_{HS:Sym}(t)\right]$	$g^{\chi^G}_{HS:\Lambda}(t)$	Degrees of primitive Sym tensors	Degrees of primitive AS tensors
A_r	$\begin{cases}[2]: r=1\\ [1,0,\dots 1]: r>1\end{cases}$	$t^2+t^3+\dots t^{r+1}$	$\left(1+t^3\right)\left(1+t^5\right)\dots\left(1+t^{2r+1}\right)$	$2,3,\dots r+1$	$3,5,\dots 2r+1$
B_r	$\begin{cases}[2]: r=1\\ [0,2]: r=2\\ [0,1,\dots 0]: r>2\end{cases}$	$t^2+t^4+\dots t^{2r}$	$\left(1+t^3\right)\left(1+t^7\right)\dots\left(1+t^{4r-1}\right)$	$2,4,\dots 2r$	$3,7,\dots 4r-1$
C_r	$[2,\dots 0]$	$t^2+t^4+\dots t^{2r}$	$\left(1+t^3\right)\left(1+t^7\right)\dots\left(1+t^{4r-1}\right)$	$2,4,\dots 2r$	$3,7,\dots 4r-1$
D_r	$\begin{cases}[2,0]\oplus[0,2]: r=2\\ [0,1,1]: r=3\\ [0,1,\dots 0]: r>3\end{cases}$	$t^2+t^4+\dots t^{2r-2}$ $+t^r$	$(1+t^3)\dots(1+t^{4r-5})$ $\times(1+t^{2r-1})$	$2,4,\dots 2r-2,$ r	$3,7,\dots 4r-5,$ $2r-1$
G_2	$[1,0]$	t^2+t^6	$\left(1+t^3\right)\left(1+t^{11}\right)$	$2,6$	$3,11$
f_4	$[1,0,0,0]$	$t^2+t^6+t^8+t^{12}$	$(1+t^3)(1+t^{11})$ $\times(1+t^{15})(1+t^{23})$	$2,6,8,12$	$3,11,15,23$
E_6	$[0,0,0,0,0,1]$	$t^2+t^5+t^6$ $+t^8+t^9+t^{12}$	$(1+t^3)(1+t^9)(1+t^{11})$ $\times(1+t^{15})(1+t^{17})(1+t^{23})$	$2,5,6,8,$ $9,12$	$3,9,11,15,$ $17,23$
E_7	$[1,0,0,0,0,0,0]$	$t^2+t^6+t^8+t^{10}$ $+t^{12}+t^{14}+t^{18}$	$(1+t^3)(1+t^{11})(1+t^{15})$ $\times(1+t^{19})(1+t^{23})$ $\times(1+t^{27})(1+t^{35})$	$2,6,8,10,$ $12,14,18$	$3,11,15,19,$ $23,27,35$
E_8	$[0,0,0,0,0,0,1,0]$	$t^2+t^8+t^{12}+t^{14}$ $+t^{18}+t^{20}+t^{24}+t^{30}$	$\left(1+t^3\right)\left(1+t^{15}\right)\left(1+t^{23}\right)$ $\times\left(1+t^{27}\right)\left(1+t^{35}\right)\left(1+t^{39}\right)$ $\times\left(1+t^{47}\right)\left(1+t^{59}\right)$	$2,8,12,14,$ $18,20,24,30$	$3,15,23,27,$ $35,39,47,59$

Table 3.2.: Sym/AS Invariants of Adjoint Irreps of Lie Groups

Casimir operator.[1] Each symmetric invariant of degree d^S is related to an antisymmetric invariant of degree $d^\Lambda = 2d^S - 1$. These AS invariants are forms over the co-cycles of a group manifold [63] and so their Hilbert series $g^{[adjoint]_G}_{HS:\Lambda}(t)$ encodes information about the cohomology of the group manifold, and is known as the Poincare polynomial of G. The sum of the degrees of the AS invariants (i.e. sum of the exponents of the Poincare polynomial) equals the dimension of the group.

We can similarly treat the the spinors of SO groups as basic irreps and calculate the degrees of their symmetric and antisymmetric invariant tensors. These are shown in Table 3.3 for orthogonal groups up to rank 5. The notation used for $SO(2r)$ can be adapted to give the invariants, either for Dirac spinors, by setting $t_1 = t_2 = t$, or for Weyl spinors, by setting t_1 or t_2 to zero. The invariant tensors are all of even degree and the degree of the AS tensors is (naturally) limited by the length of the volume form on the spinor manifold. Unfortunately, the degrees of spinor invariants do not fall into simple patterns and are difficult to generalise to higher rank groups.

Symmetric and antisymmetric invariant tensors can be combined into tensors of mixed symmetry and the number of such possible combinations compounds with increasing rank and dimension; the defining representations of exceptional groups, in particular, posses a very complicated set of invariants once invariant tensors of mixed symmetry are included [64].

It is interesting, therefore, to consider how all the invariant tensors of some representation(s) might be enumerated in a systematic manner. This question is closely related to the problem of identification of GIOs in SQCD, which is the subject of the next section.

Given some defining representation, the identification of its invariant tensors of mixed symmetry requires some way of characterising symmetry, in addition to tracking the number of indices. One solution is to map the symmetry properties of each tensor to a Young's diagram. This in turn corresponds to a representation of a unitary group of sufficiently high rank, which can be tracked by its Dynkin labels. This series of Young's diagrams can in principle be encoded as an HWG, which combines a counting fugacity t, to count the number of boxes in each Young's diagram, with highest

[1] The Casimir operators of a group form a commuting set of operators whose eigenvalues identify the irreps in which fields transform. Each set of Casimir eigenvalues is in bijective correspondence with the highest weight Dynkin labels of an irrep.[62]

Group	Spinor χ	$PL\left[g^{\chi^G}_{HS:Sym}(t)\right]$	$g^{\chi^G}_{HS:\Lambda}(t)$	Degrees of primitive Sym tensors	Degrees of AS tensors
$SO(3)$	$[1]$	0	$1+t^2$		2
$SO(4)$	$[1,0]\oplus[0,1]$	0	$\left(1+{t_1}^2\right)\left(1+{t_2}^2\right)$		$2,2,4$
$SO(5)$	$[0,1]$	0	$1+t^2+t^4$		$2,4$
$SO(6)$	$[0,1,0]\oplus[0,0,1]$	t_1t_2	$1+t_1t_2+{t_1}^4+{t_1}^2{t_2}^2$ $+{t_2}^4+{t_1}^3{t_2}^3+{t_1}^4{t_2}^4$	2	$2,\ldots,8$
$SO(7)$	$[0,0,1]$	t^2	$1+t^4+t^8$	2	$4,8$
$SO(8)$	$[0,0,1,0]\oplus[0,0,0,1]$	${t_1}^2+{t_2}^2$	$1+{t_1}^2{t_2}^2+{t_1}^8+{t_1}^6{t_2}^2+{t_1}^4{t_2}^4$ $+{t_1}^2{t_2}^6+{t_2}^8+{t_1}^6{t_2}^6+{t_1}^8{t_2}^8$	$2,2$	$4,\ldots,16$
$SO(9)$	$[0,0,0,1]$	t^2	$1+t^8+t^{16}$	2	$8,16$
$SO(10)$	$[0,0,0,1,0]\oplus[0,0,0,0,1]$	$t_1t_2+{t_1}^2{t_2}^2$	$1+t_1t_2+{t_1}^2{t_2}^2+{t_1}^3{t_2}^3+2{t_1}^4{t_2}^4+$ $2{t_1}^5{t_2}^5+2{t_1}^6{t_2}^6+2{t_1}^7{t_2}^7+{t_1}^{16}+$ ${t_1}^{14}{t_2}^2+{t_1}^{12}{t_2}^4+{t_1}^{10}{t_2}^6+3{t_1}^8{t_2}^8+$ ${t_1}^6{t_2}^{10}+{t_1}^4{t_2}^{12}+{t_1}^2{t_2}^{14}+{t_2}^{16}+$ $2{t_1}^9{t_2}^9+2{t_1}^{10}{t_2}^{10}+2{t_1}^{11}{t_2}^{11}+$ $2{t_1}^{12}{t_2}^{12}+{t_1}^{13}{t_2}^{13}+{t_1}^{14}{t_2}^{14}+$ ${t_1}^{15}{t_2}^{15}+{t_1}^{16}{t_2}^{16}$	$2,4$	$2,\ldots,32$
$SO(11)$	$[0,0,0,0,1]$	t^4	$1+t^2+t^4+t^6+t^8$ $+t^{10}+t^{12}+t^{14}+2t^{16}$ $+t^{18}+t^{20}+t^{22}+t^{24}$ $+t^{26}+t^{28}+t^{30}+t^{32}$	4	$2,\ldots,32$

Counting fugacities t_1 and t_2 are used to distinguish left and right spinors of $SO(2r)$. Full lists of AS tensors are shown.

Table 3.3.: Sym/AS Invariants of Spinor Irreps of SO Groups

weight fugacities $m_1, \ldots, m_r$ to describe its symmetry.

One method for finding such HWGs makes use of the pattern of symmetrisations that arises when a product group representation is symmetrised or anti-symmetrised. We apply the plethystic expansions A.17 and A.18 to the character of a product group representation $\chi^G(x,y) = \chi^A(x) \otimes \chi^B(y)$, where $\chi^A(x) \equiv x_1 + \ldots + x_{|\chi^A|)}$ and $\chi^B(y) \equiv y_1 + \ldots + y_{|\chi^B|}$. We take χ^A and χ^B to be the fundamental representations of unitary groups A and B and apply standard results from [60] to obtain the following:

$$\begin{aligned}\sum_{k=0}^{\infty} Sym^k\left[\chi^A \otimes \chi^B\right] &= PE\left[\chi^A \otimes \chi^B\right] \\ &= \prod_{i=1}^{|\chi^A|}\prod_{j=1}^{|\chi^B|}\frac{1}{(1-x_i y_j)} \\ &= \sum_{[n]} \chi^A_{[n]} \otimes \chi^B_{[n]}\end{aligned} \tag{3.6}$$

$$\begin{aligned}\sum_{k=0}^{|\chi^A \otimes \chi^B|} \Lambda^k\left[\chi^A \otimes \chi^B\right] &= PEF\left[\chi^A \otimes \chi^B\right] \\ &= \prod_{i=1}^{|\chi^A|}\prod_{j=1}^{|\chi^B|}(1+x_i y_j) \\ &= \sum_{[n]} \chi^A_{[n]} \otimes \chi^B_{[n]^T}\end{aligned} \tag{3.7}$$

The sums over $[n]$ are taken over all non-vanishing irreps $\chi^A_{[n]} \otimes \chi^B_{[n]}$ or $\chi^A_{[n]} \otimes \chi^B_{[n]^T}$, respectively. The Dykin labels $[n]^T$ are related to $[n]$ by transposition of their corresponding partitions or Youngs diagrams [60]. This involution exchanges symmetric and antisymmetric irreps and so the PE of a product group representation pairs up irreps with the same symmetry properties, while the PEF pairs up irreps with opposite symmetry properties.

Suppose now that we wish to enumerate all the invariant tensors of a representation χ^C, which need not be unitary. We set $B = U(N)$, where $N = \left|\chi^C\right|$ so that χ^B has dimension equal to that of the volume form on χ^C and B has sufficient Dynkin labels to track the anti-symmetry of any invariant tensor on χ^C. We also replace the unitary character χ^A within the PE in 3.6 by χ^C. Under this latter substitution, each unitary irrep $\chi^A_{[n]}$

decomposes to representations of C, which may include one or more singlets corresponding to the invariant tensors of χ^C. We select these singlets by a first Weyl integration over C:

$$\begin{aligned} g^{\chi^C}_{HS:inv.}(y) &= \oint_C d\mu^C PE\left[\chi^C \otimes \chi^{U(N)}\right] \\ &= \sum_{[n]\in inv.} a_{[n]} \chi^{U(N)}_{[n]}(y), \end{aligned} \tag{3.8}$$

where the coefficients $a_{[n]}$ track the multiplicities of the invariant tensors. It is clear that if $U(N)$ is taken as $U(1)$ with fugacity t then 3.8 reverts to 3.1 for totally symmetric invariant tensors.

As a second step, we use a generating function for the characters $\chi^{U(N)}_{[n]}$ with the Dynkin label fugacities $m \equiv m_1 \dots m_{\mathrm{N}}$ to transform the class function 3.8 into an HWG :

$$\begin{aligned} g^{\chi^C}_{HWG:inv.}(m) &= \oint_{U(N)} d\mu^{U(N)} g^{U(N)}_{\chi}(y^*, m)\, g^{\chi^C}_{HS:inv.}(y) \\ &= \sum_{[n]\in inv.} a_{[n]} m^{[n]} \end{aligned} \tag{3.9}$$

Alternatively, by noting the matching symmetry between irreps of $U(N)$ and representations of C, equations 3.8 and 3.9 can be combined:

$$g^{\chi^C}_{HWG:inv.}(m) = \oint_C d\mu^C(x')\, g^{U(N)}_{\chi}(y, m)\Big|_{y\to\chi^C(x')}, \tag{3.10}$$

where $x' \equiv x'_1, \dots, x'_{\mathrm{rank}[C]}$ are CSA coordinates for C, and the elements of the character χ^C are substituted for the y_i in the character generating function for $U(N)$.

The HWG series 3.9 or 3.10 can be presented in terms of Young tableaux for $U(N)$, with the partitions determined by the Dynkin label fugacities m, so that m^c_r represents a rectangular Young's sub-diagram with c columns and r rows, and $m^{c_1}_{r_1} \dots m^{c_N}_{r_N}$ represents the Youngs diagram formed by N sub-diagrams placed side by side.

By way of example, Table 3.4 summarises the HWGs obtained by applying 3.10 to the defining representations of low rank Classical gauge groups. Each term in the PL represents a primitive invariant tensor, or generator of invari-

Gauge Group G	Defining Irrep	Flavour Group	$PL\left[g_{HWG:inv.}^{G\otimes U(N)}\right]$
$SU(2)$	$[1]$	$U(2)$	m_2
$SU(3)$	$[1,0]$	$U(3)$	m_3
$SU(N)$	$[1,0,\ldots]$	$U(N)$	m_N
$USp(4)$	$[1,0]$	$U(4)$	m_2+m_4
$USp(2r)$	$[1,0,\ldots]$	$U(2r)$	$m_2+m_4+\ldots m_{2r}$
$SO(3)$	$[2]$	$U(3)$	${m_1}^2+{m_2}^2+m_3$
$SO(4)$	$[1,1]$	$U(4)$	${m_1}^2+{m_2}^2+{m_3}^2+m_4$
$SO(5)$	$[1,0]$	$U(5)$	${m_1}^2+{m_2}^2+{m_3}^2+{m_4}^2+m_5$
$SO(N)$	$[1,0,\ldots]$	$U(N)$	${m_1}^2+{m_2}^2+\ldots m_{N-1}^2+m_N$

Table 3.4.: Primitive Invariants of Defining Irreps of Classical Groups

ant tensors. It is clear that the defining representations of A and C series groups, which lack a symmetric tensor, only contain the wholly antisymmetric tensors previously enumerated in Table 3.1. The defining representations of $SO(N)$, however, all contain multiple primitive invariant tensors starting from the delta tensor, given by the series ${m_1}^2, {m_2}^2, \ldots, m_{N-1}^2$, plus the volume form epsilon tensor m_N, numbering N primitive invariant tensors in total. The HWGs are freely generated, so that further invariant tensors can be identified by forming monomials from products of the generators.

A related procedure can be followed, by working with the PEF in 3.7, in place of the PE in 3.6. In this case the invariant tensors of χ^C are associated to Young's diagrams of B that have been transposed.

$$\begin{aligned} g_{HS:\subset inv.}^{\chi^C}(y) &= \oint_C d\mu^C PEF\left[\chi^C \otimes \chi^{U(N)}\right] \\ &= \sum_{[n]\subset inv.} a_{[n]} \chi_{[n]^T}^{U(N)}(y), \end{aligned} \tag{3.11}$$

The series of invariants given by 3.11 are finite and incomplete, since the rank of the unitary flavour group $U(N)$ limits the degree N to which the symmetrisations of χ^C can be tracked. If $U(N)$ is taken as $U(1)$ with fugacity t then this method reverts to 3.2 for totally antisymmetric invariant tensors.

Some equivalent results can also be obtained by decomposition of tensor products [64], however, the HWG method 3.10 has the potential advan-

tage of generating the complete infinite series of invariants from a finite number of generators, thereby resolving uncertainties about the multiplicities of distinct invariants and/or their appearance at higher orders. For high dimensioned representations, where calculation with high rank unitary groups is impractical, 3.11 can be used to identify invariants, up to some finite degree of symmetrisation.

Thus, HWGs can be used to explicate how the invariant tensors of the group representations within a product group structure determine its Hilbert series. These HWG monomials identify both the orders at which such invariants are formed and the representations in which they transform. The above series for product groups incorporating $U(N)$ flavour groups are closely related to the series for the GIOs of SQCD, which are the subject of detailed examples in the next section.

There are also many invariant tensors that can be formed from combinations of representations. These can be analysed by similar plethystic methods, using refined fugacities t_i to label the different representations being symmetrised/antisymmetrised. This leads to many different moduli spaces that are outside the focus of this study.

3.2. SQCD

The moduli spaces of SQCD describe the vacuum field content of the Higgs branches of $\mathcal{N} = 1$ supersymmetric extensions of QCD and have been extensively studied. Treatments under the Plethystics Program include [13, 14, 15]. The aim here is not to give a full review of SQCD theories, but to illustrate how HWGs can provide complete and concise descriptions of their moduli spaces. While complete descriptions can be given for SQCD theories with Classical gauge groups [13, 14, 28], the moduli spaces have only been found for low flavour numbers [28] for SQCD theories with Exceptional gauge groups.

The Lagrangians for $\mathcal{N} = 1$ gauge theories are well-known, taking the form [65]:

$$\mathcal{L} = \Phi_i^\dagger e^V \Phi_i \Big|_{\theta\theta\bar{\theta}\bar{\theta}} + \left(\frac{1}{16g^2} Tr\ \mathcal{W}^\alpha \mathcal{W}_\alpha |_{\theta\theta} + W\left(\Phi_i\right)|_{\theta\theta} \right) + h.c., \qquad (3.12)$$

where h.c. denotes hermitian conjugation of the $\theta\theta$ terms. The Φ_i are

chiral superfields, transforming under some global symmetry (acting on the indices i) and also under some representation of a gauge group G (gauge indices suppressed). Their multiplets include chiral scalars ϕ_i. $W(\Phi_i)$ is the chiral superpotential. V is a vector superfield transforming with field strength $\mathcal{W}_\alpha = -\frac{1}{4}\bar{D}\bar{D}e^{-V}D_\alpha e^V$.

Expanding the Lagrangian, and requiring that its variation with respect to component fields should be zero, identifies the effective scalar potential [14]:

$$\mathcal{V}\left(\phi_i, \phi_i^\dagger\right) = \sum_i \left|\frac{\partial W}{\partial \phi_i}\right|^2 + \frac{1}{2}g^2 \sum_a \left(\sum_i \phi_i{}^\dagger T^a \phi_i\right)^2, \tag{3.13}$$

where T^a are the Lie algebra generators for G. At the SUSY vacuum, the effective scalar potential is minimised, $\mathcal{V} = 0$, giving rise to

F-term conditions, $\forall i : \frac{\partial W}{\partial \phi_i} = 0$, and

D-term conditions, $\forall a : \sum_i \phi_i{}^\dagger T^a \phi_i = 0$ or $Tr[T \cdot \sum_i \phi_i \phi_i{}^\dagger] = 0$.

In SQCD theories there is no superpotential, $W(\Phi) = 0$, so the F-terms vanish automatically. The D-term conditions require that only gauge invariant combinations of scalar fields appear at the vacuum. The vacuum field content of these theories is given by the chiral ring of gauge invariant BPS operators ("GIOs") that can be formed from the chiral scalars ϕ_i.

Quiver diagrams provide an elegant way of describing theories involving chiral scalar fields and the structure of their global symmetry (or flavour) and gauge (or colour) groups. For Classical group SQCD theories, the relevant quivers are shown in Figure 3.1.

In addition to flavour and gauge group charges, the scalar fields can also carry a variety of U(1) charges. The most important of these is the R-charge, which counts the number of chiral scalars combined within some operator.

The moduli spaces of the GIOs of all these theories can be described by the refined Hilbert series:

$$g_{HS:GIO}^{G_f \otimes G_c}(x,t) = \oint_{G_c} d\mu^{G_c}(y)\ PE\left[\chi_{bifund.}^{G_f \otimes G_c}(x,y)\, t\right]. \tag{3.14}$$

The PE generates the chiral ring of scalar field combinations by symmetrising the character $\chi_{bifund.}^{G_f \otimes G_c}(x,y)$ of the bifundamental fields. x and y are

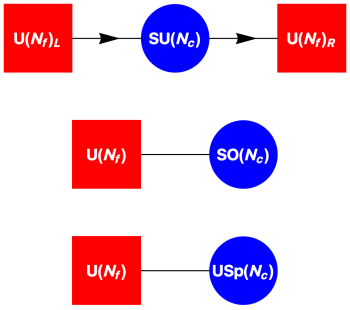

Figure 3.1.: Quiver diagrams for Classical Group SQCD. Blue nodes denote gauge groups. Red nodes denote flavour groups. The links between nodes correspond to *bifundamental* fields transforming under both the flavour and gauge groups. Fundamental and antifundamental fields are distinguished by directed links. Other U(1) charges are omitted.

weight space fugacities for the flavour and colour groups, respectively, and t is a counting fugacity for the R-charge. The D-term conditions are imposed by the Weyl integration, as described in Appendix A.2, which selects the colour/gauge group singlets that identify the GIOs.

The refined Hilbert series can most usefully be analysed in terms of its flavour group representation content by transformation into a highest weight generating function:

$$g_{HWG:GIO}^{G_f\otimes G_c}(m,t) = \oint_{G_f} d\mu^{G_f}(x)\; g_\chi^{G_f}(x^*,m)\; g_{HS:GIO}^{G_f\otimes G_c}(x,t)\,, \tag{3.15}$$

Alternatively, the refined HS 3.14 can be simplified into the unrefined Hilbert series $g_{HS:GIOs}^{G_f\otimes G_c}(1,t)$, which provides dimensional information about the moduli space. The following sections describe and comment on the moduli spaces of GIOs for some SQCD theories with low rank Classical and Exceptional groups. Much of the treatment is common between the different gauge groups.

3.2.1. GIOs of $U(N_f)_{L/R} \otimes SU(N_c)$

It is helpful to start with an explicit statement of the symmetry transformation properties of the bifundamental fields [13]. These are summarised

in Table 3.5, where the chiral scalars are referred to by their superpartner quarks or antiquarks. For convenience, the $U(N_f)$ flavour groups are initially decomposed as $SU(N_f) \otimes U(1)$.

	Gauge/Colour	Flavour				Baryon	R
Groups	$SU(N_c)$	$SU(N_f)_L$	$SU(N_f)_R$	$U(1)_L$	$U(1)_R$	$U(1)_B$	$U(1)$
Q_a^i	$[0,\ldots,1]$	$[1,0,\ldots]$	1	1	0	1	
$\bar{Q}_i^a$	$[1,0,\ldots]$	1	$[1,0,\ldots]$	0	1	- 1	
CSA Fug.	y	x_L	x_R	q	$\bar{q}$		t
HW Fug.		l	r	t_1	t_2		

Table 3.5.: SQCD Charge Assignments: $U(N_f)_{L/R} \otimes SU(N_c)$

The possible field combinations contain chiral quarks Q_a^i and/or antiquarks $\bar{Q}_i^a$, transforming in some representation of the product group, where the indices i range over the fundamentals of the $U(N_f)_{L/R}$ flavour groups and the indices a range over the fundamental or anti-fundamental of the $SU(N_c)$ colour group. The GIOs are $SU(N_c)$ colour singlets composed of quarks and/or antiquarks, with their flavour group indices determining the representation in which they transform. The fields also carry R-symmetry and baryonic $U(1)$ charges.

To obtain HWGs for these theories, we first form the product group characters of the fields:

$$\begin{aligned} &\chi_{bifund.}^{U(N_f)_{L/R} \otimes SU(N_c)}(x_L, x_R, y, q, \bar{q}) = \\ &\quad \chi_{[1,0,\ldots,0]}^{SU(N_f)_L}(x_L)\ \chi_{[0,,\ldots,0,1]}^{SU(N_c)}(y)\ q + \chi_{[1,0,\ldots,0]}^{SU(N_f)_R}(x_R)\ \chi_{[1,0,\ldots,0]}^{SU(N_c)}(y)\ \bar{q}. \end{aligned} \tag{3.16}$$

While the colour group CSA coordinates y are shared by the quarks and antiquarks, it is necessary to use different CSA coordinates x_L and x_R to distinguish the L and R flavour groups.

Application of 3.14 yields the refined Hilbert series:

$$\begin{aligned} &g_{HS:GIO}^{U(N_f)_{L/R} \otimes SU(N_c)}(x_L, x_R, t_1, t_2) = \\ &\oint_{SU(N_c)} d\mu^{SU(N_c)}(y)\ PE\left[\chi_{[1,0,\ldots,0]}^{SU(N_f)_L} \chi_{[0,,\ldots,0,1]}^{SU(N_c)}(x_L, y)\, t_1\right] PE\left[\chi_{[1,0,\ldots,0]}^{SU(N_f)_R} \chi_{[1,0,\ldots,0]}^{SU(N_c)}(x_R, y)\, t_2\right], \end{aligned} \tag{3.17}$$

where the $U(1)_{L/R}$ fugacities q and $\bar{q}$ for the quarks and anti-quarks have been combined with the R-charge fugacity as $t_1 \equiv tq$ and $t_2 \equiv t\bar{q}$, for simplification.

The HWGs follow from 3.17 by a second Weyl integration, as in 3.15:

$$
\begin{aligned}
&g_{HWG:GIO}^{U(N_f)_{L/R}\otimes SU(N_c)}(l,r,t_1,t_2) = \\
&\qquad \oint_{SU(N_f)_L \otimes SU(N_f)_R} d\mu^{SU(N_f)_L}(x_L)\; d\mu^{SU(N_f)_R}(x_R) \\
&\qquad\qquad \times\; g_\chi^{SU(N_f)}(x_L^*, l)\; g_\chi^{SU(N_f)}(x_R^*, r) \\
&\qquad\qquad \times\; g_{HS:GIO}^{\left(U(N_f)_{L/R}\otimes SU(N_c)\right)}(x_L, x_R, t_1, t_2)\,.
\end{aligned}
\tag{3.18}
$$

The highest weight fugacities $l \equiv l_1 \dots l_{N_f-1}$ and $r \equiv r_1 \dots r_{N_f-1}$ track the $SU(N_f)_{L/R}$ irreps of the (decomposed) L and R flavour groups. The HWGs from 3.18 are summarised in Table 3.6 for some low rank groups.

Theory	HWG
$U(1)_{L/R} \otimes SU(2_c)$	$1/(1-t_1t_2)$
$U(2_f)_{L/R} \otimes SU(2_c)$	$1/(1-{t_1}^2)(1-{t_2}^2)(1-l_1r_1t_1t_2)$
$U(\geq 3)_{L/R} \otimes SU(2_c)$	$1/(1-l_2{t_1}^2)(1-r_2{t_2}^2)(1-l_1r_1t_1t_2)$
$U(1)_{L/R} \otimes SU(3_c)$	$1/(1-t_1t_2)$
$U(2_f)_{L/R} \otimes SU(3_c)$	$1/(1-l_1r_1t_1t_2)(1-{t_1}^2{t_2}^2)$
$U(3_f)_{L/R} \otimes SU(3_c)$	$1/(1-{t_1}^3)(1-{t_2}^3)(1-l_1r_1t_1t_2)(1-l_2r_2{t_1}^2{t_2}^2)$
$U(\geq 4)_{L/R} \otimes SU(3_c)$	$1/(1-l_3{t_1}^3)(1-r_3{t_2}^3)(1-l_1r_1t_1t_2)(1-l_2r_2{t_1}^2{t_2}^2)$

$SU(N_f)_{L/R} \otimes U(1)_{L/R}$ highest weight fugacity notation is used.

Table 3.6.: HWGs of $U(N_f)_{L/R} \otimes SU(N_c)$ GIOs

These HWGs are all freely generated and so can be stated more succinctly in terms of their PLs, as in Table 3.7. The generators in $PL[HWG]$ encode the structure of the GIOs of the theory and the flavour group representations in which they transform.

These flavour group representations can be described either in terms of $U(N_f)$ or $SU(N_f) \otimes U(1)$. Recalling that the fugacity t counts boxes in a Young's diagram, we can translate between $SU(N) \otimes U(1)$ highest weight fugacities $\{l_i, t\}$ and $U(N)$ highest weight fugacities m_i by the map:

$$
(l_i t^i, t^N) \leftrightarrow (m_i, m_N). \tag{3.19}
$$

Theory	PL[HWG] $SU(N_f) \otimes U(1)$ fugacities	PL[HWG] $U(N_f)$ fugacities
$U(1)_{L/R} \otimes SU(2_c)$	$t_1 t_2$	$m_L m_R$
$U(2_f)_{L/R} \otimes SU(2_c)$	${t_1}^2 + {t_2}^2 + lrt_1 t_2$	$m_{L_1} m_{R_1} + m_{L_2} + m_{R_2}$
$U(\geq 3)_{L/R} \otimes SU(2_c)$	$l_2 {t_1}^2 + r_2 {t_2}^2 + l_1 r_1 t_1 t_2$	$m_{L_1} m_{R_1} + m_{L_2} + m_{R_2}$
$U(1)_{L/R} \otimes SU(3_c)$	$t_1 t_2$	$m_L m_R$
$U(2_f)_{L/R} \otimes SU(3_c)$	$lrt_1 t_2 + {t_1}^2 {t_2}^2$	$m_{L_1} m_{R_1} + m_{L_2} m_{R_2}$
$U(3_f)_{L/R} \otimes SU(3_c)$	${t_1}^3 + {t_2}^3 + l_1 r_1 t_1 t_2 + l_2 r_2 {t_1}^2 {t_2}^2$	$m_{L_1} m_{R_1} + m_{L_2} m_{R_2} + m_{L_3} + m_{R_3}$
$U(\geq 4)_{L/R} \otimes SU(3_c)$	$l_3 {t_1}^3 + r_3 {t_2}^3 + l_1 r_1 t_1 t_2 + l_2 r_2 {t_1}^2 {t_2}^2$	$m_{L_1} m_{R_1} + m_{L_2} m_{R_2} + m_{L_3} + m_{R_3}$

Table 3.7.: PLs of HWGs of $U(N_f)_{L/R} \otimes SU(N_c)$ GIOs

Taking $U(3_f)_{L/R} \otimes SU(3_c)$ as example, we can map the generators either to $U(3_f)_{L/R}$ irreps, or to $SU(3_f)_{L/R} \otimes U(1)_{L/R}$ irreps; these are described by Dynkin labels in Table 3.8.

$SU(3_f)_{L/R} \otimes U(1)_{L/R}$	Irreps	$U(3_f)_{L/R}$	Irreps
$l_1 r_1 t_1 t_2$	$[1,0]_L [1,0]_R \; q\bar{q}$	$m_{L1} m_{R1}$	$[1,0,0]_L [1,0,0]_R$
$l_2 r_2 {t_1}^2 {t_2}^2$	$[0,1]_L [0,1]_R \; q^2 \bar{q}^2$	$m_{L2} m_{R2}$	$[0,1,0]_L [0,1,0]_R$
${t_1}^3$	$[0,0]_L [0,0]_R \; q^3$	m_{L3}	$[0,0,1]_L [0,0,0]_R$
${t_2}^3$	$[0,0]_L [0,0]_R \; \bar{q}^3$	m_{R3}	$[0,0,0]_L [0,0,1]_R$

Table 3.8.: Generators of HWGs of $U(3_f)_{L/R} \otimes SU(3_c)$ GIOs

Choosing the $SU(3_f) \otimes U(1)$ notation, the monomials can be viewed, respectively, as a quark antiquark pair (meson) transforming in the $SU(N_f)_{L/R}$ fundamentals, a combination of two quarks and two antiquarks (tetraquark) transforming in the $SU(3_f)_{L/R}$ anti-fundamentals, and three quarks (baryon) or three antiquarks (antibaryon) transforming as $SU(3_f)_{L/R}$ flavour singlets. In $U(3_f)_{L/R}$ notation, the (anti)-symmetry properties of the representations are identified by their Dynkin labels; the (anti)baryons contain antisymmetric combinations of the quarks.

There are several points of interest about the structure of the generators. Most importantly, the HWGs converge for all flavour groups of fundamental dimension exceeding that of the colour group. We can interpret this in terms of complete breaking of the gauge group symmetries as N_f reaches N_c. Put another way, the anti-symmetrisation of the flavour group representation is limited by the degree of the volume form of the colour group irrep, as discussed in section 3.1. Secondly, the symmetry of the quiver leads to

pairing of the L/R flavour group representations.

These observations permit us to extrapolate Table 3.7 and to generalise the PLs of HWGs for GIOs of $U(N_f)_{L/R} \otimes SU(N_c)$ with arbitrary flavours and colours in terms of the $U(N_f)_{L/R}$ fugacities $\{m_L, m_R\}$ as:

$$PL[HWG] = \sum_{i=1}^{\min(N_f,N_c)-1} m_{L_i} m_{R_i} + \begin{cases} if\ N_f < N_c: & m_{L_{N_f}} m_{R_{N_f}} \\ if\ N_f \geq N_c: & m_{L_{N_c}} + m_{R_{N_c}} \end{cases} \tag{3.20}$$

If we restrict 3.20 to the left or right flavour group, the GIOs correspond to colour group antisymmetric invariants only; thus, setting $m_R \to 0$ recovers, for $N_f \geq N_c$, the invariants m_{N_c} of $SU(N)$ shown in 3.4.

If we are primarily interested in counting dimensions of flavour irreps, the HWGs can be transformed to unrefined HS by replacing the monomial terms in $\{l_i, r_j\}$ by the dimensions of the irreps to which they refer. This is equivalent to setting the CSA fugacities within the characters of the flavour group in the refined HS 3.17 to unity, and retaining only the overall R-charge fugacity t for counting. We then obtain the unrefined HS $g_{HS:GIO}^{U(N_f)_{L/R} \otimes SU(N_c)}(1,1,t,t)$. Some unrefined Hilbert series are shown in Table 3.9.

Theory	Unrefined Hilbert Series	|HS|
$U(1)_{L/R} \otimes SU(2_c)$	$\frac{1}{(1-t^2)}$	1
$U(2_f)_{L/R} \otimes SU(2_c)$	$\frac{1+t^2}{(1-t^2)^5}$	5
$U(3_f)_{L/R} \otimes SU(2_c)$	$\frac{(1+t^2)(1+5t^2+t^4)}{(1-t^2)^9}$	9
$U(4_f)_{L/R} \otimes SU(2_c)$	$\frac{(1+t^2)(1+14t^2+36t^4+14t^6+t^8)}{(1-t^2)^{13}}$	13
$U(5_f)_{L/R} \otimes SU(2_c)$	$\frac{(1+t^2)(1+27t^2+169t^4+321t^6+169t^8+27t^{10}+t^{12})}{(1-t^2)^{17}}$	17
$U(1)_{L/R} \otimes SU(3_c)$	$\frac{1}{(1-t^2)}$	1
$U(2_f)_{L/R} \otimes SU(3_c)$	$\frac{1}{(1-t^2)^4}$	4
$U(3_f)_{L/R} \otimes SU(3_c)$	$\frac{1-t+t^2}{(1-t)(1-t^2)^8(1-t^3)}$	10
$U(4_f)_{L/R} \otimes SU(3_c)$	$\frac{\left(1+t^2\right)\left(1+3t^2+4t^3+7t^4+4t^5+7t^6+4t^7+3t^8+t^{10}\right)}{(1-t^2)^{12}(1-t^3)^4}$	16
$U(5_f)_{L/R} \otimes SU(3_c)$	$\frac{(1-t)\left(\begin{array}{c}1+t+10t^2+23t^3+68t^4+135t^5+281t^6 \\ +446t^7+695t^8+895t^9+1090t^{10} \\ +1115t^{11}+\ldots\text{palindrome}\ldots+t^{22}\end{array}\right)}{(1-t^2)^{16}(1-t^3)^7}$	22

Table 3.9.: Unrefined HS of $U(N_f)_{L/R} \otimes SU(N_c)$ GIOs

Unlike the HWGs, the unrefined HS are not freely generated for $N_f \geq N_c$, and indeed, for $N_f > N_c$, they are not complete intersections, indicating complicated relations between generators. The unrefined HS have palindromic numerators, but these do not readily generalise to higher rank groups.

The dimensions of these unrefined HS are given, as can be verified by inspection of Table 3.9, for $N_f < N_c$, by N_f^2, and, for $N_f \geq N_c$, by $2N_fN_c - (N_c^2 - 1)$, which is the number of bifundamental fields less the number of gauge group generators [13].

A further interesting observation made in [13] is that with an $SU(2_c)$ colour group, the left and right flavour groups can be combined into a $U(2N_f)$ global symmetry. This particular feature arises for $SU(2_c)$ because the quarks and antiquarks share the same $SU(2)$ character. Thus, we can set up a fugacity map in which the CSA flavour coordinate plus fugacity degrees of freedom match between $U(N_f)_{L/R} \otimes SU(2_c)$ and $U(2N_f) \otimes SU(2_c)$.

Such alternative ways of analysing the same theory give rise to correspondences between Hilbert series and, indeed, can be identified from unrefined Hilbert series. Thus, for example, the unrefined Hilbert series for $U(2)_{L/R} \otimes SU(2_c)$ in Table 3.9 is the same as the unrefined Hilbert series for $U(4) \otimes SU(2_c)$ (not shown).

3.2.2. GIOs of $U(N_f) \otimes SO(N_c)$

In the case of $U(N_f) \otimes SO(N_c)$, the SQCD theory contains one bifundamental scalar transforming in the fundamental representation of the flavour group and the vector representation of the colour group. Charge assignments, based on [14], are as in Table 3.10. For convenience, the $U(N_f)$ flavour groups are initially decomposed as $SU(N_f) \otimes U(1)$.

The theory contains combinations of quarks Q_a^i, where the indices i and a range over the flavour group fundamental and the colour group vector representation, respectively. The GIOs are colour singlets composed of quarks and transform in some flavour group irrep. The fields also carry $U(1)$ charges, which can be absorbed, for our purposes, into a single counting fugacity $t = qt'$.

Proceeding as before, the refined HS generating functions are given by:

	Gauge/Colour	Flavour		R
Groups	$SO(N_c)$	$SU(N_f)$	$U(1)_B$	$U(1)_R$
Q_a^i	[2] for $N_c = 3$ $[1,1]$ for $N_c = 4$ $[1,0,\ldots,0]$ for $N_c > 4$	$[1,0,\ldots,0]$	1	
CSA Fugacity	y	x	q	t'
HW Fugacity		f	t	

Table 3.10.: SQCD Charge Assignments: $U(N_f) \otimes SO(N_c)$

$$g_{HS:GIO}^{U(N_f)\otimes SO(N_c)}(x,t) = \oint_{SO(N_c)} d\mu^{SO(N_c)}(y)\ PE\left[\chi_{[1,0,\ldots,0]}^{SU(N_f)}\chi_{[vec.]}^{SO(N_c)}(x,y)\,t\right], \tag{3.21}$$

and the HWGs are given by:

$$g_{HWG:GIO}^{U(N_f)\otimes SO(N_c)}(f,t) = \oint_{SU(N_f)} d\mu^{SU(N_f)}(x)\ g_{\chi}^{SU(N_f)}(x^*,f)\ g_{HS:GIO}^{U(N_f)\otimes SO(N_c)}(x,t) \tag{3.22}$$

Evaluation shows that the HWGs of these theories are are all freely generated and can be stated concisely in terms of their PLs, as set out in Table 3.11.

Theory	PL[HWG] $SU(N_f) \otimes U(1)$ fugacities	PL[HWG] $U(N_f)$ fugacities
$U(2) \otimes SO(3)$	$t^2f^2 + t^4$	${m_1}^2 + {m_2}^2$
$U(3) \otimes SO(3)$	$t^2{f_1}^2 + t^3 + t^4{f_2}^2$	${m_1}^2 + {m_2}^2 + m_3$
$U(\geq 4) \otimes SO(3)$	$t^2{f_1}^2 + t^3f_3 + t^4{f_2}^2$	${m_1}^2 + {m_2}^2 + m_3$
$U(2) \otimes SO(4)$	$t^2f^2 + t^4$	${m_1}^2 + {m_2}^2$
$U(3) \otimes SO(4)$	$t^2{f_1}^2 + t^4{f_2}^2 + t^6$	${m_1}^2 + {m_2}^2 + {m_3}^2$
$U(4) \otimes SO(4)$	$t^2{f_1}^2 + t^4{f_2}^2 + t^6{f_3}^2 + t^4$	${m_1}^2 + {m_2}^2 + {m_3}^2 + m_4$
$U(\geq 5) \otimes SO(4)$	$t^2{f_1}^2 + t^4{f_2}^2 + t^4f_4 + t^6{f_3}^2$	${m_1}^2 + {m_2}^2 + {m_3}^2 + m_4$
$U(2) \otimes SO(5)$	$t^2f^2 + t^4$	${m_1}^2 + {m_2}^2$
$U(3) \otimes SO(5)$	$t^2{f_1}^2 + t^4{f_2}^2 + t^6$	${m_1}^2 + {m_2}^2 + {m_3}^2$
$U(4) \otimes SO(5)$	$t^2{f_1}^2 + t^4{f_2}^2 + t^6{f_3}^2 + t^8$	${m_1}^2 + {m_2}^2 + {m_3}^2 + {m_4}^2$
$U(5) \otimes SO(5)$	$t^2{f_1}^2 + t^4{f_2}^2 + t^5 + t^6{f_3}^2 + t^8{f_4}^2$	${m_1}^2 + {m_2}^2 + {m_3}^2 + {m_4}^2 + m_5$
$U(\geq 6) \otimes SO(5)$	$t^2{f_1}^2 + t^4{f_2}^2 + t^5f_5 + t^6{f_3}^2 + t^8{f_4}^2$	${m_1}^2 + {m_2}^2 + {m_3}^2 + {m_4}^2 + m_5$

Table 3.11.: PLs of HWGs of $U(N_f) \otimes SO(N_c)$ GIOs

Once again, the HWGs of this SQCD theory are the same for all flavour groups of fundamental dimension exceeding the vector dimension of the $SO(N_c)$ colour group. This permits us to extrapolate Table 3.11 and to generalise the PLs of HWGs to arbitrary numbers of flavours and colours. We do this concisely, in terms of $U(N_f)$ highest weight fugacities m, using the map 3.19:

$$PL[HWG] = \sum_{i=1}^{\min(N_f,N_c)-1} m_i^2 + \begin{cases} if\ N_f < N_c: & m_{N_f}^2 \\ if\ N_f \geq N_c: & m_{N_c} \end{cases} \tag{3.23}$$

Naturally, for $N_f \geq N_c$, the results correspond exactly to the invariants of $SO(N_c)$, as shown in Table 3.4.

These results are based on taking $U(N)$ as the flavour group; however, they can be translated to any other flavour group G, which has a representation χ^G of dimension N, by using a character map $\chi^{U(N)}_{[fund]} \to \chi^G$ and reading off the representations of G associated with each monomial in the HWG series. In this manner, the series of gauge group invariants can be seen to map explicitly, via their symmetry properties, to flavour group representations.

Unrefined HS for some $U(N_f) \otimes SO(N_c)$ product groups are set out in Table 3.12. These HS are freely generated for $N_f < N_c$, complete intersections for $N_f = N_c$ and non-complete intersections for $N_f > N_c$. In all cases the numerators are palindromic. As can be verified by inspection of Table 3.12, the dimensions of these unrefined HS are given, for $N_f < N_c$, by $N_f(N_f+1)/2$ and, for $N_f \geq N_c$, by $N_f N_c - N_c(N_c-1)/2$, which is the number of bifundamental fields less the number of gauge group generators [14].

Theory	Unrefined Hilbert Series	|HS|
$U(2) \otimes SO(3)$	$\frac{1}{(1-t^2)^3}$	3
$U(3) \otimes SO(3)$	$\frac{1+t^3}{(1-t^2)^6}$	6
$U(4) \otimes SO(3)$	$\frac{1+t^2+4t^3+t^4+t^6}{(1-t^2)^9}$	9
$U(5) \otimes SO(3)$	$\frac{1+3t^2+10t^3+6t^4+6t^5+10t^6+3t^7+t^9}{(1-t^2)^{12}}$	12
$U(6) \otimes SO(3)$	$\frac{1+6t^2+20t^3+21t^4+36t^5+56t^6+36t^7+21t^8+20t^9+6t^{10}+t^{12}}{(1-t^2)^{15}}$	15
$U(7) \otimes SO(3)$	$\frac{\left(\begin{array}{c} 1+10t^2+35t^3+55t^4+126t^5+220t^6+225t^7 \\ +225t^8+220t^9+126t^{10}+55t^{11}+35t^{12}+10t^{13}+t^{15} \end{array}\right)}{(1-t^2)^{18}}$	18
$U(2) \otimes SO(4)$	$\frac{1}{(1-t^2)^3}$	3
$U(3) \otimes SO(4)$	$\frac{1}{(1-t^2)^6}$	6
$U(4) \otimes SO(4)$	$\frac{1+t^4}{(1-t^2)^{10}}$	10
$U(5) \otimes SO(4)$	$\frac{1+t^2+6t^4+t^6+t^8}{(1-t^2)^{14}}$	14
$U(6) \otimes SO(4)$	$\frac{1+3t^2+21t^4+20t^6+21t^8+3t^{10}+t^{12}}{(1-t^2)^{18}}$	18
$U(7) \otimes SO(4)$	$\frac{1+6t^2+56t^4+126t^6+210t^8+126t^{10}+56t^{12}+6t^{14}+t^{16}}{(1-t^2)^{22}}$	22
$U(2) \otimes SO(5)$	$\frac{1}{(1-t^2)^3}$	3
$U(3) \otimes SO(5)$	$\frac{1}{(1-t^2)^6}$	6
$U(4) \otimes SO(5)$	$\frac{1}{(1-t^2)^{10}}$	10
$U(5) \otimes SO(5)$	$\frac{1+t^5}{(1-t^2)^{15}}$	15
$U(6) \otimes SO(5)$	$\frac{1+t^2+t^4+6t^5+t^6+t^8+t^{10}}{(1-t^2)^{20}}$	20
$U(7) \otimes SO(5)$	$\frac{\left(\begin{array}{c} 1+3t^2+6t^4+21t^5+10t^6+15t^7 \\ +15t^8+10t^9+21t^{10}+6t^{11}+3t^{13}+t^{15} \end{array}\right)}{(1-t^2)^{25}}$	25

Table 3.12.: Unrefined HS of $U(N_f) \otimes SO(N_c)$ GIOs

3.2.3. GIOs of $U(N_f) \otimes USp(N_c)$

In the case of $U(N_f) \otimes USp(N_c)$ product groups, the bifundamental scalar fields transform in the fundamental representation of the flavour group and in the defining $N_c = 2r$ dimensional vector representation of the symplectic colour group C_r. We use the charge assignments in Table 3.13 based on [14]. For convenience, the $U(N_f)$ flavour groups are decomposed as $SU(N_f) \otimes U(1)$.

	Gauge/Colour	Flavour		R
Groups	$USp(N_c)$	$SU(N_f)$	$U(1)_B$	$U(1)_R$
Q_a^i	$[1,0,\ldots,0]$	$[1,0,\ldots,0]$	1	
CSA Fugacity	y	x	q	t'
HW Fugacity		f	t	

Table 3.13.: SQCD Charge Assignments: $U(N_f) \otimes USp(N_c)$

The theory contains combinations of quarks Q_a^i with indices i and a ranging over the flavour and colour group representations, respectively. The GIOs are colour singlets composed of quarks and transform in some flavour group irrep. The fields also carry $U(1)$ charges, which can be absorbed into a single counting fugacity $t = qt'$. Often N_f is restricted to be even, following [66], but we adopt a general treatment here.

Proceeding as before, the refined HS are given by:

$$g_{HS:GIO}^{U(N_f)\otimes USp(N_c)}(x,t) = \oint_{USp(N_c)} d\mu^{USp(N_c)}(y)\; PE\left[\chi^{SU(N_f)}_{[1,0,\ldots,0]}\chi^{USp(N_c)}_{[1,0,\ldots,0]}(x,y)\,t\right], \tag{3.24}$$

and the HWGs are given by:

$$g_{HWG:GIO}^{U(N_f)\otimes USp(N_c)}(f,t) = \oint_{SU(N_f)} d\mu^{SU(N_f)}(x)\; g_\chi^{SU(N_f)}(x^*,f)\; g_{GIOs}^{U(N_f)\otimes USp(N_c)}(x,t) \tag{3.25}$$

Evaluation shows that the HWGs of these theories are are all freely generated and can be stated concisely in terms of their PLs, as set out in Table 3.14.

Theory	PL[HWG] $SU(N_f) \otimes U(1)$ fugacities	PL[HWG] $U(N_f)$ fugacities
$U(2) \otimes USp(2)$	t^2	m_2
$U(\geq 3) \otimes USp(2)$	$t^2 f_2$	m_2
$U(2) \otimes USp(4)$	t^2	m_2
$U(3) \otimes USp(4)$	$t^2 f_2$	m_2
$U(4) \otimes USp(4)$	$t^2 f_2 + t^4$	$m_2 + m_4$
$U(\geq 5) \otimes USp(4)$	$t^2 f_2 + t^4 f_4$	$m_2 + m_4$

Table 3.14.: PLs of HWGs of $U(N_f) \otimes USp(N_c)$ GIOs

Thus, for example, the PL $t^2 f_2 + t^4$ in Table 3.14 indicates that the highest weight generators of the GIOs of an $SU(4) \otimes U(1) \otimes USp(4)$ SQCD theory consists of an antisymmetric contraction of two quarks transforming in the [0, 1, 0] irrep of the $SU(4)$ flavour group and an antisymmetric contraction of 4 quarks transforming as a [0, 0, 0] flavour singlet.

As before, the HWGs of this SQCD theory are the same for all flavour groups of fundamental dimension exceeding the vector dimension of the $USp(N_c)$ colour group. This permits us to extrapolate Table 3.14 and to generalise the HWGs for GIOs of $U(N_f) \otimes USp(N_c)$ to arbitrary flavours and colours. This is done most concisely by using the map 3.19 to convert to $U(N_f)$ fugacities m:

$$PL[HWG] = \sum_{i=1}^{\min\left(\left\lfloor \frac{N_f}{2} \right\rfloor, \frac{N_c}{2}\right)} m_{2i} \tag{3.26}$$

Naturally, for $N_f = N_c$, the GIOs correspond exactly to the antisymmetric invariants of $USp(N_c)$ as shown in Table 3.4.

Unrefined Hilbert series for some $U(N_f) \otimes USp(N_c)$ product groups are set out in Table 3.15. These HS are freely generated for $Nf \leq Nc + 1$, complete intersections for $N_f = N_c + 2$ and non-complete intersections for $N_f > N_c + 2$. In all cases the numerators are palindromic. As can be verified by inspection of Table 3.15, the dimensions of these unrefined HS are given, for $N_f < N_c$, by $N_f(N_f + 1)/2$, and, for $N_f \geq N_c$, by $N_f N_c - N_c(N_c + 1)/2$, which is the number of bifundamental fields less the number of gauge group generators [7].

Theory	Unrefined Hilbert Series	|HS|
$U(2) \otimes USp(2)$	$\frac{1}{1-t^2}$	1
$U(3) \otimes USp(2)$	$\frac{1}{(1-t^2)^3}$	3
$U(4) \otimes USp(2)$	$\frac{1+t^2}{(1-t^2)^5}$	5
$U(5) \otimes USp(2)$	$\frac{1+3t^2+t^4}{(1-t^2)^7}$	7
$U(6) \otimes USp(2)$	$\frac{(1+t^2)(1+5t^2+t^4)}{(1-t^2)^9}$	9
$U(2) \otimes USp(4)$	$\frac{1}{(1-t^2)}$	1
$U(3) \otimes USp(4)$	$\frac{1}{(1-t^2)^3}$	3
$U(4) \otimes USp(4)$	$\frac{1}{(1-t^2)^6}$	6
$U(5) \otimes USp(4)$	$\frac{1}{(1-t^2)^{10}}$	10
$U(6) \otimes USp(4)$	$\frac{1-t^6}{(1-t^2)^{15}}$	14
$U(7) \otimes USp(4)$	$\frac{1+3t^2+6t^4+3t^6+t^8}{(1-t^2)^{18}}$	18
$U(8) \otimes USp(4)$	$\frac{1+6t^2+21t^4+28t^6+21t^8+6t^{10}+t^{12}}{(1-t^2)^{22}}$	22
$U(9) \otimes USp(4)$	$\frac{\left(\begin{array}{c}1+10t^2+55t^4+136t^6+190t^8\\+136t^{10}+55t^{12}+10t^{14}+t^{16}\end{array}\right)}{(1-t^2)^{26}}$	26
$U(10) \otimes USp(4)$	$\frac{\left(\begin{array}{c}1+15t^2+120t^4+470t^6+1065t^8+1377t^{10}+\\1065t^{12}+470t^{14}+120t^{16}+15t^{18}+t^{20}\end{array}\right)}{(1-t^2)^{30}}$	30

Table 3.15.: Unrefined HS of $U(N_f) \otimes USp(N_c)$ GIOs

3.2.4. GIOs of $U(N_f) \otimes G_2$

Finally, it is interesting to examine the SQCD moduli space when the colour group is taken as an exceptional group, of which G_2 is the lowest rank example. We use the charge assignments in Table 3.16. For convenience, the $U(N_f)$ flavour groups are decomposed as $SU(N_f) \otimes U(1)$.

	Gauge/Colour	Flavour	
Groups	G_2	$SU(N_f)$	$U(1)$
Q_a^i	$[0,1]$	$[1,0,\ldots,0]$	1
CSA Fugacity	y	x	q
HW Fugacity		f	t

Table 3.16.: SQCD Charge Assignments: $U(N_f) \otimes G_2$

The bifundamental scalar fields are quarks Q_a^i, where the indices i and a range over the fundamental representation of the flavour group and defining representation $[0,1]$ of the G_2 colour group, respectively. The GIOs are colour singlets composed of quarks, with some combination of flavour indices determining the irrep in which they transform. The $U(1)$ charges are absorbed into a single counting fugacity $q \to t$.

The refined HS are given by:

$$g_{HS:GIO}^{U(N_f)\otimes G_2}(x,t) = \oint_{G_2} d\mu^{G_2}(y)\ PE\left[\chi_{[1,0,\ldots,0]}^{SU(N_f)}\ \chi_{[0,1]}^{G_2}(x,y)\,t\right], \tag{3.27}$$

and the HWGs are given by:

$$g_{HWG:GIO}^{U(N_f)\otimes G_2}(f,t) = \oint_{SU(N_f)} d\mu^{SU(N_f)}(x)\ g_{\chi}^{SU(N_f)}(x^*,f)\ g_{HS:GIO}^{U(N_f)\otimes G_2}(x,t) \tag{3.28}$$

The PLs of the HWGs for $U(N_f) \otimes G_2$ SQCD are set out in Table 3.17, where notation is shown for both $SU(N_f) \otimes U(1)$ and the corresponding $U(N_f)$ highest weight fugacities under the map 3.19.

We can identify the G_2 symmetric invariant tensor ${m_1}^2$ of order 2 and the antisymmetric invariant tensors m_3 and m_4 of order 3 and 4, along with other invariant tensors of mixed symmetry. The HWGs for $U(2)$ and $U(3)$

Theory	PL[HWG] $SU(N_f) \otimes U(1)$ fugacities	PL[HWG] $U(N_f)$ fugacities
$U(2) \otimes G_2$	$f^2t^2 + t^4$	${m_1}^2 + {m_2}^2$
$U(3) \otimes G_2$	${f_1}^2t^2 + {f_2}^2t^4 + t^6 + t^3$	${m_1}^2 + {m_2}^2 + {m_3}^2 + m_3$
$U(4) \otimes G_2$	${f_1}^2t^2 + {f_2}^2t^4 + {f_3}^2t^6 + t^8$ $+f_3t^3 + t^4 + f_1t^5$ $+f_1f_2t^7 + f_2f_3t^9 + {f_2}^2t^{12}$ $-{f_1}^2{f_2}^2t^{14} - {f_2}^2{f_3}^2t^{18}$	${m_1}^2 + {m_2}^2 + {m_3}^2 + {m_4}^2$ $+m_3 + m_4 + m_1m_4$ $+m_1m_2m_4 + m_2m_3m_4 + {m_2}^2{m_4}^2$ $-{m_1}^2{m_2}^2{m_4}^2 - {m_2}^2{m_3}^2{m_4}^2$
$U(5) \otimes G_2$	to be calculated	to be calculated

Table 3.17.: PLs of HWGs of $U(N_f) \otimes G_2$ GIOs

are freely generated. As the flavour group is increased in rank it probes further into the antisymmetric tensors of G_2. Relations exist between the invariant tensors and these manifest themselves in the negative terms in PL[HWG] for $U(4)$, which represents a complete intersection moduli space.

Recalling from section 3.2 that the G_2 defining representation has a wholly antisymmetric invariant tensor (volume form) of order 7, these HWGs should converge for flavour groups $U(7)$ and above, yielding a full enumeration of the invariant tensors of the defining representation of G_2. However, due to the complicated structure of the invariants of G_2, the contour integrations for $U(5)$ and above have so far not proved computationally feasible. Thus, in the case of a $U(5)$ flavour group, the refined Hilbert series can be obtained in the form of a $SU(5) \otimes U(1)$ class function, as in 3.29, but it has so far not proved feasible to transform this to an HWG.

$$g_{HS:GIO}^{U(5)\otimes G_2}\left(\chi^{SU(5)}, t\right) = \left(1 - t^5\right) \left(\begin{array}{r} \left(1 + t^5 - t^{15} - t^{20}\right)[0,0,0,0] \\ +t^4\left(1 + t^5 + t^{10}\right)[0,0,0,1] \\ +t^{13}[0,0,1,0] \\ -t^7[0,1,0,0] \\ -t^6\left(1 + t^5 + t^{10}\right)[1,0,0,0] \end{array} \right) \times PE\left[[2,0,0,0]\,t^2\right]\ PE\left[[0,0,1,0]\,t^3\right]. \tag{3.29}$$

It is likely that the HWGs for $U(5)$ and above will prove not to be complete intersections.

The unrefined Hilbert series for $U(N_f) \otimes G_2$ SQCD are set out in Table 3.18. The HS for $U(5)$ and above are not complete intersections, but are

Theory	Unrefined HS
$U(2) \otimes G_2$	$\frac{1}{(1-t^2)^3}$
$U(3) \otimes G_2$	$\frac{1}{(1-t^3)(1-t^2)^6}$
$U(4) \otimes G_2$	$\frac{1+t^4}{(1-t^3)^4(1-t^2)^{10}}$
$U(5) \otimes G_2$	$\frac{\left(1+t^2+3t^3+6t^4+3t^5+7t^6+8t^7+7t^8+3t^9+6t^{10}+3t^{11}+t^{12}+t^{14}\right)}{(1-t^2)^{14}(1-t^3)^7}$

Table 3.18.: Unrefined HS of $U(N_f) \otimes G_2$ GIOs

palindromic.

3.2.5. Geometric Properties of HWGs and HS of SQCD

The HWGs of SQCD explicate the structure of GIOs. In the case of Classical SQCD, the HWGs are freely generated, reflecting the limited set of invariant tensors of defining representations of Classical groups. This in turn makes it possible to extrapolate these HWGs to arbitrary numbers of colours and flavours, thus providing a full enumeration of the GIOs of any Classical SQCD theory described by the quiver in Figure 3.1. This includes theories with groups of high rank for which a direct calculation might not be feasible. The results in 3.20, 3.23 and 3.26 correspond to observations within [13, 14], but are restated concisely in the language of HWGs.

The Hilbert series of the GIOs of SQCD theories with Exceptional gauge groups are considerably more complicated than those of Classical gauge groups. It has not yet proved possible, for example, to evaluate the HWGs for $U(N_f) \otimes G_2$ for 5 or more flavours, as discussed in section 3.2.4.

HWGs differ from unrefined HS for all but the simplest theories. The description of SQCD moduli spaces in terms of unrefined HS only encodes dimensional information about flavour group representations and this can facilitate the identification of dualities between theories, as discussed in section 3.2.1. However, this simplification also leads to HS which are typically complete intersections only for small N_f.

The dimensions of HWGs for GIOs for SQCD, which follow from 3.20, 3.23 and 3.26, are lower than those of the corresponding unrefined HS, as summarised in Table 3.19. The lower dimension of the HWGs, compared with the HS, results from the projection of a moduli space on to the representation lattice of $U(N)$, which is higher dimensioned than the simple

$U(1)$ lattice used by an unrefined HS. We can give a systematic account of the difference by expanding a given HWG and analysing the structure of its irreps. For example, the expansion for $U(4)_{L/R} \otimes SU(3_c)$ in Table 3.7 takes the form:

$$PE\left[l_3 t_1^3 + r_3 t_2^3 + l_1 r_1 t_1 t_2 + l_2 r_2 t_1^2 t_2^2\right] \Leftrightarrow \sum_{n_1,n_2,n_3,n_4=0}^{\infty} [n_1,n_2,n_3]\,[n_1,n_2,n_4] t_1^{n_1+2n_2+3n_3}\; t_2^{n_1+2n_2+3n_4}. \tag{3.30}$$

The Dynkin labels in this HWG expansion require four different parameters $\{n_1, n_2, n_3, n_4\}$, corresponding to the four generators within the PE function. The parameters identify the sub-lattice of the flavour group weight lattice that is spanned by the irreps of the HWG. The dimensions of the flavour group irreps in the HWG are a polynomial function of the parameters and the degree of this polynomial indicates the dimension of the sub-lattice.

Now define HWG Irrep Degree as the total degree of the minimal polynomial that gives the dimensions of all the irreps generated by the HWG [19]. For example, the dimension formula for $SU(4)$ or $U(4)$ irreps [2] is:

$$\dim[n_1,n_2,n_3] = \frac{1}{12}(n_1{+}1)(n_2{+}1)(n_3{+}1)(n_1{+}n_2{+}2)(n_2{+}n_3{+}2)(n_1{+}n_2{+}n_3{+}3). \tag{3.31}$$

The degree of this polynomial is six. Thus the HWG Irrep Degree for $U(4)_{L/R} \otimes SU(5_c)$ is 12, being the sum of the degrees for the L and R $SU(4)$ flavour groups, and this matches the dimension $N_f(N_f-1) = 12$ for $N_f < N_c$ in Table 3.19.

As can be seen from Table 3.19, the monomials of HWGs for SQCD GIOs only span flavour group Dynkin label lattices up to m_{N_c} at most, and, in the case of USp gauge groups, only contain even Dynkin labels. In such HWGs, where some Dynkin labels are fixed at zero, the HWG Irrep Degree is reduced. In the case of $U(4)_{L/R} \otimes SU(2_c)$, for example, we find $\dim[n_1,n_2,0]$ is of degree 5 and so the HWG Irrep Degree is 10; this matches $2N_fN_c - N_c(N_c+1) = 10$ for $N_f \geq N_c$ in Table 3.19.

Case by case analysis shows that the HWG Irrep Degree, as defined,

[2] Recall that the dimensions of $U(N)$ irreps match those of $SU(N)$ irreps with the same leading Dynkin labels $[n_1, \ldots, n_{N-1}]$.

Theory		|HWG|	HWG Irrep	HWG Irrep Degree (b)	|HS|
$U(N_f)_{L/R} \otimes SU(N_c)$	$N_f < N_c$	N_f	$[n_1, \ldots, n_{N_f}]_{L/R}$	$N_f(N_f-1)$	N_f^2
	$N_f \geq N_c$	N_c+1	$[n_1, \ldots, n_{N_c}, 0, \ldots]_{L/R}$	$2N_fN_c - N_c(N_c+1)$	$2N_fN_c - (N_c^2-1)$
$U(N_f) \otimes SO(N_c)$	$N_f < N_c$	N_f	$[n_1, \ldots, n_{N_f}]$	$N_f(N_f-1)/2$	$N_f(N_f+1)/2$
	$N_f \geq N_c$	N_c	$[n_1, \ldots, n_{N_c}, 0, \ldots]$	$N_fN_c - N_c(N_c+1)/2$	$N_fN_c - N_c(N_c-1)/2$
$U(N_f) \otimes USp(N_c)$	$N_f < N_c$	$\lfloor N_f/2 \rfloor$	$[0, n_2, 0, \ldots, n_{2\lfloor N_f/2 \rfloor}, \ldots]$	$N_f(N_f-1)/2 - \lfloor N_f/2 \rfloor$	$N_f(N_f-1)/2$
	$N_f \geq N_c$	$N_c/2$	$[0, n_2, 0, \ldots, n_{N_c}, 0, \ldots]$	$N_fN_c - N_c(N_c+2)/2$	$N_fN_c - N_c(N_c+1)/2$

Table 3.19.: Dimensions of Moduli Spaces of SQCD Theories

matches the difference between the dimensions of the HWGs and the unrefined HS in Table 3.19 [28]. We can carry out a reconciliation in a similar manner for $SU(N_f) \otimes G_2$ SQCD as summarised in Table 3.20.

Theory	|HWG| (a)	HWG Irrep	HWG Irrep Degree (b)	|HS| $(a)+(b)$
$SU(2) \otimes G_2$	2	$[n]$	1	3
$SU(3) \otimes G_2$	4	$[n_1, n_2]$	3	7
$SU(4) \otimes G_2$	8	$[n_1, n_2, n_3]$	6	14
$SU(5) \otimes G_2$	*t.b.c.*	$[n_1, n_2, n_3, n_4]$	10	21

Table 3.20.: Dimensions of Moduli Spaces of $SU(N_f) \otimes G_2$ GIOs

All the HS, and also all the HWGs for GIOs of Classical SQCD are palindromic and therefore Calabi-Yau; the same is true of the Exceptional group HWGs calculated. This palindromic property of many generating functions for Hilbert series is shared with the character generating functions discussed in section 2.2 that are used to derive the HWGs and Hilbert series.

An important demonstration from the HWG analysis is that the (coefficients of the) unrefined Hilbert series of SQCD are reducible to characters of flavour group representations. This group theoretic reducibility arises because (anti-)symmetrisation of characters using the PE (or PEF) generates class functions, which can in turn always be decomposed into series of characters with polynomial coefficients. These reduced series correspond to HWGs, which precisely encode the structure of the symmetry group representations underlying a Hilbert series.

3.3. $SU(N)$-Instanton Moduli Spaces

The aim here is to construct the moduli spaces of some low rank $SU(N)$ instantons on $\mathbb{C}^2$ and to show how HWGs can be used to study their structures. Each instanton moduli space is identified with the Higgs branch of a quiver theory [8].

As elaborated in [4, 16] these Higgs branch quiver theories can be built on systems of Dp branes against a background of $Dp+4$ branes in type II string theories. Taking $p = 3$, yields a $3+1$ dimensional space-time spanned

by $D3$ branes, with $\mathcal{N} = 2$ SUSY. The instantons can be assigned positions on the transverse directions on the $D7$ branes, parameterised using $\mathbb{C}^2$.

The fields in the quiver theory transform in some representation of a product group defined by (i) the quiver gauge group, determined by the number of instantons, (ii) the Yang-Mills (or flavour) symmetry group and (iii) an $SU(2)$ global symmetry group. The instanton moduli spaces contain field combinations that are singlets of the quiver gauge group.

Following [16], $\mathcal{N} = 2$ SUSY quiver theories for the moduli spaces of k $SU(N)$ instantons on $\mathbb{C}^2$ can be described using explicit $\mathcal{N} = 1$ notation by "flower shaped" quiver diagrams, as in Figure 3.2, with their basic field content as specified in more detail in Table 3.21.

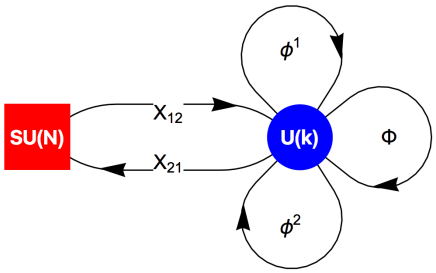

Figure 3.2.: Quiver diagram for the Moduli Space of k SU(N)-Instantons using $\mathcal{N} = 1$ notation. The square node denotes the $SU(N)$ Yang-Mills symmetry group. The round node denotes the $U(k)$ instanton quiver gauge group. The links X_{12} and X_{21} correspond to *bifundamental* fields transforming under both the Yang Mills and quiver gauge groups. The fields ϕ^α transform in the adjoint of the quiver gauge group and in a global $SU(2)$ symmetry. The field Φ transforms in the adjoint of the quiver gauge group.

It is helpful to decompose the quiver gauge group $U(k) \to SU(k) \otimes U(1)$, by extracting an overall $U(1)$ charge. Then the X_{12} and X_{21} bi-fundamental fields transform in conjugate representations with respect to both the quiver gauge and Yang-Mills symmetry groups and also carry conjugate $U(1)$ charges. The fields $\{\Phi, \phi^{(a)}\}$ transform in the $U(k)$ adjoint, which decomposes as an $SU(k)$ adjoint plus a singlet. The fugacity t, corresponding to a global $U(1)$ R-symmetry, is used to count the fields.

Field	Quiver Gauge Group : $SU(k)$	$U(k)$ $U(1)$	Yang-Mills Group $SU(N)$	Global Symmetry $SU(2_g)$	R-Charge $U(1)_R$
Φ	$[1,0,\ldots,0,1]+1$	(0)	$[0,\ldots,0]$	$[0]$	0
$\phi^{(\alpha)}$	$[1,0,\ldots,0,1]+1$	(0)	$[0,\ldots,0]$	$[1]$	(1)
X_{12}	$[1,0,\ldots,0]$	(1)	$[0,\ldots,0,1]$	$[0]$	(1)
X_{21}	$[0,\ldots,0,1]$	(-1)	$[1,0\ldots,0]$	$[0]$	(1)
CSA Fug.	$w_1,\ldots,w_{k-1}$	q	$x_1,\ldots,x_{N-1}$	y	t
HW Fug.			$m_1,\ldots,m_{N-1}$	m_g	t

Table 3.21.: Field Content of Quiver Theory for k $SU(N)$ Instantons on $\mathbb{C}^2$

The theory is defined not only by its basic fields, but also by its superpotential [16]:

$$\mathcal{W} = Tr\left(X_{21}\Phi X_{12} + \varepsilon_{\alpha\beta}\phi^{(\alpha)}\Phi\phi^{(\beta)}\right). \tag{3.32}$$

The trace is taken over all unpaired symmetry group indices. We apply variational principles, requiring that the superpotential at the SUSY vacuum should be extremised with respect to the field Φ, $\frac{\partial\mathcal{W}}{\partial\Phi} = 0$. This leads to the F-term constraints:

$$(X_{12})_a^{\ i}\,(X_{21})_i^{\ b} = \varepsilon_{\alpha\beta}\left(\phi^{(\alpha)}\right)_a^{\ c}\left(\phi^{(\beta)}\right)_c^{\ b}, \tag{3.33}$$

where quiver gauge indices are denoted by $(a,b,\ldots)$ and Yang-Mills indices by $(i,j,\ldots)$

For a quiver gauge group $U(k)$, 3.33 leads to k^2 constraints. For $k=1$, the commutator of the $\phi^{(\alpha)}$ fields vanishes and the single F-term constraint is that there should be no $SU(N)$ singlets formed from pairs of X fields. For $k>1$, the commutator does not vanish, and the F-term constraints impose an identity between the $SU(N)$ singlets formed from pairs of X fields, and the $SU(2_g)$ singlets formed by contracting pairs of $\phi^{(\alpha)}$ fields; these pairs of fields both transform in the adjoint of the quiver gauge group.

Tracing over 3.33 to obtain singlets (relative to all groups) and applying the cyclic property of the trace to the $\phi^{(\alpha)}$ yields the F-term constraint:

$$(X_{12})_a{}^i\,(X_{21})_i{}^a = \varepsilon_{\alpha\beta}\left(\phi^{(\alpha)}\right)_a{}^c\left(\phi^{(\beta)}\right)_c{}^a = 0, \tag{3.34}$$

which excludes all singlets formed from pairs of X fields, or from pairs of ϕ fields, from the moduli space.

In order to find the GIOs (quiver gauge singlets) of the theory, we continue by identifying the field representations with their characters, which follow from 3.21:

$$\begin{aligned}
\chi(\Phi) &\equiv [1,0\ldots,0,1]_{SU(k)} + 1 \\
\chi(\phi^{(\alpha)}) &\equiv [1,0\ldots,0,1]_{SU(k)}[1]_{SU(2_g)} + [1]_{SU(2_g)} \\
\chi(X_{12}) &\equiv [1,0\ldots,0,0]_{SU(k)}[0,0\ldots,1]_{SU(N)}\ q \\
\chi(X_{21}) &\equiv [0,0\ldots,0,1]_{SU(k)}[1,0\ldots,0]_{SU(N)}\ q^{-1}
\end{aligned} \tag{3.35}$$

Symmetrised combinations of the fields $\{\phi^{(\alpha)}, X_{12}, X_{21}\}$, which are also singlets of the $U(k)$ gauge group, can be generated from the characters by applying the PE, followed by Weyl integration over the gauge group, as in case of SQCD. However, these GIOs must also be subjected to the F-term constraints 3.33, and this is done by incorporating a HyperKähler quotient ("HKQ") to exclude the disallowed combinations and to avoid over-counting. The elements of the character $\chi(\Phi)$, which are equal in number to the F-term constraints, are symmetrised at order t^2 within the HKQ and cancel the field pairings identified by 3.33 or 3.34. The refined Hilbert series is thus given by the formula:

$$g_{HS}^{k,SU(N)}(x,y,t) \equiv \oint_{SU(k)\otimes U(1)} d\mu^{SU(k)} d\mu^{U(1)} \frac{PE\left[\left(\chi(\phi^{(\alpha)}) + \chi(X_{12}) + \chi(X_{21})\right)t\right]}{\underbrace{PE\left[\chi(\Phi)t^2\right]}_{\text{HyperKähler quotient}}}. \tag{3.36}$$

The HWG can be calculated by projecting $g_{HS}^{k,SU(N)}$ onto the irreps of the $SU(N)$ Yang-Mills symmetry and the global $SU(2)$ symmetry groups:

$$g_{HWG}^{k,SU(N)}(m, m_g, t) = \oint_{SU(N)\otimes SU(2_g)} d\mu^{SU(N)}(x)\; d\mu^{SU(2_g)}(y)\; g_\chi^{SU(N)}(x^*, m) \times g_\chi^{SU(2_g)}(y^*, m_g)\, g_{HS}^{k,SU(N)}(x, y, t). \tag{3.37}$$

The refined Hilbert series $g_{HS}^{k,SU(N)}(x, y, t)$ can also be summarised in unrefined form as $g_{HS}^{k,SU(N)}(1, 1, t)$, by replacing the characters of the $SU(N)$ and $SU(2_g)$ symmetry groups by their dimensions.

Instanton moduli spaces invariably contain a component generated by the fundamental of the global $SU(2)$ symmetry. This component represents the position of the instanton on the $\mathbb{R}^4 \cong \mathbb{C}^2$ manifold. For multiple instanton theories $k > 1$, this corresponds to the centre of mass. Instanton moduli spaces can be presented in reduced form by taking a quotient of the full moduli space by this $SU(2)$ symmetry. This can lead to simplifications in the HWGs for the moduli spaces, as will be shown.

The results of such calculations are set out below for one $SU(3)$ instanton on $\mathbb{C}^2$ and also for two and three $SU(2)$ instantons on $\mathbb{C}^2$.

3.3.1. Moduli Space of One $SU(3)$ Instanton

Noting that, for one instanton, the adjoint of $U(k)$ becomes the adjoint of $U(1)$, and evaluating 3.36, we obtain the refined Hilbert series:

$$g_{HS}^{1,SU(3)}(x, y, t) = (1-t^2)^2((1 + 2t^2 + 2t^4 + 2t^6 + t^8)[0, 0] - t^4[1, 1]) \times PE\left[[1, 1]t^2\right]\; PE\left[[1]t\right]. \tag{3.38}$$

For brevity, this plethystic class function has been written using character notation $[n_1, n_2](x)$ and $[n](y)$ for the irreps of the $SU(3)$ Yang-Mills and $SU(2_g)$ symmetry groups, respectively.

To obtain an HWG, we insert generating functions for the characters of $SU(2)$ and $SU(3)$, taken from Table 2.2, using Dynkin label fugacities $\{m_1, m_2\}$ for the Yang-Mills symmetry and m_g for the global symmetry,

into 3.37 and evaluate:

$$\begin{aligned} g_{HWG}^{1,SU(3)}(m_1,m_2,m_g,t) \equiv & \oint_{SU(3)} \oint_{SU(2)} d\mu^{SU(3)}(x) d\mu^{SU(2_g)}(y)\ (1-m_1 m_2) \\ & \times PE[[1,0](x^*)m_1 + [0,1](x^*)m_2] \\ & \times PE[[1](y^*)m_g]\ g_{HS}^{1,SU(3)}(x,y,t) \\ = & \frac{1}{(1-m_1 m_2 t^2)(1-m_g t)}. \end{aligned} \tag{3.39}$$

We can identify the combinations of the fields within the HWG 3.39 as shown in Table 3.22.

$SU(3); SU(2_g)$	HWG Terms	Basic Field Combinations
$[1,1;0]$	$m_1 m_2 t^2$	$SU(3)$ adjoint from X_{12} and X_{21}
$[0,0;1]$	$m_g t$	$SU(2_g)$ fundamental from $\phi^{(\alpha)}$

Table 3.22.: Generators of HWG for One $SU(3)$ Instanton Moduli Space

The Dynkin label fugacities $m_1 m_2$ always appear paired and so this is an example of the general result [16] that, for one $SU(N)$ instanton, the resulting tensor products between particles and antiparticles always transform in a real representation that is a symmetrisation $[n,0,\ldots,0,n]$ of the $SU(N)$ adjoint representation. We can also see that no t^2 singlets appear, as intended by the HyperKähler quotient.

The physical interpretation of the HWG is that the term $m_g t$ enumerates the representations of the global $SU(2)$ symmetry that describe the position of the instanton on $\mathbb{C}^2$. For $k=1$ the HWG decouples, with the $m_1 m_2 t^2$ term enumerating the holomorphic operators in the reduced single instanton moduli space ("RSIMS"), given by the one dimensional HWG:

$$g_{HWG}^{1,SU(3),red.}(m_1,m_2,t) = PE[m_1 m_2 t^2]. \tag{3.40}$$

We can unrefine the series given by the HWG 3.40, by Taylor expansion and replacement of the monomials in the HW fugacities $\{m_1,m_2\}$ by the

dimensions of the corresponding irreducible representations:

$$m_1{}^{n_1} m_2{}^{n_2} m_g{}^{n} \to \dim[n_1, n_2] \dim[n] = \frac{1}{2}(n_1{+}1)(n_2{+}1)(n_1{+}n_2{+}2)\,(n+1)\,. \tag{3.41}$$

The resulting unrefined Hilbert series matches that given in [16]:

$$g_{HS}^{1,SU(3)}(t) = \frac{1+4t^2+t^4}{(1-t)^2(1-t^2)^4}. \tag{3.42}$$

3.3.2. Moduli Space of Two $SU(2)$ Instantons

The analysis for multiple instantons is complicated by the gauge group symmetry. For $k = 2$, the characters combine the three separate non-Abelian product groups; quiver gauge $U(2)$, Yang-Mills $SU(2)$ and the global $SU(2_g)$, in addition to the $U(1)$ charges.

Proceeding as before and evaluating 3.36, we obtain the refined Hilbert series:

$$\begin{aligned} g_{HS}^{2,SU(2)}(x,y,t) = \left(1-t^2\right) & \left(\begin{array}{r} \left(1+t^2-t^{14}-t^{16}\right)[0;0] \\ +t^3\left(1-t^{10}\right)[0;1] \\ -t^6\left(1-t^4\right)[2;0] \\ -t^5\left(1-t^6\right)[2;1] \end{array} \right) \\ & \times PE\left[[0;1]t + [2;0]t^2 + [0;2]t^2 + [2;1]t^3 - [0;1]t^3\right]. \end{aligned} \tag{3.43}$$

This has been written as a plethystic class function using condensed character notation $[n_1;n](x,y) \equiv [n_1](x)[n]_g(y)$ for the irreps of the $SU(2)\otimes SU(2_g)$ product group.

Applying 3.37,by inserting the character generating functions for $g_\chi^{SU(2)}(x^*, m_1)$ and $g_\chi^{SU(2)}(y^*, m_g)$, which use the HW fugacities m_1 and m_g to track the Yang-Mills $SU(2)$ and $SU(2_g)$ irreps, gives the HWG:

$$\begin{aligned} g_{HWG}^{2,SU(2)}(m_1, m_g, t) \equiv & \oint_{SU(2)\otimes SU(2_g)} d\mu^{SU(2)}(x) d\mu^{SU(2_g)}(y) \\ & \times PE\left[[1](x)m_1\right]\ PE\left[[1](y)m_g\right]\ g_{HS}^{2,SU(2)}(x,y,t) \end{aligned} \tag{3.44}$$

Carrying out the contour integrations, this evaluates as:

$$g_{HWG}^{2,SU(2)}(m_1, m_g, t) = \frac{P(m_1, m_g, t)}{(1 - m_g t)(1 - {m_g}^2 t^2)(1 - {m_1}^2 t^2)(1 - m_g {m_1}^2 t^3)(1 - t^4)^2 (1 - {m_1}^2 t^4)}, \tag{3.45}$$

where

$$P(m_1, m_g, t) = 1 + m_g t^3 + m_g {m_1}^2 t^5 + {m_1}^2 t^6 - {m_g}^2 {m_1}^2 t^6 - m_g {m_1}^2 t^7 - m_g {m_1}^4 t^9 - {m_g}^2 {m_1}^4 t^{12}. \tag{3.46}$$

Table 3.23 identifies the combinations of the fields giving rise to the HWG denominator terms. The exponents of the fugacities $\{m_1, m_g\}$ are the

$SU(2); SU(2_g)$	HWG Terms	Basic Field Combinations
$[0;0]$	t^4	Singlets
$[0;1]$	$m_g t$	$SU(2_g)$ fundamental from $\phi^{(\alpha)}$
$[0;2]$	${m_g}^2 t^2$	$SU(2_g)$ adjoint from $\phi^{(\alpha)}$
$[2;0]$ $[2;0]$	${m_1}^2 t^2$ ${m_1}^2 t^4$	$SU(2)$ adjoint from X_{12} and X_{21}
$[2;1]$	$m_g {m_1}^2 t^3$	$SU(2_g)$ fundamental $\otimes$ $SU(2)$ adjoint from $\phi^{(a)}, X_{12}$ and X_{21}

Table 3.23.: Generators of HWG for Two $SU(2)$ Instanton Moduli Space

Dynkin labels that identify the generators of the moduli space according to the irreps in which they transform. While the $SU(2_g)$ generators transform in both the fundamental and adjoint, the Yang-Mills $SU(2)$ generators are limited to the adjoint. The generator $m_g {m_1}^2 t^3$ gives rise to mixing between the global and Yang-Mills symmetries.

Interestingly, the polynomial $P(m_1, m_g, t)$ is anti-palindromic of degree (4,2,12) in the variables $\{m_1, m_g, t\}$. The numerator $P(m_1, m_g, t)$ also contains the monomial term $m_g t^3$, which is not just a product of the generators.

Some of these generators can be recognised from the refined HS in 3.43, however, the HWG gives a complete account of the resulting representation content.

We can easily verify that the HyperKähler quotient has had the desired effect of excluding Yang-Mills singlets formed from pairs of fields. Thus, if we specialise the HWG 3.45 to Yang-Mills singlets, by setting m_1 to zero, we obtain:

$$g_{HWG}^{2,SU(2)}(0, m_g, t) = \frac{1 + m_g t^3}{(1 - t^4)^2 (1 - m_g t)(1 - {m_g}^2 t^2)}. \tag{3.47}$$

This series does not contain any t^2 monomials, confirming that all simple pairs of fields that are Yang-Mills singlets have been excluded from the generators. The only singlets are at orders of t^4, showing that they only contain even numbers of pairs of X or ϕ fields [28].

Returning to the HWG given by 3.45 and 3.46, we can see that the global $SU(2_g)$ symmetry only appears amongst the generators as m_g or ${m_g}^2$. This appears to be part of a more general pattern, where the global symmetry appears amongst the HWG generating monomials at orders up to ${m_g}^k$, where k is the instanton number and equals the maximum degree of the Casimirs of the $U(k)$ quiver gauge group [19].

As for the case of $k = 1$, we can simplify the moduli space by factoring out the tensor products that result from $PE[[0;1]t]$. Physically, the fundamental of $SU(2_g)$ corresponds to the centre of mass of a system of instantons, and so working with such a reduced moduli space corresponds to an analysis in the instanton rest frame. If we reduce the HS 3.43 by taking a quotient by this centre of mass term, the HWG 3.45 evaluates to the reduced two $SU(2)$ instanton moduli space:[3]

$$g_{HWG}^{2,SU(2),red.}(m_1, m_g, t) = \frac{1 + m_g {m_1}^2 t^5}{(1 - {m_g}^2 t^2)(1 - {m_1}^2 t^2)(1 - m_g {m_1}^2 t^3)(1 - t^4)}. \tag{3.48}$$

Unlike the HWG 3.45 for the full moduli space, the reduced HWG 3.48 constitutes a complete intersection. The reduced HWG has dimension 4 and includes the monomial terms $m_g {m_1}^2 t^3$ and $m_g {m_1}^2 t^5$ that mix up the $SU(2)$ and $SU(2_g)$ symmetries. Such coupling between global $SU(2_g)$ and Yang-Mills symmetries appears to be an inherent feature of instanton moduli spaces for $k > 1$.

3.3.3. Moduli Space of Three $SU(2)$ Instantons

The case $k = 3$ gives rise to a $U(3)$ quiver gauge symmetry, and the field characters combine three separate non-Abelian product groups: quiver gauge $SU(3)$, Yang-Mills $SU(2)$ and the global $SU(2_g)$, in addition to the local and global $U(1)$ symmetries. Application of 3.35 thus gives rise to a

[3] This result is equivalent to a character expansion presented in [19], but uses the more concise HWG notation.

complicated collection of fields to be symmetrised.

In this case, it is more convenient to work with the Hilbert series for the reduced 3 instanton moduli space.

$$g_{HS}^{3,SU(2),red.}(x,y,t) \equiv PE\left[-[0;1]\,t\right]\ g_{HS}^{3,SU(2)}(x,y,t). \tag{3.49}$$

The plethystic class function for the refined Hilbert series $g_{HS}^{3,SU(2),red.}$ is nonetheless extremely unwieldy, so is not shown here. The HWG of the reduced HS follows from 3.37 as:

$$\begin{aligned} g_{HWG}^{3,SU(2),red.}(m_1,m_g,t) \equiv \oint_{SU(2)\otimes SU(2_g)} & d\mu^{SU(2)}(x) d\mu^{SU(2_g)}(y)\ PE\left[[1](x)m_1\right] \\ & \times\ PE\left[[1](y)m_g\right]\ g_{HS}^{3,SU(2),red.}(x,y,t) \end{aligned} \tag{3.50}$$

Evaluation yields:

$$g_{HWG}^{3,SU(2),red.}(m_1,m_g,t) = \frac{P(m_1,m_g,t)}{Q(m_1,m_g,t)}, \tag{3.51}$$

where the denominator is given by:

$$\begin{aligned} Q(m_1,m_g,t) = & \left(1-t^4\right)^2\left(1-t^6\right)\left(1-t^8\right) \\ & \times \left(1-{m_g}^2t^2\right)\left(1-m_gt^3\right)\left(1-{m_g}^3t^3\right) \\ & \times \left(1-{m_1}^2t^2\right)\left(1-{m_1}^2t^4\right)\left(1-{m_1}^6t^{10}\right) \\ & \times \left(1-m_g{m_1}^2t^3\right)\left(1-{m_g}^2{m_1}^2t^4\right), \end{aligned} \tag{3.52}$$

and the numerator $P(m_1,m_g,t)$ consists of 1 followed by 248 monomial terms, being palindromic of degree (12,7,43) in the variables (m_1,m_g,t).[4]

Table 3.24 identifies the combinations of the fields in the denominator $Q(m_1,m_g,t)$ that are the generators of the HWG. While the generators include field combinations in the $SU(2_g)$ fundamental, the only Yang-Mills $SU(2)$ irreps that occur are the adjoint and its symmetrisations. The generators do not include singlets comprised of pairs of fields, so we can verify that the F-term constraints have been implemented as intended by the Hyper Kähler quotient.

[4]See [28] for details.

$SU(2);SU(2_g)$	HWG Terms	Basic Field Combinations
$[0;0]$	t^4, t^6, t^8	Singlets
$[0;1]$	$m_g t^3$	$SU(2_g)$ irreps from $\phi^{(\alpha)}$
$[0;2]$	${m_g}^2 t^2$	
$[0;3]$	${m_g}^3 t^3$	
$[2;1]$	${m_1}^2 m_g t^3$	$SU(2)$ adjoint and $SU(2_g)$ irreps
$[2;2]$	${m_1}^2 {m_g}^2 t^4$	from $\phi^{(\alpha)}$, X_{12} and X_{21}
$[2;0]$	${m_1}^2 t^2$	$SU(2)$ adjoint from X_{12} and X_{21}
$[2;0]$	${m_1}^2 t^4$	
$[6;0]$	${m_1}^6 t^{10}$	$SU(2)$ symmetrised adjoint from X_{12} and X_{21}

Table 3.24.: Generators of HWG for Three $SU(2)$ Instanton Reduced MS

As before, we can also simplify the HWG into an unrefined version by either (a) setting the Yang-Mills gauge and global $SU(2)$ CSA coordinates in 3.49 to unity or (b) replacing monomial terms in the m_g and m_1 Dynkin label fugacities in a Taylor expansion of 3.51 by the corresponding irrep dimensions using the mapping:

$$ {m_g}^n {m_1}^{n_1} \rightarrow \dim[n]\dim[n_1] = (n+1)(n_1+1). \tag{3.53} $$

We obtain the palindromic Hilbert series:[5]

$$ g_{HS}^{3,SU(2),red.}(t) = \frac{\left(\begin{array}{c} 1 + 3t^2 + 6t^3 + 12t^4 + 16t^5 + 31t^6 + 36t^7 + 55t^8 + \\ 54t^9 + 60t^{10} + \ldots \text{palindrome} \ldots + t^{20} \end{array} \right)}{(1-t^2)^3(1-t^3)^4(1-t^4)^3}. \tag{3.54} $$

It is clear from the significant increase in complexity between the moduli spaces of two and three SU(2)-instanton theories that the mixing between the Yang-Mills and global $SU(2_g)$ irreps becomes highly non-trivial for $k >> 1$. This mixing results from the coupling between the fundamental of the global $SU(2_g)$ and the adjoint of the $U(k)$ quiver gauge group, introduced by the quiver diagram.

[5]This is consistent with the series obtained by using instanton counting methods set out in [67].

3.3.4. Geometric Properties of HWGs and HS of Instantons

As illustrated by the examples above, the representation structures and HWGs of instanton moduli spaces are generally considerably more complicated than those of SQCD. This arises due to the number of different symmetry groups involved and because they involve symmetrisations of the higher dimensioned adjoint representation of the quiver gauge group, in addition to those of basic irreps. This leads to many relations within the Hilbert series and so, while the generating functions for the HWGs and HS of instanton moduli spaces remain palindromic, only some of these moduli spaces are freely generated. The examples illustrate that while the HWGs for single instanton theories are freely generated [16], this is not the case for $k > 1$ instanton theories.

As in the case of SQCD, it is possible to decompose the dimensions of instanton moduli spaces into the dimensions of their HWGs and the degrees of the dimensional polynomials of the HWG irreps. This can be seen from Table 3.25.

Theory	|HWG| (a)	HWG Irrep	HWG Irrep Degree (b)	|HS| $(a)+(b)$
One $SU(2)$-Instanton	2	$[2n_1, n]$	2	4
Two $SU(2)$-Instantons	6	$[2n_1; n]$	2	8
Three $SU(2)$-Instantons	10	$[2n_1; n]$	2	12
One $SU(3)$-Instanton	2	$[n_1, n_1; n]$	4	6

Table 3.25.: Dimensions of Moduli Spaces of Selected Instanton Theories

The instanton moduli spaces calculated in Table 3.25 all include a contribution from global $SU(2)$ symmetries. If this contribution is excluded, we obtain reduced instanton moduli spaces, as discussed earlier.

As discussed in [16], when G is a simple Lie group, the Hilbert series for the reduced moduli spaces of one G-instanton ("RSIMS") take the form:

$$g_{HS}^{1,G,red.}(x,t) = \sum_{k=0}^{\infty} [k\theta]\,(x)\,t^{2k}, \tag{3.55}$$

where $k\theta$ is some multiple of the Dynkin labels θ of the adjoint representa-

tion of G. This expression is equivalent to the HWG:

$$g_{HWG}^{1,G,red.}(m,t) = PE\left[m^{\theta}t^2\right], \tag{3.56}$$

which is one dimensional. For example, the HWG of the RSIMS for $SU(3)$ is just $m_1 m_2 t^2$.

This leads to an elegant decomposition of the dimensions of RSIMS for simple Classical and Exceptional Lie groups into one dimensional HWGs and the degrees of their dimensional polynomials. These are calculated in the same manner as previously and are set out in Table 3.26. All the reduced one instanton moduli spaces have a HS (complex) dimension equal to twice the sum of the dual Coxeter labels of G [16]. This important observation holds the key to the Coulomb branch constructions that will be discussed for RSIMS and other nilpotent orbits in Chapter 6.

Series	Adjoint	HWG	|HWG| (a)	HWG Irrep Degree (b)	|HS| $(a)+(b)$
A_n	$A_1:[2]$	m^2t^2	1	1	2
	$A_2:[1,1]$	$m_1m_2t^2$	1	3	4
	$A_{\geq 3}:[1,0,\ldots,1]$	$m_1m_nt^2$	1	$2n-1$	$2n$
B_n	$B_1:[2]$	m^2t^2	1	1	2
	$B_2:[0,2]$	${m_2}^2t^2$	1	3	4
	$B_{\geq 3}:[0,1,\ldots,0]$	m_2t^2	1	$4n-5$	$4n-4$
C_n	$C_1:[2]$	m^2t^2	1	1	2
	$C_2:[2,0]$	${m_1}^2t^2$	1	3	4
	$C_{\geq 3}:[2,0,\ldots,0]$	${m_1}^2t^2$	1	$2n-1$	$2n$
D_n	$D_3:[0,1,1]$	$m_2m_3t^2$	1	5	6
	$D_{\geq 4}:[0,1,\ldots,0]$	m_2t^2	1	$4n-7$	$4n-6$
E_6	$[0,0,0,0,0,1]$	m_6t^2	1	21	22
E_7	$[1,0,0,0,0,0,0]$	m_1t^2	1	33	34
E_8	$[0,0,0,0,0,0,1,0]$	m_7t^2	1	57	58
f_4	$[1,0,0,0]$	m_1t^2	1	15	16
G_2	$[1,0]$	m_1t^2	1	5	6

Table 3.26.: Dimensions of RSIMS of Simple Lie Groups

We now turn to the subject of the nilpotent orbits of a Classical or Exceptional group, of which the RSIMS is the simplest non-trivial example.

4. Introduction to Nilpotent Orbits

4.1. Nilpotent Matrices, Nilpositive Elements and Nilpotent Orbits

The subject of nilpotent orbits can be approached in a variety of ways. Traditional approaches involve the analysis of the matrices and/or generators of the Lie algebra $\mathfrak{g}$ of some Lie group G. From the perspective of this study, the closure of a nilpotent orbit can be considered as a moduli space described by class functions on the representation lattice of G. So, as a necessary preliminary to motivating the use of SUSY quiver theories and their moduli spaces in this context, it is useful to review the relationships between a group G, the nilpotent matrices or generators X of its Lie algebra $\mathfrak{g}$, and the nilpotent orbits $\mathcal{O}_X$ to which they give rise.

A nilpotent matrix X over some field (taken as $\mathbb{C}$) is one that vanishes at some power $X^k = 0$ for $k \geq d$, where d is defined as the nilpotent degree of the matrix. By similarity transformation, all the eigenvalues of X are zero and all its invariants vanish: $\det[X] = 0, \ldots, \mathrm{tr}[X] = 0$. Examples of nilpotent matrices include strictly upper (or lower) triangular matrices. Thus, a *nilpositive* raising operator X of a Lie algebra $\{H_i, E^+_\alpha, E^-_\alpha\}$, defined as $X \equiv \sum_\alpha u_\alpha E^+_\alpha$, for some coefficients u_α, acts as a nilpotent matrix on the vector space of representations.[1] Importantly, matrices obtained by applying a similarity transformation to X retain zero eigenvalues and remain nilpotent. This leads naturally to the concept of a nilpotent orbit defined as an equivalence class [33]:

$$\mathcal{O}_X = \{M : M = AXA^{-1} \text{ for } A \in G\}. \tag{4.1}$$

[1] See section 4.2.3 for Lie algebra notational conventions.

The simple restriction that a matrix should be nilpotent can be combined with further restrictions, with respect to nilpotent degree, matrix rank, etc., to define a poset (partially ordered set) of equivalence classes of nilpotent matrices. This poset can be graphed to give a distinct *Hasse diagram* for each Lie group. A similar Hasse diagram can be drawn based on the moduli space inclusion relations between nilpotent orbits.

The boundary of all the nilpotent orbits associated with these equivalence classes is known as the *closure of the maximal nilpotent orbit* or *nilpotent cone* $\mathcal{N}$. Similarly, each equivalence class gives rise to the *closure* of a nilpotent orbit. By a common abuse of terminology, the closures of nilpotent orbits are often referred to simply as nilpotent orbits, and this is the convention generally adopted in this study.

If we consider the simple condition that a Lie algebra matrix generator X should be nilpotent, it follows, from the vanishing eigenvalues of X, that the Casimir operators [62] formed from the traces of symmetrised products of X should vanish:

$$\forall d : d \in \{\text{Degrees of Symmetric Casimirs of G}\} \rightarrow \text{tr}\left[X^d\right] = 0, \qquad (4.2)$$

and this vanishing of Casimir operators generalises to non-matrix groups.

The degrees $\{d\}$ of symmetric Casimir invariants, which are equal in number to the rank of G, are shown in Table 3.2. Viewed as a moduli space, the nilpotent cone $\mathcal{N}$ is therefore the quotient of the moduli space of Lie algebra generators of G (the PE of the adjoint representation) divided by the moduli space of Casimir invariants. The resulting Hilbert series takes the form:

$$\begin{aligned} g_{HS}^{G,\mathcal{N}} &= \frac{PE\left[\chi^G_{[adj.]}t\right]}{\prod\limits_{d\in\text{Casimirs}[G]} PE\left[t^d\right]} \\ &= \prod_{d\in\text{Casimirs}[G]} \left(1-t^d\right) PE\left[\chi^G_{[adj.]}t\right] \\ &= mHL^G_{[0,\ldots,0]}(t) \end{aligned} \qquad (4.3)$$

This exactly matches the definition of the modified Hall Littlewood function $mHL^G_{[0,\ldots,0]}$ in 2.17. So, the Hilbert series of the (closure of the) maximal nilpotent orbit is equal to $mHL^G_{[singlet]}$ and has the dimension:

$$|\mathcal{N}| = |\mathfrak{g}| - \text{rank}[\mathfrak{g}]. \tag{4.4}$$

This compares with the dimension $|\mathcal{O}_X| \leq |\mathcal{N}|$ of the nilpotent orbit associated with general X, which is given by [33]:

$$|\mathcal{O}_X| = |\mathfrak{g}| - |\mathfrak{g}^X|, \tag{4.5}$$

where $\mathfrak{g}^X$ is the centraliser of X in $\mathfrak{g}$, defined as $\mathfrak{g}^X \equiv \{\mathfrak{c} : \mathfrak{c} \in \mathfrak{g}\ \&\ [X, \mathfrak{c}] = 0\}$. Thus $|\mathfrak{g}^X| \geq \text{rank}[\mathfrak{g}]$.

To give examples, first consider $SU(2)$, which has one non-trivial nilpotent orbit. $SU(2)$ has a three dimensional Lie algebra matrix generator given by $M = \begin{pmatrix} z & x-iy \\ x+iy & -z \end{pmatrix}$. Imposing the nilpotence condition $M^2 = 0$ entails $x^2 + y^2 + z^2 = 0$, so a general nilpotent matrix from the complexified Lie algebra of $SU(2)$ has *two* free complex parameters. Turning to the adjoint representation, the corresponding matrix generator is $M = i \begin{pmatrix} 0 & z & -y \\ -z & 0 & x \\ y & -x & 0 \end{pmatrix}$. In both cases, the single SU(2) Casimir invariant is of degree two, $\text{tr}[M.M] = 2(x^2+y^2+z^2)$, and vanishes under the nilpotence condition, as expected from 4.2. From a Lie algebra perspective, the $SU(2)$ raising operator E_1^+ has itself as a single centraliser, so, in accordance with 4.5, the dimension of the nilpotent orbit is *two*.

Or, consider $SU(3)$, which has two non-trivial nilpotent orbits. The nilpotence condition $M^2 = 0$ places 4 conditions on the 8 dimensional Lie algebra and yields a matrix generator with *four* free complex parameters. From a Lie algebra perspective, the $SU(3)$ raising operator $X = E_{12}^+$, has the centraliser $\mathfrak{g}^X = \{E_1^+, E_2^+, E_{12}^+, H_1 - H_2\}$, so, by 4.5, the dimension of this nilpotent orbit is *four*.

Alternatively, the weaker nilpotence condition $M^3 = 0$ places 2 conditions on the Lie algebra of $SU(3)$ and yields a matrix with *six* free parameters. Taking the $SU(3)$ raising operator as $X = E_1^+ + E_2^+$, this has the centraliser $\mathfrak{g}^X = \{E_1^+ + E_2^+, E_{12}^+\}$, so, by 4.5, the dimension of this nilpotent orbit is *six*. $SU(3)$ has $|\mathfrak{g}| = 8$ and two Casimir invariants, so this is the maximal nilpotent orbit.

These examples illustrate the correspondence between the degrees of freedom of nilpotent matrices and the dimensions of orbits described by equivalence classes of nilpotent Lie algebra elements or their moduli spaces.

While the general relationship between nilpositive elements and moduli spaces requires a more thorough account, the principle of analysing the closures of nilpotent orbits in terms of the moduli spaces of representations extends in a natural way from Classical groups through Exceptional groups, as will be shown.

4.2. SU(2) Homomorphisms and Standard Triples

As a further preliminary, it is important to review the means of identifying and classifying the nilpotent orbits of G. This can be done in terms of $SU(2)$ homomorphisms, partitions or dimensions, amongst other methods to be discussed later.

As described in [33], the Jacobson-Morozov theorem shows that each nilpotent element X of $\mathfrak{g}$ falls within some *standard triple* $\{H, X, Y\}$ of some $SU(2)$ subalgebra of $\mathfrak{g}$. Also, a theorem of Kostant shows that the map from standard triples to nilpotent elements is injective (or one to one), up to conjugation of the nilpotent elements. Taken together, these theorems establish a bijection between standard triples and conjugacy classes of nilpotent elements. By arguing a bijection between conjugacy classes of nilpotent elements and nilpotent orbits, (Theorem 3.2.10) [33] further claims a bijection between standard triples and (closures of) nilpotent orbits $\mathcal{O}_X$. Each standard triple $\{H, X, Y\}$ is in turn defined by a homomorphism (or embedding) ρ from G to $SU(2)$ and this implies a bijection between $SU(2)$ homomorphisms ρ and distinct nilpotent orbits $\mathcal{O}_X$.

The possible embeddings of $SU(2)$ into G were first systematically enumerated, for both Classical and Exceptional groups, by Dynkin [54]. The *standard tables* of nilpotent orbits in the recent Literature, for example in [33], are essentially unchanged from the list of $SU(2)$ subalgebras identified by Dynkin.

4.2.1. SU(2) Homomorphisms

From the perspective of character analysis, each such homomorphism ρ corresponds to a fugacity map between the CSA coordinates $\{x_1, \ldots, x_r\}$ of G and $\{x\}$ of $SU(2)$, under which the character of every representation of G decomposes into a sum of characters of $SU(2)$ irreps:

$$\begin{aligned} \rho : \{x_1, \ldots, x_r\} &\to \{x^{\omega_1}, \ldots, x^{\omega_r}\}, \\ \rho : \chi^G(x_1, \ldots, x_r) &\to \sum\nolimits_n^{\oplus} a_n [n](x), \end{aligned} \tag{4.6}$$

where the coefficients a_n are non-negative integers. The exponents $[\omega_1, \ldots, \omega_r]$ in 4.6 are referred to as the *weight map* of ρ in this study. The enumeration of nilpotent orbits via $SU(2)$ homomorphisms is therefore equivalent to the problem of identifying all such valid weight maps.

We can refine the problem as follows. The exponents of x that appear in a valid map $\rho(R)$ of some representation R of G are weight space Dynkin labels of SU(2) and must therefore be integers. Moreover, the highest exponent of x that can appear must be an integer below $|R|$, otherwise the monomials within $\rho(R)$ could not form a complete representation. Furthermore, once we establish that a map ρ is valid for all the basic irreps of G (those with highest weight Dynkin labels of the form $[0, \ldots, 1, \ldots, 0]$), it follows that the map must be valid for all representations of G [58]. This limits the number of possible weight maps at most to the product of the dimensions of the basic irreps of G.

Indeed, the number of possible homomorphisms can be limited further by a theorem [54], which entails that ρ, when expressed in terms of simple root fugacities $\{z_1, \ldots, z_r\}$ of G and $\{z\}$ of $SU(2)$, must be conjugate under the action of the Weyl group of G to a map of the form:

$$\rho : \{z_1, \ldots z_r\} \to \{z^{\frac{q_1}{2}}, \ldots, z^{\frac{q_r}{2}}\}, \tag{4.7}$$

where $q_i \in \{0, 1, 2\}$. The labels $[q_1, \ldots, q_r]$ are termed the *Characteristic* of a nilpotent orbit [54]. In this study, the Characteristic is also refered to as the *root map* of ρ.[2] Thus, there are at most $3^{\text{rank}[G]}$ root maps that need to be tested, which is a straightforward computational procedure for low rank groups.[3]

These homomorphisms can also be labelled by the $SU(2)$ decomposition of $\rho(R)$, where R is some representation of G. R is usually chosen to be the

[2]The Literature also refers to a Characteristic $G[\rho]$ as the Dynkin labels (of a nilpotent orbit), not to be confused with the weight space Dynkin labels (of irreps) $[n]_G$. Since the labels in a Characteristic can only be 0, 1 or 2, it can be convenient to omit the separators ",".

[3]Note that root and weight fugacities and maps are related by the Cartan matrix of G as $z = x^A$ and $q = A\omega$, respectively.

fundamental representation for A series groups, or the vector representation for BCD series groups. Such decompositions of $\rho(R)$ are conventionally expressed using condensed partition notation, under which each $SU(2)$ irrep $[n]$ with non-zero multiplicity a_n is assigned an element in the partition equal to its dimension, with an exponent equal to its multiplicity:

$$\begin{aligned} \rho(R) &= \sum_{n=0}^{n_{\max}} a_n\,[n], \\ &\Leftrightarrow \left(|[n_{\max}]|^{a_{n_{\max}}}, \ldots, |[n]|^{a_n}, \ldots, 1^{a_0}\right). \end{aligned} \tag{4.8}$$

Additional selection rules are required to ensure that the representations $\rho(R)$ assigned to each irrep R of G are consistent with its bilinear invariants. Recall that an irrep can be classified as (i) real, (ii) pseudo real or (iii) complex, depending, respectively, on whether it has (i) a symmetric bilinear invariant with itself, (ii) an antisymmetric bilinear invariant with itself, or (iii) a bilinear invariant with its contragredient representation (complex conjugate in the case of unitary representations). As shown in [33], when R has bilinear symmetric or antisymmetric invariants, this requires *irrep selection rules*, to exclude any homomorphisms ρ under which such bilinears change type:

1. Real R. If a partition element (i.e. $SU(2)$ irrep) of even dimension appears, it must appear an even number of times. This ensures that any pseudo real $SU(2)$ irreps come in pairs. These are often referred to as B partitions or D partitions.

2. Pseudo real R. If a partition element (i.e. $SU(2)$ irrep) of odd dimension appears, it must appear an even number of times. This ensures that any real $SU(2)$ irreps come in pairs. These are often referred to as C partitions.

3. Complex R. Complex irreps have bilinear invariants with their complex conjugates, rather than with themselves. Conjugate pairs of representations have identical $SU(2)$ partitions, so no selection rules apply.

It is important to appreciate that these irrep selection rules depend on the type of representation R of the parent group, upon which ρ acts, and not

on the parent group series (as implied in some of the Literature). The Real and Pseudo real rules apply across all representations of both Classical and Exceptional groups, although they are largely redundant in the case of A series groups, where the fundamental irreps are complex and not subject to these restrictions.

Appendix B tabulates these homomorphisms for Classical groups up to rank 5 and for Exceptional groups. The homomorphisms are described by their dimensions, their Characteristics (or root maps) and weight maps, and the resulting partitions of the key irreps of G. While partial tables are often presented in the Literature [33, 30], this fuller presentation, including vectors/fundamentals, spinors and the adjoint representation, is helpful for the analysis of nilpotent orbits.

As an example, A_3 has five nilpotent orbits and these can be referred to uniquely, either by the partition data assigned (under ρ) to one of its representations, or by the Characteristic (root map), or by the weight map. Taking the character of the fundamental of A_3 as $[1,0,0] = x_1 + x_2/x_1 + x_3/x_2 + 1/x_3$ and the simple root fugacities of A_3 as $\{z_1 = {x^2}_1/x_2, z_2 = {x^2}_2/x_1/x_3, z_3 = {x_3}^2/x_2\}$, the homomorphism ρ with Characteristic [222] can be written in any one of the following equivalent ways:

$$\begin{aligned}
\rho : (z_1, z_2, z_3) &\to (z, z, z)\,, \\
\rho : (x_1, x_2, x_3) &\to \left(x^3, x^4, x^3\right), \\
\rho : (x_1 + x_2/x_1 + x_3/x_2 + 1/x_3) &\to \left(x^3 + x + 1/x + 1/x^3\right), \\
\rho : [1,0,0] &\to [3], \\
\rho : [1,0,0] &\to (4).
\end{aligned} \tag{4.9}$$

Intriguingly, while these $SU(2)$ homomorphisms identify all the Characteristics of Exceptional and Classical group nilpotent orbits that appear in standard tables, this method also leads to a few extra root maps for some Exceptional groups, as highlighted in Appendix B.5. One extra root map arises in F_4; there are 3 in E_6, 8 in E_7 and 39 in E_8. Their moduli spaces are examined and discussed in Chapter 7.

4.2.2. Partitions

For Classical groups, there is a bijective correspondence between $SU(2)$ homomorphisms that satisfy the irrep selection rules and partitions [33]. As an alternative to finding the partitions of nilpotent orbit from $SU(2)$ homomorphisms, they can also be found from partition generating functions that encapsulate the irrep selection rules. We introduce fugacities $\{\nu_1, \ldots, \nu_N\}$, indexed according to the possible dimensions of $SU(2)$ irreps, where N is the fundamental/vector dimension of G, and use exponents to count the multiplicities of irreps. For example, $\rho \equiv (4)$ maps to the monomial ν_4 and $\rho \equiv (1^2, 2)$ maps to the monomial $\nu_1^2\nu_2$. We use the overall counting fugacity t. A short calculation then leads to the generating functions for partitions set out in Table 4.1.

Group	Partition Series	Generating Function
$SU(N)$	$\sum_{i=1}^{\infty} P_{SU}(\nu_1, \ldots, \nu_\infty)\, t^i$	$\prod_{i=1}^{\infty} \frac{1}{1-\nu_i t^i} - 1$
$USp(N)$	$\sum_{i=1}^{\infty} P_{USp}(\nu_1, \ldots, \nu_\infty)\, t^i$	$\prod_{i=1}^{\infty} \frac{1}{1-\nu_i t^i} \prod_{j=0}^{\infty} \frac{1}{1+\nu_{2j+1} t^{2j+1}} - 1$
$SO(N)$	$\sum_{i=1}^{\infty} P_{SO}(\nu_1, \ldots, \nu_\infty)\, t^i$	$\prod_{i=1}^{\infty} \frac{1}{1-\nu_i t^i} \prod_{j=1}^{\infty} \frac{1}{1+\nu_{2j} t^{2j}} + \prod_{j=1}^{\infty} \frac{1}{1+\nu_{2j}^2 t^{4j}} - 2$

Table 4.1.: Generating Functions for Partitions of Classical Orbits

For example, to obtain the partitions for the fundamental of $SU(4)$, we find the coefficient of t^4 in the Taylor expansion of the generating function for $\sum_{i=1}^{\infty} P_{SU}(\nu_1, \ldots, \nu_\infty)\, t^i$. This is $\nu_1^4 + \nu_1^2\nu_2 + \nu_1\nu_3 + \nu_2^2 + \nu_4$, corresponding to the set of five partitions $\{(1^4), (1^2, 2), (1, 3), (2^2), (4)\}$.

In the case of Exceptional groups, there is no such bijective correspondence between partitions of the vector/fundamental representation and $SU(2)$ homomorphisms. For example, both G_2 and B_3 have 7 dimensional vector/fundamental representations, but G_2 only has 5 nilpotent orbits, compared with the 7 of B_3.

It is also noteworthy that a description of nilpotent orbits, by partitions of the vector representation alone, does not give a unique labelling for D_{even} groups. Recalling that the spinor is a more fundamental representation than a vector, we can see in appendix B.4, for example, that the (2^4) and (4^2) vector partitions of D_4 both correspond to pairs of nilpotent orbits that are

distinguished only by their spinor partitions.

Partitions that only contain pairs of even elements are referred to as *very even*. The very even vector partitions of $SO(4k)$ groups all correspond to *spinor pairs* of nilpotent orbit moduli spaces and can be encoded in a simple generating function, as shown in Table 4.2.

Group	Partition Series	Generating Function
$SO(4k)$	$\sum_{i=1}^{\infty} P_{SO}^{\text{Spinor Pair}}(\nu_1, \ldots, \nu_\infty)\, t^i$	$\prod_{i=1}^{\infty} \frac{1}{1-\nu_{2i}^2 t^{4i}} - 1$

Table 4.2.: Generating Functions for Partitions of Spinor Pair Orbits

The partitions of $N = 4k$ are given by the coefficients of t^N. The generating function can be unrefined, by setting $\nu_i \to 1$, to find the number of $SO(4k)$ spinor pair nilpotent orbits as a function of the vector dimension.

4.2.3. Standard Triples

It is useful to elaborate on the relationship between $SU(2)$ homomorphisms and standard triples $\{H, X, Y\}$. Standard triples are defined by the commutation relations $[H, X] = 2X, [H, Y] = -2Y, [X, Y] = H$. These operators are embedded in the Lie algebra $\mathfrak{g}$ of G, which is given by the operators $\{H_i, E_{\alpha+}, E_{\alpha-}\}$, as detailed in Appendix A.4.

Now, consider a Characteristic $[q] \equiv [q_1, \ldots, q_r]$, with corresponding weight map $[w] \equiv [w_1, \ldots, w_r]$, related by $[q] = A \cdot [w]$. Each root, $\alpha = \sum_i a_i \alpha_i$, where $\{\alpha_1, \ldots, \alpha_r\}$ are simple roots, is assigned a Characteristic height, $[\alpha] \equiv \sum_{i=1}^{r} a_i q_i$.

The elements of the standard triple $\{H, X, Y\}$ are chosen as:

$$\begin{aligned} H &= \sum_{i=1}^{r} w_i H_i, \\ X &= \sum_{\alpha \in \Phi_G : [\alpha]=2} u_\alpha E_{\alpha+}, \\ Y &= \sum_{\alpha \in \Phi_G : [\alpha]=2} v_\alpha E_{\alpha-}, \end{aligned} \tag{4.10}$$

for some coefficients u_α and v_α. X contains only those roots with $[\alpha] = 2$, and each of these satisfies the commutation relations $[H, E_{\alpha+}] = 2E_{\alpha+}$,

so $[H, X] = 2X$. Similarly, Y satisfies $[H, Y] = -2Y$. The commutation relation $[X, Y] = H$ determines u_α and v_α, up to scaling freedoms [54].

As the simplest example, consider the $SU(2)$ homomorphism with the Characteristic [2]. This maps the positive root of $G = SU(2)$ to the positive root of an $SU(2)$ subalgebra and so the nilpositive element is just $X = E_{1+}$. The relationship between the standard triple $\{H, X, Y\}$ of the SU(2) subalgebra and its parent $SU(2)$ algebra $\{H_1, E_{1+}, E_{1-}\}$ follows directly, as set out in Table 4.3. The coefficient of H_1 in the standard triple matches the *weight* map, which is [1].

Parent group	Lie algebra
$SU(2)$	$[H_1, E_{1\pm}] = \pm 2E_{1\pm} \quad [E_{1+}, E_{1-}] = H_1$
	Nilpotent element
Characteristic	[2]
Weight map	[1]
Positive roots	E_{1+}
$\{H, X, Y\}$	$\{H_1, E_{1+}, E_{1-}\}$

Table 4.3.: Standard Triple for SU(2) Homomorphism

The analysis for $SU(3)$ in Table 4.4 is more interesting. In this case there are two non-trivial nilpotent orbits, so that the Characteristic [11] generates the nilpositive element E_{12+}, while the Characteristic [22] generates the nilpositive element $(E_{1+} + E_{2+})$. Once again, the coefficients of H_1 and H_2 match the labels [1 1] and [2 2] in the corresponding weight maps. The standard triples can be verified using the Lie algebra relations.

This analysis generalises to any $SU(2)$ homomorphism of G. The nilpotent operators E_α in the standard triple follow directly from the Characteristic. The coefficients u_α and v_α can, in principle, be determined, up to scaling freedoms, from the Lie algebra $\mathfrak{g}$.

Notwithstanding the received bijective relationship between standard triples and nilpotent orbits, there is no simple prescription in the Literature for finding the closure of a nilpotent orbit from its standard triple, although its dimensions can be obtained from 4.5. Accordingly, this study focuses first on methods based on partitions, which lead to the Higgs branch constructions of Chapter 5. The Coulomb branch constructions of Chapter 6 draw directly on Characteristics and weight maps. By way of integrating

Parent group	Lie algebra
$SU(3)$	$[H_1, E_{1\pm}] = \pm 2E_{1\pm}$ $[H_2, E_{1\pm}] = \mp E_{1\pm}$ $[H_1, E_{2\pm}] = \mp E_{2\pm}$ $[H_2, E_{2\pm}] = \pm 2E_{2\pm}$ $[H_{1 \text{ or } 2}, E_{12\pm}] = \pm E_{12\pm}$ $[E_{1+}, E_{1-}] = H_1$ $[E_{2+}, E_{2-}] = H_2$ $[E_{12+}, E_{12-}] = H_1 + H_2$ $[E_{1\pm}, E_{2\pm}] = \pm E_{12\pm}$ $[E_{1\pm}, E_{12\mp}] = \mp E_{2\mp}$ $[E_{2\pm}, E_{12\mp}] = \pm E_{1\mp}$ (other commutators zero)
	Nilpotent elements
Characteristic	[11]
Weight map	[11]
Positive roots	$\{E_{12+}\}$
$\{H, X, Y\}$	$\{H_1 + H_2, E_{12+}, E_{12-}\}$
Characteristic	[22]
Weight map	[22]
Positive roots	$\{E_{1+}, E_{2+}\}$
$\{H, X, Y\}$	$\{2H_1 + 2H_2, E_{1+} + E_{2+}, 2E_{1-} + 2E_{2-}\}$

Table 4.4.: Standard Triples for SU(3) Homomorphisms

these approaches, a method developed in the course of this study, for calculating the Hilbert series of the closures of nilpotent orbits, based on their Characteristics, is presented in Chapter 7.

4.3. Dimensions of Nilpotent Orbits

The dimensions $|\mathcal{O}_\rho|$ of a nilpotent orbit $\mathcal{O}_\rho \sim \mathcal{O}_X$ can be found directly by subtracting from $|G|$ the length of the adjoint partition (i.e. the number of $SU(2)$ representations into which the adjoint representation of G is split by $\rho^G(adj.)$):

$$|\mathcal{O}_\rho| = |G| - \left|\rho^G(adj.)\right|. \tag{4.11}$$

This can be checked by inspection of Appendix B. Comparing 4.5, it appears that the dimension of the centralizer $\mathfrak{g}^X$ is equal to the length of the partition $\left|\rho^G(adj.)\right|$.

For a Classical group, the dimension $|\mathcal{O}_\rho|$ can also be calculated, as set out in [33], from the partition data of the defining fundamental/vector representation. Consider the ordered partition (in standard notation) $\rho(def.) = (\rho_1, \ldots, \rho_n)$, with ρ_1 being the greatest element appearing in ρ. The trans-

pose partition $\sigma \equiv \rho^T$, where $\sigma = (\sigma_1, \ldots, \sigma_{\rho_1})$, can be obtained using Young's diagrams. It is convenient, for our purposes, to restate (6.1.4) of [33] more simply in terms of rank r and this transposed partition $\sigma(def.)$, to obtain the dimension formulae shown in Table 4.5. These dimensions are based on a lattice over a complex space and are always even.

Group	$\lvert\mathcal{O}_\rho\rvert$
A_r	$(r+1)^2 - \sum_i \sigma_i^2$
B_r	$r(2r+1) - \frac{1}{2}\sum_{i\ odd} \sigma_i(\sigma_i - 1) - \frac{1}{2}\sum_{i\ even} \sigma_i(\sigma_i + 1)$
C_r	$r(2r+1) - \frac{1}{2}\sum_{i\ odd} \sigma_i(\sigma_i + 1) - \frac{1}{2}\sum_{i\ even} \sigma_i(\sigma_i - 1)$
D_r	$r(2r-1) - \frac{1}{2}\sum_{i\ odd} \sigma_i(\sigma_i - 1) - \frac{1}{2}\sum_{i\ even} \sigma_i(\sigma_i + 1)$

Table 4.5.: Dimension Formulae for Classical Orbits

We can identify within the expressions for $|\mathcal{O}_\rho|$, the dimension of G, reduced by a sequence of dimensions of square matrices defined by σ. For the A series, this sequence is associated with unitary matrices, while for BCD series, this sequence is associated with alternating symmetric and antisymmetric real matrices.

Importantly, identical dimensions can also be obtained by assigning a Higgs branch quiver theory to a Classical vector/fundamental partition that satisfies the Real and Pseudo real rules selection rules, as will be shown in Chapter 5.

4.4. Terminology

Before proceeding, it is helpful to collect some of the elaborate terminology that permeates the classification of nilpotent orbits.

4.4.1. Canonical Orbits

The dimensions of nilpotent orbits have a partial ordering, which is often expressed using Hasse diagrams. Formally, this partial ordering is defined by inclusion relations amongst the closures $\bar{\mathcal{O}}$ of nilpotent orbits $\mathcal{O}$.[4] There

[4]The closures $\bar{\mathcal{O}}$ correspond to the quiver theory moduli spaces that are calculated in this study.

are a number of canonical orbits within this partial ordering:

1. The *trivial orbit*. This is associated with the partitions $\rho^G(R) = (1^{|R|})$ and always has zero dimension.

2. The *minimal orbit*. This is the first orbit with non-zero dimension and is always unique. Its complex dimension is equal to twice the sum of the dual Coxeter labels of G. This equals the dimension of the reduced single instanton moduli space of G.

3. The *sub-regular orbit*. This is the orbit with next to highest dimension. It is always unique, having a complex dimension equal to the number of the roots of G, less 2.

4. The *maximal orbit*. This is the orbit with highest dimension and is always unique. Its complex dimension is equal to the number of roots of G. This equals the dimension of the modified Hall Littlewood function $mHL^G_{[0,\ldots,0]}$.

The above orbits are not distinct for low rank groups. For example, in A_1, the minimal and maximal orbits coincide, as do the trivial and sub-regular.

4.4.2. Distinguished Orbits

A *distinguished* nilpotent element is associated with an $SU(2)$ homomorphism in which $\rho^G(adj.)$ contains no $SU(2)$ singlets [33]. This rule leads to the following list of distinguished nilpotent orbits:[5]

A_r: Maximal nilpotent orbit only,

B_r: Partitions of $2r+1$ into distinct odd parts,

C_r: Partitions of $2r$ into distinct even parts,

D_r: Partitions of $2r$ into distinct odd parts,

G_2: [20] and [22],

F_4: [0200], [0202], [2202] and [2222],

E_6: [202020] [220222] and [222222],

[5]The list of distinguished Exceptional group Characteristics appears in Table 23 of [54].

E_7: [0020020], [2020020], [2020220], [2202022], [2202222] and [2222222],

E_8: [00020000], [00200020], [00200200], [00200220], [20200200], [20200220], [20202020], [20202220], [22020222], [22022222] and [22222222].

The vector partitions of SO and USp groups that correspond to distinguished nilpotent orbits can be encoded as the simple generating functions in Table 4.6. The partitions of N are given by the coefficients of t^N, as

Group	Partition Series	Generating Function
$USp(N)$	$\sum_{i=1}^{\infty} P_{USp}^{\text{Dist.}}(\nu_1, \ldots, \nu_\infty)\, t^i$	$\prod_{i=1}^{\infty} \left(1 + \nu_{2i} t^{2i}\right)$
$SO(N)$	$\sum_{i=1}^{\infty} P_{SO}^{\text{Dist.}}(\nu_1, \ldots, \nu_\infty)\, t^i$	$\prod_{i=0}^{\infty} \left(1 + \nu_{2i+1} t^{2i+1}\right)$

Table 4.6.: Generating Functions for Distinguished BCD Partitions

described in section 4.2.2. These generating functions can be unrefined, by setting $\nu_i \to 1$, to find the number of distinguished nilpotent orbits as a function of the vector dimension N.

4.4.3. Even Orbits

An *even* nilpotent orbit is one that has a Characteristic containing the labels 0 or 2 only. All distinguished orbits are even [33].

4.4.4. Richardson Orbits

A *Richardson* nilpotent orbit is one that can be induced from the the trivial nilpotent orbit of a subgroup [33]. Every nilpotent orbit that has a Characteristic containing only the labels 0 or 2 has a quotient group G/H structure and can be induced, as will be explained in section 7.1, from the trivial nilpotent orbit of the subgroup H, whose Dynkin diagram is defined by the 0 labels of the Characteristic. All even orbits are thus Richardson orbits. In addition, some groups have *non-even Richardson* orbits, with the rules for identifying such orbits being given in [68]. Richardson orbits have polarizations [69] and symplectic resolutions [68]. The complete set of Richardson orbits is:

A_r: All nilpotent orbits,

B_r: Partitions of $2r+1$, whose first q parts are odd, where q is *odd*, with the remaining parts even,

C_r: Partitions of $2r$, whose first q parts are odd, where q is *even*, with the remaining parts even,

D_r: Partitions of $2r$, whose first q parts are odd, with the remaining parts even, and either (i) q is even but $q \neq 2$, or (ii) $q = 2$ and the two odd parts are located at positions $2k-1$ and $2k$ for some integer k,

EFG: All even orbits, plus

F_4: [1012],

E_6: [100010], [010100], [100012], [110111] and [110112],

E_7: [0100011], [1010100], [2010100], [2101101] and [2101021],

E_8: [01001002], [101010000], [21010220], [01000120], [10101010], [10101020] and [20101020].

4.4.5. Rigid vs Non-Rigid Orbits

A *non-rigid* nilpotent orbit is one that can be induced from some nilpotent orbit of a subgroup. All Richardson orbits are thus non-rigid, being induced from a trivial nilpotent orbit. Importantly, any orbit whose Characteristic contains 2 can be induced from the orbit of the subgroup defined by the Dynkin diagram and Characteristic that remains after removing one or more nodes with Characteristic 2 from the parent diagram.

Conversely, a *rigid* nilpotent orbit is one that *cannot* be induced from a nilpotent orbit of a subgroup. A rigid nilpotent orbit has a Characteristic containing 0 and 1 only, as a necessary, but not sufficient, condition. Notably, the minimal nilpotent orbits of simple groups, other than those isomorphic to the A series, are rigid [33]. Also, for example, $D_4[1011]$ is rigid amongst orbits of low rank groups. Rigid orbits of Exceptional groups are identified in [70].

The inclusion relations between the above types of orbit provide a classi-

fication scheme:

$$\{Nilpotent\ Orbits\} = \{Rigid\} \cup \{Non - Rigid\}$$
$$\{Non - Rigid\} \supset \{Richardson\} \supset \{Even\} \supset \{Distinguished\} \tag{4.12}$$

4.4.6. Special Orbits

A *special* nilpotent orbit is one that is invariant under two applications of the Spaltenstein map. For Classical groups the Spaltenstein map is defined by fundamental/vector partition transposition, followed, if the transpose partition is not valid under the Real/Pseudo real selection rules, by BCD-collapse to a lower partition. The Spaltenstein map d is thus many to one, often described as $d^3 = d$, and can lead to the conflation of distinct nilpotent orbits, as discussed in [24]. All A series nilpotent orbits are special. A special BC series nilpotent orbit is one whose Spaltenstein map does not require BC collapse.

A Spaltenstein map can also be defined for Exceptional groups. All Richardson orbits are special, as is any orbit of a higher rank group induced from a special orbit [33]. Some rigid orbits are also special.

4.4.7. Normal vs Non-Normal Orbits

From the perspective of this study, a more important distinction is that between *normal* and *non-normal* nilpotent orbits. A normal symplectic variety only contains singularities that are rational Gorenstein [71] and this entails that it is Calabi-Yau with a palindromic Hilbert series [13]. Consistent with this, the *normal* nilpotent orbits of Classical groups (calculated up to rank 4, as tabulated in Chapter 5) were found in [24] to have palindromic Hilbert series; however, *non-normal* nilpotent orbits were found to have non-palindromic Hilbert series.

The *normalisation* of a nilpotent orbit can be defined as a palindromic moduli space of the same dimension that forms a covering space. A normal nilpotent orbit is its own normalisation. Normalisations of non-normal nilpotent orbits contain elements outside the nilpotent cone $\mathcal{N}$.

For Classical groups, it was shown in [6], based on a geometric analysis, that the vector partition of a non-normal orbit is always related to that of the orbit immediately below it, by a particular degeneration of its Young's

diagram. In this degeneration, a pair of even rows in some *sub-diagram*, described by the partition $(2r, 2r)$, degenerates to $(2r-1, 2r-1, 1, 1)$; all the rows above and all the columns to the left of the sub-diagram remain unchanged. Such degenerations result from a D_{2r} subalgebra of a BCD series parent and are termed $A_{2r-1} \cup A_{2r-1}$ degenerations. A D_{2r} group may have several degenerations associated with its spinor pairs, including $A_{2r-1} \cup A_{2r-1}$ and $A_1 \cup A_1$ degenerations.

All A series nilpotent orbits are normal. The Classical non-normal nilpotent orbits up to rank 5 are:

B: $[101], [2101], [10001], [22101]$,

C: $[0200], [02000]$,

D: $[02] \cup [20], [0002] \cup [0020], [0202] \cup [0220], [01011]$.

These are all Richardson orbits of non-distinguished type.

A similar situation arises in Exceptional groups, where non-normal nilpotent orbits are also associated with particular degenerations of their partitions [71]. The non-normal nilpotent orbits of Exceptional groups are identified in [72], being:

G_2: [01],

F_4: [0002], [2001], [0101], [1010], [1012], (5 cases),

E_6: [100011], [200020], [100012], [010101], [200022], (5 cases),

E_7: [2000100], [2000020], [1010000], [1001010], [0100011], [0010100], [2000200], [2000220], [0101021], [2101021], (10 cases),

E_8: [10000020], [00001010], [00000220], [0100010], [10001000], [20000020], [00000121], [10001020], [20001010], [00100020], [00000022], [20000200], [20000220], [10100010], [01001010], [01000101], [10010100], [00101000], [10010120], [20002000], [01000121], [00101020], [20002020], [21000121], [20002220], [20101020], [20020020], [01010221], [21010221], (29 cases).

The non-normal orbits of Exceptional groups occur amongst all types other than distinguished and their relationships with their normalisations are complicated [71]. It is conjectured in [72] that all distinguished nilpotent orbits are *normal*.

5. Higgs Branch Constructions of Nilpotent Orbits

5.1. Quivers for Minimal Classical Nilpotent Orbits

This exposition of the Higgs branch constructions of the moduli spaces that match Classical group nilpotent orbits starts with a review of reduced single instanton moduli spaces. For a $k = 1$ G-instanton theory, the $SU(2_g)$ global symmetry decouples, as discussed in section 3.3, and this permits simple SUSY quiver theories for the RSIMS of Classical groups, whch coincide with minimal nilpotent orbits.

These theories are all $\mathcal{N} = 2$ SUSY theories consisting of (i) hypermultiplets containing bifundamental scalars, transforming in a Classical Yang-Mills (or flavour) group and a particular gauge group, (ii) a vector multiplet transforming in the adjoint of the gauge group and (iii) a superpotential. The theories have interpretations in terms of brane systems, as will be developed in Chapter 6. The brane constructions corresponding to unitary theories are straightforward, however, the orthogonal and symplectic theories require the use of orientifold planes [16]. The quivers are shown in Figure 5.1 using $\mathcal{N} = 2$ notation and the field charges and superpotential are as specified in Table 5.1, adapted from [16] by the elimination of the $SU(2_g)$ fields.

These moduli spaces give the refined Hilbert series of GIOs for the various product groups. Their generating functions are constructed as in section 3.3: the fields in Table 5.1 are symmetrised using the PE; the F-term vacuum constraints are imposed by the HyperKähler quotient, which contains the adjoint of the gauge group and takes the form $PE[[adj.]\ t^2]$. The results are shown in in Table 5.2.

The GIOs (or singlets) of the quiver gauge group are selected through

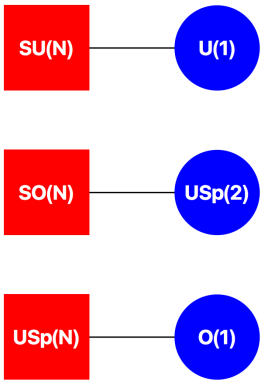

Figure 5.1.: Quivers for Classical Reduced Single Instanton Moduli Spaces using $\mathcal{N} = 2$ notation. The square nodes denotes the Yang-Mills symmetry groups. The round nodes denotes the instanton quiver gauge groups. The links correspond to *bifundamental* fields transforming under the Yang Mills and quiver gauge groups. The superpotential fields transforming in the adjoint of the quiver gauge group are implicit in the gauge nodes.

Fields	Quiver Gauge Group	Yang-Mills Group	R-Charge $U(1)_R$	Superpotential
$SU(N)_{YM} \otimes U(1)_{gauge} \otimes \bar{U}(1)_{gauge}$:				
Φ	1	$[0,\dots 0]$	(0)	$Tr\left(X_{21}\Phi X_{12}\right)$
X_{12}	$1/q$	$[1,\dots 0]$	(1)	
X_{21}	q	$[0,\dots 1]$	(1)	
$SO\left(N\right)_{YM} \otimes USp(2)_{gauge}$:				
S	$[2]$	$[0,\dots 0]$	0	$Tr\left(Q_a \varepsilon^{ab} S_{bc} \varepsilon^{cd} Q_d\right)$
Q	$[1]$	$[1,\dots 0]$	(1)	
$USp\left(N\right)_{YM} \otimes O(1)_{gauge}$:				
A	1	$[0,\dots 0]$	0	$Tr\left(QAQ\right)$
Q	± 1	$[1,\dots 0]$	(1)	
CSA Fugacities	y	x	t	
HW Fugacities		m	t	

Table 5.1.: Field Content of Quivers for Classical RSIMS

Weyl integration or a Molien average (see Appendix A.2). Different quiver gauge groups are required to yield RSIMS, depending on the Yang-Mills group. The chosen quiver gauge groups contain bilinear invariants (discussed in section 3.1), that act, via the mediacy of the bifundamental fields, to contract the vector/fundamental of the Yang-Mills group, giving its adjoint. The Molien average for a C series flavour group is taken over the two characters ± 1 of the $O(1)$ gauge group; these are reflected in the $\pm t$ fugacities.

Evaluation of the contour integrals gives the refined Hilbert series shown in Table 5.3. These are written using class function notation as:

$$g^G_{HS:RSIMS}\left(\chi^G(x),t\right) = P^G_{RSIMS}\left(\chi^G(x),t\right) PE\left[[adj.]^G(x)\ t^2\right]. \qquad (5.1)$$

The refined Hilbert series $g^G_{HS:RSIMS}\left(\chi^G(x),t\right)$ can be transformed, through a further contour integration using a character generating function to give the HWG $g^G_{HWG:RSIMS}\left(m,t\right)$, as in 2.14. These HWGs are shown in Tables 5.2 and 5.3 and correspond to highest weight symmetrisations of the adjoint representation $[k\theta^G]$ for $k = \{0, 1, \ldots \infty\}$, where $[\theta^G]$ are the Dynkin labels of the adjoint representation of G.

As noted in section 3.3, the unrefined Hilbert series $g^G_{HS:RSIMS}(t)$ have dimensions equal to twice the sum of the dual Coxeter labels of G and these coincide with the dimensions of minimal nilpotent orbits tabulated in Appendix B.

Moreover, it is straightforward to show that the RSIMS of G is included within the nilpotent cone $\mathcal{N}$, by comparison with the moduli space defined by the modified Hall Littlewood function $mHL^G_{singlet}$. Such moduli space inclusion calculations are described in detail later in this Chapter.

This combination of dimensional matching and inclusion relations uniquely identifies the RSIMS as the minimal nilpotent orbit of G. Thus, the quiver theories in Figure 5.1 yield all the minimal nilpotent orbits of Classical groups. The correspondence between each quiver diagram and a partition of the vector/fundamental representation under the homomorphism ρ is described in the next section. The accidental isomorphisms between Classical Lie group algebras give rise to alternative possible Yang-Mills and quiver gauge group choices.

Yang-Mills Group	Adjoint	HWG	Product Group	Higgs Branch Formula
$A_1 \cong B_1 \cong C_1$	$[2]$	m^2t^2	$A_1 \otimes U(1) \otimes \bar{U}(1)$	$\oint_{U(1)} d\mu^{U(1)} \frac{PE\left[([1]q+[1]q^{-1})t\right]}{PE[1,t^2]}$
$A_{r\geq 2}$	$[1,\ldots,1]$	$m_1 m_r t^2$	$A_r \otimes U(1) \otimes \bar{U}(1)$	$\oint_{U(1)} d\mu^{U(1)} \frac{PE\left[([1,0,\ldots]q+[0,\ldots,1]q^{-1})t\right]}{PE[1,t^2]}$
$B_2 \cong C_2$	$[0,2]$	${m_2}^2t^2$	$B_2 \otimes C_1$	$\oint_{C_1} d\mu^{C_1} \frac{PE[[1,0][1]t]}{PE[[2],t^2]}$
$B_{r\geq 3}$	$[0,1,\ldots 0]$	m_2t^2	$B_r \otimes C_1$	$\oint_{C_1} d\mu^{C_1} \frac{PE[[1,0,\ldots 0][1]t]}{PE[[2],t^2]}$
$C_1 \cong A_1 \cong B_1$	$[2]$	m^2t^2	$C_1 \otimes O(1)$	$\frac{1}{2}\left(PE\left[[1]\,t\right] + PE\left[[1]\,t,(-t)\right]\right)$
$C_{r\geq 2}$	$[2,0,\ldots]$	${m_1}^2t^2$	$C_r \otimes O(1)$	$\frac{1}{2}\left(PE\left[[1,0,\ldots]\,t\right] + PE\left[[1,0,\ldots]\,t,(-t)\right]\right)$
D_2	$[2,0] \oplus [0,2]$	${m_1}^2t^2 + {m_2}^2t^2$	$D_2 \otimes C_1$	$\oint_{C_1} d\mu^{C_1} \frac{PE[[1,1][1]t]}{PE[[2]t^2]}$
D_3	$[0,1,1]$	$m_2m_3t^2$	$D_3 \otimes C_1$	$\oint_{C_1} d\mu^{C_1} \frac{PE[[1,0,0][1]t]}{PE[[2],t^2]}$
$D_{r\geq 4}$	$[0,1,\ldots,0]$	m_2t^2	$D_r \otimes C_1$	$\oint_{C_1} d\mu^{C_1} \frac{PE[[1,0,0,\ldots,0][1]t]}{PE[[2]t^2]}$

Table 5.2.: Higgs branch formulae for Classical RSIMS

Series	$g^G_{HWG:RSIMS}$	$P^G_{RSIMS}(\chi^G, t^2)$	$PE[[adj.]^G\ t^2]$
A_1	m^2t^2	$\left(1-t^4\right)[0,0]$	$PE\left[[2]\,t^2\right]$
A_2	$m_1m_2t^2$	$\begin{pmatrix} 1-t^4-t^8+t^{12} & [0,0] \\ -t^4+2t^6-t^8 & [1,1] \end{pmatrix}$	$PE\left[[1,1]\,t^2\right]$
A_3	$m_1m_3t^2$	$P^{A_3}_{\text{RSIMS}}$	$PE\left[[1,0,1]\,t^2\right]$
B_2	${m_2}^2t^2$	$\begin{pmatrix} 1-t^4-t^{12}+t^{16} & [0,0] \\ t^6-2t^8+t^{10} & [0,2] \\ -t^4+t^6+t^{10}-t^{12} & [1,0] \\ t^6-2t^8+t^{10} & [1,2] \\ -t^4+t^6+t^{10}-t^{12} & [2,0] \end{pmatrix}$	$PE\left[[0,2]\,t^2\right]$
B_3	m_2t^2	$P^{B_3}_{\text{RSIMS}}$	$PE\left[[0,1,0]\,t^2\right]$
C_2	${m_1}^2t^2$	$\begin{pmatrix} 1-t^4-t^{12}+t^{16} & [0,0] \\ -t^4+t^6+t^{10}-t^{12} & [0,1] \\ -t^4+t^6+t^{10}-t^{12} & [0,2] \\ t^6-2t^8+t^{10} & [2,0] \\ t^6-2t^8+t^{10} & [2,1] \end{pmatrix}$	$PE\left[[2,0]\,t^2\right]$
C_3	${m_1}^2t^2$	$P^{C_3}_{\text{RSIMS}}$	$PE\left[[2,0,0]\,t^2\right]$
D_2	${m_1}^2t^2+{m_2}^2t^2$	$\begin{pmatrix} 2-2t^4-2t^6+2t^{10} & [0,0] \\ -t^2+t^4+t^6-t^8 & [0,2] \\ -t^2+t^4+t^6-t^8 & [2,0] \end{pmatrix}$	$PE\left[[2,0]\,t^2+[0,2]\,t^2\right]$
D_3	$m_2m_3t^2$	$P^{D_3}_{\text{RSIMS}}$	$PE\left[[0,1,1]\,t^2\right]$
D_4	m_2t^2	$P^{D_4}_{\text{RSIMS}}$	$PE\left[[0,1,0,0]\,t^2\right]$

$P^{A_3}_{\text{RSIMS}}$, $P^{B_3}_{\text{RSIMS}}$, $P^{C_3}_{\text{RSIMS}}$, $P^{D_3}_{\text{RSIMS}}$, $P^{D_4}_{\text{RSIMS}}$ are given in [29].

Table 5.3.: HWGs and Refined HS for RSIMS of Classical Groups

Constructions of this type are not known when the Yang-Mills group is Exceptional; while the adjoint of an Exceptional group can be formed by anti-symmetrising the fundamental representation, many other irreps are also generated, so the resulting moduli spaces are not minimal nilpotent orbits.

5.2. Quivers for General Classical Nilpotent Orbits

The SUSY quiver theories whose Higgs branches correspond to nilpotent orbits of unitary groups can all be described by an $SU(N_f)$ flavour node linked to a linear chain of unitary gauge nodes $U(N_i)$ [7]. Such quivers, which are shown in Figure 5.2 using $\mathcal{N}=2$ notation, contain a descending sequence of unitary gauge nodes and can be referred to by the mnemonic $[N_f]-(N_1)-\ldots(N_{max})$.

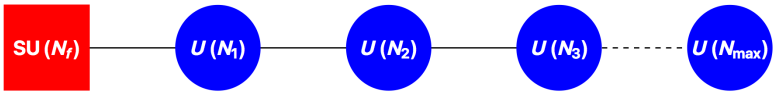

Figure 5.2.: Unitary Linear Quiver. Square (red) nodes denote flavour nodes. Round (blue) nodes denote gauge nodes. The links represent pairs of bifundamental fields transforming in the fundamental and antifundamental representations. The quiver is ordered such that $N_f \geq N_1 \geq N_i \geq \ldots \geq N_{max}$.

If we consider the Higgs branch of such a quiver: each link represents a bifundamental hypermultiplet containing a conjugate pair of scalar fields X_{ij} and X_{ji} transforming under the flavour and/or gauge groups associated with its nodes; each gauge node is associated with a scalar field Φ_{ii} transforming in the adjoint representation of the gauge group. A superpotential is formed from contractions of bifundamental and adjoint fields. The F-terms obtained by application of vacuum minima conditions to the superpotential lead to the imposition on each node of a HyperKähler quotient. The ring of gauge invariant operators formed by symmetrising the bifundamental fields, modulo the HKQ, can be enumerated in a Hilbert series.

The Higgs branch formula for this Hilbert series, expressed in terms of characters χ and a counting fugacity t, is:

$$g^{A}_{HS:Higgs}\left(\chi(x),t\right) = \oint_{gauge} d\mu^{gauge} \prod_{j<i} \frac{PE\left[\chi\left(X_{ij}+X_{ji}\right)t\right]}{g_{HK}(\chi^{U(N_i)},t)}. \tag{5.2}$$

The integrand is a product of terms similar to those appearing in Table 5.2 and the Weyl integration is carried out over each gauge group.

One delicate aspect of this calculation is that of the HyperKähler quotient g_{HK}. This has the effect of ensuring, for each Weyl integration, that the flavour group Hilbert series excludes any singlets (or vacuum bubbles), which would otherwise result, under the PE, from invariants of the gauge group. As described in section 3.3, one method of calculation [25] involves applying vacuum conditions to the superpotential terms that can be constructed from the bifundamental fields and adjoint gauge fields. A more direct route, which we adopt here, is to find the HKQ from the moduli space of the gauge fields that correspond to the flavour group singlets that

we wish to exclude:

$$g_{HK}\left(\chi^{U(N_i)},t\right)=\oint\limits_{U(N_j)}d\mu^{U(N_j)}\;PE\left[\chi\left(X_{ij}+X_{ji}\right)t\right]. \tag{5.3}$$

For a linear A series quiver of the type in fig 5.2, this HyperKähler quotient invariably evaluates to the PE of the adjoint of the gauge group: $g_{HK}(\chi^{U(N_i)},t)=PE[\chi(\Phi_{ii})\;t^2]$. The Hilbert series for the Higgs branch is thus given by:

$$g^A_{HS:Higgs}\left(\chi(x),t\right)=\oint\limits_{gauge}d\mu^{gauge}\left(\prod_{j<i}\frac{PE\left[\chi\left(X_{ij}+X_{ji}\right)\;t\right]}{PE\left[\chi\left(\Phi_{ii}\right)\;t^2\right]}\right) \tag{5.4}$$

The dimension of this Hilbert series, when unrefined by setting all the flavour group CSA coordinates x to unity, is given by the formula:

$$\left|g^A_{HS:Higgs}\left(\chi(1),t\right)\right|=\sum_{ij}\left|\chi\left(X_{ij}\right)\right|-\sum_{i\in gauge}\left|\chi\left(\Phi_{ii}\right)\right|-\sum_{i\in gauge}\left|[adj.]^{U(N_i)}\right| \tag{5.5}$$

The last two terms on the RHS follow from the HyperKähler quotient and the Weyl integration over each gauge group, respectively, and have identical dimensions.

Assuming that the sequence of node dimensions $\{N_f,N_1,\ldots,N_{max}\}$ is non-increasing, unordered partition data can be assigned to the quiver as:

$$\sigma=\{\sigma_i:\sigma_1=N_f-N_1;\sigma_i=N_{i-1}-N_i;\sigma_{max}=N_{max}\}. \tag{5.6}$$

Note that the σ_i from this construction are non-negative, but are not necessarily ordered. We now use the identity, $N_f=\sum\limits_{i=1}^{max}\sigma_i$, to rearrange the dimension formula 5.5 as:

$$\begin{aligned}\left|g^A_{HS:Higgs}\left(1,t\right)\right|&=\sum_{n=1}^{max-1}\underbrace{2\left(N_f-\sum_{i=1}^{n-1}\sigma_i\right)\left(N_f-\sum_{i=1}^{n}\sigma_i\right)}_{hypers}-\underbrace{2\left(N_f-\sum_{i=1}^{n}\sigma_i\right)^2}_{vectors}\\&={N_f}^2-\sum_{i=1}^{max}{\sigma^2}_i.\end{aligned} \tag{5.7}$$

Thus, we have recovered the dimensions of the A series nilpotent orbits in

Table 4.5 from the unitary quivers defined by the sequence $\{N_f, N_1, \ldots, N_{max}\}$, and can use the partition data associated with each A series nilpotent orbit to identify a unitary linear quiver, whose moduli space has a Hilbert series of the same dimension as the nilpotent orbit.

The process of matching partition data from the nilpotent orbits of BCD series groups to quiver theories is similar, but with some refinements. The dimension formulae in Table 4.5 for BCD groups invite association with alternating O/USp groups. As a development from diagrams outlined in [7], it was proposed in [20] that linear quivers for BCD groups could take the form of alternating chains of O/USp groups. It is therefore natural to examine the mapping of partition data from nilpotent orbits to the vector/fundamental dimensions of an alternating chain of O/USp groups.

One issue that arises is that some partitions require USp groups with odd fundamental dimension; however, homomorphisms ρ with such partitions are precisely those excluded by the B/D and C-partition selection rules described in section 4.2. The B/D and C-partition selection rules in effect correspond to the restriction of nilpotent orbit root maps for BCD groups to the Characteristics of homomorphisms ρ that can consistently be described by an alternating O/USp chain.

So, the linear BCD quivers to investigate take the form of chains of alternating O/USp nodes, with the first node being a flavour node and the remaining nodes being gauge nodes, ordered with non-increasing vector/fundamental dimension, as in Figures 5.3 and 5.4.

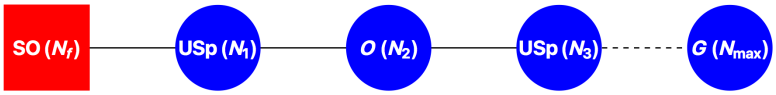

Figure 5.3.: Orthogonal Linear Quiver. Square (red) nodes denote flavour nodes. Round (blue) nodes denote gauge nodes. The links represent bifundamental fields transforming in the vector/fundamental representations. The quiver is ordered such that $N_f \geq N_1 \geq N_i \geq \ldots \geq N_{max}$.

We can calculate the Hilbert series for the Higgs branches of such BCD series quivers and find their dimensions using a prescription similar to 5.4.

Figure 5.4.: Symplectic Linear Quiver. Square (red) nodes denote flavour nodes. Round (blue) nodes denote gauge nodes. The links represent bifundamental fields transforming in the vector/fundamental representations. The quiver is ordered such that $N_f \geq N_1 \geq N_i \geq \ldots \geq N_{max}$.

$$g^{BCD}_{HS:Higgs}\left(\chi(x),t\right) = \oint_{gauge} d\mu^{gauge} \left(\prod_{j<i} \frac{PE\left[\chi\left(X_{ij}\right)t\right]}{PE\left[\chi\left(\Phi_{ii}\right)\ t^2\right]} \right) \tag{5.8}$$

The fields X_{jk} are now half-hypermultiplets, so that there is just one field X_{jk} between nodes $\{j,k\}$. There are complications relating to the structure of the HyperKähler quotient and the use of orthogonal rather than SO groups; these do not, however, affect the dimensions of a Hilbert series, so we defer a discussion of these topics to section 5.4. The dimensional formula necessarily reflects both the series of the flavour group and the position of a node, with the gauge group series matching (or complementing) the flavour group on even (or odd) indexed N_i nodes. Otherwise, the Higgs branch dimension formula for BCD quivers follows in a similar manner to that for A series quivers:

$$\begin{aligned}
\left|g^{B/D}_{HS:Higgs}\left(1,t\right)\right| = & \sum_{n} \left(N_f - \sum_{k=1}^{n-1} \sigma_k \right) \left(N_f - \sum_{k=1}^{n} \sigma_k \right) \\
& - \sum_{n\ odd} \left(N_f + 1 - \sum_{k=1}^{n} \sigma_k \right) \left(N_f - \sum_{k=1}^{n} \sigma_k \right) \\
& - \sum_{n\ even} \left(N_f - 1 - \sum_{k=1}^{n} \sigma_k \right) \left(N_f - \sum_{k=1}^{n} \sigma_k \right) \\
= & \frac{1}{2} N_f \left(N_f - 1 \right) - \frac{1}{2} \sum_{i\ odd} \sigma_i \left(\sigma_i - 1 \right) - \frac{1}{2} \sum_{i\ even} \sigma_i \left(\sigma_i + 1 \right)
\end{aligned} \tag{5.9}$$

$$
\begin{aligned}
\left|g^{C}_{HS:Higgs}\left(1,t\right)\right| = & \sum_{n}\left(N_f-\sum_{k=1}^{n-1}\sigma_k\right)\left(N_f-\sum_{k=1}^{n}\sigma_k\right) \\
& -\sum_{n\ odd}\left(N_f-1-\sum_{k=1}^{n}\sigma_k\right)\left(N_f-\sum_{k=1}^{n}\sigma_k\right) \\
& -\sum_{n\ even}\left(N_f+1-\sum_{k=1}^{n}\sigma_k\right)\left(N_f-\sum_{k=1}^{n}\sigma_k\right) \\
= & \frac{1}{2}N_f\left(N_f+1\right)-\frac{1}{2}\sum_{i\ odd}\sigma_i\left(\sigma_i+1\right)-\frac{1}{2}\sum_{i\ even}\sigma_i\left(\sigma_i-1\right)
\end{aligned}
\tag{5.10}
$$

Thus, in a similar manner to the A series, we can recover the dimensions of the BCD series nilpotent orbits in Table 4.5 from quivers with alternating O/USp nodes. We can, therefore, use the partition data from a BCD series nilpotent orbit to identify a linear BCD quiver, whose moduli space has a Hilbert series with the same dimension as the nilpotent orbit. Before concluding that these quiver theories all lead to moduli spaces matching nilpotent orbits, it remains to establish their inclusion relations.

These moduli spaces are constructed on a case by case basis in the following sections and their structures and inclusion relations are analysed in terms of their Hilbert series and decompositions into representations of G. It turns out that both characters and mHL functions of G provide useful bases for these decompositions, with the latter providing a means of encoding infinite series of class functions as finite polynomials.

Clearly the set of well-ordered partitions does not exhaust the set of all the possible quivers defined by Figures 5.2, 5.3 and 5.4. It is interesting to ask whether there are dualities, such that different A or BCD quivers share the same moduli space. The dimension formulae in Table 4.5 do not depend upon the strict ordering of the partition data, so dualities do indeed arise, as will be shown in sections 5.3.4 and 5.4.6.

5.3. A Series Orbits from Higgs Branch Moduli Spaces

Quivers whose Higgs branches have Hilbert series with dimensions corresponding to those of nilpotent orbits are listed in Appendix B.1. The constructions are in all cases defined by the partition data for the vec-

tor/fundamental representation under the homomorphism ρ. The extremal quiver diagrams that can be constructed from partitions of N are represented by the minimal and maximal nilpotent orbits.

5.3.1. Maximal and Minimal A Series Orbits

In the case of the minimal nilpotent orbit of A_r, which corresponds to the reduced single instanton moduli space, the fundamental partition takes the form $\rho = (2, 1^{r-1})$. The transpose of this partition gives the quiver increments $\sigma = (r, 1)$, which correspond to the unitary quivers $[r+1] - (1)$ shown in Figure 5.5, whose Higgs branches were evaluated in section 5.1.

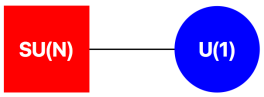

Figure 5.5.: Quiver for A Series Minimal Nilpotent Orbit. $SU(N)$ has two nodes, with square (red) nodes denoting flavour and round (blue) nodes denoting gauge groups. The links represent pairs of bifundamental chiral scalars transforming in the fundamental and anti-fundamental representations.

The maximal nilpotent orbit of A_r, which corresponds to the modified Hall Littlewood polynomial $mHL^{A_r}_{[singlet]}$, has the fundamental partitions $\rho = (N) = (r+1)$. This transposes to the quiver increments $\sigma = (1^{r+1})$, corresponding to the quiver shown in Figure 5.6.

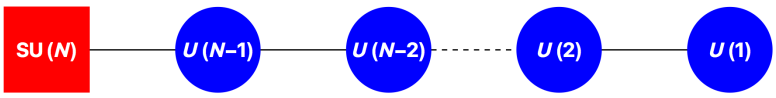

Figure 5.6.: Quiver for A Series Maximal Nilpotent Orbit. $SU(N)$ has N nodes, with square (red) nodes denoting flavour and round (blue) nodes denoting gauge groups. The links represent pairs of bifundamental chiral scalars transforming in the fundamental and anti-fundamental representations.

5.3.2. Evaluation of A Series Quivers

The refined Hilbert series $g_{HS:Higgs}^{[N_f]-(N_1)-\ldots(N_{max})}$ of the A series quivers shown in Figure 5.2, which include all the A series nilpotent orbits, can be calculated from 5.4.

It is convenient to carry out the Weyl integrations sequentially and, to this end, 5.4 can be rearranged into a recursive procedure:

$$\begin{aligned} g_{HS:Higgs}^{[N_i]-(N_{i+1})-\ldots(N_{max})}\left(\chi^{SU(N_i)},t\right) = & \oint_{U(N_{i+1})} d\mu^{U(N_{i+1})} \\ & \times \frac{PE\left[\left(\chi_{fund.}^{U(N_i)}\otimes\chi_{anti.}^{U(N_{i+1})}+\chi_{anti.}^{U(N_i)}\otimes\chi_{fund.}^{U(N_{i+1})}\right)t\right]}{PE\left[\chi_{adj.}^{U(N_{i+1})}t^2\right]} \\ & \times g_{HS:Higgs}^{[N_{i+1}]-\ldots(N_{max})}\left(\chi^{SU(N_{i+1})},t\right). \end{aligned} \tag{5.11}$$

The definitions $g_{HS:Higgs}^{[N_{max}]}=1$ and $U(N_0)\equiv U(N_f)$ are used. This is an example of quiver *gluing* discussed in [25]. Note that gauge invariance under the $U(1)$ subgroup within each $U(N)$ gauge group entails that each HS in the sequence contains only the characters of $SU(N_i)$. In effect, each nilpotent orbit in the sequence, $[N_{max}]\rightarrow[N_{max-1}]-(N_{max})\rightarrow\ldots\rightarrow[N_f]-(N_1)-\ldots-(N_{max})$, induces orbits in groups of higher rank and this permits efficient calculation of all A_r nilpotent orbits up to a given rank.

As discussed in the previous section, the partition data associated with a nilpotent orbit defines a sequence of dimensions, whose separation is non-increasing, such that $N_i-N_{i+1}\geq N_{i+1}-N_{i+2}$. However, these quivers represent only a subset of those within the more general schema in Figure 5.2. Analysis of the full set allows us to examine dualities between quiver theories and so we include these *non-partition* quivers in the analysis.

5.3.3. Analysis of A Series Moduli Spaces

Once a generating function $g_{HS:Higgs}^{quiver}$ for a refined Hilbert series has been calculated, this moduli space can be analysed in a number of different ways, as discussed in Chapter 2. Both characters and modified Hall Littlewood polynomials provide a basis of orthogonal functions that can be used to decompose these class functions. For low rank groups, these moduli spaces often have a simple description in terms of one but not always both bases,

which thus provide complementary modes of analysis. The following methods are of most relevance:

1. A refined Hilbert series for a nilpotent orbit can be rearranged into the canonical form:

$$g^{quiver}_{HS:Higgs}(\chi,t) \equiv P^{G}_{HS:Higgs}(\chi,t)\ \ PE\left[\chi^{G}_{adj.}t^{2}\right], \tag{5.12}$$

   where $P^{G}_{HS:Higgs}(\chi,t)$ is the character decomposition of some finite polynomial class function of G. Rearrangements of this form are given in Table 5.3 for some minimal nilpotent orbits. The expression 4.3 for a maximal nilpotent orbit is also in this form. However, expressions for the refined HS of nilpotent orbits can be extremely unwieldy, and are generally not tabulated in this study, but rather transformed to more concise forms.

2. A Hilbert series can be unrefined as $g^{G}_{HS:Higgs}(1,t)$ by setting all the CSA coordinates to unity. This permits the counting of dimensions, generators and relations.

3. A refined Hilbert series can be decomposed as a character expansion in irreps of G. These infinite series can be described by an HWG $g^{G}_{HWG:Higgs}(m,t)$ for the coefficients of each irrep, identified by its Dynkin labels. The HWGs are found using a character generating function and Weyl integration, as in 2.14.

4. A refined Hilbert series can be decomposed in terms of mHL functions of G. Significantly, these series turn out to be finite for nilpotent orbits and can be described by an HWG $g^{G}_{HWG(mHL):Higgs}(h,t^2)$ for the mHL coefficients. It is necessary to define the Hall Littlewood polynomials with respect to the counting fugacity t^2 to obtain a match with the powers of t appearing in the Hilbert series for a Higgs branch. The HWGs are found by Weyl integration over an orthonormal $\overline{mHL}$ generating function, as in 2.27.

5. A further important matter concerns the analysis of inclusion relations between moduli spaces. Consider two moduli spaces defined by common fugacities $f \equiv f_1 \dots f_k$ and carrying positive coefficients a_n and b_n, such that $g_1 \equiv \sum_n a_n f^n$ and $g_2 \equiv \sum_n b_n f^n$. Then:

The union of the moduli spaces is given by $g_1 \cup g_2 = \sum_n \max[a_n, b_n] f^n$

The intersection of the moduli spaces is given by $g_1 \cap g_2 = \sum_n \min[a_n, b_n] f^n$

A moduli space g_1 includes g_2: $g_1 \supseteq g_2$ iff $\forall n : a_n \geq b_n$

Knowledge of the unrefined Hilbert series permits an ordering relative to t, but sums of dimensions are not always sufficient to identify differences between representations. The definitive analysis of the inclusion relations amongst the nilpotent orbit moduli spaces is therefore obtained over class functions, using character HWGs with the fugacities $\{m, t\}$. [1]

Tables 5.4 and 5.5 set out the results of these calculations for A_1 through A_4, for quivers associated with descending sequences of unitary gauge nodes as per Figure 5.2. Several observations can be made:

1. All the moduli spaces of these Higgs branch quiver theories constructed using partition data have dimensions equal to those of the corresponding nilpotent orbits.

2. All the moduli spaces are contained within the nilpotent cone $\mathcal{N}$. Furthermore, the moduli spaces observe ordering relations consistent with those in the Hasse diagrams of nilpotent orbits in the Literature, e.g. [6, 33], as can be verified by Taylor expansion of the character HWGs and/or the unrefined HS.

3. The unrefined HS of these moduli spaces are palindromic, indicating Calabi Yau surfaces, and consistent with the property of being HyperKähler. The unrefined HS of maximal nilpotent orbits are complete intersections [25].

4. The character HWGs that are not freely generated or complete intersections are palindromic.

5. The moduli space decompositions into characters identify their generators, such as the A_1 generator m^2t^2 or the A_2 generator $m_1 m_2 t^2$. Each generator (or monomial) of these moduli spaces $m_1^{n_1} \dots m_r^{n_r}$ is

[1] Ordering with respect to the mHL HWGs is not helpful since the mHL functions already encode the fugacity t.

Partition	Quiver	Dim.	Unrefined HS	Character HWG	mHL HWG
(1^2)	[2]	0	1	1	$1-h^2t^2$
(2)	[2]-(1)	2	$\frac{1-t^4}{(1-t^2)^3}$	$\frac{1}{1-m^2t^2}$	1
(1^3)	[3]	0	1	1	$1-h_1h_2t^2+{h_1}^3t^4$ $-h_1h_2t^4+{h_2}^3t^4-{h_1}^2{h_2}^2t^6$
$(2,1)$	[3]-(1) [3]-(2)	4	$\frac{1+4t^2+t^4}{(1-t^2)^4}$	$\frac{1}{1-m_1m_2t^2}$	$1-h_1h_2t^4$
(3)	[3]-(2)-(1)	6	$\frac{(1-t^4)(1-t^6)}{(1-t^2)^8}$	$\frac{1-m_1^3m_2^3t^{12}}{(1-m_1m_2t^2)(1-m_1m_2t^4)(1-{m_1}^3t^6)(1-{m_2}^3t^6)}$	1
(1^4)	[4]	0	1	1	$1-h_1h_3t^2-h_1h_3t^4+{h_1}^2h_2t^4+h_2{h_3}^2t^4$ $-h_1h_3t^6-h_1{h_2}^2h_3t^6+{h_1}^2h_2t^6$ $+h_2{h_3}^2t^6-{h_1}^2{h_3}^2t^6+{h_2}^2t^6-{h_3}^4t^6$ $-{h_1}^4t^6+{h_1}^3h_2h_3t^8-h_1{h_2}^2h_3t^8$ $-{h_1}^2{h_3}^2t^8+h_1h_2{h_3}^3t^8+{h_2}^4t^8$ $+h_1h_2{h_3}^3t^{10}-{h_2}^3{h_3}^2t^{10}$ $+{h_1}^3h_2h_3t^{10}-{h_1}^3{h_3}^3t^{10}$ $-{h_1}^2{h_2}^3t^{10}+{h_1}^2{h_2}^2{h_3}^2t^{12}$
$(2,1^2)$	[4]-(1)	6	$\frac{(1+t^2)(1+8t^2+t^4)}{(1-t^2)^6}$	$\frac{1}{1-m_1m_3t^2}$	$1-h_1h_3t^4-{h_2}^2t^4$ $-h_1h_3t^6+{h_1}^2h_2t^6+h_2{h_3}^2t^6$ $+{h_2}^2t^6-{h_1}^2{h_3}^2t^8$
(2^2)	[4]-(2)	8	$\frac{(1+t^2)^2(1+5t^2+t^4)}{(1-t^2)^8}$	$\frac{1}{(1-m_1m_3t^2)(1-{m_2}^2t^4)}$	$1-h_1h_3t^4-h_1h_3t^6+{h_2}^2t^6$
$(3,1)$	[4]-(2)-(1) [4]-(3)-(1) [4]-(3)-(2)	10	$\frac{(1+t^2)(1+4t^2+10t^4+4t^6+t^8)}{(1-t^2)^{10}}$	$\frac{1-{m_1}^2{m_2}^2{m_3}^2t^{12}}{\left(\begin{array}{c}(1-m_1m_3t^2)(1-{m_2}^2t^4)(1-m_1m_3t^4)\\ \times(1-{m_1}^2m_2t^6)(1-m_2{m_3}^2t^6)\end{array}\right)}$	$1-h_1h_3t^6$
(4)	[4]-(3)-(2)-(1)	12	$\frac{(1-t^4)(1-t^6)(1-t^8)}{(1-t^2)^{15}}$	$\frac{1+\ldots 56\ terms\ldots+{m_1}^6{m_2}^4{m_3}^6t^{42}}{\left(\begin{array}{c}(1-m_1m_3t^2)(1-{m_2}^2t^4)(1-m_1m_3t^4)\\ \times(1-{m_1}^2m_2t^6)(1-m_2{m_3}^2t^6)\\ \times(1-{m_2}^2t^8)(1-{m_1}^4t^{12})(1-{m_3}^4t^{12})\end{array}\right)}$	1

[N] denotes an SU(N) flavour node. (N) denotes a U(N) gauge node.
An mHL HWG of 1 denotes $mHL_{[0,\ldots,0]}(t^2)$.
Where multiple quivers have the same Hilbert series, the nilpotent orbit partition is given first.
The numerator of the character HWG for the [4]-(3)-(2)-(1) quiver has been truncated.

Table 5.4.: Quivers, HWGs and HS for Orbits of A_1, A_2 and A_3

Partition	Quiver	Dim.	Unrefined HS	Character HWG	mHL HWG
(1^5)	[5]	0	1	1	...
$(2,1^3)$	[5]-(1)	8	$\frac{1+16t^2+36t^4+16t^6+t^8}{(1-t^2)^8}$	$\frac{1}{1-m_1m_4t^2}$	not shown
$(2^2,1)$	[5]-(2) [5]-(3)	12	$\frac{1+12t^2+53t^4+88t^6+53t^8+12t^{10}+t^{12}}{(1-t^2)^{12}}$	$\frac{1}{(1-m_1m_4t^2)(1-m_2m_3t^4)}$	$1-h_1h_4t^4-h_1h_4t^6-h_1h_4t^8$ $+h_2h_3t^8+{h_1}^2h_3t^8+h_2{h_4}^2t^8$ $+h_2h_3t^{10}-{h_3}^2h_4t^{10}$ $-{h_1}^2{h_4}^2t^{10}-h_1{h_2}^2t^{10}$ $+h_1h_2h_3h_4t^{14}$
$(3,1^2)$	[5]-(2)-(1)	14	$\frac{1+9t^2+45t^4+65t^6+45t^8+9t^{10}+t^{12}}{(1-t^2)^{15}(1-t^4)^{-1}}$	$\frac{1-m_1^2m_2m_3m_4^2t^{12}}{\left(\begin{array}{c}(1-m_1m_4t^2)(1-m_1m_4t^4)(1-m_2m_3t^4)\\ \times(1-{m_1}^2m_3t^6)(1-m_2{m_4}^2t^6)\end{array}\right)}$	$1-h_1h_4t^6-h_2h_3t^6$ $-h_1h_4t^8+{h_1}^2h_3t^8+h_2{h_4}^2t^8$ $+h_2h_3t^{10}-{h_1}^2{h_4}^2t^{10}$
$(3,2)$	[5]-(3)-(1) [5]-(3)-(2) [5]-(4)-(2)	16	$\frac{1+6t^2+22t^4+37t^6+22t^8+6t^{10}+t^{12}}{(1-t^2)^{18}(1-t^4)^{-2}}$	not shown	$1-h_1h_4t^6$ $-h_1h_4t^8+h_2h_3t^{10}$
$(4,1)$	[5]-(3)-(2)-(1) [5]-(4)-(2)-(1) [5]-(4)-(3)-(1) [5]-(4)-(3)-(2)	18	$\frac{1+4t^2+10t^4+20t^6+10t^8+4t^{10}+t^{12}}{(1-t^2)^{20}(1-t^4)^{-1}(1-t^6)^{-1}}$	not shown	$1-h_1h_4t^8$
(5)	[5]-(4)-(3)-(2)-(1)	20	$\frac{(1-t^4)(1-t^6)(1-t^8)(1-t^{10})}{(1-t^2)^{24}}$	...	1

[N] denotes an SU(N) flavour node. (N) denotes a U(N) gauge node.
An mHL HWG of 1 denotes $mHL_{[0,\ldots,0]}(t^2)$.
Where multiple quivers have the same Hilbert series, the nilpotent orbit partition is given first.
The character or mHL HWGs for some quivers are not shown for brevity.

Table 5.5.: Quivers, HWGs and HS for Orbits of A_4

a root lattice object, with *N-ality* zero: $\mod \left[\sum_{i=1}^{r} i n_i, N\right] = 0$, where $N = r + 1$.

6. All the moduli spaces decompose into finite sums of mHL functions. Each monomial is also a root lattice object with *N-ality* zero with respect to the h_i fugacities.

7. The character and mHL descriptions are complementary; orbits close to the minimal nilpotent orbit have character HWGs that are freely generated or complete intersections; orbits close to the maximal nilpotent orbit decompose to a small number of mHL functions.

8. The canonical A series nilpotent orbits have distinct signatures in terms of Hilbert series, character HWGs and/or mHL HWGs. These are summarised in Table 5.6 for future reference.

9. There are several dualities, where multiple quivers correspond to the same nilpotent orbit. The circumstances under which these arise are discussed further below.

5.3.4. Dualities of A Series Quivers

It is significant that there are a number of quivers, such as $[3]-(2)$, $[4]-(3)-(1)$ and $[4]-(3)-(2)$, that cannot be described by partitions, since their increments σ_i are not well-ordered. However, the nilpotent orbit dimensions set out in Table 4.5 are insensitive to the order of the σ_i, and so, any such *non-partition* quiver with $N_i \geq N_{i+1}$ has a Hilbert series with the same dimension as the quiver obtained by reordering the σ_i into a partition. Indeed, calculations using 5.4 show that in many (but not all) cases, the refined Hilbert series of non-partition quivers, including the above examples, match those of the quivers from nilpotent orbit partitions.

There are nonetheless limits to the extent to which the σ_i can be reordered to obtain a dual quiver with the same Hilbert series. For example, a calculation of the Hilbert series of the quiver $[4]-(3)$ yields a non-palindromic result that does not match $[4]-(1)$.

The concept of quiver *balance*, defined in section 6.1.1, can be used to predict when the Higgs branch Hilbert series of a non-partition quiver will match that of a quiver from a nilpotent orbit partition.

Orbit	Dimension	Quiver	Unrefined HS	PL[Character HWG]	mHL HWG
Trivial	0	$[n+1]$	1	1	...
Minimal	$2n$	$[n+1]-(1)$	$\frac{\sum_{i=0}^{n}\binom{n}{i}^2 t^{2i}}{(1-t^2)^{2n}}$	$m_1 m_n t^2$	...
Supra Minimal $n \geq 3$	$4n-4$	$[n+1]-(2)$	...	$m_1 m_n t^2 + m_2 m_{n-1} t^4$	...
Supra Supra Minimal $n \geq 3$	$4n-2$	$[n+1]-(2)-(1)$	...	$m_1 m_n t^2$ $+m_1 m_n t^4 + m_2 m_{n-1} t^4$ $+{m_1}^2 m_{n-1} t^6 + m_2 m_n^2 t^6$ $-{m_1}^2 m_2 m_{n-1} m_n^2 t^{12}$	...
2-Node Quiver $n+1 \geq 2k$	$2k(n+1-k)$	$[n+1]-(k)$	...	$\sum_{i=1}^{k} m_i m_{n+1-i} t^{2i}$	...
Sub Sub Regular $n \geq 3$	$n(n+1)-4$	$[n+1]-(n-1)-$ $(n-3)-[\ldots]-(1)$	...	...	$1+h_2 h_{n-1} t^{4n-6}$ $-h_1 h_n t^{2n-2} - h_1 h_n t^{2n}$
Sub Regular	$n(n+1)-2$	$[n+1]-(n-1)-$ $(n-2)-[\ldots]-(1)$	...	...	$1-h_1 h_n t^{2n}$
Maximal	$n(n+1)$	$[n+1]-[\ldots]-(1)$	$\frac{\prod_{i=1}^{n}\left(1-t^{2(i+1)}\right)}{(1-t^2)^{n(n+2)}}$	...	1

Within a quiver, $[\ldots]$ denotes a maximal sub-chain

Table 5.6.: Generalised A Series Nilpotent Orbit HS and HWGs

If all gauge nodes in a quiver have a balance of zero, the quiver is termed *balanced*. If one or more gauge nodes have a positive balance and no gauge nodes have a negative balance, the quiver is described as *positively balanced*. If one or more gauge nodes have a balance of -1, the quiver is described as *minimally unbalanced*. If one or more gauge nodes have a balance of -2 or less, the quiver is described as *very unbalanced*. With these definitions, Tables 5.4 and 5.5 show:

1. A quiver specified by the partition data from a nilpotent orbit is either balanced or positively balanced. [2] Amongst such quivers, only those for maximal nilpotent orbits are balanced.

2. A quiver that does not correspond to a nilpotent orbit partition is minimally or very unbalanced.

3. A minimally unbalanced quiver, with increments σ_i, has a Hilbert series that matches the quiver from the nilpotent orbit partition given by a reordering of the σ_i.

4. Very unbalanced quivers, if evaluated using 5.4, have Hilbert series that are non-palindromic and do not match those of the nilpotent orbit partitions given by a reordering of the σ_i. [3]

This pattern of Higgs branch dualities between A series quivers is consistent with findings in [73].

A different class of dualities arises between ordered linear quivers of the type in Figure 5.2, which contain one or more *duplicate* nodes, such that $N_k = N_{k+1} = \ldots = N_{k+i}$. Formula 5.7 indicates that the dimension of a Higgs branch moduli space should be unaffected by the addition of duplicate nodes to any given node. Indeed, calculation indicates that refined Hilbert series are also unaffected by this addition, providing the duplicate nodes are added within maximal quiver sub-chains, so that quivers do *not* become *very unbalanced*.

[2] This condition entails that a quiver gauge theory has a superconformal IR fixed point [20].

[3] As discussed in [31], for the case of $[N_f] - (N_c)$ quivers, whenever $N_f < 2N_c - 1$, the theory becomes *very unbalanced*, and extra dimensions of the moduli space result from incomplete breaking of the gauge group. These extra dimensions and non-palindromic features of the moduli space may be eliminated by the introduction of Fayet-Iliopoulos terms.[56]

Thus, for example:

$$\begin{aligned} g_{Higgs}^{[4]-(3)-(2)-(1)} &= g_{Higgs}^{[4]-(3)-(2)-(2)-(1)} = g_{Higgs}^{[4]-(4)-(3)-(2)-(1)}, \\ g_{Higgs}^{[4]-(2)-(1)} &= g_{Higgs}^{[4]-(2)-(2)-(1)}, \\ &\text{but} \\ g_{Higgs}^{[4]-(2)} &\neq g_{Higgs}^{[4]-(2)-(2)}. \end{aligned} \tag{5.13}$$

Clearly this opens up a large further class of dualities, and, while this area merits further study, it may be conjectured that any ordered linear A series quiver, that is not *very unbalanced*, has the same Higgs branch moduli space as the nilpotent orbit quiver obtained by reordering increments and/or eliminating duplicate nodes to give a well formed partition.

5.4. BCD Series Orbits from Higgs Branch Moduli Spaces

We now turn to the more intricate matter of carrying through a comparable analysis for BCD series groups. Orthogonal and symplectic groups are complementary in terms of the symmetry of their matrix generators and invariants of degree 2, and the interplay between the two series is necessary to construct moduli spaces that match the dimensions of all B, C and D series nilpotent orbits. As shown in section 3.1, the bilinear invariants of C series are antisymmetric and therefore act on B/D vectors to generate the adjoint representation, while the bilinear invariants of the B/D series are symmetric, and so act on C vectors also to generate the adjoint representation. The complementary interplay of these groups, when paired as gauge/flavour groups, generates representations transforming in the root space of the flavour group, as required for a nilpotent orbit.

As observed in [20], unitary and orthosymplectic quivers are related by a $\mathbb{Z}_2$ orbifold action and the orthogonal and symplectic groups in a quiver must alternate so that this action can be defined. This does not, however, entail that a quiver should not contain both B and D series groups and, accordingly, we proceed with quivers that can be of mixed BCD type.

These quivers are tabulated, based on vector representation partitions, for the nilpotent orbits of BCD groups up to rank 5, in Appendices B.2,

B.3 and B.4. For brevity, the quivers are shown as BCD chains, but should properly be interpreted, for the purpose of Higgs branch calculations, as chains headed by a flavour group and with O/USp gauge groups.

The Higgs branches of all these quivers can be calculated using some version of schema 5.8, however, there are a number of complications relating to the necessity, in general, of using $O(N)$ gauge groups [7], rather than $SO(N)$, to obtain moduli spaces that match nilpotent orbits, and also relating to the calculation of HyperKähler quotients for $O(N)$ gauge groups. These complications are least severe for maximal and minimal nilpotent orbits and so these are a good place to start.

5.4.1. Maximal and Minimal BCD Series Orbits

For minimal nilpotent orbits, the vector partitions ρ and the quiver increments $\sigma = \rho^T$ take the forms in Table 5.7, with the resulting quivers shown in Figure 5.7.

Group	Partition ρ	Quiver Increments σ
$B_{r\geq 2}$	$(2^2, 1^{2r-3})$	$(2r-1, 2)$
$C_{r\geq 1}$	$(2, 1^{2r-2})$	$(2r-1, 1)$
$D_{r\geq 2}$	$(2^2, 1^{2r-4})$	$(2r-2, 2)$

Table 5.7.: Partition Data for BCD Series Minimal Nilpotent Orbits

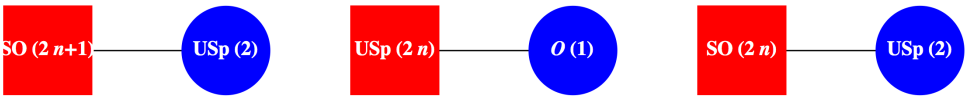

Figure 5.7.: Quivers for BCD Series Minimal Nilpotent Orbits. Square (red) nodes denote flavour and round (blue) nodes denote gauge groups. The links represent bifundamental half-hypermultiplets with scalar fields transforming in the vector representations.

Consequently, as discussed in section 5.1, quivers for B/D series minimal nilpotent orbits have a $C_1 \cong USp(2)$ gauge group, while those for C series minimal nilpotent orbits have a $B_0 \cong O(1)$ gauge group. B_0 is a finite group, with two elements that can be represented by the characters $\{1, -1\}$, so the group average is provided by a Molien sum, rather than by Weyl integration

[13]. The HyperKähler quotient in the integrations is given by the adjoint of the gauge group, with counting fugacity t^2, as shown in Table 5.2. Note that B_0 has no adjoint representation.

Turning to maximal nilpotent orbits, the vector partitions and quiver increments take the forms in Table 5.8, with the resulting quivers shown in Figure 5.8. The maximal nilpotent orbits of BCD groups are constructed from quiver chains of O/USp groups with adjacent dimensions, as shown in Figure 5.8. In the case of the BC chain, the fundamental dimension decreases by one between adjacent nodes, whereas in a DC chain the fundamental dimension decreases by alternating steps of zero or two; it is important to note the ordering, with C series nodes of a given rank, which have higher group dimension, taking precedence over D.

Group	Partition ρ	Quiver Increments σ
$B_{r\geq 1}$	$(2r+1)$	(1^{2r+1})
$C_{r\geq 1}$	$(2r)$	(1^{2r})
$D_{r\geq 2}$	$(2r-1,1)$	$(2,1^{2r-2})$

Table 5.8.: Partition Data for BCD Series Maximal Nilpotent Orbits

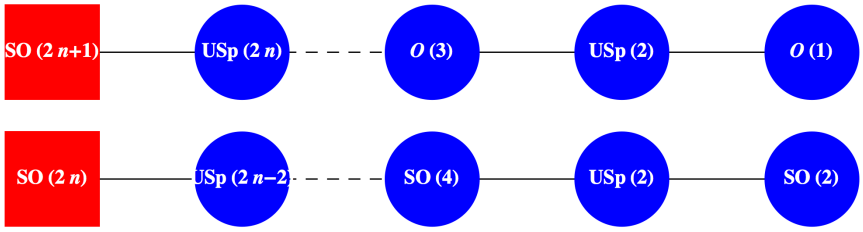

Figure 5.8.: Quivers for BCD Series Maximal Nilpotent Orbits. Square (red) nodes denote flavour and round (blue) nodes denote gauge groups. The links represent bifundamental fields transforming in the vector representations. A maximal chain for a symplectic group can be obtained by truncating either the BC or DC chain and taking the highest rank symplectic group as the new flavour group.

An interesting situation arises for B_1, where, by isomorphism with A_1, the minimal and maximal nilpotent orbits coincide. Figure 5.8, indicates that this orbit is given by $SO(3) - USp(2) - O(1)$, whereas Figure 5.7 and

the results of section 5.1 show that the minimal nilpotent orbit of B_1 is given by $SO(3) - USp(2)$. This is another example of quiver duality, where two different quivers lead to identical moduli spaces.

A further example of duality arises in the case of the maximal nilpotent orbit of C_r. This can be obtained from either a BC or DC maximal chain in Figure 5.8, by truncation to make $USp(2r)$ the flavour group. The partition for the maximal nilpotent orbit of $USp(2r)$ is given by the quiver increments of $\sigma = (1^{2r})$ in Table 5.8, as in a BC chain, however, the dimension formula for a C series nilpotent orbit in Table 4.5 shows that the dimension of moduli space with quiver increments of $\sigma = (0,2)^r$, corresponding to a DC chain, is the same.

Furthermore, these two types of maximal chain: BC and DC, represent special cases, and this gives rise to further quiver dualities, since we can substitute between $C_n - D_n - C_{n-1}$ and $C_n - B_{n-1} - C_{n-1}$ links in a *maximal* chain without affecting the moduli space. The consequence is that the partitions for maximal nilpotent orbits can be dualised to a variety of maximal BCD chains.

All the above dualities between maximal nilpotent orbits of BCD groups can be confirmed by evaluation of the moduli spaces.

The first link in a maximal BC or DC chain is $C_1 - B_0$ or $C_1 - D_1 \cong A_1 - U(1)$. This corresponds to the minimal nilpotent orbit of $C_1 \cong A_1$, which is also the maximal nilpotent orbit $mHL^{C_1}_{[singlet]}(t^2)$. Using recursion and making use of the identity 4.3, this leads to some relatively simple formulae for calculating maximal nilpotent orbits:

$$\begin{aligned} g^{B_r\,\max}_{HS:Higgs}\left(\chi^{B_r},t\right) &= \oint_{C_r} d\mu^{C_r} \frac{PE\left[\chi^{B_r}_{vec.}\otimes\chi^{C_r}_{vec.}t\right]}{PE\left[\chi^{C_r}_{adj.}t^2\right]} g^{C_r\,\max}_{HS:Higgs}\left(\chi^{C_r},t\right) \\ &= \prod_{d\in \text{Casimirs}[C_r]}\left(1-t^{2d}\right)\oint_{C_r} d\mu^{C_r} PE\left[\chi^{B_r}_{vec.}\otimes\chi^{C_r}_{vec.}t\right] \end{aligned} \tag{5.14}$$

$$g^{C_r\,\max}_{HS:Higgs}\left(\chi^{C_r},t\right) = \oint\limits_{B_{r-1}} d\mu^{B_{r-1}} \frac{1}{2} \sum_{t=\{t,-t\}} \frac{PE\left[\chi^{C_r}_{vec.} \otimes \chi^{B_{r-1}}_{vec.} t\right]}{PE\left[\chi^{B_{r-1}}_{adj.} t^2\right]} g^{B_{r-1}\,\max}_{HS:Higgs}\left(\chi^{B_{r-1}},t\right)$$
$$= \frac{1}{2} \prod_{d\in \text{Casimirs}[B_{r-1}]} \left(1-t^{2d}\right) \oint\limits_{B_{r-1}} d\mu^{B_{r-1}} \sum_{t=\{t,-t\}} PE\left[\chi^{C_r}_{vec.} \otimes \chi^{B_{r-1}}_{vec.} t\right] \tag{5.15}$$

$$g^{C_r\,\max}_{HS:Higgs}\left(\chi^{C_r},t\right) = \oint\limits_{D_r} d\mu^{D_r} \frac{PE\left[\chi^{C_r}_{vec.} \otimes \chi^{D_r}_{vec.} t\right]}{PE\left[\chi^{D_r}_{adj.} t^2\right]} g^{D_r\,\max}_{HS:Higgs}\left(\chi^{D_r},t\right)$$
$$= \prod_{d\in \text{Casimirs}[D_r]} \left(1-t^{2d}\right) \oint\limits_{D_r} d\mu^{D_r} PE\left[\chi^{C_r}_{vec.} \otimes \chi^{D_r}_{vec.} t\right] \tag{5.16}$$

$$g^{D_r\,\max}_{HS:Higgs}\left(\chi^{D_r},t\right) = \oint\limits_{C_{r-1}} d\mu^{C_{r-1}} \frac{PE\left[\chi^{D_r}_{vec.} \otimes \chi^{C_{r-1}}_{vec.} t\right]}{PE\left[\chi^{C_{r-1}}_{adj.} t^2\right]} g^{C_{r-1}\,\max}_{HS:Higgs}\left(\chi^{C_{r-1}},t\right)$$
$$= \prod_{d\in \text{Casimirs}[C_{r-1}]} \left(1-t^{2d}\right) \oint\limits_{C_{r-1}} d\mu^{C_{r-1}} PE\left[\chi^{D_r}_{vec.} \otimes \chi^{C_{r-1}}_{vec.} t\right] \tag{5.17}$$

As discussed in the next section, each B series gauge group, taken as $O(2r+1)$, requires both a Weyl integration over its $SO(2r+1)$ subgroup and a Molien average over the $\mathbb{Z}_2$ factor corresponding to the sign of the determinant of the $O(2r+1)$ representation matrix. Algebraically, this $\mathbb{Z}_2$ factor is introduced in 5.15 by changing the sign of the fugacity t within the PE function.

Calculation for BCD groups of low rank verifies that 5.14 to 5.17 correspond to the modified Hall Littlewood functions $mHL^G_{[singlet]}(t^2)$, as required by 4.3. It may be reasoned, following from the patterns of BCD group invariants, that this correspondence holds for BCD maximal nilpotent orbits of all rank. This is similar to the situation for A series maximal nilpotent orbits [25].

5.4.2. Orthogonal Gauge Groups

In order for a moduli space to be HyperKähler, the gauge groups must be connected [7], which in turn entails that a BCD quiver should contain O rather than SO gauge groups.

For a B series gauge group, the sign of the determinant of an $O(2r+1)$ representation matrix gives a $\mathbb{Z}_2$ factor that decouples from the vector representation as $\chi_{vec.}^{O(2r+1)} \to \pm 1 \otimes \chi_{vec.}^{SO(2r+1)}$. The projection of $O(2r+1)$ gauge group singlets therefore requires both the usual Weyl integration over the $SO(2r+1)$ subgroup and a Molien average (see Appendix A.2) over the $\mathbb{Z}_2$ factor. This factor is implemented in 5.15 as a sign change in the fugacity t that couples to the characters in the vector representation.

Gauge Groups $O(2r)$

Turning to D series gauge groups, the introduction of a $\mathbb{Z}_2$ factor has no effect on the Molien-Weyl integrals for quivers of *maximal nilpotent orbits*, calculated in the previous section, but is pertinent to the calculation of more general BCD nilpotent orbits.

Characters of $O(2r)$

Recall that an orthogonal representation matrix O obeys the defining identity $O.O^T = I$ and so $|O| = \pm 1$. A complication arises when constructing the character of an $O(2r)$ representation matrix, since the $\mathbb{Z}_2$ factor which acts to change the sign of its determinant is not a multiple of the identity matrix and therefore does not commute with the matrix. As a consequence, the character of an $O(2r)$ matrix with negative determinant, denoted $O(2r)^-$, does not have the same structure as the character of an $SO(2r)$ matrix. Indeed, it is necessary to calculate the character of an $O(2r)^-$ matrix from first principles. While the calculation for $O(2)^-$ is relatively straightforward, the general result for $O(2r)^-$ is surprising, since it involves both a reduction in rank and a partly symplectic character.

An illuminating method of calculating the character (i.e. sum of the eigenvalues) of a representation matrix is to find its eigenvalues, or at least their structure, as encoded in the characteristic polynomial.

Consider the $D_1 \cong SO(2) \cong U(1)$ matrix, $O = \begin{pmatrix} \cos\theta & \sin\theta \\ -\sin\theta & \cos\theta \end{pmatrix}$. The characteristic polynomial $|O - \lambda I| = 0$ evaluates as $1-(e^{i\theta}+e^{-i\theta})\lambda+\lambda^2 = 0$,

and the eigenvalues of O follow as $\lambda = e^{\pm i\theta}$, corresponding, under the substitution $e^{i\theta} \to x$, to the D_1 character $x + 1/x$. If we now apply the $\mathbb{Z}_2$ factor $\begin{pmatrix} 0 & 1 \\ 1 & 0 \end{pmatrix}$, the characteristic polynomial becomes $1 - \lambda^2 = 0$, with eigenvalues $\lambda = \pm 1$. Thus the character for $O(2)^-$ has zero rank and is just $1 + (-1)$. An equivalent treatment is given in [19].

Now consider O(4) and O(6) matrices acting on the vector representation. The structures of their eigenvalues differ between SO and O^- matrices, since the characteristic polynomials of $SO(2r)$ matrices are palindromic, while those of $O(2r)^-$ are anti-palindromic. Their eigenvalues rearrange to the forms in Table 5.9, where we use canonical unimodular CSA coordinates to indicate the groups from which characters are taken: $\{x, y, \ldots\}$ for D_r and $\{a, b, \ldots\}$ for C_r. Importantly, this decomposition of the character of

Matrix	Characteristic Polynomial	Eigenvalues (λ)
$SO(2)$	$1 - a_1\lambda + \lambda^2 = 0$	$\{x, 1/x\}$
$O(2)^-$	$1 - \lambda^2 = 0$	$\{1, -1\}$
$SO(4)$	$1 - a_1\lambda + a_2\lambda^2 - a_1\lambda^3 + \lambda^4 = 0$	$\{xy, 1/xy, x/y, y/x\}$
$O(4)^-$	$1 - a_1\lambda + a_1\lambda^3 - \lambda^4 = 0$	$\{1, -1, a, 1/a\}$
$SO(6)$	$1 - a_1\lambda + a_2\lambda^2 - a_3\lambda^3 + a_2\lambda^4 - a_1\lambda^5 + \lambda^6 = 0$	$\left\{\frac{x}{yz}, \frac{yz}{x}, x, \frac{1}{x}, \frac{z}{y}, \frac{y}{z}\right\}$
$O(6)^-$	$1 - a_1\lambda + a_2\lambda^2 - a_2\lambda^4 + a_1\lambda^5 - \lambda^6 = 0$	$\left\{1, -1, a, \frac{1}{a}, \frac{a}{b}, \frac{b}{a}\right\}$

Table 5.9.: Characteristic Polynomials and Eigenvalues of O(2r)

an $O(2r)^-$ matrix in the vector representation generalises to higher rank $O(2r)$ groups, as $\chi_{vec.}^{O(2r)^-} \cong \chi_{vec.}^{O(2)^-} \oplus \chi_{vec.}^{C_{r-1}}$.

Before proceeding, it is useful to verify that the use of the characters $\chi_{vec.}^{O(2r)^-}$ and $\chi_{vec.}^{SO(2r)}$ for the two types of $O(2r)$ vector representation leads to the required invariants. The Hilbert series for symmetric and antisymmetric invariants can be found by applying the PE or PEF, respectively, to a character, in both cases followed by Weyl integration. The Weyl integration is carried out using the Haar measures for the corresponding D or C groups and we obtain the results in Table 5.10. The exponents of the fugacity t give the degrees of the invariants and show that both types of $O(2r)$ vector representation matrices are associated with symmetric and antisymmetric invariants in the form of delta and epsilon tensors, but with a change of sign in the antisymmetric invariants (i.e. determinants). Thus, when we take a group average over $O(2r)$, the antisymmetric invariants encoded in

a Hilbert series cancel out.

Matrix	Det.	$\chi^{O}_{vec.}$	$\oint d\mu\ PE\left[\chi^{O}_{vec.}t\right]$	$\oint d\mu\ PEF\left[\chi^{O}_{vec.}t\right]$
$SO(2)$	$+1$	$q+1/q$	$\frac{1}{1-t^2}$	$1+t^2$
$O(2)^-$	-1	$1+(-1)$	$\frac{1}{1-t^2}$	$1-t^2$
$SO(4)$	$+1$	$xy+\frac{1}{xy}+\frac{x}{y}+\frac{y}{x}$	$\frac{1}{1-t^2}$	$1+t^4$
$O(4)^-$	-1	$1+(-1)+x+\frac{1}{x}$	$\frac{1}{1-t^2}$	$1-t^4$
$SO(6)$	$+1$	$\frac{x}{yz}+\frac{yz}{x}+x+\frac{1}{x}+\frac{z}{y}+\frac{y}{z}$	$\frac{1}{1-t^2}$	$1+t^6$
$O(6)^-$	-1	$1+(-1)+x+\frac{1}{x}+\frac{x}{y}+\frac{y}{x}$	$\frac{1}{1-t^2}$	$1-t^6$
$SO(2r)$	$+1$	$\chi^{SO(2r)}_{vec.}$	$\frac{1}{1-t^2}$	$1+t^{2r}$
$O(2r)^-$	-1	$1+(-1)+\chi^{C_{r-1}}_{vec.}$	$\frac{1}{1-t^2}$	$1-t^{2r}$

Table 5.10.: Characters and Invariants of O(2r) Matrices

HyperKähler Quotients for $C_k - O(2r)$

The peculiar form of character for $\chi^{O(2r)^-}_{vec.}$ leads to a HyperKähler quotient for a quiver with C_k flavour group and $O(2r)^-$ gauge group that varies from the usual $PE[\chi^{SO(2r)}_{adj.}t^2]$. We can find this HKQ by integrating over the C_k flavour group, where $k \geq r$ for the quivers under study:

$$g_{HK}\left(\chi^{O(2r)^-},t\right) = \oint_{C_k} d\mu^{C_k} PE\left[\chi^{C_k}_{vec.}\otimes\chi^{O(2r)^-}_{vec.}t\right] \tag{5.18}$$

Carrying out the calculation for $O(2r)^-$ characters up to $r=5$ gives the results in Table 5.11. Based on these, this study conjectures that the HKQ for higher rank $O(2r)^-$ characters is as shown.

The structure of the HKQ terms follows from the invariant tensors of the C_k flavour group fundamental, which are antisymmetric of degree $2,4,\ldots,2k$. Under the PE of the bifundamental of the $C_k\otimes O(2r)^-$ product group, these C_k invariants map the character $\chi^{O(2r)^-}_{vec.}$ to a series of characters of C_{r-1} irreps. The PEs in Table 5.11 that generate this series contain terms at t^4, in addition to the usual term at t^2 from the anti-symmetrisation of an orthogonal group vector representation.

Bifundamental	$g_{HK}^{O(2r)^-}\left(\chi^{C_{r-1}},t\right)$
$C_{k\geq 1}\otimes O(2)^-$	$1/(1+t^2)$
$C_{k\geq 2}\otimes O(4)^-$	$PE[[2]_C,t^4]$
$C_{k\geq 3}\otimes O(6)^-$	$PE[[0,1]_C,t^2]\ PE[[2,0]_C-[0,1]_C,t^4]$
$C_{k\geq 4}\otimes O(8)^-$	$PE[[0,1,0]_C,t^2]\ PE[[2,0,0]_C-[0,1,0]_C,t^4]$
$C_{k\geq 5}\otimes O(10)^-$	$PE[[0,1,0,0]_C,t^2]\ PE[[2,0,0,0]_C-[0,1,0,0]_C,t^4]$
$C_{k\geq r}\otimes O(2r)^-$	$PE\left[[0,1,0,\ldots\ldots,0]_{C_{r-1}},t^2\right]\ PE\left[[2,0,0,\ldots,0]_{C_{r-1}}-[0,1,0\ldots,0]_{C_{r-1}},t^4\right]$

Table 5.11.: HyperKähler Quotients for $O(2r)^-$

Based on the foregoing, we can express the group averaged Weyl integration over a quiver containing a bifundamental field with C_k flavour group and $O(2)$ gauge group, as:

$$g_{HS:Higgs}^{C_k-O(2)}\left(\chi^{C_k},t\right)=\frac{1}{2}\left(g_{HS:Higgs}^{C_k-SO(2)}\left(\chi^{C_k},t\right)+g_{HS:Higgs}^{C_k-O(2)^-}\left(\chi^{C_k},t\right)\right), \quad (5.19)$$

where

$$g_{HS:Higgs}^{C_k-SO(2)}\left(\chi^{C_k},t\right)=\oint_{SO(2)}d\mu^{SO(2)}\frac{PE\left[\chi_{vec.}^{C_k}\otimes\chi_{vec.}^{SO(2)}t\right]}{PE\left[t^2\right]} \quad (5.20)$$

and

$$g_{HS:Higgs}^{C_k-O(2)^-}\left(\chi^{C_k},t\right)=\frac{PE\left[\chi_{vec.}^{C_k}t\right]PE\left[\chi_{vec.}^{C_k}(-t)\right]}{1/\left(1+t^2\right)}. \quad (5.21)$$

The vector character of $D_1\cong SO(2)$ is represented as $x+1/x$ and the unitary Haar measure $1/x$ is used, when calculating 5.20. The action of the $\mathbb{Z}_2$ factor encoded in 5.21 is trivial for the maximal chain C_1-D_1, but has an impact on the Hilbert series for quivers containing non-maximal chains, from C_2-D_1 upwards.

The corresponding Weyl integral for a C_k flavour group and $O(2r)$ gauge

group where $k \geq r > 1$ is:

$$g_{HS:Higgs}^{C_k-O(2r)}\left(\chi^{C_k},t\right) = \frac{1}{2}\oint_{D_r} d\mu^{D_r}\frac{PE\left[\chi_{vec.}^{C_k}\otimes\chi_{vec.}^{SO(2r)}t\right]}{PE\left[\chi_{adj.}^{SO(2r)}t^2\right]} + \frac{1}{2}\oint_{C_{r-1}} d\mu^{C_{r-1}}\frac{PE\left[\chi_{vec.}^{C_k}\otimes\chi_{vec.}^{C_{r-1}}t\right]PE\left[\chi_{vec.}^{C_k}t\right]PE\left[\chi_{vec.}^{C_k}(-t)\right]}{g_{HK}^{O(2r)^-}\left(\chi^{C_{r-1}},t\right)} \tag{5.22}$$

where $g_{HK}^{O(2r)^-}$ is as in Table 5.11. These group averaging procedures, which do not affect the dimensions of a moduli space, but may affect its structure, are included within the evaluation of general BCD quivers in the following.

5.4.3. Evaluation of BCD Series Quivers

Using the averaging procedures over orthogonal gauge groups, as elaborated in section 5.4.2, we can calculate the Hilbert series of a BCD quiver from the general formula, adapted from 5.8:

$$g_{HS:Higgs}^{SO/USp(N_0)}\left(\chi^{SO/USp(N_0)},t\right) = \frac{1}{2^{\#O}}\sum_{O\pm}\oint_{\substack{USp/O(N_1)\otimes\\ O/USp(N_2)\otimes\ldots}} d\mu^{\substack{USp/O(N_1)\otimes\\ O/USp(N_2)\otimes\ldots}} \times\prod_{\substack{gauge(i)\\ =USp}}\frac{PE\left[\chi_{vec.}^{O(N_{i-1})}\otimes\chi_{vec.}^{USp(N_i)}t\right]}{PE\left[\chi_{adj.}^{USp(N_i)}t^2\right]}\times\prod_{\substack{gauge(i)\\ =O}}\frac{PE\left[\chi_{vec.}^{USp(N_{i-1})}\otimes\chi_{vec.}^{O(N_i)}t\right]}{g_{HK}^{O(N_i)}\left(\chi_{adj.}^{O(N_i)},t\right)}, \tag{5.23}$$

where $\#O$ equals the number of orthogonal gauge groups and the summation indicates that all possible combinations of SO/O^- gauge group characters should be evaluated. As before, the calculations can be arranged in a recursive manner, inducing a nilpotent orbit from the orbits defined by the subchains in a quiver.

5.4.4. Analysis of BCD Series Moduli Spaces

Once the Hilbert series for a BCD quiver has been calculated, it can be restated in a similar manner to the A series quivers. The results for BCD groups of rank up to 4 are set out in Tables 5.12 to 5.17.

Orbit	Quiver	$\lvert\mathcal{O}\rvert$	Unrefined Hilbert Series	Character HWG	mHL HWG
(1^3)	B_1	0	1	1	$1-h^2t^2$
(3)	B_1, C_1, B_0	2	$\frac{1+t^2}{(1-t^2)^2}$	$\frac{1}{1-m^2t^2}$	1
(1^5)	B_2	0	1	1	$1-{h_2}^2t^2-h_1t^4$ $+h_1{h_2}^2t^4+h_1{h_2}^2t^6$ $-{h_1}^3t^6-{h_2}^4t^6+{h_1}^2{h_2}^2t^8$
$(2^2,1)$	B_2, C_1	4	$\frac{1+6t^2+t^4}{(1-t^2)^4}$	$\frac{1}{1-{m_2}^2t^2}$	$1-h_1t^4-{h_1}^2t^4+h_1{h_2}^2t^6$
$(3,1^2)$	B_2, C_1, B_0	6	$\frac{(1+t^2)(1+3t^2+t^4)}{(1-t^2)^6}$	$\frac{1}{(1-{m_2}^2t^2)(1-{m_1}^2t^4)}$	$1-h_1t^4$
(5)	B_2, C_2, B_1, C_1, B_0	8	$\frac{(1+t^2)^2(1+t^4)}{(1-t^2)^8}$	$\frac{1+m_1{m_2}^2t^8}{\left(\begin{array}{c}(1-{m_2}^2t^2)(1-m_1t^4)\\ \times(1-{m_1}^2t^4)(1-{m_2}^2t^6)\end{array}\right)}$	1
(1^7)	B_3	0	1	1	not shown
$(2^2,1^3)$	B_3, C_1	8	$\frac{1+13t^2+28t^4+13t^6+t^8}{(1-t^2)^8}$	$\frac{1}{1-m_2t^2}$	not shown
$(3,1^4)$	B_3, C_1, B_0	10	$\frac{1+10t^2+20t^4+10t^6+t^8}{(1-t^2)^{10}(1+t^2)^{-1}}$	$\frac{1}{(1-m_2t^2)(1-{m_1}^2t^4)}$	$1-{h_3}^2t^4-h_2t^6+h_1h_2t^6$ $-h_1t^6+h_1h_2t^8+{h_3}^2t^8$ $-{h_1}^3t^8-{h_2}^2t^{10}+{h_1}^2h_2t^{12}$
$(3,2^2)$	B_3, C_2, B_0	12	$\frac{1+8t^2+36t^4+92t^6+t^8-6t^{10}}{(1-t^2)^{12}(1+t^2)^{-1}}$	$\frac{1+m_1{m_3}^2t^6}{(1-m_2t^2)(1-{m_1}^2t^4)(1-{m_3}^2t^4)}$	$1-h_1t^6-h_2t^6-{h_2}^2t^8$ $+{h_3}^2t^8+{h_1}^2h_2t^{10}$ $+h_2{h_3}^2t^{10}-{h_1}^2{h_3}^2t^{12}$
$(3^2,1)$	B_3, C_2, D_1	14	$\frac{1+6t^2+21t^4+28t^6+21t^8+6t^{10}+t^{12}}{(1-t^2)^{14}(1+t^2)^{-1}}$	$\frac{1+m_1m_2{m_3}^2t^{10}}{\left(\begin{array}{c}(1-m_2t^2)(1-{m_1}^2t^4)(1-{m_3}^2t^4)\\ \times(1-m_1{m_3}^2t^6)(1-{m_2}^2t^8)\end{array}\right)}$	$1-h_2t^6-h_1t^6+{h_3}^2t^8$
$(5,1^2)$	B_3, C_2, B_1, C_1, B_0	16	$\frac{1+3t^2+6t^4+3t^6+t^8}{(1-t^2)^{16}(1+t^2)^{-2}(1+t^4)^{-1}}$	not shown	$1-h_1t^6$
(7)	$B_3, C_3, B_2, C_2, B_1, C_1, B_0$	18	$\frac{(1-t^4)(1-t^8)(1-t^{12})}{(1-t^2)^{21}}$	not shown	1

B/D gauge nodes in a quiver indicate averages over the corresponding O gauge groups
An mHL HWG of 1 denotes $mHL^B_{[0,\ldots,0]}(t^2)$.
The character or mHL HWGs for some quivers are not shown for brevity.

Table 5.12.: Quivers, HWGs and HS for Orbits of B_1, B_2 and B_3

Orbit	Quiver	Dim.	Unrefined Hilbert Series	Character HWG	mHL HWG
(1^9)	B_4	0	1	1	not shown
$(2^2,1^5)$	B_4, C_1	12	$\frac{1+24t^2+129t^4+220t^6+129t^8+24t^{10}+t^{12}}{(1-t^2)^{12}}$	$\frac{1}{1-m_2t^2}$	not shown
$(3,1^6)$	B_4, C_1, B_0	14	$\frac{1+21t^2+105t^4+175t^6+105t^8+21t^{10}+t^{12}}{(1-t^2)^{14}(1+t^2)^{-1}}$	$\frac{1}{(1-{m_1}^2t^4)(1-m_2t^2)}$	not shown
$(2^4,1)$	B_4, C_2	16	$\frac{1+20t^2+165t^4+600t^6+924t^8}{+600t^{10}+165t^{12}+20t^{14}+t^{16}}{(1-t^2)^{16}}$	$\frac{1}{(1-m_2t^2)(1-{m_4}^2t^4)}$	not shown
$(3,2^2,1^2)$	B_4, C_2, B_0	20	$\frac{1+14t^2+106t^4+454t^6+788t^8}{+454t^{10}+106t^{12}+14t^{14}+t^{16}}{(1-t^2)^{20}(1+t^2)^{-2}}$	$\frac{1+m_1m_3t^6}{(1-{m_1}^2t^4)(1-m_2t^2)(1-{m_3}^2t^8)(1-{m_4}^2t^4)}$	not shown
$(3^2,1^3)$	B_4, C_2, D_1	22	$\frac{1+13t^2+91t^4+335t^6+737t^8+946t^{10}}{+737t^{12}+335t^{14}+91t^{16}+13t^{18}+t^{20}}{(1-t^2)^{22}(1+t^2)^{-1}}$	$\frac{1+m_1m_2m_3t^{10}}{\left(\begin{array}{c}(1-m_2t^2)(1-{m_1}^2t^4)(1-{m_4}^2t^4)\\ \times(1-m_1m_3t^6)(1-{m_2}^2t^8)(1-{m_3}^2t^8)\end{array}\right)}$	not shown
(3^3)	B_4, C_3, B_1	24	$\frac{1+10t^2+56t^4+194t^6+438t^8+578t^{10}}{+438t^{12}+194t^{14}+56t^{16}+10t^{18}+t^{20}}{(1-t^2)^{24}(1+t^2)^{-2}}$	not shown	$1-h_2t^6-h_1t^8-h_2t^{10}$ $+h_3t^{10}+h_1h_3t^{12}-{h_2}^2t^{14}$ $+h_3t^{14}+h_1h_3t^{14}-h_1{h_4}^2t^{14}$ $-h_1{h_4}^2t^{16}+h_2h_3t^{18}$
$(5,1^4)$	B_4, C_2, B_1, C_1, B_0	24	$\frac{1+10t^2+55t^4+136t^6+190t^8}{+136t^{10}+55t^{12}+10t^{14}+t^{16}}{(1-t^2)^{24}(1+t^2)^{-2}(1+t^4)^{-1}}$	not shown	$1-h_3t^6-h_1t^8+h_1h_2t^8$ $-{h_1}^3t^{10}-h_2t^{10}+h_1h_2t^{10}$ $-{h_2}^2t^{14}+h_3t^{14}+{h_1}^2h_2t^{16}$
$(4^2,1)$	B_4, C_3, D_2, C_1	26	$\frac{1+9t^2+45t^4+165t^6+441t^8+854t^{10}}{+1050t^{12}+\ldots\text{palindrome}\ldots+t^{24}}{(1-t^2)^{26}(1+t^2)^{-1}}$	not shown	$1-h_1t^8-{h_1}^2t^8-h_2t^{10}$ $+h_1h_2t^{14}+h_3t^{14}+h_1h_3t^{14}$ $-h_1{h_4}^2t^{16}$
$(5,2^2)$	B_4, C_3, B_1, C_1, B_0	26	$\frac{1+7t^2+30t^4+98t^6+259t^8+554t^{10}}{+484t^{12}+71t^{14}-15t^{16}-2t^{18}+t^{20}}{(1-t^2)^{26}(1+t^2)^{-3}}$	not shown	$1-h_1t^8-h_2t^{10}-{h_2}^2t^{12}$ $+{h_1}^2h_2t^{14}+h_3t^{14}$ $+h_2h_3t^{16}-{h_1}^2h_3t^{18}$
$(5,3,1)$	B_4, C_3, D_2, C_1, B_0	28	$\frac{1+6t^2+22t^4+62t^6+138t^8+227t^{10}}{+264t^{12}+\ldots\text{palindrome}\ldots+t^{24}}{(1-t^2)^{28}(1+t^2)^{-2}}$	$\ldots$	$1-h_1t^8-h_2t^{10}+h_3t^{14}$
$(7,1^2)$	$B_4, C_3, B_2,$ C_2, B_1, C_1, B_0	30	$\frac{1+3t^2+6t^4+10t^6+6t^8+3t^{10}+t^{12}}{(1-t^2)^{33}(1-t^4)^{-1}(1-t^8)^{-1}(1-t^{12})^{-1}}$	$\ldots$	$1-h_1t^8$
(9)	$B_4, C_4, B_3, C_3,$ B_2, C_2, B_1, C_1, B_0	32	$\frac{(1-t^4)(1-t^8)(1-t^{12})(1-t^{16})}{(1-t^2)^{36}}$	$\ldots$	1

B/D gauge nodes in a quiver indicate averages over the corresponding O gauge groups
An mHL HWG of 1 denotes $mHL^B_{[0,\ldots,0]}(t^2)$.
The character or mHL HWGs for some quivers are not shown for brevity.

Table 5.13.: Quivers, HWGs and HS for Orbits of B_4

Orbit	Quiver	Dim.	Unrefined Hilbert Series	Character HWG	mHL HWG
(1^2)	C_1	0	1	1	$1-h^2t^2$
(2)	C_1, B_0	2	$\frac{1+t^2}{(1-t^2)^2}$	$\frac{1}{1-m^2t^2}$	1
(1^4)	C_2	0	1	1	$1-{h_1}^2t^2-h_2t^4$ $+{h_1}^2h_2t^4+{h_1}^2h_2t^6$ $-{h_2}^3t^6-{h_1}^4t^6+{h_1}^2{h_2}^2t^8$
$(2,1^2)$	C_2, B_0	4	$\frac{1+6t^2+t^4}{(1-t^2)^4}$	$\frac{1}{1-{m_1}^2t^2}$	$1-h_2t^4-{h_2}^2t^4+{h_1}^2h_2t^6$
(2^2)	C_2, D_1	6	$\frac{1+3t^2+t^4}{(1-t^2)^6(1+t^2)^{-1}}$	$\frac{1}{(1-{m_1}^2t^2)(1-{m_2}^2t^4)}$	$1-h_2t^4$
(4)	C_2, B_1, C_1, B_0	8	$\frac{(1-t^4)(1-t^8)}{(1-t^2)^{10}}$	$\frac{1+{m_1}^2m_2t^8}{\left(\begin{array}{c}(1-{m_1}^2t^2)(1-m_2t^4)\\ \times(1-{m_2}^2t^4)(1-{m_1}^2t^6)\end{array}\right)}$	1
(1^6)	C_3	0	1	1	not shown
$(2,1^4)$	C_3, B_0	6	$\frac{1+14t^2+t^4}{(1-t^2)^6(1+t^2)^{-1}}$	$\frac{1}{1-{m_1}^2t^2}$	not shown
$(2^2,1^2)$	C_3, D_1	10	$\frac{1+10t^2+41t^4+10t^6+t^8}{(1-t^2)^{10}(1+t^2)^{-1}}$	$\frac{1}{(1-{m_1}^2t^2)(1-{m_2}^2t^4)}$	$1-h_2t^4-{h_3}^2t^6$ $+h_1h_2h_3t^8+h_1h_3t^8-h_2t^8$ $+h_1h_2h_3t^{10}+h_1h_3t^{10}-{h_1}^3h_3t^{10}$ $-{h_2}^2t^{10}-{h_2}^3t^{10}+{h_1}^2{h_2}^2t^{12}$
(2^3)	C_3, B_1	12	$\frac{1+7t^2+15t^4+7t^6+t^8}{(1-t^2)^{12}(1+t^2)^{-2}}$	$\frac{1}{(1-{m_1}^2t^2)(1-{m_2}^2t^4)(1-{m_3}^2t^6)}$	$1-h_2t^4+h_1h_3t^8$ $-h_2t^8+h_1h_3t^{10}$ $-{h_2}^2t^{10}$
(3^2)	C_3, D_2, C_1	14	$\frac{1+6t^2+21t^4+35t^6+21t^8+6t^{10}+t^{12}}{(1-t^2)^{14}(1+t^2)^{-1}}$	$\frac{1+m_1m_2m_3t^8}{\left(\begin{array}{c}(1-{m_1}^2t^2)(1-{m_2}^2t^4)(1-{m_2}^2t^4)\\ \times(1-m_1m_3t^6)(1-{m_3}^2t^6)\end{array}\right)}$	$1-{h_1}^2t^6-h_2t^8+h_1h_3t^{10}$
$(4,1^2)$	C_3, B_1, C_1, B_0	14	$\frac{1+6t^2+21t^4+56t^6+21t^8+6t^{10}+t^{12}}{(1-t^2)^{14}(1+t^2)^{-1}}$	not shown	$1-h_2t^8-{h_2}^2t^8+{h_1}^2h_2t^{10}$
(4, 2)	C_3, D_2, C_1, B_0	16	$\frac{1+3t^2+7t^4+13t^6+7t^8+3t^{10}+t^{12}}{(1-t^2)^{16}(1+t^2)^{-2}}$	not shown	$1-h_2t^8$
(6)	$C_3, B_2, C_2, B_1, C_1, B_0$	18	$\frac{(1-t^4)(1-t^8)(1-t^{12})}{(1-t^2)^{21}}$	not shown	1

B/D gauge nodes in a quiver indicate averages over the corresponding O gauge groups
An mHL HWG of 1 denotes $mHL^C_{[0,\ldots,0]}(t^2)$.
The character or mHL HWGs for some quivers are not shown for brevity.

Table 5.14.: Quivers, HWGs and HS for Orbits of C_1, C_2 and C_3

Orbit	Quiver	Dim.	Unrefined Hilbert Series	Character HWG	mHL HWG
(1^8)	C_4	0	1	1	not shown
$(2,1^6)$	C_4, B_0	8	$\frac{1+28t^2+70t^4+28t^6+t^8}{(1-t^2)^8}$	$\frac{1}{1-{m_1}^2t^2}$	not shown
$(2^2,1^4)$	C_4, D_1	14	$\frac{1+21t^2+204t^4+406t^6}{+204t^8+21t^{10}+t^{12}}{(1-t^2)^{14}(1+t^2)^{-1}}$	$\frac{1}{(1-{m_1}^2t^2)(1-{m_2}^2t^4)}$	not shown
$(2^3,1^2)$	C_4, B_1	18	$\frac{1+17t^2+126t^4+537t^6+894t^8}{+537t^{10}+126t^{12}+17t^{14}+t^{16}}{(1-t^2)^{18}(1+t^2)^{-1}}$	$\frac{1}{(1-{m_1}^2t^2)(1-{m_2}^2t^4)(1-{m_3}^2t^6)}$	not shown
(2^4)	C_4, D_2	20	$\frac{1+14t^2+79t^4+223t^6+317t^8}{+223t^{10}+79t^{12}+14t^{14}+t^{16}}{(1-t^2)^{20}(1+t^2)^{-2}}$	$\frac{1}{\left(\begin{array}{c}(1-{m_1}^2t^2)(1-{m_2}^2t^4)\\ \times(1-{m_3}^2t^6)(1-{m_4}^2t^8)\end{array}\right)}$	not shown
$(4,1^4)$	C_4, B_1, C_1, B_0	20	$\frac{1+14t^2+106t^4+574t^6+722t^8}{+574t^{10}+106t^{12}+14t^{14}+t^{16}}{(1-t^2)^{20}(1+t^2)^{-2}}$	$\frac{1+m_1m_3t^6+m_1m_2m_3t^8+{m_1}^2m_2t^8}{\left(\begin{array}{c}(1-{m_1}^2t^2)(1-{m_1}^2t^6)(1-m_2t^4)\\ \times(1-{m_2}^2t^4)(1-{m_3}^2t^6)\end{array}\right)}$	not shown
$(3^2,1^2)$	C_4, D_2, C_1	22	$\frac{1+13t^2+91t^4+419t^6+1346t^8+2365t^{10}}{+1841t^{12}+476t^{14}-56t^{16}-29t^{18}+t^{20}}{(1-t^2)^{22}(1+t^2)^{-1}}$	$\frac{1+m_2m_4t^8+m_1m_2m_3t^8+m_1m_3m_4t^{10}}{+m_1m_2m_3m_4t^{12}-m_1m_2m_3m_4t^{14}}{\left(\begin{array}{c}(1-{m_1}^2t^2)(1-{m_2}^2t^4)(1-m_2t^4)\\ \times(1-{m_3}^2t^6)(1-m_1m_3t^6)(1-{m_4}^2t^8)\end{array}\right)}$	not shown
$(3^2,2)$	C_4, B_2, C_1	24	$\frac{1+10t^2+56t^4+194t^6+405t^8+512t^{10}}{+405t^{12}+194t^{14}+56t^{16}+10t^{18}+t^{20}}{(1-t^2)^{24}(1+t^2)^{-2}}$	not shown	$1-{h_1}^2t^6-h_2t^8-h_4t^8+h_1h_3t^{10}$ $-h_2t^{12}+h_1h_3t^{12}+h_4t^{12}$ $-{h_2}^2t^{14}+2h_1h_3t^{14}-h_2h_4t^{14}$ $+{h_3}^2t^{16}-h_2h_4t^{16}$
$(4,2,1^2)$	C_4, D_2, C_1, B_0	24	$\frac{1+10t^2+56t^4+230t^6+701t^8+776t^{10}}{+701t^{12}+230t^{14}+56t^{16}+10t^{18}+t^{20}}{(1-t^2)^{24}(1+t^2)^{-2}}$	not shown	$1-h_2t^8-h_4t^8-{h_3}^2t^{10}-h_2t^{12}$ $+h_1h_3t^{12}+h_1h_2h_3t^{12}+h_4t^{12}$ $-{h_2}^2t^{14}-{h_2}^3t^{14}+h_1h_3t^{14}$ $-{h_1}^3h_3t^{14}+h_1h_2h_3t^{14}+{h_1}^2{h_2}^2t^{16}$
$(4,2^2)$	C_4, B_2, C_1, B_0	26	$\frac{1+7t^2+30t^4+98t^6+199t^8+230t^{10}}{+199t^{12}+98t^{14}+30t^{16}+7t^{18}+t^{20}}{(1-t^2)^{29}(1-t^4)^{-3}}$	not shown	$1-h_2t^8-h_4t^8-h_2t^{12}+h_1h_3t^{12}$ $+h_4t^{12}-{h_2}^2t^{14}+h_1h_3t^{14}$
(4^2)	C_4, D_3, C_2, D_1	28	$\frac{1+6t^2+21t^4+56t^6+99t^8+117t^{10}}{+99t^{12}+56t^{14}+21t^{16}+6t^{18}+t^{20}}{(1-t^2)^{30}(1-t^4)^{-1}(1-t^8)^{-1}}$	$\ldots$	$1-h_2t^8-h_2t^{12}+h_4t^{12}$
$(6,1^2)$	$C_4, B_2, C_2,$ B_1, C_1, B_0	28	$\frac{1+6t^2+21t^4+56t^6+126t^8+252t^{10}}{+126t^{12}+56t^{14}+21t^{16}+6t^{18}+t^{20}}{(1-t^2)^{30}(1-t^4)^{-1}(1-t^8)^{-1}}$	$\ldots$	$1-h_2t^{12}-{h_2}^2t^{12}+{h_1}^2h_2t^{14}$
$(6,2)$	$C_4, D_3, C_2,$ B_1, C_1, B_0	30	$\frac{1+3t^2+7t^4+13t^6+22t^8+34t^{10}}{+22t^{12}+13t^{14}+7t^{16}+3t^{18}+t^{20}}{(1-t^2)^{33}(1-t^4)^{-2}(1-t^8)^{-1}}$	$\ldots$	$1-h_2t^{12}$
(8)	$C_4, B_3, C_3, B_2,$ C_2, B_1, C_1, B_0	32	$\frac{(1-t^4)(1-t^8)(1-t^{12})(1-t^{16})}{(1-t^2)^{36}}$	$\ldots$	1

B/D gauge nodes in a quiver indicate averages over the corresponding O gauge groups
An mHL HWG of 1 denotes $mHL^C_{[0,\ldots,0]}(t^2)$.
The character or mHL HWGs for some quivers are not shown for brevity.

Table 5.15.: Quivers, HWGs and HS for Orbits of C_4

Orbit	Quiver	Dim.	Unrefined Hilbert Series	Character HWG	mHL HWG
(1^4)	D_2	0	1	1	$1-h_2{}^2t^2-h_1{}^2t^2+h_1{}^2h_2{}^2t^4$
$(2^2)^{I/II}$	D_2, C_1	2	$\frac{1+4t^2-t^4}{(1-t^2)^2}$	$\frac{1-m_1{}^2m_2{}^2t^4}{(1-m_1{}^2t^2)(1-m_2{}^2t^2)}$	$1-h_1{}^2h_2{}^2t^4$
$(3,1)$	D_2, C_1, B_0	4	$\frac{(1-t^4)^2}{(1-t^2)^6}$	$\frac{1}{(1-m_1{}^2t^2)(1-m_2{}^2t^2)}$	1
(1^6)	D_3	0	1	1	$1-h_2h_3t^2-h_2h_3t^4$ $+h_1h_3{}^2t^4+h_1h_2{}^2t^4-h_2h_3t^6$ $-h_1{}^2h_2h_3t^6+h_1h_3{}^2t^6-h_2{}^2h_3{}^2t^6$ $+h_1h_2{}^2t^6+h_1{}^2t^6-h_3{}^4t^6$ $-h_2{}^4t^6-h_1{}^2h_2h_3t^8+h_1h_2{}^3h_3t^8$ $-h_2{}^2h_3{}^2t^8+h_1h_2h_3{}^3t^8+h_1{}^4t^8$ $+h_1h_2{}^3h_3t^{10}-h_1{}^3h_3{}^2t^{10}$ $-h_1{}^3h_2{}^2t^{10}+h_1h_2h_3{}^3t^{10}$ $-h_2{}^3h_3{}^3t^{10}+h_1{}^2h_2{}^2h_3{}^2t^{12}$
$(2^2,1^2)$	D_3, C_1	6	$\frac{1+8t^2+t^4}{(1-t^2)^6(1+t^2)^{-1}}$	$\frac{1}{1-m_2m_3t^2}$	$1-h_2h_3t^4-h_1{}^2t^4$ $-h_2h_3t^6+h_1h_3{}^2t^6$ $+h_1h_2{}^2t^6+h_1{}^2t^6-h_2{}^2h_3{}^2t^8$
$(3,1^3)$	D_3, C_1, B_0	8	$\frac{1+5t^2+t^4}{(1-t^2)^8(1+t^2)^{-2}}$	$\frac{1}{(1-m_2m_3t^2)(1-m_1{}^2t^4)}$	$1-h_2h_3t^4+h_1{}^2t^6-h_2h_3t^6$
(3^2)	D_3, C_2, D_1	10	$\frac{1+4t^2+10t^4+4t^6+t^8}{(1-t^2)^{10}(1+t^2)^{-1}}$	$\frac{1-m_1{}^2m_2{}^2m_3{}^2t^{12}}{\left(\begin{array}{c}(1-m_2m_3t^2)(1-m_1{}^2t^4)(1-m_2m_3t^4)\\ \times(1-m_1m_2{}^2t^6)(1-m_1m_3{}^2t^6)\end{array}\right)}$	$1-h_2h_3t^6$
$(5,1)$	D_3, C_2, B_1, C_1, B_0	12	$\frac{(1-t^4)(1-t^6)(1-t^8)}{(1-t^2)^{15}}$	not shown	1

B/D gauge nodes in a quiver indicate averages over the corresponding O gauge groups
An mHL HWG of 1 denotes $mHL^D_{[0,\ldots,0]}(t^2)$.
The character or mHL HWGs for some quivers are not shown for brevity.

Table 5.16.: Quivers, HWGs and HS for Orbits of D_2 and D_3

Orbit	Quiver	Dim.	Unrefined Hilbert Series	Character HWG	mHL HWG
(1^8)	D_4	0	1	1	not shown
$(2^2,1^4)$	D_4, C_1	10	$\frac{1+17t^2+48t^4+17t^6+t^8}{(1-t^2)^{10}(1+t^2)^{-1}}$	$\frac{1}{1-m_2t^2}$	not shown
$(2^4)^{I/II}$	D_4, C_2	12	$\frac{1+15t^2+85t^4+162t^6+15t^8-13t^{10}-t^{12}}{(1-t^2)^{12}(1+t^2)^{-1}}$	$\frac{1-{m_3}^2{m_4}^2t^8}{(1-m_2t^2)(1-{m_3}^2t^4)(1-{m_4}^2t^4)}$	not shown
$(3,1^5)$	D_4, C_1, B_0	12	$\frac{1+14t^2+36t^4+14t^6+t^8)}{(1-t^2)^{12}(1+t^2)^{-2}}$	$\frac{1}{(1-{m_1}^2t^4)(1-m_2t^2)}$	not shown
$(3,2^2,1)$	D_4, C_2, B_0	16	$\frac{1+12t^2+77t^4+296t^6+476t^8}{+296t^{10}+77t^{12}+12t^{14}+t^{16}}{(1-t^2)^{16}}$	$\frac{1+m_1m_3m_4t^6}{\left(\begin{array}{c}(1-{m_1}^2t^4)(1-m_2t^2)\\ \times(1-{m_3}^2t^4)(1-{m_4}^2t^4)\end{array}\right)}$	$1-2h_2t^6+{h_1}^2t^8-{h_2}^2t^8$ $+{h_3}^2t^8+{h_4}^2t^8-h_2t^{10}$ $+{h_1}^2h_2t^{10}+h_2{h_3}^2t^{10}$ $+h_2{h_4}^2t^{10}-{h_1}^2{h_3}^2t^{12}$ $-{h_1}^2{h_4}^2t^{12}-{h_3}^2{h_4}^2t^{12}$ $-h_1h_3h_4t^{14}+h_1h_2h_3h_4t^{16}$
$(3^2,1^2)$	D_4, C_2, D_1	18	$\frac{1+9t^2+45t^4+109t^6+152t^8}{+109t^{10}+45t^{12}+9t^{14}+t^{16}}{(1-t^2)^{18}(1+t^2)^{-1}}$	$\frac{1+m_1m_2m_3m_4t^{10}}{\left(\begin{array}{c}(1-{m_1}^2t^4)(1-m_2t^2)\\ \times(1-{m_2}^2t^8)(1-{m_3}^2t^4)\\ \times(1-{m_4}^2t^4)(1-m_1m_3m_4t^6)\end{array}\right)}$	$1-2h_2t^6+{h_1}^2t^8+{h_3}^2t^8$ $+{h_4}^2t^8-h_2t^{10}-h_1h_3h_4t^{14}$
$(4^2)^{I/II}$	D_4, C_3, D_2, C_1	20	$\frac{1+7t^2+28t^4+84t^6+173t^8+238t^{10}}{+133t^{12}+28t^{14}-14t^{16}-5t^{18}-t^{20}}{(1-t^2)^{20}(1+t^2)^{-1}}$	not shown	$1-{h_1}^2t^8-h_2t^{10}+h_1h_3h_4t^{14}$
$(5,1^3)$	D_4, C_2, B_1, C_1, B_0	20	$\frac{1+6t^2+21t^4+28t^6}{+21t^8+6t^{10}+t^{12}}{(1-t^2)^{20}(1+t^2)^{-2}(1+t^4)^{-1}}$	not shown	$1-h_2t^6+{h_1}^2t^8-h_2t^{10}$
$(5,3)$	D_4, C_3, D_2, C_1, B_0	22	$\frac{1+3t^2+8t^4+16t^6+28t^8}{+16t^{10}+8t^{12}+3t^{14}+t^{16}}{(1-t^2)^{22}(1+t^2)^{-3}}$	not shown	$1-h_2t^{10}$
$(7,1)$	$D_4, C_3, B_2,$ C_2, B_1, C_1, B_0	24	$\frac{(1-t^4)(1-t^8)^2(1-t^12)}{(1-t^2)^{28}}$	not shown	1

B/D gauge nodes in a quiver indicate the corresponding O gauge groups
An mHL HWG of 1 denotes $mHL^D_{[0,\ldots,0]}(t^2)$.
The character or mHL HWGs for some quivers are not shown for brevity.

Table 5.17.: Quivers, HWGs and HS for Orbits of D_4

It is noteworthy that, for all the BCD nilpotent orbit partitions, this construction yields moduli spaces that (i) have the correct dimensions, (ii) are invariant under the accidental isomorphisms, (iii) have character expansions that are free of singlets (i.e. satisfy the vacuum conditions) and (iv) decompose into finite sums of modified Hall Littlewood polynomials. The inclusion relations between the moduli spaces can be read off either from the character HWGs or from the subgroup relations amongst the quivers. These inclusion relations confirm that all the lower dimensioned moduli spaces are contained in both the maximal and sub-regular nilpotent orbits and, moreover, are consistent with the standard Hasse diagrams of nilpotent orbits in the Literature [33].

Drawing on the analysis in Tables 5.12 to 5.17, the structure and representation content of the moduli spaces for certain canonical nilpotent orbits can be generalised to higher rank groups, as set out in Tables 5.18, 5.19 and 5.20. In all cases:

1. The minimal nilpotent orbit contains irreps whose highest weight Dynkin labels are integer multiples of the adjoint representation.

2. The supra-minimal nilpotent orbit has dimension two more than the minimal. For For B/D groups, its irreps are generated by the adjoint representation and the graviton. For the C series, the structure of nilpotent orbits further inside the body of the Hasse diagram can be generalised.

3. The sub-regular nilpotent orbit has dimension two less than the maximal. Its mHL decomposition differs from the maximal nilpotent orbit by $mHL^{B/D}_{[1,0,\ldots]}t^{2n}$ or $mHL^{C}_{[0,1,0,\ldots]}t^{4n-4}$.

4. The maximal orbit is a complete intersection [25].

Interestingly, the character HWGs for a O/USp quiver with only two nodes can also be generalised to any rank. The patterns of HWG generators for 2-node quivers with SO flavour groups follow from the antisymmetric invariants of even degree of USp fundamentals; the patterns for 2-node quivers with USp flavour groups follow from the invariants of mixed symmetry of O vectors [28, 16, 14]. While there are several similarities between the forms of these HWGs for B_n and D_n flavour groups, there are differences in

Orbit	Dimension	Quiver	Unrefined HS	PL[Character HWG]	mHL HWG
Trivial	0	B_n	1	1	...
Minimal	$4n-4$	B_n, C_1	...	$m_2 t^2$	...
Supra Minimal	$4n-2$	B_n, C_1, B_0	...	$m_2 t^2 + {m_1}^2 t^4$	...
2-Node Quiver $n > 2k$	$4k(n-k)$	$B_n - C_k$	...	$\sum_{i=1}^{k} m_{2i} t^{2i}$	...
2-Node Quiver $n = 2k$	$4k(n-k)$	$B_n - C_k$	...	$\sum_{i=1}^{k-1} m_{2i} t^{2i} + m_{2k}^2 t^{2k}$	...
Sub Regular	$2n^2-2$	$B_n, C_{n-1}, \ldots, B_0$	...	...	$1 - h_1 t^{2n}$
Maximal	$2n^2$	$B_n, C_n, \ldots, B_0$	$\frac{\prod_{i=1}^{n}\left(1-t^{4i}\right)}{(1-t^2)^{n(2n+1)}}$	...	1

B/D gauge nodes in a quiver indicate the corresponding O gauge groups.
The maximal and sub-regular quivers contain maximal chains of O/USp gauge groups,
in which substitutions between B_{k-1} and D_k gauge groups are permitted. Assumes rank > 2

Table 5.18.: Generalised B Series Nilpotent Orbit HS and HWGs

Orbit	Dimension	Quiver	Unrefined HS	PL[Character HWG]	mHL HWG
Trivial	0	C_n	1	1	...
Minimal	$2n$	$C_n - B_0$	...	${m_1}^2t^2$	...
Supra Minimal $n \geq 2$	$4n-2$	$C_n - D_1$	...	${m_1}^2t^2 + {m_2}^2t^4$	...
Supra Supra Minimal $n \geq 3$	$6n-6$	$C_n - B_1$	...	${m_1}^2t^2 + {m_2}^2t^4 + {m_3}^2t^6$	...
2-Node Quiver $n \geq k$	$k(2n-k+1)$	$C_n - O_k$	...	$\sum_{i=1}^{k} m_i^2 t^{2i}$	...
Sub-Regular	$2n^2-2$	C_n, D_{n-1}, C_{n-2} $\dots D_2, C_1, D_1$	...	...	$1 - h_2 t^{4n-4}$
Maximal	$2n^2$	C_n, B_{n-1}, C_{n-1} $\dots B_1, C_1, B_0$	$\frac{\prod_{i=1}^{n}(1-t^{4i})}{(1-t^2)^{n(2n+1)}}$	...	1

B/D gauge nodes in a quiver indicate the corresponding O gauge groups.
The maximal and sub-regular quivers contain maximal chains of O/USp gauge groups,
in which substitutions between B_{k-1} and D_k gauge groups are permitted.

Table 5.19.: Generalised C Series Nilpotent Orbit HS and HWGs

Orbit	Dimension	Quiver	Unrefined HS	PL[Character HWG]	mHL HWG
Trivial	0	D_n	1	1	$\ldots$
Minimal	$4n-6$	D_n, C_1	$\ldots$	$m_2 t^2$	$\ldots$
Supra Minimal	$4n-4$	D_n, C_1, B_0	$\ldots$	$m_2 t^2 + {m_1}^2 t^4$	$\ldots$
2-Node Quiver $n \geq 2k+2$	$2k(2n-2k-1)$	$D_n - C_k$	$\ldots$	$\sum_{i=1}^{k} m_{2i} t^{2i}$	$\ldots$
2-Node Quiver $n = 2k+1$	$2k(2n-2k-1)$	$D_n - C_k$	$\ldots$	$\sum_{i=1}^{k-1} m_{2i} t^{2i} + m_{2k} m_{2k+1} t^{2k}$	$\ldots$
2-Node Quiver $n = 2k$	$2k(2n-2k-1)$	$D_n - C_k$	$\ldots$	$\sum_{i=1}^{k-1} m_{2i} t^{2i} + m_{2k-1}^2 t^{2k} + m_{2k}^2 t^{2k} - m_{2k-1}^2 m_{2k}^2 t^{4k}$	$\ldots$
Sub Regular	$2n(n-1)-2$	$D_n, C_{n-2}, \ldots, D_1$	$\ldots$	$\ldots$	$1 - h_1 t^{2n}$
Maximal	$2n(n-1)$	$D_n, C_{n-1}, \ldots, D_1$	$\frac{\left(1-t^{2n}\right)\prod_{i=1}^{n-1}\left(1-t^{4i}\right)}{\left(1-t^2\right)^{n(2n-1)}}$	$\ldots$	1

B/D gauge nodes in a quiver indicate the corresponding O gauge groups.
The maximal and sub-regular quivers contain maximal chains of O/USp gauge groups,
in which substitutions between B_{k-1} and D_k gauge groups are permitted. Assumes rank ≥ 3

Table 5.20.: Generalised D Series Nilpotent Orbit HS and HWGs

relation to the appearance of spinors, as can be seen from Tables 5.18 and 5.20.

5.4.5. Non-Palindromic Nilpotent Orbits

Almost all the moduli spaces are normal with palindromic Hilbert series and those that are not fall into two categories.

In the case of D_{2r} groups, the Higgs branch construction does not yield palindromic moduli spaces for nilpotent orbits associated with pairs of spinor partitions. Specifically, as can be seen from appendix B.4, the vector partitions $\{(2^2), (2^4), (4^2)\}$ all correspond to pairs of orbits distinguished by their spinor partitions. While we can identify palindromic moduli spaces associated with each of the spinors, the unions of these spaces are non-palindromic. Since the Higgs branch construction, which is based on fields transforming in the vector representation, does not distinguish between the spinors, it naturally yields these unions of spinor moduli spaces. In the case of D_2, the palindromic 2 dimensional moduli spaces are provided by the 2 dimensional nilpotent orbits of the Weyl spinors, analysed in section 5.3. In the case of D_4, we can obtain the 12 and 20 dimensional palindromic moduli spaces by applying triality to the orbits from the vector partitions $\{3, 1^5\}$ and $\{5, 1^3\}$. These algebraic relations between these moduli spaces are described in 5.24, 5.25 and 5.26, and hold equally well for all the types of moduli space description: Hilbert series, character HWG and mHL HWG.

$$g^{D_2}_{(2^2)} = g^{A_1}_{(2)} \otimes g^{A_1}_{(1^2)} + g^{A_1}_{(1^2)} \otimes g^{A_1}_{(2)} - g^{D_2}_{(1^4)} \tag{5.24}$$

$$g^{D_4}_{(2^4)} = g^{D_4}_{(3,1^5)}\Big|_{\substack{m_1 \Leftrightarrow m_3 \\ h_1 \Leftrightarrow h_3}} + g^{D_4}_{(3,1^5)}\Big|_{\substack{m_1 \Leftrightarrow m_4 \\ h_1 \Leftrightarrow h_4}} - g^{D_4}_{(2^2,1^4)} \tag{5.25}$$

$$g^{D_4}_{(4^2)} = g^{D_4}_{(5,1^3)}\Big|_{\substack{m_1 \Leftrightarrow m_3 \\ h_1 \Leftrightarrow h_3}} + g^{D_4}_{(5,1^3)}\Big|_{\substack{m_1 \Leftrightarrow m_4 \\ h_1 \Leftrightarrow h_4}} - g^{D_4}_{(3^2,1^2)} \tag{5.26}$$

These non-palindromic moduli spaces are unions of two palindromic moduli spaces (i.e. their sum less their intersection, given by the palindromic nilpotent orbit of lower dimension). The vector partitions of D_{2r} spinor pair orbits are always *very even*, as noted in 4.2.2. The palindromic spinor moduli spaces can also be obtained from the Coulomb branch or NOL constructions, to be discussed in later Chapters.

The remaining non-palindromic moduli spaces of BCD groups up to rank 4 are generated by the quivers $B_3 - C_2 - B_0$, $B_4 - C_3 - B_1 - C_1 - B_0$ and $C_4 - D_2 - C_1$. We can identify relationships between these non-palindromic quivers and the non-palindromic *spinor pair* quivers of D_{2r} discussed above. Specifically,

1. the quivers $B_3 - C_2 - B_0$ and $B_4 - C_3 - B_1 - C_1 - B_0$ are related to the non-palindromic $D_4 - C_2$ and $D_6 - C_3$, under character maps between vector representations $D_4 \to B_3 \otimes B_0$ and $D_6 \to B_4 \otimes B_1$, and

2. $C_4 - D_2 - C_1$ contains the non-palindromic $D_2 - C_1$ as a subchain.

Both categories of non-normal nilpotent orbit are related to the orbits below in their Hasse diagrams by particular transitions between partitions [6], as summarised in section 4.4.7. The D_2 and D_4 examples can be described by the Kraft-Procesi degenerations $A_1 \cup A_1$ or $A_3 \cup A_3$ within D_2 or D_4 subalgebras. In the D_5 example in section 4.4.7, the non-palindromic nature of the orbit follows from the $A_1 \cup A_1$ Kraft-Procesi degeneration of a D_2 subalgebra within the partition $(3^2, 2^2)$. The other BCD non-normal orbits can be analysed in a similar manner. Non-normal nilpotent orbits all induce families of non-normal orbits of higher rank and so non-palindromic features occur throughout higher rank BCD groups.

It can be noted that, while many of the character HWGs calculated for BCD groups are palindromic, there is no bijective correspondence between the palindromy of HWGs and Hilbert series. Thus, some non-normal orbits with Characteristic height 2 or 3, have character HWGs that are complete intersections, and some normal orbits have character HWGs that are non-palindromic (for example, $C_3[210], C_4[2100], C_4[2010]$). The mHL HWGs are generally not palindromic.

5.4.6. Dualities of BCD Series Quivers

The pattern of dualities between BCD quivers differs from that between A quivers due to the alternation of gauge group types. Consider the general case of a $USp - O - USp$ sub-chain described by the partition data $(\ldots, \sigma_i, \sigma_{i+1}, \ldots)$. It follows from the dimension formulae 5.9 and 5.10 that

the mapping,

$$(\ldots,\sigma_i,\sigma_{i+1},\ldots)\rightarrow(\ldots,{\sigma'}_{i+1},{\sigma'}_i,\ldots)=(\ldots,\sigma_{i+1}-1,\sigma_i+1,\ldots), \tag{5.27}$$

preserves the dimension of a Hilbert series, while switching between $USp-O(\text{even})-USp$ and $USp-O(\text{odd})-USp$, or vice versa. The resulting sequence is not a well ordered partition and detailed calculations are required to see if the moduli spaces are the same and the quivers are dual to each other.

In the case of $(\sigma_i,\sigma_{i+1})=(1,1)\rightarrow(2,0)$, which arises between maximal sub-chains, $C_rB_{r-1}C_{r-1}$ and $C_rD_rC_{r-1}$, the duality holds, as discussed in section 5.4.1. Some further examples where calculation confirms that the duality holds are shown in Table 5.21.

Quiver	Partition σ	Sequence σ'	Dual Quiver
C_1-B_0	$(1,1)$	$(0,2)$	C_1-D_1
C_2-D_1	$(2,2)$	$(1,3)$	C_2-B_1
C_3-B_1	$(3,3)$	$(2,4)$	C_3-D_2
$C_3-D_2-C_1$	$(2,2,2)$	$(1,3,2)$	$C_3-B_2-C_1$
$C_3-D_2-C_1-B_0$	$(2,2,1,1)$	$(1,3,0,2)$	$C_3-B_2-C_1-B_0$

Table 5.21.: Examples of Dual BCD Quivers

An example where the duality does not hold is given by C_2B_0, which is related to C_2D_2 by the dimension shift $(\sigma_i,\sigma_{i+1})=(3,1)\rightarrow(0,4)$. Calculation of further examples indicates that the shifted quiver has the same Higgs branch moduli space, if the elements of the partition σ are shifted by a single unit, but not if the shift is greater. (This can be viewed as an analogue of the "*not very unbalanced*" rule that applies for unitary quivers.) The constraint on shifts requires that a quiver should contain some equally spaced pairs of nodes, and, consequently, this *dimension shifting* duality only applies between sub-chains of the form:

$$\begin{aligned}&\ldots-USp(2N)-O(2N-k)-USp(2N-2k)-\ldots\\&\qquad\qquad\leftrightarrow\\&\ldots-USp(2N)-O(2N+1-k)-USp(2N-2k)-\ldots\end{aligned} \tag{5.28}$$

This duality allows many, *but not all*, BCD quivers for nilpotent orbits to be restated either as a BC or as a DC chain, including all *special* orbits up to rank 5 (and perhaps generally). This facilitates brane constructions using orientifolds [20], since the restriction of gauge theories to BC or DC chains avoids QFT parity anomalies.

Similarly to the case of the A series, dimensional calculations using 5.9 and 5.10 indicate that Higgs branch dimensions of BCD quivers are unaffected by subchain additions of the form $C_k \to C_k - D_k - C_k$ or $C_k \to C_k - B_k - C_k$. Evaluation of Hilbert series, verifies that the Higgs branch moduli spaces themselves are also unaffected by this addition, providing the subchains are added within maximal quiver sub-chains. As examples:

$$\begin{gathered} g_{Higgs}^{C_2-D_2-C_1-D_1} = g_{Higgs}^{C_2-D_2-C_2-D_2-C_1-D_1}, \\ \text{but} \\ g_{Higgs}^{C_2-B_0} \neq g_{Higgs}^{C_2-D_2-C_2-B_0}. \end{gathered} \tag{5.29}$$

Also, as noted in section 5.4.2, the moduli spaces of *maximal* DC chains with $O(N)$ and $SO(N)$ gauge groups are the same.

The combination of all these dualities entails that many ordered linear O/USp quivers have the same Higgs branches as one of the BCD nilpotent orbit quivers. A more comprehensive analysis of such dualities could be an interesting area of further study.

6. Coulomb Branch Constructions of Nilpotent Orbits

6.1. Monopole Formula

The monopole formula, introduced in [20] and refined in [21], provides a systematic method for the construction of the Coulomb branches of particular SUSY quiver theories, being $\mathcal{N} = 4$ superconformal gauge theories in 2+1 dimensions. The Coulomb branches of these theories are HyperKähler manifolds. The formula draws upon a lattice of monopole charges, often referred to as a GNO lattice [74], that is applied to a linked system of gauge and flavour nodes defined by a quiver diagram.

Each gauge node carries adjoint valued fields from the vector multiplet and the links between nodes correspond to complex scalars within the hypermultiplets of the theory. The monopole formula generates the Coulomb branch of the quiver by projecting monopole charge configurations from the GNO lattice into the root space lattice of G, according to the monopole flux over each gauge node, under a grading determined by the conformal dimension of the overall monopole flux.

The *conformal dimension* (equivalent to R-charge or the highest weight of the $SU(2)_R$ global symmetry) of a monopole flux is given by applying the following general schema [20, 21] to the quiver diagram:

$$\Delta(q) = \underbrace{\frac{1}{2}\sum_{i=1}^{r}\sum_{\rho_i \in R_i} |\rho_i(q)|}_{\substack{\textit{contribution of } N=4 \\ \textit{hyper multiplets}}} - \underbrace{\sum_{\alpha \in \Phi_+} |\alpha(q)|}_{\substack{\textit{contribution of } N=4 \\ \textit{vector multiplets}}} \quad . \tag{6.1}$$

The positive R-charge contribution in the first term is from the matter fields that link adjacent nodes in the quiver diagram. These are bifundamental chiral operators within the $\mathcal{N} = 4$ hypermultiplets. The second

term describes the negative R-charge contribution from the $\mathcal{N} = 4$ vector multiplets; this arises due to symmetry breaking, whenever the monopole flux q over a gauge node contains a number of different charges.

The focus here is on Coulomb branch constructions where the gauge groups are unitary, so it is useful to specialise to a *unitary monopole formula*, as distinct from versions that have been proposed using other gauge groups [21].

The relevant quivers can be described by gauge nodes indexed by i, where i runs from 1 to r, with each $U(N_i)$ gauge node carrying a *monopole flux* $q_i \equiv (q_{i,1}, \ldots, q_{i,N_i})$ comprising one or more *monopole charges* $q_{i,j}$. The fluxes are assigned the collective coordinate $q \equiv (q_1, \ldots, q_r)$. A $P_q^{U(N)} \equiv \prod_i P_{q_i}^{U(N_i)}$ symmetry factor, explained below, is associated to the gauge nodes. The monopole flux over the gauge nodes is counted by the fugacity $z \equiv (z_1, \ldots, z_r)$.

The gauge nodes may also be attached to some number f of flavour nodes, indexed by j, where j runs from 1 to f, with each flavour node having N_j flavours. The flavour nodes may also carry fixed external charges described by the collective coordinate $\lambda \equiv (\lambda_1, \ldots, \lambda_f)$, where $\lambda_j \equiv (\lambda_{j,1}, \ldots, \lambda_{j,N_j})$.

Conformal dimension $\Delta(q, \lambda)$ is tracked using the counting fugacity t. With these definitions, the *unitary monopole formula* is given by the schema, refined from [21]:

$$g_{\text{Coulomb}}(\lambda, z, t) \equiv \sum_q P_q^{U(N)}(t)\, z^q z^{\phi(\lambda)} t^{\Delta(q,\lambda)}. \tag{6.2}$$

The notation in 6.2 requires some further explication:

1. The limits of summation for the monopole charges are $\infty \geq q_{i,1} \geq \ldots q_{i,j} \geq \ldots q_{i,N_i} \geq -\infty$ for $i = 1, \ldots r$. (In the case of $U(1)$ symmetry it can be convenient to drop the redundant second index on $q_{i,j}$.)

2. The monomial z^q combines the monopole fluxes q_i into total charges for each z_i and is expanded as $z^q \equiv \prod_{i=1}^{r} z_i^{\sum_{j=1}^{N_i} q_{i,j}}$.

3. The term $P_q^{U(N)}$ encodes the degrees $d_{i,j}$ of the Casimirs of the residual $U(N)$ symmetries that remain at the gauge nodes under a monopole flux q.

$$P_q^{U(N)} \equiv \prod_{i,j} \frac{1}{\left(1-t^{d_{i,j}(q)}\right)} = \prod_{i=1}^{r} \prod_{j=1}^{N_i} \prod_{k=1}^{\lambda_{ij}(q_i)} \frac{1}{1-t^k}. \tag{6.3}$$

The determination of residual symmetries follows [21]. We construct a partition of N_i for each node, which counts how many of the charges $q_{i,j}$ are equal, such that $\lambda(q_i) = (\lambda_{i,1}, \ldots, \lambda_{i,N_i})$, where $\sum_{j=1}^{N_i} \lambda_{i,j} = N_i$ and $\lambda_{i,j} \geq \lambda_{i,j+1} \geq 0$. The non-zero terms $\lambda_{i,j}$ in the partition give the ranks of the residual $U(N)$ symmetries associated with each node, so that it is a straightforward matter to compound the terms in the degrees of Casimirs, recalling that a $U(N)$ group has Casimirs of degrees 1 through N. For example, if $q_{i,j} = q_{i,k}$ for all j, k, then $\{d_{i,1}, \ldots d_{i,N_i}\} = \{1, \ldots, N_i\}$ and if $q_{i,j} \neq q_{i,k}$ for all j, k, then $\{d_{i,1}, \ldots d_{i,N_i}\} = \{1, \ldots, 1\}$.

4. The conformal dimension $\Delta(q, \lambda)$ associated with each monopole flux q against a background of external charges λ is given by the formula:

$$\Delta(q,\lambda) = \underbrace{\frac{1}{2}\sum_{j>i}^{r}\sum_{m,n}|q_{i,m}A_{ij} - q_{j,n}A_{ji}|}_{\text{gauge - gauge hypers}} + \underbrace{\frac{1}{2}\sum_{j>i}\sum_{m,n}|q_{i,m}A_{ij} - \lambda_{j,n}A_{ji}|}_{\text{gauge - flavour hypers}} - \underbrace{\sum_{i=1}^{r}\sum_{m>n}|q_{i,m} - q_{i,n}|}_{\text{gauge vplets}}, \tag{6.4}$$

where (i) the summations are taken over all the monopole charges in the flux q and (ii) the linking pattern between nodes is defined by the A_{ij} off-diagonal matrix terms, which are only non-zero for linked nodes [1].

5. The external charge factor $\phi(\lambda)$ is zero for nilpotent orbit moduli spaces. It is relevant for $T(SU(N))$ theories discussed in section 8.1.

It is instructive to compare the explicit formula 6.4 with the schema 6.1. Importantly, 6.4 specifies a number of matters precisely, including the dimensional measures $|\rho_i(q)|$ and $|\alpha(q)|$, the linking matrices A_{ij} and the

[1] For theories with simply laced quivers of ADE type, for $i \neq j$, $A_{ij} = 0$ or -1

pattern of summations over the monopole fluxes. This version of the unitary monopole formula can be applied to a wide variety of quivers to obtain Coulomb branch moduli spaces.

It is remarkable that with a little further specialisation, the unitary monopole formula 6.2, together with 6.3 and 6.4, exactly generates the moduli spaces of certain nilpotent orbits of both Classical and Exceptional groups. This specialisation involves mapping the gauge nodes of a quiver to the Dynkin diagram of the chosen group G, taking the z as fugacities for the simple roots of G and setting the linking factors A_{ij} to the Cartan matrix of G, extended to incorporate any flavour nodes. Various choices are possible for the $U(N)$ charges on the gauge nodes and the number and linking of flavour nodes, providing that the quiver diagrams remain *balanced*, as explained in section 6.1.1. The moduli spaces of these theories live in the root space of G and conformal dimension takes integer values.

Based on early work in [1], it was shown in [21] how the unitary monopole formula can be combined with quivers based on the affine Dynkin diagrams of simply laced ADE groups, and with their $U(N)$ gauge groups defined by Coexter labels, to construct RSIMS or minimal nilpotent orbits. In [22] this program was extended to non-simply laced BCFG groups, by working with dual Coexter labels and modifying the linking factors to reflect different root lengths. In [29] it was shown that quivers based on twisted affine Dynkin diagrams and/or based on the Characteristics of nilpotent orbits can be used to construct the moduli spaces of near to minimal nilpotent orbits of Classical groups. One of the findings of this study is that such constructions extend to near to minimal nilpotent orbits of Exceptional groups. These matters are summarised in the sections that follow.

There are, however, a number of aspects that are pertinent to all the monopole constructions of nilpotent orbit moduli spaces and it is useful to clarify these before proceeding.

6.1.1. Quiver Balance

Since the conformal dimension formula offsets positive half-integer R-charge shifts from hypermultiplets, by negative integer R-charge shifts from vector multiplets, this leads to a situation where, depending on the quiver specification, conformal dimension could be positive or negative and half-integer

as well as integer. Clearly, negative conformal dimensions would not be consistent with t acting as a well-formed counting fugacity.

The desirability of such general quivers is discussed from a field theory perspective in [20]; broadly speaking, *good* theories are defined therein as those with non-negative integer conformal dimension, *ugly* theories are those with non-negative half integer conformal dimension and *bad* theories are those with zero or negative conformal dimensions. Such potential problems can be avoided by requiring that a quiver should observe constraints, which can be expressed effectively in terms of *balance*.

The concept of balance, introduced in [20] for simply laced groups, can be adapted to reflect the different root lengths encoded in the off-diagonal terms of the Cartan matrix for a non-simply laced group. After extending the Cartan matrix as $\tilde{A}_{ij}$ to include links to any flavour nodes, a quiver can be defined as *balanced*, if the $U(N)$ charge on each *gauge* node i obeys the rule:

$$N_i = \frac{1}{2} \sum_{j \in \left\{ \begin{smallmatrix} \text{adjacent} \\ \text{nodes} \end{smallmatrix} \right\}} \left| \tilde{A}_{ij} \right| N_j, \tag{6.5}$$

where the linking factors $|\tilde{A}_{ij}|$ are taken from the extended Cartan matrix and the N_j include the ranks of any flavour nodes in addition to those of gauge nodes. Flavour nodes are not required to be balanced.

Since, by definition, $A_{ii} = 2$ for each gauge node, 6.5 can be rearranged to define *balance* for each node i as:

$$\text{Balance}(i) \equiv -\sum_j \tilde{A}_{ij} N_j, \tag{6.6}$$

with the quiver balance condition becoming, $\text{Balance}(i) = 0$, for all gauge nodes i.

In the case of an affine Dynkin diagram, the vector N_j of ranks of unitary groups equals the vector formed by the dual Coxeter labels; these form the kernel of the affine Cartan matrix, and so $\text{Balance}(i) = 0$ for all nodes, including the flavour nodes. This corresponds to the degeneracy of an affine Cartan matrix, which permits branching to other groups, as discussed in appendix A.3.

Now consider a monopole flux q with a single non-zero monopole charge $q_{i,1} = 1$. In the absence of external charges λ, the conformal dimension is

given by:

$$\begin{aligned}\Delta(q_{i,1} \to 1) &= \frac{1}{2} \sum_{j \in \left\{ \substack{\text{adjacent} \\ \text{nodes}} \right\}} \left| \tilde{A}_{ij} \right| N_j - (N_i - 1) \\ &= \frac{1}{2}\text{Balance}(i) + 1.\end{aligned} \tag{6.7}$$

When a quiver is balanced, any unit monopole gauge charge has a conformal dimension of 1. When a quiver is *minimally unbalanced*, with one or more nodes having $\text{Balance}(i) = -1$, at least one monopole has a conformal dimension of $1/2$. When a quiver is *very unbalanced*, with one or more nodes having $\text{Balance}(i) \leq -2$, at least one monopole has a conformal dimension that is zero or negative. The quivers whose Coulomb branches correspond to the moduli spaces of nilpotent orbits all have integer conformal dimension and are balanced.

A balanced quiver diagram, *whose flavour nodes are each simply linked to a single gauge node*, has flavour node dimensions and gauge node dimensions that are mediated by the regular Cartan matrix A of G. Define the gauge node ranks by the vector $N_g \equiv (N_{g_1}, \ldots, N_{g_r})$ and the flavour node dimensions by $N_f \equiv (N_{f_1}, \ldots, N_{f_r})$, where both vectors are ordered by the Dynkin diagram of G, with N_f having zero entries for gauge nodes that do not have a flavour node attached. It then follows from 6.6 that, for such a balanced quiver:

$$N_f = A \cdot N_g \tag{6.8}$$

Almost all the quivers for Coulomb branch constructions of nilpotent orbit moduli spaces are of this type.

6.1.2. Coulomb Branch Dimension

Consider the unrefined Hilbert series $g_{Coulomb}(1,t)$, which is obtained by setting the z fugacities in 6.2 to unity. Since the number of poles contributed by each $U(N_i)$ gauge group depends only on rank N_i, and is invariant under gauge group breaking by the monopole flux q, the dimension of this moduli space can be expanded as:

$$|g_{HS:Coulomb}(1,t)| = \left| \sum_q t^{\Delta(q)} \right| + \left| \prod_{i,j} \frac{1}{(1-t)} \right|. \tag{6.9}$$

The dimension of each of the RHS terms is determined by the sum of the ranks of the $U(N_i)$ gauge groups. Hence, the dimension of the Coulomb branch is equal to *twice* the sum of the gauge group ranks N_i.

So, in order to find a Coulomb branch construction for a given nilpotent orbit, based on the unitary monopole formula, it is necessary to identify a balanced quiver with $U(N)$ gauge group ranks summing to half the (complex) dimension of the orbit. However, not all balanced quivers correspond to nilpotent orbits. There are several methods for finding those that do, including from affine Dynkin diagrams, from nilpotent orbit Characteristics, and, in the case of the A series, from 3d mirror symmetry.

6.2. Minimal Nilpotent Orbits

The quiver for a Coulomb branch construction of a minimal nilpotent orbit or RSIMS of G, is specified by the extended (untwisted affine) Dynkin diagram of G, as shown in Figures 2.1 and 2.2.

The zero central charge of the affine Lie algebra corresponds to an overall gauge invariance condition on the field combinations. Since the extra affine root and its Dynkin label are redundant, by virtue of the degeneracy of the affine Cartan matrix, they can be gauged away. Thus, the affine root, labelled by $i = 0$, can be treated as a flavour node and assigned a charge $q_0 \equiv \lambda_0$ of zero; however, the affine node still plays a role in the gauge-flavour hyper contribution to conformal dimension, in accordance with the linking pattern of the extended Cartan matrix.

The quiver diagrams follow directly from the extended Dynkin diagrams by setting the affine node to a single flavour node. The dual Coxeter labels $\breve{a}_i$ determine the ranks of the $U(N_i)$ gauge fields. Applying the unitary monopole formulae 6.2, 6.3 and 6.4 gives a Coulomb branch construction of the RSIMS for any Classical or Exceptional group. There are other possible gauge choices, as will be discussed, but these choices all construct the same moduli space.

The quivers are balanced, in accordance with 6.8, and so have integer conformal dimension. Their Coulomb branch has dimension equal to twice the sum of the dual Coxeter labels, consistent with the dimensions of RSIMS calculated in 3.3.4.

The construction of an RSIMS requires the collection of the root space

monomials z^q, into class functions of G, at the correct positive and negative integer powers and multiplicities; however, collections of root space monomials do not necessarily form complete representations. It is an interesting question, therefore, to examine how the Weyl group symmetry of G is realised by the monopole formula.

For the A and C series, and their isomorphisms, where the gauge nodes are all $U(1)$, Weyl reflections of the simple roots z_i are in one to one correspondence with Weyl reflections of the monopole charges q_i. In these cases it is straightforward to show that conformal dimension $\Delta(q)$ is Weyl invariant. Conformal dimension thus effects a foliation of the root space monomials z^q into sets of dominant weights and orbits that have the same R-charge.

In the case of other Classical and Exceptional series, however, some $U(N_i)$ gauge groups are of rank greater than one, and Weyl group reflections of simple roots z_i do not map uniquely to linear transformations of the monopole charges $q_{i,j}$. This makes it difficult to establish the invariance of the monopole formula under the Weyl group of G, other than by full calculation of the moduli space. Nonetheless, it appears that the restriction imposed by building each quiver upon a Dynkin diagram of G is sufficient to ensure that the moduli space obtained has the necessary Weyl group symmetries and is a class function of G.

At this time, a proof of the equality between these Coulomb branch moduli spaces and the RSIMS of G, for arbitrary rank, is not known. However, the equivalence can in principle be verified analytically on on a case by case basis, and has been carried out in [21, 22, 29] for low rank Classical and Exceptional groups. Checks have also been carried out based on unrefined Hilbert series and the first few terms of the Taylor expansions of the refined Hilbert series of these Coulomb branch moduli spaces.

6.2.1. Simply Laced Groups

This section sets out details of the Coulomb branch constructions of refined HS for ADE series RSIMS from the unitary monopole formula given by 6.2, 6.3 and 6.4. The treatment is largely taken from [29] and [22].

A Series

The formal equivalence of Coulomb branch constructions for A_1 and A_2 RSIMS to those based on character generating functions is proved below. The root structure of A_2 is used to illustrate the Weyl group invariance of conformal dimension for A series groups.

The monopole construction for A series RSIMS is based on the extended Cartan matrix, defined in accordance with A.31, and the dual Coxeter labels of the simple roots (shown as a column vector), where the affine root is labelled as z_0:

$$\left|\begin{array}{c|cccccc|c} z_1 & 2 & -1 & \dots & 0 & 0 & -1 & 1 \\ z_2 & -1 & 2 & \dots & 0 & 0 & 0 & 1 \\ \dots & \dots & \dots & \dots & \dots & \dots & \dots & 1 \\ z_{r-1} & 0 & 0 & \dots & 2 & -1 & 0 & 1 \\ z_r & 0 & 0 & \dots & -1 & 2 & -1 & 1 \\ z_0 & -1 & 0 & \dots & 0 & -1 & 2 & 1 \end{array}\right|. \tag{6.10}$$

For A_1, the extended Cartan matrix and dual Coxeter labels are:

$$\left|\begin{array}{c|cc|c} z_1 & 2 & -2 & 1 \\ z_0 & -2 & 2 & 1 \end{array}\right|. \tag{6.11}$$

Applying 6.2, 6.3 and 6.4, we obtain the monopole formula for an A series RSIMS:

$$g^{A_r}_{HS:RSIMS}(z,t) = \frac{1}{(1-t)^r} \sum_{q_1,\dots,q_r=-\infty}^{\infty} {z_1}^{q_1} {z_2}^{q_2} \dots {z_r}^{q_r}\ t^{\Delta(q)}, \tag{6.12}$$

where

$$\Delta\left(q\right) = \frac{1}{2}\left(|q_1| + \sum_{i=1}^{r-1} |q_i - q_{i+1}| + |q_r|\right). \tag{6.13}$$

The constructions for A_1 and A_2 can be rearranged into the character generating functions for RSIMS. For A_1, where we are working with simple roots expressed as z_1 in terms of root space fugacities, rather than as x^2 in

terms of weight space fugacities, we have:

$$\begin{aligned} g^{A_1}_{HS:RSIMS}(z,t) &= \frac{1}{(1-t)} \sum_{q_1=-\infty}^{\infty} z_1^{q_1} t^{|q_1|} \\ &= \frac{1}{(1-t)} \left(\sum_{q_1=0}^{\infty} z_1^{q_1} t^{q_1} + \sum_{q_1=0}^{\infty} z_1^{-q_1} t^{q_1} - 1 \right) \\ &= \frac{1-t^2}{(1-t)(1-z_1 t)(1-t/z_1)} \\ &= \left(1-t^2\right) PE\left[[2]\, t\right]. \end{aligned} \tag{6.14}$$

This yields the minimal nilpotent orbit character generating function for A_1 whose Higgs branch calculation is given in Table 5.3. [2]

For A_2, the rearrangement, which follows the boundaries of Weyl chambers, is more intricate:

$$\begin{aligned} g^{A_2}_{HS:RSIMS}(z,t) &= \frac{1}{(1-t)^2} \sum_{q_1,q_2=-\infty}^{\infty} z_1^{q_1} z_2^{q_2} t^{\frac{1}{2}(|q_1|+|q_1-q_2|+|q_2|)} \\ &= \frac{1}{(1-t)^2} \left(\begin{array}{l} \sum_{q_2=0}^{\infty} \sum_{q_1=0}^{q_2} \left(z_1^{q_1} z_2^{q_2} + z_1^{-q_1} z_2^{-q_2} + z_1^{q_2} z_2^{q_1} + z_1^{-q_2} z_2^{-q_1} \right) t^{q_2} \\ - \sum_{q_1=0}^{\infty} \left(z_1^{q_1} z_2^{q_1} + z_1^{-q_1} z_2^{-q_1} \right) t^{q_1} \\ - \sum_{q_1=0}^{\infty} \left(z_1^{q_1} + z_1^{-q_1} + z_2^{q_1} + z_2^{-q_1} \right) t^{q_1} \\ + \sum_{q_1=0}^{\infty} \sum_{q_2=0}^{\infty} \left(z_1^{-q_1} z_2^{q_2} + z_1^{q_1} z_2^{-q_2} \right) t^{(q_1+q_2)} + 1 \end{array} \right) \\ &= \frac{\left(1-t^2-t^4+t^6\right) - \left(t^2-2t^3+t^4\right)\left(z_1+z_2+z_1 z_2+z_1^{-1}+z_2^{-1}+z_1^{-1}z_2^{-1}+2\right)}{(1-z_1 t)(1-z_2 t)(1-z_1 z_2 t)\left(1-z_1^{-1}t\right)\left(1-z_2^{-1}t\right)\left(1-z_1^{-1}z_2^{-1}t\right)(1-t)^2} \\ &= \left(\left(1-t^2-t^4+t^6\right)[0,0] - \left(t^2-2t^3+t^4\right)[1,1]\right) PE[[1,1]\, t]. \end{aligned} \tag{6.15}$$

This matches the minimal nilpotent orbit character generating function for A_2, as given in Table 5.3 (up to counting conventions).

Some insight into the complexities of the monopole formula can be obtained by reversing the above procedure and seeking to derive the monopole formula from the Weyl character generating function 2.7. For A_1 the deriva-

[2] Note that the Coulomb branch conventionally counts R-charge by orders of t while the Higgs branch counts by orders of t^2.

tion proceeds as below:

$$
\begin{aligned}
g^{A_1}_{HS:RSIMS}(z,t) &= \frac{1}{(1-z)\left(1-\frac{t}{z}\right)} + \frac{1}{\left(1-\frac{1}{z}\right)(1-tz)} \\
&= \sum_{a=0}^{\infty}\sum_{b=0}^{\infty} t^a z^{b-a} + \sum_{a=0}^{\infty}\sum_{b=0}^{\infty} t^a z^{a-b} \\
&= \sum_{q=-\infty}^{\infty}\sum_{b=\max(0,-q)}^{\infty} t^{b+q} z^q + \sum_{q=-\infty}^{\infty}\sum_{b=\max(0,q)}^{\infty} t^{b-q} z^q \\
&= \frac{1}{1-t}\sum_{q=-\infty}^{\infty}\left(t^{\max(0,-q)+q} + t^{\max(0,q)-q}\right) z^q \\
&= \frac{1}{1-t}\left(\sum_{q=-\infty}^{\infty} t^{|q|} z^q + \sum_{q=-\infty}^{\infty} z^q\right) \\
&= \frac{1}{1-t}\sum_{q=-\infty}^{\infty} t^{|q|} z^q .
\end{aligned}
\tag{6.16}
$$

The key steps in the derivation include (i) Taylor expansion of the summand associated with each long root, (ii) rearrangement of the limits of summation, such that the summands share the same simple root fugacities z^q and the charges q range from $-\infty$ to ∞, (iii) implementation of sums with the respect to the charges that are not carried by the simple roots and (iv) simplification of the resulting piecewise functions. When boiling down the latter it is useful to draw on identities that follow from the complex unimodular nature of the root space coordinates.

While we should in principle be able to find such derivations for higher rank groups, the simplification of the piecewise functions becomes increasingly non-trivial.

Thus, for $SU(3)$, we have:

$$\begin{aligned}
g^{A_2}_{HS:RSIMS}(z,t) &= \sum_{\text{Weyl}} \frac{1}{\left(1-\frac{1}{z_1}\right)\left(1-\frac{1}{z_1 z_2}\right)(1-z_2)(1-tz_1)} \\
&= \sum_{\text{Weyl}} \sum_{a=0}^{\infty}\sum_{b=0}^{\infty}\sum_{c=0}^{\infty}\sum_{d=0}^{\infty} t^a z_1^{a-b-c} z_2^{d-c} \\
&= \sum_{\text{Weyl}} \sum_{q_1=-\infty}^{\infty}\sum_{q_2=-\infty}^{\infty}\sum_{c=\max(0,-q_2)}^{\infty}\sum_{b=\max(0,-c-q_1)}^{\infty} z_1^{q_1} z_2^{q_2} t^{b+c+q_1} \\
&= \frac{1}{(1-t)} \sum_{\text{Weyl}} \sum_{q_1=-\infty}^{\infty}\sum_{q_2=-\infty}^{\infty}\sum_{c=\max(0,-q_2)}^{\infty} z_1^{q_1} z_2^{q_2} t^{\max(0,c+q_1)} \\
&= \frac{1}{(1-t)} \sum_{\text{Weyl}} \sum_{q_1=-\infty}^{\infty}\sum_{q_2=-\infty}^{\infty}\sum_{a=0}^{\infty} z_1^{q_1} z_2^{q_2} t^{\max(0,a+q_1,a+q_1-q_2)} \\
&= \frac{1}{(1-t)^2} \sum_{\text{Weyl}} \sum_{q_1=-\infty}^{\infty}\sum_{q_2=-\infty}^{\infty} z_1^{q_1} z_2^{q_2} \left(t^{\max(0,q_1,q_1-q_2)} - (1-t)\min\left(0,\max\left(q_1,q_1-q_2\right)\right)\right) \\
&= \frac{1}{(1-t)^2} \sum_{\text{Weyl}} \sum_{q_1=-\infty}^{\infty}\sum_{q_2=-\infty}^{\infty} z_1^{q_1} z_2^{q_2} t^{\max(0,q_1,q_1-q_2)},
\end{aligned} \tag{6.17}$$

where we have used an identity, which is valid for unimodular root fugacities:

$$\sum_{q_1=-\infty}^{\infty}\sum_{q_2=-\infty}^{\infty} z_1^{q_1} z_2^{q_2} \min\left(0,\max\left(q_1,q_1-q_2\right)\right) = 0. \tag{6.18}$$

We continue by carrying out the Weyl reflections to obtain:

$$\begin{aligned}
g^{A_2}_{HS:RSIMS}(z,t) &= \frac{1}{(1-t)^2} \sum_{q_1=-\infty}^{\infty}\sum_{q_2=-\infty}^{\infty} z_1^{q_1} z_2^{q_2} (t^{\max(0,-q_1,q_2-q_1)} + t^{\max(0,q_1,q_1-q_2)} \\
&\qquad + t^{\max(0,-q_2,-q_1)} + t^{\max(0,-q_2,q_1-q_2)} + t^{\max(0,q_2,q_2-q_1)} + t^{\max(0,q_2,q_1)}) \\
&= \frac{1}{(1-t)^2} \sum_{q_1=-\infty}^{\infty}\sum_{q_2=-\infty}^{\infty} z_1^{q_1} z_2^{q_2} \left(2 + t^{|q_1|} + t^{|q_2|} + t^{|q_1-q_2|} + t^{\frac{1}{2}|q_1-q_2|+\frac{1}{2}|q_1|+\frac{1}{2}|q_2|}\right) \\
&= \frac{1}{(1-t)^2} \sum_{q_1=-\infty}^{\infty}\sum_{q_2=-\infty}^{\infty} z_1^{q_1} z_2^{q_2} \left(t^{\frac{1}{2}|q_1-q_2|+\frac{1}{2}|q_1|+\frac{1}{2}|q_2|}\right),
\end{aligned} \tag{6.19}$$

where we have rearranged the parts of the six piecewise functions and used identities involving the unimodular fugacities z_i to eliminate five of the resulting functions:

$$\sum_{q_1=-\infty}^{\infty} z_1^{q_1} = 0 = \sum_{q_1=-\infty}^{\infty}\sum_{q_2=-\infty}^{\infty} z_1^{q_1} z_2^{q_2} t^{|q_1-q_2|}. \tag{6.20}$$

D Series

The Coulomb branch construction for D series RSIMS is based on the extended Cartan matrix and dual Coxeter labels:

$$\left|\begin{array}{c|ccccccc|c} z_1 & 2 & -1 & \dots & 0 & 0 & 0 & 0 & 1 \\ z_2 & -1 & 2 & \dots & 0 & 0 & 0 & -1 & 2 \\ \dots & \dots & \dots & \dots & \dots & \dots & \dots & \dots & 2 \\ z_{r-2} & 0 & 0 & \dots & 2 & -1 & -1 & 0 & 2 \\ z_{r-1} & 0 & 0 & \dots & -1 & 2 & 0 & 0 & 1 \\ z_r & 0 & 0 & \dots & -1 & 0 & 2 & 0 & 1 \\ z_0 & 0 & -1 & \dots & 0 & 0 & 0 & 2 & 1 \end{array}\right|. \tag{6.21}$$

Applying 6.2, 6.3 and 6.4, we obtain the equation for a $D_{r\geq 4}$ series RSIMS:

$$g^{D_r}_{HS:RSIMS}(z,t) = \sum_{q_1,q_{r-1},q_r=-\infty}^{\infty} \sum_{\substack{q_{j,1}\geq q_{j,2}\geq -\infty \\ r-2\geq j\geq 2}}^{\infty} {z_1}^{q_1} {z_2}^{q_{2,1}+q_{2,2}} \dots {z_{r-2}}^{q_{r-2,1}+q_{r-2,2}} {z_{r-1}}^{q_{r-1}} {z_r}^{q_r} \times P^{U(N)}_q(t)\, t^{\Delta(q)}, \tag{6.22}$$

where

$$P^{U(N)}_q(t) = \frac{1}{(1-t)^r} \prod_{j=2}^{r-2} \begin{cases} q_{j,1} = q_{j,2} : 1/(1-t^2) \\ q_{j,1} \neq q_{j,2} : 1/(1-t) \end{cases} \tag{6.23}$$

and

$$\Delta(q) = \frac{1}{2} \left(\begin{array}{c} \sum_{i=1}^{2} |q_{2,i}| + \sum_{i=1}^{2} |q_1 - q_{2,i}| + \sum_{k=2}^{r-3} \sum_{i,j=1}^{2} |q_{k,i} - q_{k+1,j}| \\ + \sum_{i=1}^{2} |q_{r-2,i} - q_{r-1}| + \sum_{i=1}^{2} |q_{r-2,i} - q_r| \\ - \sum_{k=2}^{r-2} |q_{k,1} - q_{k,2}| \end{array} \right) \tag{6.24}$$

The construction can, in principle, be rearranged into a character generating function similar to Table 5.3.

Interestingly, the gauge choice $q_0 = 0$ has alternatives and, indeed, any one of the monopole charges can be defined to be zero, providing (i) the limits and summand are modified to include both q_0 and z_0, and (ii) care

is taken over the symmetry factors, since the node with the zero monopole charge carries the Casimirs of $SU(N)$ rather than $U(N)$. For star shaped quivers, such as D_4, a particularly convenient choice of gauge is $q_{2,2} = 0$, and this leads directly to a decomposition into a symmetric sum over all the representations of four $T(SU(2))$ quiver theories, discussed in Chapter 8.

E Series

The Coulomb branch construction for E_6 RSIMS is based on the extended Cartan matrix and dual Coxeter labels:

$$\begin{array}{c|ccccccc|c} z_1 & 2 & -1 & 0 & 0 & 0 & 0 & 0 & 1 \\ z_2 & -1 & 2 & -1 & 0 & 0 & 0 & -1 & 2 \\ z_3 & 0 & -1 & 2 & -1 & 0 & -1 & 0 & 3 \\ z_4 & 0 & 0 & -1 & 2 & -1 & 0 & 0 & 2 \\ z_5 & 0 & 0 & 0 & -1 & 2 & 0 & 0 & 1 \\ z_6 & 0 & 0 & -1 & 0 & 0 & 2 & -1 & 2 \\ z_0 & 0 & 0 & 0 & 0 & 0 & -1 & 2 & 1 \end{array} . \tag{6.25}$$

Applying the prescription set out in 6.2, 6.3 and 6.4, we obtain the monopole equation for an E_6 instanton:

$$\begin{aligned} g^{E_6}_{HS:RSIMS}(z,t) = \sum_{q_1,q_5=-\infty}^{\infty} \sum_{\substack{q_{j,1}\geq q_{j,2}\geq -\infty \\ j=2,4,6}}^{\infty} \sum_{q_{3,1}\geq q_{3,2}\geq q_{3,3}\geq -\infty}^{\infty} & {z_1}^{q_1} {z_2}^{q_{2,1}+q_{2,2}} {z_3}^{q_{3,1}+q_{3,2}+q_{3,3}} \\ & \times {z_4}^{q_{4,1}+q_{4,2}} {z_5}^{q_5} {z_6}^{q_{6,1}+q_{6,2}} \; P^{E_6}_{U(N)}(q,t)\, t^{\Delta(q)}, \end{aligned} \tag{6.26}$$

where

$$\begin{aligned} P^{E_6}_{U(N)}(q,t) = & \frac{1}{(1-t)^6(1-t^2)^4(1-t^3)} \\ & \times If\left[q_{3,1}\neq q_{3,2} \vee q_{3,1}\neq q_{3,3} \vee q_{3,2}\neq q_{3,3}, \left(1+t+t^2\right)\right] \\ & \times If\left[q_{3,1}\neq q_{3,2} \wedge q_{3,1}\neq q_{3,3} \wedge q_{3,2}\neq q_{3,3}), (1+t)\right] \\ & \times \prod_{j=2,4,6} If\left[q_{j,1}\neq q_{j,2}, (1+t)\right] \end{aligned} \tag{6.27}$$

and

$$\Delta(q) = \frac{1}{2}\left(\sum_{i=1}^{2}|q_1 - q_{2,i}| + \sum_{k=2,4,6}\sum_{i,j=1}^{i=2,j=3}|q_{3,j} - q_{k,i}| + \sum_{i=1}^{2}|q_{4,i} - q_5| + \sum_{i=1}^{2}|q_{6,i}|\right) - \sum_{k=2,4,6}\sum_{i>j\geq 1}^{2}|q_{k,i} - q_{k,j}| - \sum_{i>j\geq 1}^{3}|q_{3,i} - q_{3,j}|. \tag{6.28}$$

The RSIMS constructions for E_7 and E_8 groups follow a similar pattern to E_6.

Again, the gauge choice $q_0 = 0$ has alternatives. For star shaped quivers, such as E_6, a convenient choice of gauge is $q_{3,3} = 0$, and this leads directly to a decomposition into a symmetric sum over all the representations of three $T(SU(3))$ quiver theories, discussed in Chapter 8.

6.2.2. Non-Simply Laced Groups

B Series

The Coulomb branch construction for B series RSIMS is based on the extended Cartan matrix and dual Coxeter labels:

$$\left|\begin{array}{cccccccc} z_1 & 2 & -1 & \dots & 0 & 0 & 0 & 1 \\ z_2 & -1 & 2 & \dots & 0 & 0 & -1 & 2 \\ \dots & \dots & \dots & \dots & \dots & \dots & \dots & 2 \\ z_{r-1} & 0 & 0 & \dots & 2 & -2 & 0 & 2 \\ z_r & 0 & 0 & \dots & -1 & 2 & 0 & 1 \\ z_0 & 0 & -1 & \dots & 0 & 0 & 2 & 1 \end{array}\right|. \tag{6.29}$$

Applying 6.2, 6.3 and 6.4, gives the monopole formula for the RSIMS of $B_{r>2}$:

$$g^{B_r}_{HS:RSIMS}(z,t) = \sum_{q_1,q_r=-\infty}^{\infty}\sum_{\substack{q_{j,1}\geq q_{j,2}\geq -\infty \\ r-1\geq j\geq 2}}^{\infty} {z_1}^{q_1}{z_2}^{q_{2,1}+q_{2,2}}\dots{z_{r-1}}^{q_{r-1,1}+q_{r-1,2}}{z_r}^{q_r} \times P^{B_r}_{U(N)}(q,t)\, t^{\Delta(q)}, \tag{6.30}$$

where

$$P_{U(N)}^{B_r}(q,t) = \frac{\prod_{j=2}^{r-1} If\left[q_{j,1} \neq q_{j,2}, (1+t)\right]}{(1-t)^r (1-t^2)^{r-2}} \tag{6.31}$$

and

$$\begin{aligned}\Delta(q) = \frac{1}{2}\left(\sum_{i=1}^{2}\left(|q_1 - q_{2,i}| + |q_{2,i}| + |2q_{r-1,i} - q_r|\right) + \sum_{k=2}^{r-2}\sum_{i,j=1}^{2}|q_{k,i} - q_{k+1,j}|\right) \\ - \sum_{k=2}^{r-1}\sum_{i>j}|q_{k,i} - q_{k,j}|.\end{aligned} \tag{6.32}$$

This Coulomb branch construction for B_2 can be rearranged into the B_2 RSIMS in Table 5.3:

$$\begin{aligned} g_{HS:Coulomb}^{B_2}(z,t) &= \frac{1}{(1-t)^2}\sum_{q_1,q_2=-\infty}^{\infty} {z_1}^{q_1}{z_2}^{q_2} t^{\frac{1}{2}(|2q_1-q_2|+|q_2|)} \\ &= \frac{1}{(1-t)^2}\left(\begin{array}{l} \sum_{q_1=0}^{\infty}\sum_{q_2=0}^{2q_1}\left({z_1}^{q_1}{z_2}^{q_2} + {z_1}^{-q_1}{z_2}^{-q_2}\right)t^{q_1} \\ + \sum_{q_1=0}^{\infty}\sum_{q_2=2q_1}^{\infty}\left({z_1}^{q_1}{z_2}^{q_2} + {z_1}^{-q_1}{z_2}^{-q_2}\right)t^{(q_2-q_1)} \\ - \sum_{q_1=0}^{\infty}\left({z_1}^{q_1}{z_2}^{2q_1} + {z_1}^{-q_1}{z_2}^{-2q_1}\right)t^{q_1} \\ + \sum_{q_1=0}^{\infty}\sum_{q_2=0}^{\infty}\left({z_1}^{q_1}{z_2}^{-q_2} + {z_1}^{-q_1}{z_2}^{q_2}\right)t^{(q_1+q_2)} \\ - \sum_{q_1=0}^{\infty}\left({z_1}^{q_1} + {z_1}^{-q_1}\right)t^{q_1} \\ - \sum_{q_2=0}^{\infty}\left({z_2}^{q_2} + {z_2}^{-q_2}\right)t^{q_2} \\ +1 \end{array}\right) \\ &\cdots \\ &= \begin{pmatrix} 1-t^2-t^6+t^8 & [0,0] \\ t^3-2t^4+t^5 & [0,2] \\ -t^2+t^3+t^5-t^6 & [1,0] \\ t^3-2t^4+t^5 & [1,2] \\ -t^2+t^3+t^5-t^6 & [2,0] \end{pmatrix} PE\left[[0,2]\,t\right]. \end{aligned} \tag{6.33}$$

The monopole formula for the B_2 RSIMS can also be obtained from the character generating function 2.12. This permits us to take advantage of the invariance of the highest root of B_2 under the Weyl reflections of an A_1 subgroup and to work with the W_{B_2/A_1} quotient group. This quotient group has dimension $|W_{B_2/A_1}| = 4$ and transforms amongst the long roots of B_2 which are $\{z_1, z_1{z_2}^2, {z_1}^{-1}, {z_1}^{-1}{z_2}^{-2}\}$. We obtain:

$$\begin{aligned}
g^{B_2}_{HS:RSIMS}(z,t) &= \sum_{W_{B_2/A_1}} \frac{1}{(1-tz_1)\,(1-1/z_1)\,(1-z_2)\,(1-1/z_1z_2)} \\
&= \sum_{W_{B_2/A_1}} \sum_{a=0}^{\infty}\sum_{b=0}^{\infty}\sum_{c=0}^{\infty}\sum_{d=0}^{\infty} t^a z_1^{a-b-d} z_2^{c-d} \\
&= \sum_{W_{B_2/A_1}} \sum_{q_1=-\infty}^{\infty}\sum_{q_2=-\infty}^{\infty}\sum_{d=\max(0,-q_2)}^{\infty}\sum_{b=\max(0,-d-q_1)}^{\infty} {z_1}^{q_1}{z_2}^{q_2} t^{b+d+q_1} \\
&= \frac{1}{(1-t)} \sum_{W_{B_2/A_1}} \sum_{q_1=-\infty}^{\infty}\sum_{q_2=-\infty}^{\infty}\sum_{d=0}^{\infty} {z_1}^{q_1}{z_2}^{q_2} t^{\max(0,d+q_1,d+q_1-q_2)} \\
&= \frac{1}{(1-t)^2} \sum_{W_{B_2/A_1}} \sum_{q_1=-\infty}^{\infty}\sum_{q_2=-\infty}^{\infty} z_1^{q_1} z_2^{q_2} \left(\begin{array}{c} t^{\max(0,q_1,q_1-q_2)} - \\ (1-t)\min(0,\max(q_1,q_1-q_2)) \end{array} \right) \\
&= \frac{1}{(1-t)^2} \sum_{W_{B_2/A_1}} \sum_{q_1=-\infty}^{\infty}\sum_{q_2=-\infty}^{\infty} z_1^{q_1} z_2^{q_2} t^{\max(0,q_1,q_1-q_2)},
\end{aligned} \tag{6.34}$$

where we have used the identity 6.18 to eliminate piecewise terms. Carrying out the Weyl reflections and rearranging or eliminating piecewise terms, using the identities 6.20, recovers the RSIMS monopole formula 6.33:

$$\begin{aligned}
g^{B_2}_{HS:RSIMS}(z,t) &= \frac{1}{(1-t)^2} \sum_{q_1=-\infty}^{\infty}\sum_{q_2=-\infty}^{\infty} z_1^{q_1} z_2^{q_2} (t^{\max(0,-q_1,q_2-q_1)} + t^{\max(0,-q_1,q_1-q_2)} \\
&\quad + t^{\max(0,q_1,q_2-q_1)} + t^{\max(0,q_1,q_1-q_2)}) \\
&= \frac{1}{(1-t)^2} \sum_{q_1=-\infty}^{\infty}\sum_{q_2=-\infty}^{\infty} z_1^{q_1} z_2^{q_2} (t^{\frac{1}{2}|2q_1-q_2|+\frac{1}{2}|q_2|} + t^{|q_1-q_2|} + t^{|q_1|} + 1) \\
&= \frac{1}{(1-t)^2} \sum_{q_1=-\infty}^{\infty}\sum_{q_2=-\infty}^{\infty} z_1^{q_1} z_2^{q_2} t^{\frac{1}{2}|2q_1-q_2|+\frac{1}{2}|q_2|}.
\end{aligned} \tag{6.35}$$

C Series

The Coulomb branch construction for C series RSIMS is based on the extended Cartan matrix and dual Coxeter labels:

$$\left|\begin{array}{c|cccccc|c} z_1 & 2 & -1 & \dots & 0 & 0 & -1 & 1 \\ z_2 & -1 & 2 & \dots & 0 & 0 & 0 & 1 \\ \dots & \dots & \dots & \dots & \dots & \dots & \dots & 1 \\ z_{r-1} & 0 & 0 & \dots & 2 & -1 & 0 & 1 \\ z_r & 0 & 0 & \dots & -2 & 2 & 0 & 1 \\ z_0 & -2 & 0 & \dots & 0 & 0 & 2 & 1 \end{array}\right|. \tag{6.36}$$

Applying 6.2, 6.3 and 6.4, we obtain the monopole formula for a $C_{r\geq 2}$ RSIMS:

$$g^{C_r}_{HS:RSIMS}(z,t) = \frac{1}{(1-t)^r} \sum_{q_i=-\infty}^{\infty} {z_1}^{q_1} {z_2}^{q_2} \dots {z_r}^{q_r} t^{\Delta(q)}, \tag{6.37}$$

where

$$\Delta(q) = \frac{1}{2}\left(|q_1| + \sum_{i=1}^{r-2} |q_i - q_{i+1}| + |q_{r-1} - 2q_r| \right). \tag{6.38}$$

The constructions for B_2 and C_2 are isomorphic under interchange of root labels.

$\mathbf{G_2}$

The Coulomb branch construction for the G_2 RSIMS is based on the extended Cartan matrix and dual Coxeter labels:

$$\left|\begin{array}{c|ccc|c} z_1 & 2 & -3 & -1 & 2 \\ z_2 & -1 & 2 & 0 & 1 \\ z_0 & -1 & 0 & 2 & 1 \end{array}\right|. \tag{6.39}$$

Applying 6.2, 6.3 and 6.4, we obtain the monopole formula for a G_2 RSIMS:

$$g^{G_2}_{HS:RSIMS}(z,t) = \sum_{q_{1,1}\geq q_{1,2}\geq -\infty}^{\infty} \sum_{q_2=-\infty}^{\infty} {z_1}^{q_{1,1}+q_{1,2}} {z_2}^{q_2} P^{G_2}_{U(N)} t^{\Delta(q)}, \tag{6.40}$$

where

$$P^{G_2}_{U(N)}(q,t) = \frac{If\left[q_{1,1} \neq q_{1,2}, (1+t)\right]}{(1-t)^2(1-t^2)} \tag{6.41}$$

and

$$\Delta(q) = \frac{1}{2}\sum_{i=1}^{2}\left(|q_{1,i}| + |3q_{1,i} - q_2|\right) - |q_{1,1} - q_{1,2}|\,. \tag{6.42}$$

$\mathbf{F_4}$

The Coulomb branch construction for the F_4 RSIMS is based on the extended Cartan matrix and dual Coxeter labels:

$$\begin{array}{c|ccccc|c|} z_1 & 2 & -1 & 0 & 0 & -1 & 2 \\ z_2 & -1 & 2 & -2 & 0 & 0 & 3 \\ z_3 & 0 & -1 & 2 & -1 & 0 & 2 \\ z_4 & 0 & 0 & -1 & 2 & 0 & 1 \\ z_0 & -1 & 0 & 0 & 0 & 2 & 1 \\ \end{array}\,. \tag{6.43}$$

Applying 6.2, 6.3 and 6.4, we obtain the monopole formula for a F_4 RSIMS:

$$g^{F_4}_{HS:RSIMS}(z,t) = \sum_{\substack{q_{j1}\geq q_{j,2}\geq -\infty \\ j=1,3}}^{\infty} \sum_{q_{2,1}\geq q_{2,2}\geq q_{2,3}\geq -\infty}^{\infty} \sum_{q_4=-\infty}^{\infty} z_1{}^{q_{1,1}+q_{1,2}} z_2{}^{q_{2,1}+q_{2,2}+q_{2,3}} z_3{}^{q_{3,1}+q_{3,2}} z_4{}^{q_4} \times P^{F_4}_{U(N)} t^{\Delta(q)}, \tag{6.44}$$

where

$$\begin{aligned} P^{F_4}_{U(N)}(q,t) =& \frac{\prod_{j=1,3} If\left[q_{j,1} \neq q_{j,2}, 1+t\right]}{(1-t)^4(1-t^2)^3(1-t^3)} \\ & \times If\left[\exists i,j : q_{2i} \neq q_{2j}, (1+t+t^2)\right] \\ & \times If\left[!\exists i,j : q_{2,i} = q_{2,j}, (1+t)\right] \end{aligned} \tag{6.45}$$

and

$$\begin{aligned} \Delta(q) =& \frac{1}{2}\left(\sum_{i=1}^{2}|q_{1,i}| + \sum_{i=1}^{2}\sum_{j=1}^{3}\left(|q_{1,i} - q_{2,j}| + |2q_{2,j} - q_{3,i}|\right) + \sum_{i=1}^{2}|q_{3,i} - q_4|\right) \\ & - \sum_{k=1,3}|q_{k,1} - q_{k,2}| - \sum_{i>j}|q_{2,i} - q_{2,j}|. \end{aligned} \tag{6.46}$$

6.2.3. Root Space Foliation

A key feature of the Coulomb branch construction is the way in which conformal dimension foliates the root space into sets of Weyl group orbits of dominant weights. This is illustrated for A_2, B_2 C_2 and G_2 RSIMS in Figures 6.1, 6.2, 6.3 and 6.4. Roots are labelled using root space coordinates, rather than weight space coordinates/Dynkin labels.

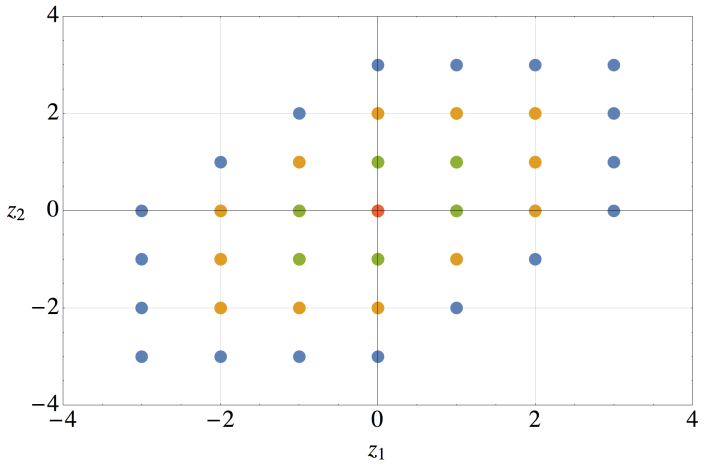

Figure 6.1.: Root Space of A_2 Foliated by RSIMS Conformal Dimension. The colour sequence corresponds to conformal dimensions of 0 for (0,0), 1 for the Weyl orbit of (1,1), 2 for the Weyl orbits of (2,2), (1,2) and (2,1), and 3 for the Weyl orbits of (3,3), (2,3) and (3,2). The adjoint representation is given by the orbit of (1,1) with conformal dimension 1 plus 2 orbits with conformal dimension 0.

In all cases, the RSIMS can be expressed as sums of orbits of dominant weights, combined at multiplicities determined by the $P^{U(N)}$ factors. Conformal dimension remains constant around each orbit. More than one dominant weight can have the same conformal dimension. For all rank 2 groups, the adjoint is given by the orbits with conformal dimension 1 plus two orbits with conformal dimension 0. The isomorphism between B_2 and C_2 is evident upon interchange of simple roots.

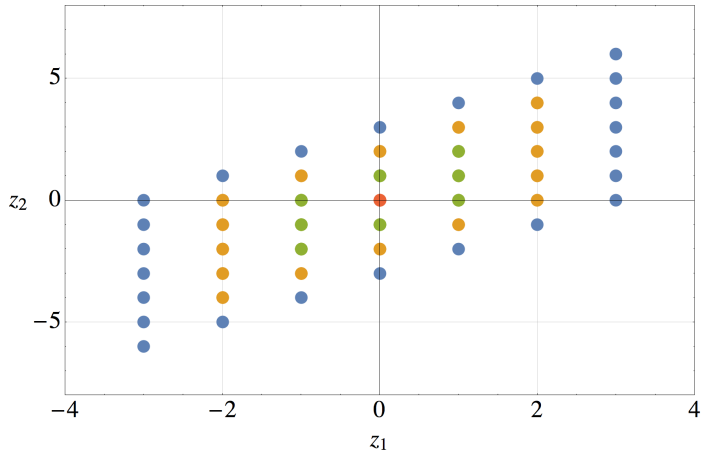

Figure 6.2.: Root Space of B_2 Foliated by RSIMS Conformal Dimension. The colour sequence corresponds to conformal dimensions of 0 for (0,0), 1 for the Weyl orbits of (1,2) and (1,1), 2 for the Weyl orbits of (2,4), (2,3) and (2,2), and 3 for the Weyl orbits of (3,6), (3,5), (3,4) and (3,3). The long root of the adjoint representation is (1,2).

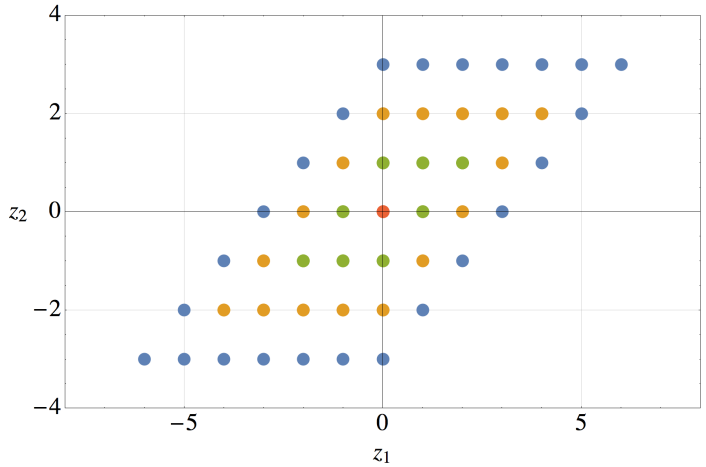

Figure 6.3.: Root Space of C_2 Foliated by RSIMS Conformal Dimension.The colour sequence corresponds to conformal dimensions of 0 for (0,0), 1 for the Weyl orbits of (2,1) and (1,1), 2 for the Weyl orbits of (4,2), (3,2) and (2,2), and 3 for the Weyl orbits of (6,3), (5,3), (4,3) and (3,3). The long root of the adjoint representation is (2,1).

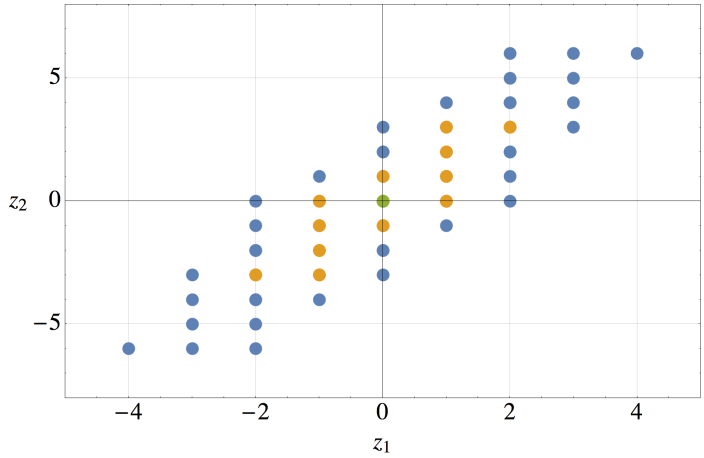

Figure 6.4.: Root Space of G_2 Foliated by RSIMS Conformal Dimension. The colour sequence corresponds to conformal dimensions of 0 for (0,0), 1 for the Weyl orbits of (2,3) and (1,2), and 2 for the Weyl orbits of (4,6), (3,6), (3,5) and (2,4). The long root of the adjoint representation is (2,3).

6.3. Near to Minimal Nilpotent Orbits

6.3.1. Twisted Affine Quivers

Coulomb branch constructions of near to minimal nilpotent orbits from affine Dynkin diagrams proceed in a similar manner to those for RSIMS. One option is to replace a node of an untwisted affine diagram, other than the affine node, by a flavour node. Alternatively, one can start with a twisted affine Dynkin diagram (see appendix A.3). Both types of affine diagram are balanced and therefore replacement of any node by a flavour node of equal $U(N)$ rank leads to a balanced quiver diagram. By judicious choice, we can obtain a simple algebra of the same rank as the starting algebra. The node that is replaced becomes a flavour node (with zero background charge) in the quiver diagram.

Figures 6.5 and 6.6 show the branching options for some extended (untwisted affine) Classical and Exceptional Dynkin diagrams, expressed in terms of the quivers to which they give rise. These include, for reference, the quivers for RSIMS examined in section 6.2.

The Classical (untwisted) affine Dynkin diagrams give rise to one class of quivers over and above those for RSIMS. This class of quivers is derived

from the B_r affine Dynkin diagram and yields Coulomb branch constructions over D_r. Gauge node counting shows that the Coulomb branch dimension of these quivers is $4r-4$, which is 2 above the dimension of the minimal nilpotent orbit of D_r. This indicates that these moduli spaces correspond to the next to minimal orbits of D_r.

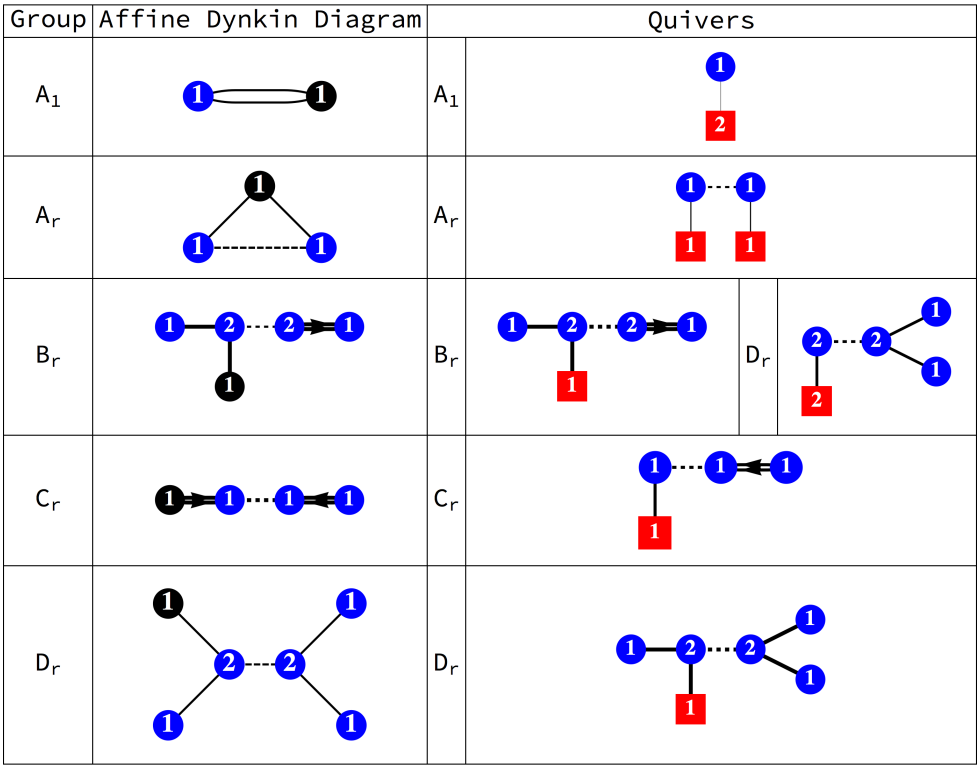

Figure 6.5.: Quivers from Classical Affine Dynkin Diagrams. Round (blue) nodes denote gauge nodes in the regular Dynkin diagram. The affine diagram is obtained by adding a gauge node (black). The dual Coxeter labels of each node are shown. Square (red) nodes denote flavour nodes. When a short root attached to a long root in the affine diagram is taken as a flavour node, its rank is doubled.

The Exceptional (untwisted) affine Dynkin diagrams also give rise to a number of quivers over and above those for RSIMS. These extra quivers provide Coulomb branch constructions for moduli spaces of A_2, B_4, A_7, A_8 and D_8, and these appear to correspond to nilpotent orbits.

1. $G_2 \to A_2$. This quiver gives the Coulomb branch construction for the

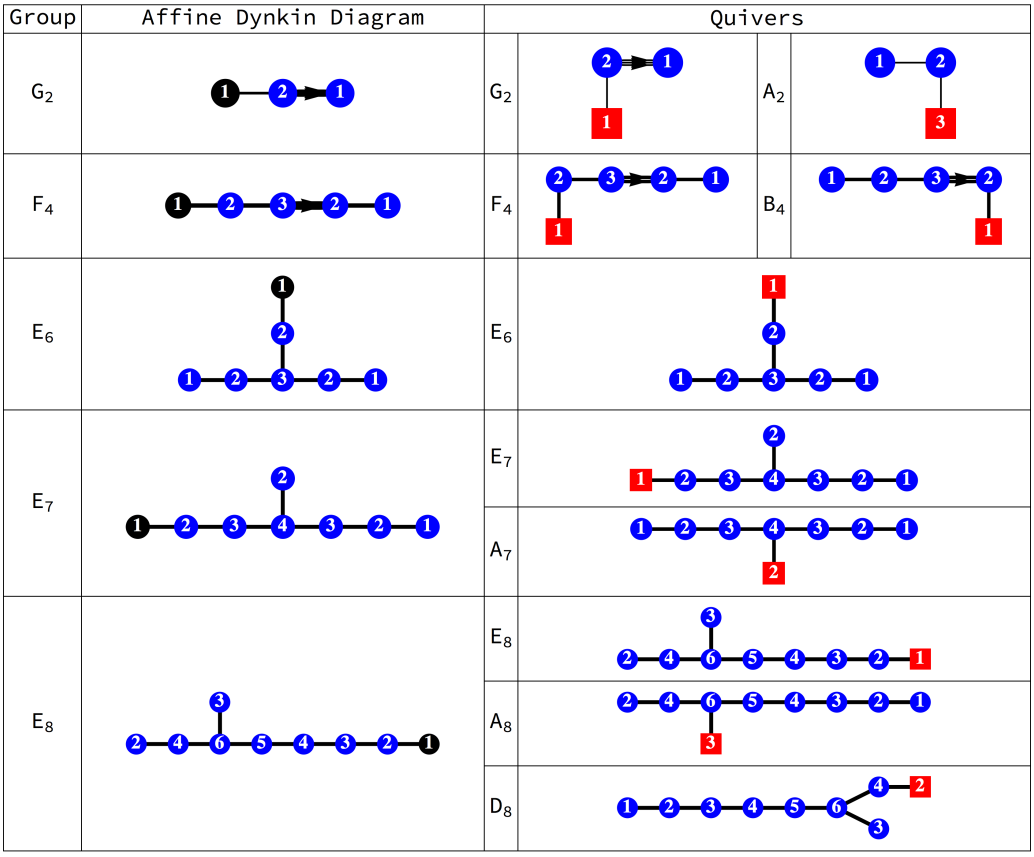

Figure 6.6.: Quivers from Exceptional Affine Dynkin Diagrams. Round (blue) nodes denote gauge nodes in the regular Dynkin diagram. The affine diagram is obtained by adding a gauge node (black). The dual Coxeter labels of each node are shown. Square (red) nodes denote flavour nodes. When a short root attached to a long root in the affine diagram is taken as a flavour node, its rank is doubled or tripled according to the ratio of root lengths.

6 dimensional maximal nilpotent orbit of A_2.

2. $F_4 \to B_4$. This quiver appears to be the Coulomb branch construction for the 16 dimensional nilpotent orbit of B_4, which is two orbits above the minimal. The quiver diagram is consistent with the Characteristic of this nilpotent orbit, as discussed in 6.5.

3. $E_7 \to A_7$. This quiver gives the Coulomb branch construction for the 32 dimensional nilpotent orbit of A_7. This can be established by 3d mirror duality, as discussed in 6.4.

4. $E_8 \to A_8$. This quiver gives the Coulomb branch construction for the 58 dimensional nilpotent orbit of A_8. This can be established by 3d mirror duality, as discussed in 6.4.

5. $E_8 \to D_8$. This quiver appears to be the Coulomb branch construction for the 56 dimensional spinor pair nilpotent orbit of D_8, which is seven above the minimal. The quiver diagram is consistent with the Characteristic of this nilpotent orbit, as discussed in 6.5.

Figure 6.7 shows the branching options for twisted affine Dynkin diagrams. The three infinite families give rise to a series of quivers that provide Coulomb branch constructions for nilpotent orbits. In addition, $A_1^{(2)}, G_2^{(3)}$ and $F_4^{(2)}$ branch to some further quivers.

1. $A_1^{(2)} \to A_1$. This quiver gives the Coulomb branch construction for the nilpotent orbit of A_1.

2. $G_2^{(3)} \to A_2$. This quiver gives the Coulomb branch construction for the 6 dimensional maximal nilpotent orbit of A_2.

3. $B_r^{(2)}$ or $\tilde{B}_r^{(2)} \to B_r$. This quiver gives the Coulomb branch construction for the $4r-2$ dimensional next to minimal nilpotent orbit of B_r.

4. $C_r^{(2)} \to D_r$. This quiver gives the Coulomb branch construction for the $4r-4$ dimensional next to minimal nilpotent orbit of D_r.

5. $C_r^{(2)} \to C_r$. This quiver gives the Coulomb branch construction for the $4r-2$ dimensional next to minimal nilpotent orbit of C_r.

6. $F_4^{(2)} \to C_4$. This quiver gives the Coulomb branch construction for the 20 dimensional nilpotent orbit of C_4.

7. $F_4^{(2)} \to F_4$. This quiver gives the Coulomb branch construction for the 22 dimensional next to minimal nilpotent orbit of F_4.

Taken together, the affine quivers yield Coulomb branch constructions for moduli spaces of minimal nilpotent orbits of all groups, next to minimal nilpotent orbits of all BCD groups and F_4, plus a number of other near to minimal nilpotent orbits.

However, calculation shows that a few of the branching options from twisted affine Dynkin diagrams lead to quivers that do *not* correspond to the moduli space of any nilpotent orbit:

1. $A_1^{(2)} \to A_1$: The quiver $[4] - (2)$ has a 4 dimensional Coulomb branch, which is clearly not the A_1 orbit.

2. $G_2^{(3)} \to G_2$: The quiver $(3) \equiv> (2) - [1]$ has a 10 dimensional Coulomb branch, but this does not match the G_2 nilpotent orbit of the same dimension.

3. $B_r^{(2)}$ or $\tilde{B}_r^{(2)} \to C_r$: The C_r quivers have $4r$ dimensional Coulomb branches, but these do not match C_r nilpotent orbits.

The reasons for these exceptions amongst the quivers from twisted affine branchings are unclear. In practice, therefore, it is necessary to verify, on a case by case basis, the correspondence between these Coulomb branch constructions and the Higgs branch constructions for nilpotent orbit moduli spaces set out in Tables 5.4 to 5.6 and 5.12 to 5.20.

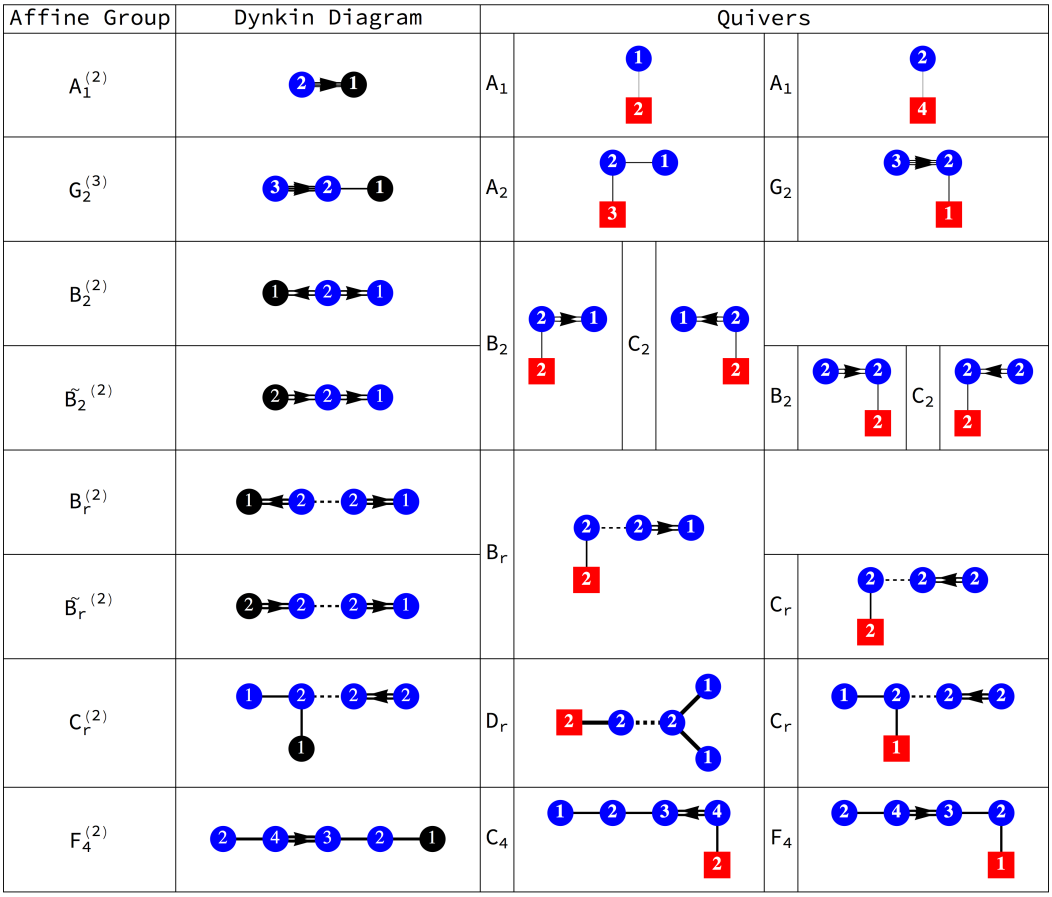

Figure 6.7.: Quivers from Twisted Affine Dynkin Diagrams. Twisted affine groups are labelled using the notation of [58]. Round (blue) nodes denote gauge nodes in the regular Dynkin diagram. The twisted affine diagram is obtained by adding a gauge node (black). The dual Coxeter labels of each node are shown. Square (red) nodes denote flavour nodes. When a short root attached to a long root in the affine diagram is taken as the flavour node in a quiver, its rank is multiplied according to the ratio of root lengths.

6.3.2. Evaluation of Affine Coulomb Branches

As an example, applying the monopole formula to the quiver $[2]-(2) => (1)$ from $B_2^{(2)} \to B_2$ yields the Coulomb branch:

$$g^{B_2}_{HS:Coulomb}(z,t) = \sum_{q_{1,1}=-\infty}^{\infty} \sum_{q_{1,2}=-\infty}^{q_{1,1}} \sum_{q_2=-\infty}^{\infty} P_q^{U(N)}(t)\ {z_1}^{q_{1,1}+q_{1,2}} {z_2}^{q_2}\ t^{\Delta(q)}, \tag{6.47}$$

where

$$\Delta(q) = \frac{1}{2}\left(|2q_{1,1}| + |2q_{1,2}| + |2q_{1,1} - q_2| + |2q_{1,2} - q_2|\right) - |q_{1,1} - q_{1,2}| \tag{6.48}$$

and

$$P_q^{U(N)}(t) = \begin{cases} q_{1,1} = q_{1,2} : 1/\left((1-t)^2(1-t^2)\right) \\ q_{1,1} \neq q_{1,2} : 1/(1-t)^3 \end{cases} . \tag{6.49}$$

It is important to note that, under the monopole formula, the quivers $[1] \Leftarrow (2) \Rightarrow (1)$ and $[2]-(2) \Rightarrow (1)$ evaluate identically for an uncharged flavour node. Implementing the summation piecewise and replacing the simple root fugacities of B_2 by weight space fugacities $\{z_1, z_2\} \to \left\{\frac{x^2}{y^2}, \frac{y^2}{x}\right\}$, we obtain:

$$g^{B_2}_{HS:Coulomb}(x,y,t) = \frac{(t+1)x^3y^4(t^4xy^2 + t^3xy^2 - t^2x^2y^2 - t^2x^2 - t^2y^4 - t^2y^2 + txy^2 + xy^2)}{(t-x)(tx-1)(t-y^2)(ty^2-1)(tx-y^2)(tx^2-y^2)(ty^2-x)(ty^2-x^2)}$$

$$= \left((1 - t^2 - t^5 + t^7)[0,0] + (-t^2 + t^3 + t^4 - t^5)[1,0]\right) PE\left[[0,2]t\right] \tag{6.50}$$

As before, we can restate this in terms of an unrefined Hilbert series and in terms of a character HWG:

$$g^{B_2}_{HS:Coulomb}(1,t) = \frac{(1+t)(1+3t+t^2)}{(1-t)^6}, \tag{6.51}$$

$$g^{B_2}_{HWG:Coulomb}(m_1,m_2,t) = \frac{1}{(1-{m_2}^2t)(1-{m_1}^2t^2)}, \tag{6.52}$$

Comparison with Table 5.12, shows that we have obtained the moduli space for the 6 dimensional next to minimal nilpotent orbit of B_2, under the counting fugacity map, Higgs $\to$ Coulomb : $t^2 \to t$.

In principle, this calculation can be repeated for the quivers identified in Figure 6.7. Subject to some qualifications, discussed below, calculations up

to rank 4 confirm a match between the Coulomb branches of these quivers and those of the Higgs branches of BCD quivers corresponding to nilpotent orbits. This match is summarised in Figures 6.8, 6.9 and 6.10, giving the dimensions of the nilpotent orbits, their Higgs branch quivers and the equivalent Coulomb branch quivers, which are all balanced. The flavour nodes in these Coulomb branch quivers do not carry external charges.

Turning to the near minimal nilpotent orbits associated with pairs of D_n spinor partitions; calculation shows that their Coulomb branch constructions form a pair of palindromic moduli spaces, according to the choice of spinor linked to the flavour node. Their Higgs branch constructions are non-palindromic unions of these two Coulomb branches.

Thus, in the case of D_4, as indicated in Figure 6.10, the Coulomb branch quiver for the 12 dimensional $D_4 - C_1 - B_0$ nilpotent orbit is related by triality to a pair of 12 dimensional moduli spaces, and the union of this pair forms the $D_4 - C_2$ I/II nilpotent orbit construction on the Higgs branch, consistent with 5.25.

Similarly, it can be anticipated that the Higgs branch construction from the $D_8 - C_4$ quiver of the 56 dimensional nilpotent orbit of D_8 equals the union of the spinor pair Coulomb branch constructions from the E_8 affine Dynkin diagram identified in section 6.3.

Group	Dimension	Higgs Quiver	Coulomb Quiver
B_1	2	$B_1-C_1-B_0$	
B_2	4	B_2-C_1	
	6	$B_2-C_1-B_0$	
	8	$B_2-C_2-B_1-C_1-B_0$	...?...
B_3	8	B_3-C_1	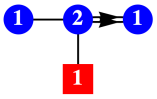
	10	$B_3-C_1-B_0$	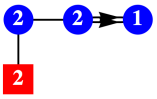
	12	$B_3-C_2-B_0$	...?...
	14	$B_3-C_2-D_1$	
	16	$B_3-C_2-B_1-C_1-B_0$	
	18	$B_3-C_3-B_2-C_2-B_1-C_1-B_0$	
B_4	12	B_4-C_1	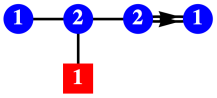
	14	$B_4-C_1-B_0$	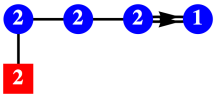
	16	B_4-C_2	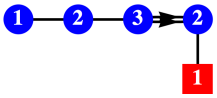
	20	$B_4-C_2-B_0$	...?...
	22	$B_4-C_2-D_1$	
	24	$B_4-C_3-B_1$	
	24	$B_4-C_2-B_1-C_1-B_0$	
	26	$B_4-C_3-D_2-C_1$	
	26	$B_4-C_3-B_2-C_2-B_1-C_1-B_0$	
	28	$B_4-C_3-D_2-C_1-B_0$	
	30	$B_4-C_3-B_2-C_2-B_1-C_1-B_0$	
	32	$B_4-C_4-B_3-C_3-B_2-C_2-B_1-C_1-B_0$	

Figure 6.8.: Higgs/Coulomb Quivers for B Series Nilpotent Orbits up to rank 4. B/D gauge nodes in a Higgs quiver indicate the corresponding O group. Round (blue) nodes denote U(N) gauge nodes. Square (red) nodes denote flavour nodes. The nilpotent orbits can be calculated from either the Higgs or Coulomb branches of the dual quivers using the Higgs branch or monopole formulae, respectively.

Group	Dimension	Higgs Quiver	Coulomb Quiver
C_1	2	C_1–B_0	
C_2	4	C_2–B_0	
	6	C_2–D_1	
	8	C_2–B_1–C_1–B_0	...?...
C_3	6	C_3–B_0	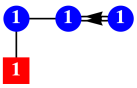
	10	C_3–D_1	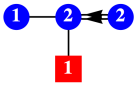
	12	C_3–B_1	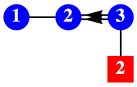
	14	C_3–D_2–C_1	...?...
	14	C_3–B_1–C_1–B_0	
	16	C_3–D_2–C_1–B_0	
	18	C_3–B_2–C_2–B_1–C_1–B_0	
C_4	8	C_4–B_0	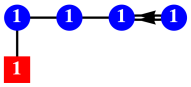
	14	C_4–D_1	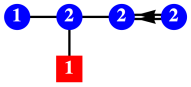
	18	C_4–B_1	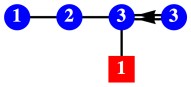
	20	C_4–D_2	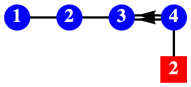
	20	C_4–B_1–C_1–B_0	...?...
	22	C_4–D_2–C_1	
	24	C_4–B_2–C_1	
	24	C_4–D_2–C_1–B_0	
	26	C_4–B_2–C_1–B_0	
	28	C_4–D_3–C_2–D_1	
	28	C_4–B_2–C_2–B_2–C_1–B_0	
	30	C_4–D_3–C_2–B_1–C_1–B_0	
	32	C_4–B_3–C_3–B_2–C_2–B_1–C_1–B_0	

Figure 6.9.: Higgs/Coulomb Quivers for C Series Nilpotent Orbits up to rank 4. B/D gauge nodes in a Higgs quiver indicate the corresponding O group. Round (blue) nodes denote U(N) gauge nodes. Square (red) nodes denote flavour nodes. The nilpotent orbits can be calculated from either the Higgs or Coulomb branches of the dual quivers using the Higgs branch or monopole formulae, respectively.

Group	Dimension	Higgs Quiver	Coulomb Quiver
D_3	6	D_3-C_1	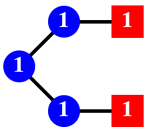
	8	$D_3-C_1-B_0$	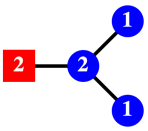
	10	$D_3-C_2-D_1$	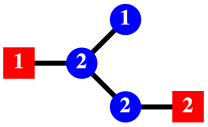
	12	$D_3-C_2-B_1-C_1-B_0$	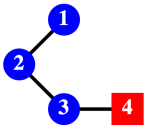
D_4	10	D_4-C_1	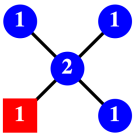
	12	$D_4-C_1-B_0$	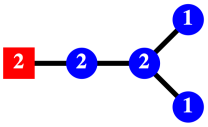
		$D_4-C_2{}^{I/II}$	
	16	$D_4-C_2-B_0$	...?...
	18	$D_4-C_2-D_1$	
	20	$D_4-C_3-D_2-C_1$	
	20	$D_4-C_2-B_1-C_1-B_0$	
	22	$D_4-C_3-D_2-C_1-B_0$	
	24	$D_4-C_3-B_2-C_2-B_1-C_1-B_0$	

Figure 6.10.: Higgs/Coulomb Quivers for D Series Nilpotent Orbits up to rank 4. B/D gauge nodes in a Higgs quiver indicate the corresponding O group. Round (blue) nodes denote U(N) gauge nodes. Square (red) nodes denote flavour nodes. The nilpotent orbits can be calculated from either the Higgs or Coulomb branches of the dual quivers using the Higgs branch or monopole formulae, respectively. The three 12 dimensional nilpotent orbits of D_4 are related by triality.

6.4. 3d Mirror Symmetry

6.4.1. A Series

Since early work in [1], it has been known that the Higgs branches of A series quivers have moduli spaces that are identical to those of the Coulomb branches of certain unitary dual quivers, under $3d$ *mirror symmetry*. A pair of quivers $\mathcal{A}$ and $\mathcal{B}$ that are $3d$ mirror dual obeys the relationship:

$$\begin{aligned} g^{\mathcal{A}}_{\text{HS:Higgs}} &= g^{\mathcal{B}}_{\text{HS:Coulomb}} \\ g^{\mathcal{A}}_{\text{HS:Coulomb}} &= g^{\mathcal{B}}_{\text{HS:Higgs}} \end{aligned} \tag{6.53}$$

Given an A series quiver containing a linear sequence of gauge nodes, its mirror dual can be calculated using brane combinatorics, as set out in [2, 25, 31], and this provides a method of finding A series quivers with Coulomb branch moduli spaces equal to the Higgs branch constructions of nilpotent orbits in Tables 5.4 to 5.6.

Briefly, the brane system can be described in type IIB string theory in terms of D5, NS5 and D3 branes in $9+1$ space-time. The branes all extend along the space-time directions x_0, x_1 and x_2. The D3 branes also extend along x_3. The D5 and NS5 branes extend along x_4, x_5, x_6 and x_7, x_8, x_9, respectively, being interchanged by S-duality. The D3 branes begin and end on 5-branes, so moving a D5 and NS5 through each other in the x_3 direction creates or destroys a D3 brane. Each set of D3 branes linking two adjacent NS5 branes defines a unitary symmetry. The D5 branes carry a flavour symmetry.

The brane manipulations to transform the quiver for the Higgs branch construction of the maximal nilpotent orbit of A_3 into its mirror are shown in Figure 6.11. The quiver starts with the D5 branes disconnected from the D3 branes (i.e. with no *net* left or right linking), with the only links being between the D3 and NS5 branes. S-duality is used to interchange the D5 and NS5 branes. Adjacent pairs of D5 and NS5 branes are then moved through each other, with D3 branes being destroyed, until the D5 branes are one again disconnected from the D3 branes. In this example, the resulting quiver matches the initial quiver, and is said to be *self-mirror*.

Figure 6.12 displays those quivers that yield the nilpotent orbits for A_1 to A_3 on their Higgs branches along with the $3d$ mirror duals that produce the

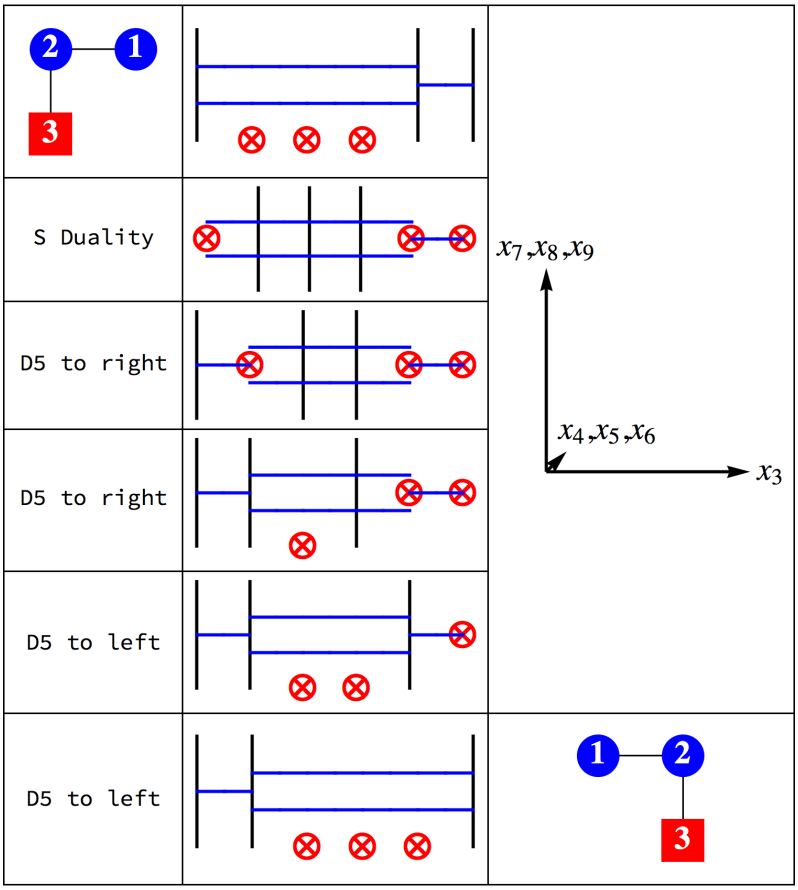

Figure 6.11.: Mirror Dual A Series Quiver from Brane Transformations. NS5 branes are denoted by vertical lines, D3 branes by horizontal lines and D5 branes by $\otimes$. S-duality interchanges NS5 and D5 branes. When a D5 brane is moved to the right (left) through an NS5 brane, its net D3 linking from the right (left) is reduced by one. Unlinked D5 branes are moved to the bottom of the diagrams. The final quiver matches the initial quiver under reflection in the x_3 direction

same moduli spaces on on their Coulomb branches. The analysis generalises to higher ranks.

Group	Nilpotent Orbit	Dimension	Higgs Branch Quiver	Coulomb Branch Quiver
A_1	(2)	2		
A_2	(2,1)	4		
A_2	(3)	6		
A_3	$(2,1^2)$	6	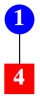	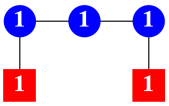
A_3	(2^2)	8	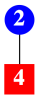	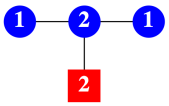
A_3	(3,1)	10	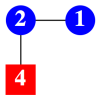	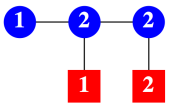
A_3	(4)	12	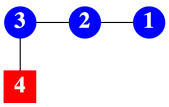	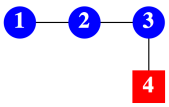

Figure 6.12.: Mirror Dual A Series Quivers for Nilpotent Orbits. Round (blue) nodes denote unitary gauge nodes of the indicated rank. Square (red) nodes denote numbers of flavour nodes.

The quivers of the A series maximal nilpotent orbits are all self-mirror and their Coulomb branches correspond to $T(SU(N))$ quiver theories, discussed in Chapter 8.

6.4.2. BCD Series

As shown in sections 6.2 and 6.3, quivers exist whose Coulomb branches yield the moduli spaces of minimal and near to minimal nilpotent orbits of BCD groups. Also brane configurations for Higgs branch constructions of

BCD nilpotent orbits are known. For example, it was shown in [22], how instantons of BCD groups can be constructed, using orientifold planes, from D2 branes against a background of D6 branes.[3]

However, finding Coulomb branch counterparts of Higgs branch quivers for general BCD nilpotent orbits via $3d$ mirror symmetry remains problematic for a number of reasons. Firstly, the proposals for mirror symmetric duals of BCD Higgs branch quivers via brane manipulations involving $O3$ orientifold planes [75, 21, 31] lead to Coulomb branch quivers with non-unitary gauge nodes that are not equal in number to the simple roots of the BCD group, and which cannot, therefore, be calculated using the unitary monopole formula. Secondly, while versions of the monopole formula for non-unitary gauge nodes have been proposed [55], these have not been successful at generating moduli spaces with refined Hilbert series that match those of the purported mirrors. Indeed, one method currently used for working with the maximal nilpotent orbits ($T(G)$ theories) of BCD series [55, 31], is simply to bypass the problem, by conjecturing the equivalence of the Coulomb branches of the unknown quivers to BCD modified Hall Littlewood polynomials.

6.5. Quivers from Characteristics

As a final method of finding quivers for the Coulomb branch constructions of nilpotent orbits, a remarkable match can be observed between the structures of near to minimal Coulomb branch quivers, and their respective Characteristics and weight maps (in Appendix B). Specifically, the flavour and gauge nodes of the Coulomb branch quivers in Figures 6.8 to 6.10, and also several of the quivers in 6.12, when ordered as vectors N_f and N_g, as per section 6.1.1, match their Characteristics and weight maps. This match only appears for nilpotent orbits whose complex dimensions are exactly twice the sum of their weight map labels. (This is because the unitary monopole formula always leads to a Coulomb branch moduli space whose complex dimension is twice that of the sum of the ranks of the gauge nodes.)

The observed match extends to the RSIMS and near to minimal nilpotent orbits of Exceptional Groups and this invites the conjecture that, for any Classical or Exceptional group G:

[3]The orientifold planes are required to reproduce the root systems of the Lie algebras.

> "If a nilpotent orbit of G has a complex dimension equal to twice the sum of the Dynkin labels in its weight map, then application of the unitary monopole formula to a quiver defined by the Dynkin diagram of G, with gauge nodes defined by the weight map and flavour nodes defined by the Characteristic (root map), yields a Coulomb branch construction for the moduli space of the nilpotent orbit".

Empirically, whenever a Characteristic $[q]$ obeys this rule, the Characteristic height $[\theta]$ (as defined in section 4.2.3) of the highest root equals 2, so θ is contained in the nilpotent element X. As observed in [76], $[\theta] \equiv \sum_{i=1}^{r} a_i q_i$, where the a_i are taken as the Coxeter labels of G.

All the nilpotent orbits covered by this Characteristic rule have character HWGs of a *freely generated* type. In the case of nilpotent orbits higher up a Hasse diagram, some generators have Characteristic height greater than 2, so the moduli spaces can be complicated by relations between generators, with the result that the HWGs are usually not freely generated.

Figure 6.9 includes the quivers whose Coulomb branches yield the 12 and 18 dimensional nilpotent orbits of C_3 and C_4, which have been found by this rule. Figure 6.13 shows the quivers for nilpotent orbits of Exceptional groups that follow from this rule; these include the orbits that can be found from affine Dynkin diagrams. Evaluation of the Hilbert series of these Coulomb branch constructions gives results that are consistent with the NOL formula calculations carried out in the next Chapter.

Group	Characteristic	Dimension	Quiver
G_2	[1,0]	6	
F_4	[1,0,0,0]	16	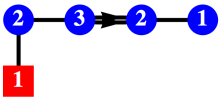
	[0,0,0,1]	22	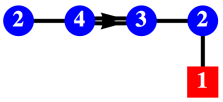
E_6	[0,0,0,0,0,1]	22	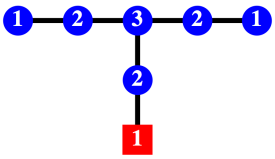
	[1,0,0,0,1,0]	32	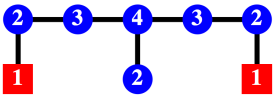
E_7	[1,0,0,0,0,0,0]	34	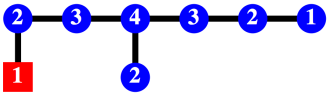
	[0,0,0,0,1,0,0]	52	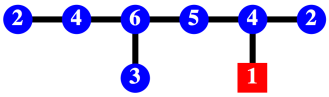
	[0,0,0,0,0,2,0]	54	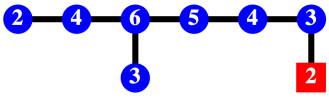
E_8	[0,0,0,0,0,0,1,0]	58	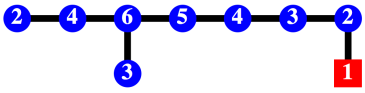
	[1,0,0,0,0,0,0,0]	92	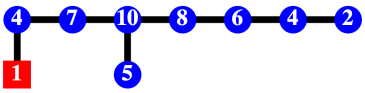

Figure 6.13.: Quivers from Characteristics of Exceptional Groups. Round (blue) nodes denote unitary gauge nodes of the indicated rank. Square (red) nodes denote numbers of flavour nodes. The Characteristics coincide with the numbers of flavour nodes attached to each gauge node. The dimension of a Coulomb branch nilpotent orbit construction equals twice the sums of the ranks of its gauge nodes.

7. Localisation Constructions of Nilpotent Orbits

7.1. Nilpotent Orbit Localisation formula

This study continues by presenting a generating function for the normalisation of a nilpotent orbit, which can in principle be restricted to yield the nilpotent orbit itself. This is referred to as the *Nilpotent Orbit Localisation* ("NOL") formula in this study and is given in 7.5. It is defined by the fixed points under the Weyl group, of plethystic functions, which are parameterised by subsets of roots and background charges, over the root space of G.

By way of motivation, a more general localisation formula, which is an extension of (4.23) in [31], and from which many relevant generating functions emerge as special instances, is given by:

$$g^{G}_{HS}\left(x,t,[n]\right) \equiv \sum_{w\in W_{G/H}} w\cdot\left(x^{[n]}\prod_{\alpha\in\tilde{\Phi}^{+}_{G/H}\subseteq\Phi^{+}_{G/H}}\frac{1}{1-z^{\alpha}t}\prod_{\beta\in\Phi^{+}_{G/H}}\frac{1}{1-z^{-\beta}}\right). \tag{7.1}$$

As usual, x represents the weight space fugacities and $z=x^{A}$ represents the root space fugacities of some Lie group G, with Dynkin labels $[n]$ and positive root space Φ^{+}_{G}. The group H, with positive root space Φ^{+}_{H}, is a semi-simple regular subgroup of G, such that the quotient G/H contains the positive roots $\Phi^{+}_{G/H}{=}\Phi^{+}_{G}\ominus\Phi^{+}_{H}$, and $\tilde{\Phi}^{+}_{G/H}$ is some subset of $\Phi^{+}_{G/H}$. The summation is over the action of representative elements w of the cosets $W_{G/H}$ [1], which act as $x\rightarrow w\cdot x$ and $z(x)\rightarrow z(w\cdot x)$. A key requirement of the construction is that the summand should be invariant under W_{H}. Since $\Phi^{+}_{G/H}$ is W_{H} invariant by construction, this requires that $x^{[n]}$ and $\tilde{\Phi}^{+}_{G/H}$

[1] See equation 2.12 for notation surrounding quotient group partition.

should be W_H invariant.

The NOL formula is part of a family of plethystic functions, which includes the Weyl character formula and the modified Hall Littlewood formula, treated in Chapter 2. We can note some special cases of 7.1:

1. $H = \emptyset, t = 0$ recovers the Weyl formula 2.3 for the character of the irrep with Dynkin label $[n]$:

$$\chi^G_{[n]}(x) = \sum_{w \in W_G} w \cdot \left(x^{[n]} \prod_{\beta \in \Phi^+_G} \frac{1}{1 - z^{-\beta}} \right). \tag{7.2}$$

2. $H = \emptyset, \tilde{\Phi}^+_{G/H} = \Phi^+_G$ recovers the formula 2.18 for the modified Hall Littlewood of G with Dynkin label $[n]$:

$$mHL^G_{[n]}(x,t) = \sum_{w \in W_G} w \cdot \left(x^{[n]} \prod_{\beta \in \Phi^+_G} \frac{1}{(1 - z^{\beta} t)(1 - z^{-\beta})} \right). \tag{7.3}$$

3. $H = G_0, [n] = [0], \tilde{\Phi}^+_{G/H} = \{\theta\}$, where G_0 is the stability group of the (highest weight Dynkin labels of the) highest root θ, recovers a character generating function for a RSIMS, specialised from 2.12:[2]

$$g^G_{RSIMS}(x,t) = \sum_{w \in W_{G/G_0}} w \cdot \left(\frac{1}{1 - z^{\theta} t} \prod_{\beta \in \Phi^+_{G/G_0}} \frac{1}{1 - z^{-\beta}} \right). \tag{7.4}$$

It is a key finding of this study that, with appropriate choice of parameters, the localisation formula 7.1 can be adapted to yield the normalisation of a nilpotent orbit. Considerations motivated by the above special cases, along with explicit checking versus Higgs/Coulomb branch calculations, identify a *Nilpotent Orbit Localisation* formula that appears common to all *normal* nilpotent orbits.

[2]The G_0 stability group of θ is implemented in an equivalent manner in [18, 17], where the RSIMS generating function is implemented as a sum over long roots.

NOL formula

Notably, the parameters of the NOL formula can be fixed directly from the Characteristic of a nilpotent orbit root via a simple algorithm. The basic NOL formula follows from 7.1, by setting $[n]$ to $[0]$, which selects the singlet from the more general family of moduli spaces that can be associated to a given nilpotent orbit, and by precise choices of H and $\tilde{\Phi}$:

$$g_{NOL}^{G[\rho]}(x,t) \equiv \sum_{w \in W_{G/G_0}} w \cdot \left(\prod_{\alpha \in \tilde{\Phi}^+_{G/G_0}} \frac{1}{1-z^{\alpha}t} \prod_{\beta \in \Phi^+_{G/G_0}} \frac{1}{1-z^{-\beta}} \right), \tag{7.5}$$

where $\tilde{\Phi}^+_{G/G_0} \equiv \Phi^+_{G/G_0} \ominus \Phi_G^{[1]}$, as elaborated below. In principle, the nilpotent orbit, denoted $g_{NO}^{G[\rho]}$, can be found by *restricting* $g_{NOL}^{G[\rho]}$ to the nilpotent cone $\mathcal{N}$ [3]:

$$g_{NO}^{G[\rho]}(x,t) = g_{NOL}^{G[\rho]}(x,t)\Big|_{\mathcal{N}}. \tag{7.6}$$

The $SU(2)$ homomorphism ρ, introduced in section 4.1, induces a grading of the root system of G. Adapting notation introduced in [54], define the following subsets of roots:

$$\Phi_G^{[k]} \equiv \left\{ \alpha \in \Phi_G^+ : \text{Characteristic height } [\alpha] = k \right\}. \tag{7.7}$$

Then:

$$\Phi_G^+ = \bigcup_{k \geq 0} \Phi_G^{[k]}; \quad \Phi^+_{G/G_0} = \bigcup_{k \geq 1} \Phi_G^{[k]}; \quad \tilde{\Phi}^+_{G/G_0} = \bigcup_{k \geq 2} \Phi_G^{[k]}. \tag{7.8}$$

Each $SU(2)$ homomorphism selects a subset $\tilde{\Phi}^+_{G/G_0}$ of positive roots for symmetrisation with t within the NOL formula. This subset invariably includes the highest root, plus some system of positive roots connected to the highest root in the Hasse diagram.

The Weyl denominator identity, $\sum_{w \in W_{G_0}} \prod_{\beta \in \Phi^+_{G_0}} \frac{1}{1-z^{-\beta}} = 1$, which follows

[3] For Classical groups, this restriction is achievable with the Higgs branch formula; for Exceptional groups, its analytical implementation can be a non-trivial exercise, as will be discussed.

from 7.2, permits rearrangement of 7.5 into the equivalent form:

$$g^{G[\rho]}_{NOL}(x,t) = \sum_{w\in W_G} w\cdot\left(\prod_{\alpha\in\tilde{\Phi}^+_{G/G_0}}\frac{1}{1-z^{\alpha}t}\prod_{\beta\in\Phi^+_G}\frac{1}{1-z^{-\beta}}\right). \tag{7.9}$$

For computational purposes 7.5 is often simpler, involving smaller denominator terms and fewer Weyl group reflections.[4]

We can easily check that the NOL formula matches known results for canonical types of nilpotent orbit. In particular, choosing a Characteristic of $[22\ldots2]$ entails that both $\Phi^{[0]}_G$ and $\Phi^{[1]}_G$ are empty and so 7.5 reduces to 7.3, corresponding to $mHL^G_{[0]}$, the maximal nilpotent orbit of G. Also, it is straightforward to check that the Characteristic of a minimal nilpotent orbit leads to $\Phi^{[2]}_G$ containing just the highest root, so that $\tilde{\Phi}^+_{G/G_0} = \{\theta\}$ and 7.9 reduces to 7.4.

NOL formula: Even and Richardson Orbits

In the case of an even orbit, whose Characteristic contains only the labels 0 and 2, $\Phi^{[1]}_G = \emptyset$ and the NOL formula simplifies:

$$g^{G[\rho]}_{NOL(even)}(x,t) = \sum_{w\in W_{G/G_0}} w\cdot\left(\prod_{\alpha\in\Phi^+_{G/G_0}}\frac{1}{(1-z^{\alpha}t)(1-z^{-\alpha})}\right). \tag{7.10}$$

All Richardson nilpotent orbits can also be treated within this category. If the Richardson orbit is even, its $H \equiv G_0$ subgroup follows directly from the zeros of the Characteristic of G. If the Richardson orbit is not even, one or more H subgroup embeddings still exist, even if these cannot be read directly from the Characteristic.

NOL formula: Induced Orbits

A different and important rearrangement can be made to the NOL formula to induce a given nilpotent orbit (or its normalisation) from the nilpotent

[4] As discussed earlier, the quotient group construction in 7.5 requires that $\Phi^{[1]}_G$ be invariant under W_{G_0}. This appears to be the case for all Characteristics derived from $SU(2)$ homomorphisms of G. When calculating using the NOL formula, it is a straightforward matter to check this invariance on a case by case basis. If such invariance did not apply, 7.9 would remain valid.

orbit of a subgroup, whenever its Characteristic contains at least one 2. Essentially, we define a $G/H/G_0$ quotient group structure, by taking H as the semi-simple subgroup defined by the Dynkin diagram of G that remains after any nodes corresponding to 2 in the Characteristic have been eliminated. As a result, the Characteristic for the nilpotent orbit in H contains only 0 and 1.

Starting from 7.5, we set $G/G_0 \rightarrow G/H \otimes H/G_0$, such that $\Phi_G^{[1]}$ falls within Φ_H. We obtain:

$$\begin{aligned} g_{NOL}^{G[\rho]}(x,t) &= \sum_{w \in W_{G/G_0}} w \cdot \left(\prod_{\alpha \in \tilde{\Phi}^+_{G/G_0}} \frac{1}{1-z^{\alpha}t} \prod_{\beta \in \Phi^+_{G/G_0}} \frac{1}{1-z^{-\beta}} \right) \\ &= \sum_{w \in W_{G/H}} w \cdot \left(g_{NOL}^{H[\rho]}(x,t) \prod_{\alpha \in \Phi^+_{G/H}} \frac{1}{(1-z^{\alpha}t)(1-z^{-\alpha})} \right) \end{aligned} \tag{7.11}$$

where

$$g_{NOL}^{H[\rho]}(x,t) = \sum_{W_{H/G_0}} w \cdot \left(\prod_{\gamma \in \tilde{\Phi}^+_{H/G_0}} \frac{1}{1-z^{\gamma}t} \prod_{\delta \in \Phi^+_{H/G_0}} \frac{1}{1-z^{-\delta}} \right). \tag{7.12}$$

Since 7.12 takes the same form as 7.5, the nilpotent orbit (or its normalisation) $g_{NOL}^{G[\rho]}$ is shown to be induced from the nilpotent orbit $g_{NOL}^{H[\rho]}$. One feature of the induction method 7.11 is that it opens the door to hybrid constructions in which an Exceptional orbit can be induced from a Classical orbit that has been calculated using the Higgs branch formula. For example, $g_{Induced}^{F_4[1012]}$ can be induced in this manner from $g_{Higgs}^{B_3[101]}$, which we write as:

$$g_{Induced}^{F_4[1012]}(x,t) = g_{NOL}^{F_4[0002]}(x,t) \left[g_{Higgs}^{B_3[101]}(x,t) \right]. \tag{7.13}$$

The fugacity maps between the weight space x coordinates of G and H follow from equating the respective simple root fugacities z that are involved in the branchings, as discussed in section 2.6.[5]

[5]When carrying out induction calculations it is important to match root space (not weight space) fugacities of G and H.

Charged NOL formula

Finally, it is helpful to generalise version 7.9 of the NOL formula to deal with root systems that are modulated by background charges, as in 7.1. Define the *charged* NOL formula:

$$g^{G[\rho]}_{NOL}\left(x,t\right)\left[x^{[n]}\right] \equiv \sum_{w\in W_G} w\cdot\left(x^{[n]}\prod_{\alpha\in\tilde{\Phi}^+_{G/G_0}}\frac{1}{1-z^{\alpha}t}\prod_{\beta\in\Phi^+_G}\frac{1}{1-z^{-\beta}}\right), \tag{7.14}$$

where $x^{[n]}$ is a weight given by the CSA coordinates x and Dynkin labels $[n]$. Note that the quotient group W_{G/G_0} structure is not used in order to permit general Dynkin labels.[6]

The charged functions 7.14 constitute an orthogonal basis (under an appropriate measure) only in special cases. Specifically, $t\to 0$ yields the Weyl Character formula and $\Phi^{[0]}_G = \emptyset = \Phi^{[1]}_G$ yields charged functions of the maximal nilpotent orbit, which equal the modified Hall Littlewood functions. Unfortunately, the charged functions defined by a nilpotent orbit do not generally constitute an orthogonal basis. This limits their general utility, although they can be used to provide a description of relations between nilpotent orbits.

HWGs from NOL formula

The refined Hilbert series from the NOL formula can be converted either to character HWGs or to orthogonal mHL HWGs by applying A.29:

$$\begin{aligned} g^{G[\rho]}_{NOL}\left(m,t\right) &= \oint_G d\mu^{G-}\ \prod_{i=1}^{r}\frac{1}{1-m_i/x_i}\ g^{G[\rho]}_{NOL}\left(x,t\right)\\ \tilde{g}^{G[\rho]}_{NOL}\left(h,t\right) &= \oint_G d\mu^{G-}\ \prod_{\alpha\in\Phi^+}(1-z^{\alpha}t)\ \prod_{i=1}^{r}\frac{1}{1-h_i/x_i}\ g^{G[\rho]}_{NOL}\left(x,t\right) \end{aligned} \tag{7.15}$$

Note that the $\tilde{g}^{G[\rho]}_{NOL}\left(h,t\right)$ need to be glued to $1/v^G_{[n]}(t)$ normalisation factors via a further transformation, as discussed in 2.4, to obtain $g^{G[\rho]}_{NOL}\left(h,t\right)$.

[6] A quotient group structure can be introduced if the Weyl group symmetries of $[n]$ permit.

Relationship of NOL formula to $T^*(G/H)$ theory

It is instructive to relate the NOL formula to the result that appears in [77] for the Highest Weight Generating function of the representation content of a $T^*(G/H)$ theory. This moduli space selects a subset of the representations of G from within the HWG for the characters of G, by gauging a reductive subgroup H:

$$g^{T^*(G/H)}(m) \equiv \oint_H d\mu^H(y)\; g^G_\chi(y,m), \tag{7.16}$$

where $g^G_\chi(y,m)$ is the HWG and $d\mu^H(y)$ is the Haar measure for H. It can be shown that $g^{T^*(G/H)}(m)$ emerges as a special case from the HWG $g^{G[even]}_{NOL}(m,t)$, as follows.

First, we define a Levi subgroup of G, $H \equiv G_0 \otimes U(1)^{\text{rank}[G]-\text{rank}[G_0]}$, such that H and G have the same rank. This allows us to establish a diffeomorphism between the weight space coordinates x of G and y of H. We then transform the refined Hilbert series $g^{G[even]}_{NOL}(x,t)$, calculated from 7.10, to an HWG by projection onto a character generating function for G:

$$g^{G[even]}_{NOL}(m,t) = \oint_G d\mu^G(x)\; g^G_\chi(x^*,m)\, g^{G[even]}_{NOL}(x,t) \tag{7.17}$$

The Haar measure $d\mu^G(x)$ for G can be decoupled to separate off the Haar measure $d\mu^H(x)$ of the H subgroup:

$$\begin{aligned} d\mu^G(x) &= \frac{1}{|W_G|}\left(\prod_{i=1}^{\text{rank}[G]}\frac{dx_i}{x_i}\right)\left(\prod_{\alpha\in\Phi_G}(1-z^\alpha)\right) \\ &= \frac{1}{|W_{G_0}|}\left(\prod_{i=1}^{\text{rank}[G]}\frac{dx_i}{x_i}\right)\left(\prod_{\beta\in\Phi_{G_0}}\left(1-z^\beta\right)\right)\frac{|W_{G_0}|}{|W_G|}\left(\prod_{\alpha\in\Phi_{G/G_0}}(1-z^\alpha)\right) \\ &= d\mu^H(x)\,\frac{|W_{G_0}|}{|W_G|}\left(\prod_{\alpha\in\Phi_{G/G_0}}(1-z^\alpha)\right). \end{aligned} \tag{7.18}$$

Under the fugacity simplification $t \to 1$, 7.10 reduces to:

$$\begin{aligned} g_{NOL}^{G[even]}(x,1) &= \sum_{w \in W_{G/G_0}} w \cdot \left(\prod_{\alpha \in \Phi^+_{G/G_0}} \frac{1}{(1-z^{\alpha})(1-z^{-\alpha})} \right) \\ &= \sum_{w \in W_{G/G_0}} w \cdot \left(\prod_{\alpha \in \Phi_{G/G_0}} \frac{1}{(1-z^{\alpha})} \right) \end{aligned} \tag{7.19}$$

Inserting 7.18 and 7.19 into 7.17, we obtain:

$$\begin{aligned} g_{NOL}^{G[even]}(m,1) &= \oint d\mu^H(x)\; g_{\chi}^{G}(x^*,m) \frac{|W_{G_0}|}{|W_G|} \prod_{\alpha \in \Phi_{G/G_0}} (1-z^{\alpha}) \\ &\qquad \times \sum_{w \in W_{G/G_0}} w \cdot \left(\prod_{\alpha \in \Phi_{G/G_0}} \frac{1}{(1-z^{\alpha})} \right) \\ &= \oint d\mu^H(x)\; g_{\chi}^{G}(x^*,m) \frac{|W_{G_0}|}{|W_G|} \frac{|W_G|}{|W_{G_0}|} \\ &= \oint_H d\mu^H(y)\; g_{\chi}^{G}(y,m) \\ &= g^{T^*(G/H)}(m), \end{aligned} \tag{7.20}$$

where we have replaced one Weyl group summation $\sum_{w \in W_{G/G_0}}$ by $\frac{|W_G|}{|W_{G_0}|}$, as discussed in Appendix A.2 (equation A.28), and transformed the conjugate x^* coordinates of G to the y coordinates of H. Thus, $g^{T^*(G/H)}(m)$ is a specialisation to $t=1$ of $g_{NOL}^{G[even]}(m,t)$.

7.2. Classical Group Orbits from the NOL formula

The Classical group moduli spaces obtained from the NOL formula 7.5 all have palindromic Hilbert series and are similar in this regard to the Coulomb branch constructions with the unitary monopole formula. For normal nilpotent orbits, as defined in section 4.4.7, the NOL formula yields the same moduli spaces as the Higgs branch constructions tabulated in Chapter 5. For non-normal orbits, the NOL formula yields a moduli space that is either (i) a normal component, or (ii) a normalisation.

The cases that require discussion are the *non-normal* nilpotent orbits. The number of these increases with rank; their Characteristics are listed in section 4.4.7, up to rank 5, and the moduli spaces obtained from the NOL formula are summarised in Table 7.1, up to rank 4.

In the case of the D_{2r} spinor pairs of nilpotent orbits, discussed in section 5.4.5, the NOL formula gives the individual palindromic spinor moduli spaces, according to the Characteristic chosen. Examples in Table 7.1 include $D_2[20]$, $D_4[0020]$ and $D_4[0220]$. The moduli spaces of the conjugate spinors have identical unrefined Hilbert series and their HWGs are related by the exchange of spinor fugacities. These spinor moduli spaces are the normal components of the non-normal nilpotent orbits, constructed on the Higgs branch, which are their unions:

$$g_{Higgs}^{D_{2r}[...20]I/II} = g_{Higgs}^{D_{2r}[...02]I/II} = g_{NOL}^{D_{2r}[...20]} + g_{NOL}^{D_{2r}[...02]} - g_{NOL}^{D_{2r}[...20]\cap D_{2r}[...02]\}}. \tag{7.21}$$

For all the other non-normal nilpotent orbits, the NOL formula yields a normalisation. Examples in Table 7.1 include $B_3[101]$, $B_4[2101]$ and $C_4[0200]$. Classical non-normal nilpotent orbits are related to their normalisations by some Z_2 quotient [6]. In each case the (non-normal) Higgs branch construction can be recovered from the normalisation by excluding those elements that fall outside the nilpotent cone $\mathcal{N}$. Thus:

$$\begin{aligned} g_{Higgs}^{B_3[101]} &= g_{NOL}^{B_3[101]} - g_{NOL}^{B_3[200]}\left[x_1 t\right], \\ g_{Higgs}^{B_4[2101]} &= g_{NOL}^{B_4[2101]} - g_{NOL}^{B_4[2200]}\left[x_1 t^2\right], \\ g_{Higgs}^{C_4[0200]} &= g_{NOL}^{C_4[0200]} - g_{NOL}^{C_4[0002]}\left[x_4 t^2\right]. \end{aligned} \tag{7.22}$$

The moduli spaces outside the nilpotent cone can be described by the charged NOL formula 7.14. The nilpotent orbit upon which each of these charged moduli spaces is built is related to its parent orbit by the $A_{2r-1} \cup A_{2r-1}$ Kraft-Procesi degeneration, discussed in section 4.4.7, and lies beneath the parent orbit in the Hasse diagram.

It can be seen from Table 7.1, that $g_{\mathrm{NOL}}^{D_4[0020]}$ and $g_{Higgs}^{B_3[101]}$ have the same unrefined Hilbert series. This is an example of a branching relationship between two nilpotent orbits; these are discussed further in Chapter 8.

Orbit	Dim.	Unrefined HS	Character HWG	mHL HWG
$g_{\mathrm{NOL}}^{D_2[20]}$	2	$\frac{1+t}{(1-t)^2}$	$\frac{1}{(1-m_1{}^2t)}$	$1-h_2{}^2t$
$g_{\mathrm{NOL}}^{D_4[0020]}$	12	$\frac{(1+14t+36t^2+14t^3+t^4)}{(1-t)^{12}(1+t)^{-2}}$	$\frac{1}{(1-m_2t)(1-m_3{}^2t)}$	$1-h_1{}^2t^2-h_4{}^2t^2-2h_2t^3$ $+h_1h_3h_4t^3+h_1{}^2t^4+h_3{}^2t^4$ $+h_4{}^2t^4+2h_1h_3h_4t^4-h_2h_3{}^2t^4$ $-h_2t^5-2h_2{}^2t^5-h_2h_3{}^2t^5$ $+2h_1h_3h_4t^5+h_3{}^4t^5-h_1{}^2h_4{}^2t^5$ $-h_1{}^2h_4{}^2t^6+h_1h_2h_3h_4t^6$ $-h_2{}^3t^7-h_1h_3h_4t^7+2h_1h_2h_3h_4t^7$ $-h_1h_3{}^3h_4t^7+h_1h_2h_3h_4t^8$ $+h_2{}^2h_3{}^2t^8-h_1h_3{}^3h_4t^8$
$g_{\mathrm{NOL}}^{D_4[0220]}$	20	$\frac{(1+6t+21t^2+28t^3+21t^4+6t^5+t^6)}{(1-t)^{20}(1+t)^{-2}(1+t^2)^{-1}}$	$\frac{\left(\begin{array}{c}1+m_1m_3m_4t^4\\ +m_1m_3m_4t^5+m_1m_2m_3m_4t^5\\ +m_2m_3{}^2t^6+m_1m_2m_3m_4t^7\\ +m_1{}^2m_2m_4{}^2t^8-m_1m_2{}^2m_3m_4t^8\\ +m_1{}^2m_3{}^2m_4{}^2t^9-m_1m_2m_3{}^3m_4t^9\\ -m_1{}^2m_2m_3{}^2m_4{}^2t^{10}-m_1{}^3m_2m_3m_4{}^3t^{11}\\ -m_1{}^2m_2m_3{}^2m_4{}^2t^{12}-m_1{}^2m_2{}^2m_3{}^2m_4{}^2t^{12}\\ -m_1{}^2m_2{}^2m_3{}^2m_4{}^2t^{13}-m_1{}^3m_2{}^2m_3{}^3m_4{}^3t^{17}\end{array}\right)}{\left(\begin{array}{c}(1-m_2t)(1-m_1{}^2t^2)(1-m_3{}^2t^2)\\ \times(1-m_4{}^2t^2)(1-m_2t^3)(1-m_1m_3m_4t^3)\\ \times(1-m_2{}^2t^4)(1-m_3{}^2t^4)(1-m_1{}^2m_4{}^2t^6)\end{array}\right)}$	$1-h_2t^3+h_3{}^2t^4-h_2t^5$
$g_{\mathrm{NOL}}^{B_3[101]}$	12	$\frac{(1+14t+36t^2+14t^3+t^4)}{(1-t)^{12}(1+t)^{-2}}$	$\frac{1}{(1-m_1t)(1-m_2t)(1-m_3{}^2t^2)}$	$1+h_1t-h_3{}^2t^2-h_1t^3$ $-2h_2t^3+h_3{}^2t^4+h_1h_3{}^2t^4$ $-h_2{}^2t^5+h_1h_3{}^2t^5$
$g_{\mathrm{NOL}}^{C_4[0200]}$	22	$\frac{\left(\begin{array}{c}1+13t+133t^2+608t^3+1478t^4+2002t^5\\ +1478t^6+608t^7+133t^8+13t^9+t^{10}\end{array}\right)}{(1-t)^{22}(1+t)^{-1}}$	$\frac{1+m_1m_2m_3t^4}{\left(\begin{array}{c}(1-m_1{}^2t)(1-m_2{}^2t)(1-m_2t^2)\\ \times(1-m_3{}^2t^3)(1-m_4t^2)(1-m_1m_3t^3)\end{array}\right)}$	$1+h_4t^2-h_1{}^2t^3-h_1h_3t^3-h_2t^4$ $+h_1{}^2h_2t^4-h_1h_3t^4-h_4t^4$ $-h_1{}^4t^5+h_1{}^2h_2t^5+h_2{}^2t^5+h_2h_4t^5$ $-h_2t^6+h_1h_3t^6-h_3{}^2t^6+h_4t^6$ $-h_1{}^2h_4t^6+h_2h_4t^6-h_2{}^2t^7-h_2{}^3t^7$ $+2h_1h_3t^7-h_1{}^2h_4t^7-h_2h_4t^7$ $+h_1{}^2h_2{}^2t^8+h_3{}^2t^8-h_2h_4t^8$ $+h_1{}^3h_3t^9+h_2{}^2h_4t^9-h_1{}^2h_2h_4t^{10}$
$g_{\mathrm{NOL}}^{B_4[2101]}$	26	$\frac{\left(\begin{array}{c}1+7t+39t^2+152t^3+340t^4+410t^5\\ +340t^6+152t^7+39t^8+7t^9+t^{10}\end{array}\right)}{(1-t)^{26}(1+t)^{-3}}$	...	$1+h_1t-h_3{}^2t^2-h_1t^3-2h_2t^3$ $+h_3{}^2t^4+h_1h_3{}^2t^4$ $-h_2{}^2t^5+h_1h_3{}^2t^5$

D series moduli spaces are normal components of spinor pair nilpotent orbits; B/C moduli spaces are normalisations. NOL/Coulomb branch HS counted by t correspond to Higgs branch HS counted by t^2.

Table 7.1.: Non-Normal Classical Orbit Components and Normalisations

7.3. Exceptional Group Orbits

The construction of Exceptional group nilpotent orbits poses a number of challenges. Firstly, Exceptional groups do not act in a similar manner to $SL(n, \mathbb{R}/\mathbb{C})$ rotation matrices on their fundamental vector spaces, so the Higgs branch method is not available [6]. This limits the construction methods to those based on the Coulomb branch or NOL formulae. These in turn have their own limitations; the unitary monopole formula only works for minimal and near minimal orbits; and the NOL formula yields the normalisation of a nilpotent orbit, which only equals the orbit if it is normal. Finally, the high dimensions of the Weyl groups of the E series entail that explicit calculations, using the methods developed during this study, are not always feasible in terms of computing memory and/or time.

In principle, however, those Exceptional group Characteristics for which the NOL formula does yield nilpotent orbits can be identified by verifying that the moduli spaces are entirely contained within the nilpotent cone $\mathcal{N}$, which is known for every group. Such results can be cross-checked for completeness by comparison with the known non-normal orbits listed in section 4.4.7. Moreover, even without a systematic formula for calculating the non-normal Exceptional group orbits, it is often possible to find candidates on a case by case basis, by restricting their normalisations to exclude charged nilpotent orbits of lower dimension, as will be shown. The findings presented below are derived from a combination of established results, full HS and HWG calculations, and inferences based on unrefined HS expansions, checked to the highest order practicable.

In this study, Exceptional group nilpotent orbits are labelled by their Characteristics for various reasons. Firstly, a Characteristic provides the structure and parameters of the Coulomb branch and NOL formulae. Secondly, while a Characteristic provides a clear and unambiguous specification of a nilpotent element X, the same is not true of the various alternative labelling methods based on sub-groups, developed, inter alia, by Dynkin [54], Bala-Carter [78, 79], Hesselink [69]. Amongst these, the method that is closest to the use of Characteristics is given by Hesselink, who identifies the semi-simple subgroup G_0 under which a nilpotent element X is invariant; this labelling method works for most Richardson orbits, but not for other types. The Bala-Carter labelling method, which does not play a role in the

NOL formula, is summarised and discussed in Appendix A.5.

As is clear from the discussion on the variants of the NOL formula in section 7.1, there is often a choice to be made as to whether an orbit is calculated directly from the roots of G, or induced from an orbit of a subgroup H, using 7.11. Either choice leads to the same refined HS under the NOL formula, but the induction method permits the incorporation, for example, of a non-normal nilpotent orbit of H calculated on the Higgs branch.

The following sub-sections analyse the nilpotent orbits of Exceptional groups, starting from the Characteristics of $SU(2)$ homomorphisms, classifying the type of each orbit, giving its constructions, calculating, where practicable, unrefined HS, character HWGs and mHL HWGs, and identifying whether the moduli spaces are nilpotent orbits or normalisations of non-normal orbits. For G_2, F_4 and E_6, nilpotent orbit Hasse diagrams are drawn, based on moduli space inclusion relations.

7.3.1. Orbits of G_2

Table 7.2 classifies the 5 nilpotent orbits of G_2 and gives their unrefined HS. Table 7.3 gives the character and mHL HWGs, calculated from the refined HS. To comment on the various orbits:

[10]: 6 dimensional nilpotent orbit. This is the minimal nilpotent orbit and is both rigid and normal. It can be calculated either from a Coulomb branch quiver theory built on the affine Dynkin diagram, as discussed in section 6.2.2, or from the NOL formula. Both its HS and character HWG are palindromic.

[01]: 8 dimensional nilpotent orbit. This next to minimal orbit is rigid, but not normal, and does not have a Coulomb branch construction.[7] The NOL formula yields a normalisation. The non-normal orbit is found by excluding from this normalisation a subspace expressed in terms of the charged NOL formula for the minimal nilpotent orbit:

$$g_{NO}^{G_2[01]}(x,t) = g_{NOL}^{G_2[01]}(x,t) - g_{NOL}^{G_2[10]}(x,t)\,[x_2 t]\,. \tag{7.23}$$

[7] If the G_2 twisted affine Dynkin diagram is used as a Coulomb branch quiver, it leads to a moduli space that is not a nilpotent orbit, since the Characteristic does not have the correct sum of gauge node ranks to yield an 8 dimensional HS.

[20]: 10 dimensional nilpotent orbit. The sub-regular nilpotent orbit is distinguished and has an invariant subgroup $G_0 = A_1$. It can be calculated from the NOL formula 7.10. Both its HS and character HWG are palindromic.

[22]: 12 dimensional nilpotent orbit. The maximal nilpotent orbit is distinguished. It can be calculated from the NOL formula. Both its HS and character HWG are palindromic, in the latter case with degree $m_1{}^3 m_2{}^5 t^{18}$.

It can easily be checked, both from the unrefined HS and the character HWGs, that these nilpotent orbits satisfy the expected inclusion relations $g_{NO}^{G_2[00]} \subset g_{NO}^{G_2[10]} \subset g_{NO}^{G_2[01]} \subset g_{NO}^{G_2[20]} \subset g_{NO}^{G_2[22]}$, providing that the non-normal 8 dimensional nilpotent orbit is used. These inclusion relations are graphed in the Hasse diagram in Figure 7.1.

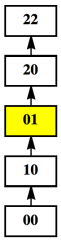

Figure 7.1.: Hasse Diagram of G_2 Nilpotent Orbits. The diagram is derived from Hilbert series inclusion relations, with the yellow node indicating a non-normal nilpotent orbit.

It is worth commenting that the normalisation $g_{NOL}^{G_2[01]}$ has the same unrefined Hilbert series as $g_{Higgs}^{B_3[010]}$ in Table 5.12 (up to t counting conventions) and can be obtained from this using a character map that folds the B_3 vector and spinor together [80].

Characteristic	Type	Construction	Dim.	Hilbert Series
[00]	Even	Trivial	0	1
[10]	Rigid	$g^{G_2[10]}_{Coulomb}(x,t)$ or $g^{G_2[10]}_{NOL}(x,t)$	6	$\frac{(1+t)\left(1+7t+t^2\right)}{(1-t)^6}$
[01]	Rigid, Non-normal	$g^{G_2[01]}_{NOL}(x,t) - g^{G_2[10]}_{NOL}(x,t)\,[x_2 t]$	8	$\frac{1+6t+20t^2+43t^3-7t^4-7t^5}{(1-t)^8}$
[20]	Distinguished	$g^{G_2[20]}_{NOL}(x,t)$	10	$\frac{(1+t)\left(1+3t+6t^2+3t^3+t^4\right)}{(1-t)^{10}}$
[22]	Distinguished	$g^{G_2[22]}_{NOL}(x,t)$	12	$\frac{\left(1-t^2\right)\left(1-t^6\right)}{(1-t)^{14}}$
[01]	Rigid, Normalisation	$g^{G_2[01]}_{NOL}(x,t)$	8	$\frac{1+13t+28t^2+13t^3+t^4}{(1-t)^8}$

Both the non-normal 8 dimensional nilpotent orbit and its normalisation are shown.

Table 7.2.: G_2 Orbit Constructions and Hilbert Series

Characteristic	Character HWG	mHL HWG
[00]	1	$1 - h_1 t + {h_2}^3 t^2 - {h_1}^2 t^3 - h_2 t^3$ $+ h_1 h_2 t^3 - {h_2}^4 t^3 + h_1 h_2 t^4 - {h_2}^3 t^4$ $+ h_1 {h_2}^3 t^4 - {h_1}^3 t^5 + h_1 {h_2}^3 t^5$ $- {h_2}^5 t^5 + {h_1}^2 {h_2}^2 t^6$
[10]	$\frac{1}{1-m_1 t}$	$1 - {h_2}^2 t^2 - h_2 t^3 + h_1 h_2 t^3$ $+ h_1 h_2 t^4 - {h_2}^3 t^4$
[01]	$\frac{1-{m_2}^6 t^6}{(1-m_1 t)(1-{m_2}^2 t^2)(1-{m_2}^3 t^3)}$	$1 - h_2 t^3 - {h_1}^2 t^4 + h_1 {h_2}^2 t^5$
[20]	$\frac{1+m_1 {m_2}^3 t^5}{(1-m_1 t)(1-{m_2}^2 t^2)(1-{m_2}^3 t^3)(1-{m_1}^2 t^4)}$	$1 - h_2 t^3$
[22]	$\frac{\left(\begin{array}{c} 1 - m_2 t^2 - m_1 t^4 + {m_2}^2 t^4 \\ + m_1 m_2 t^5 + m_1 {m_2}^3 t^5 + m_1 m_2 t^6 + m_1 {m_2}^2 t^6 \\ + m_1 m_2 t^7 - m_1 {m_2}^2 t^7 - m_1 {m_2}^4 t^7 \\ + {m_1}^2 t^8 - m_1 {m_2}^2 t^8 - m_1 {m_2}^3 t^8 - m_1 {m_2}^4 t^8 \\ - m_1 {m_2}^2 t^9 - {m_1}^2 {m_2}^3 t^9 \\ - {m_1}^2 m_2 t^{10} - {m_1}^2 {m_2}^2 t^{10} - {m_1}^2 {m_2}^3 t^{10} + m_1 {m_2}^5 t^{10} \\ - {m_1}^2 m_2 t^{11} - {m_1}^2 {m_2}^3 t^{11} + {m_1}^2 {m_2}^4 t^{11} \\ + {m_1}^2 {m_2}^3 t^{12} + {m_1}^2 {m_2}^4 t^{12} + {m_1}^2 {m_2}^2 t^{13} + {m_1}^2 {m_2}^4 t^{13} \\ + {m_1}^3 {m_2}^3 t^{14} - {m_1}^2 {m_2}^5 t^{14} - {m_1}^3 {m_2}^4 t^{16} + {m_1}^3 {m_2}^5 t^{18} \end{array}\right)}{\left(\begin{array}{c} (1 - m_1 t)\,(1 - m_2 t^2)\,(1 - {m_2}^2 t^2)\,(1 - m_2 t^3) \\ \times (1 - {m_2}^3 t^3)\,(1 - {m_1} t^4)\,(1 - {m_1}^2 t^4)\,(1 - m_1 t^5) \end{array}\right)}$	1
[01] (Normalisation)	$\frac{1}{(1-m_1 t)(1-m_2 t)}$	$1 + h_2 t - {h_2}^2 t^2 - h_1 t^3$ $- h_2 t^3 + h_1 h_2 t^4$

Both the non-normal 8 dimensional nilpotent orbit and its normalisation are shown.

Table 7.3.: G_2 Orbits and HWGs

7.3.2. Orbits of F_4

The 16 nilpotent orbits of F_4 are described in Tables 7.5 to 7.8, which give their classification, constructions, unrefined HS and, where practicable, character HWGs and modified Hall Littlewood HWGs. Tables 7.9 and 7.10 contain similar information for the normalisations of the non-normal orbits. Many of the orbits have distinctive features:

[1000] and [0001]: 16 dimensional minimal and 22 dimensional next to minimal nilpotent orbits. These orbits are rigid and have the invariant subgroups C_3 and B_3, respectively. The Hilbert series can be calculated either (i) from the Coulomb branch of a quiver theory built, respectively, on the affine or twisted affine Dynkin diagram of F_4, or (ii) from the NOL formula 7.5. Their HS and character HWGs are palindromic.

[0100]: 28 dimensional nilpotent orbit. This orbit is rigid and has the invariant subgroup $A_1 \otimes A_2$. Its Hilbert series can be calculated either from the NOL formula, or as the intersection of the two 30 dimensional orbits. Both the HS and character HWG are palindromic.

[2000]: 30 dimensional nilpotent orbit. This orbit is even, has the invariant subgroup C_3, and is normal. Its Hilbert Series can be calculated from the NOL formula. Both the HS and character HWG are palindromic.

[0002]: 30 dimensional nilpotent orbit. This orbit is even, has the invariant subgroup B_3, and is non-normal. The NOL formula yields a normalisation. The candidate for the non-normal orbit is found by excluding from this normalisation a subspace expressed in terms of the charged NOL formula for the 28 dimensional orbit:

$$g_{NO}^{F_4[0002]}(x,t) = g_{NOL}^{F_4[0002]}(x,t) - g_{NOL}^{F_4[0100]}(x,t)\left[x_4 t^2\right], \tag{7.24}$$

with notation as per 7.14. Both the HS and character HWG are non-palindromic.

[0010]: 34 dimensional nilpotent orbit. This orbit is rigid and has the invariant subgroup $A_2 \otimes A_1$. It can be calculated from the NOL formula. The HS and character HWG (not shown) are palindromic.

[2001]: 36 dimensional nilpotent orbit. This orbit is non-rigid, has the invariant subgroup $B_2 \cong C_2$, and is non-normal. Its normalisation can be calculated from the NOL formula. The candidate for the non-normal nilpotent orbit is found by excluding from its normalisation a subspace expressed by applying the charged NOL formula to the 34 dimensional orbit:

$$g_{NO}^{F_4[2001]}(x,t) = g_{NOL}^{F_4[2001]}(x,t) - g_{NOL}^{F_4[0010]}(x,t)\left[x_1 t^3\right]. \tag{7.25}$$

The HS is non-palindromic.

[0101]: 36 dimensional nilpotent orbit. This orbit is rigid, has the invariant subgroup $A_1 \otimes A_1$, and is non-normal. Its normalisation can be calculated from the NOL formula. The candidate for the non-normal nilpotent orbit is found by excluding from its normalisation a subspace expressed by applying the charged NOL formula to the 34 dimensional orbit:

$$g_{NO}^{F_4[0101]}(x,t) = g_{NOL}^{F_4[0101]}(x,t) - g_{NOL}^{F_4[0010]}(x,t)\left[x_4 t^2\right]. \tag{7.26}$$

Note the difference in charges between 7.26 and 7.25. The HS is non-palindromic.

[1010]: 38 dimensional nilpotent orbit. This orbit is non-rigid, has the invariant subgroup $A_1 \otimes A_1$, and is non-normal. Its normalisation is found from the NOL formula. The candidate for the non-normal nilpotent orbit is found by excluding from this normalisation a subspace expressed in terms of charged NOL formulae for the two 36 dimensional orbits:

$$\begin{aligned} g_{NO}^{F_4[1010]}(x,t) = g_{NOL}^{F_4[1010]}(x,t) &- g_{NOL}^{F_4[2001]}(x,t)\left[x_1 t^3 + x_4 t^2\right] \\ &- g_{NOL}^{F_4[0101]}(x,t)\left[x_3 x_4 t^6\right] \end{aligned} \tag{7.27}$$

Its HS is non-palindromic.

[1012]: 42 dimensional nilpotent orbit. This orbit is Richardson, has the invariant subgroup A_1, and is non-normal. Its normalisation can be calculated from the NOL formula. Possible candidates for the non-normal nilpotent orbit can be found either (i) by excluding from its

normalisation a subspace expressed in terms of the charged NOL formula for the 40 dimensional orbit $g_{NO}^{F_4[0200]}$, or (ii) by induction (using 7.11) from $g_{Higgs}^{B_3[101]}$:

$$\begin{aligned} g_{NO}^{F_4[1012]}(x,t) &= g_{NOL}^{F_4[1012]}(x,t) - g_{NOL}^{F_4[0200]}(x,t)\left[x_4t^2 + x_3t^6\right] \\ g_{Induced}^{F_4[1012]}(x,t) &= g_{NOL}^{F_4[0002]}(x,t)\left[g_{Higgs}^{B3[101]}\right] \end{aligned} \tag{7.28}$$

The former is taken as the candidate for the non-normal orbit $g_{NO}^{F_4[1012]}(x,t)$, on the grounds that it is consistent with the restriction method detailed below, and that it includes [0200], as in the standard Hasse diagram. Its HS is non-palindromic.

[0200], [0202], [2202] and [2222]: 40 dimensional , 44 dimensional, 46 dimensional sub-regular, and 48 dimensional maximal nilpotent orbits. These orbits are distinguished and contain the invariant subgroups $A_1 \otimes A_2$, $A_1 \otimes A_1$, A_1 and $\emptyset$, respectively. They are found from the NOL formula. Their HS are palindromic.

The above list excludes the moduli space defined by the $SU(2)$ homomorphism with the root map [2002]. Detailed calculation of Hilbert series shows that $g_{NOL}^{F_4[2002]}$ is not a nilpotent orbit, but is an extension of the distinguished $g_{NO}^{F_4[0200]}$, which can be described using the charged NOL formula:

$$g_{NOL}^{F_4[2002]}(x,t) = g_{NO}^{F_4[0200]}(x,t)\left[1 + x_1t^3 + x_4t^2\right]. \tag{7.29}$$

It is necessary to make some caveats in relation to the non-normal orbits. Firstly, the method of finding the charged NOL formula descriptions that restrict their normalisations to $\mathcal{N}$ is partly empirical, guided by unrefined HS and character HWGs, where known. The *restricted NOL* method used for F_4 has been (i) to fix the moduli space inclusion relations below a non-normal orbit using its normalisation and (ii) to exclude from the normalisation a subspace containing one (or sometimes more) *charged* normalisations of orbits lying immediately below in the Hasse diagram. The charges are selected such that the resulting non-normal moduli spaces lie within the nilpotent cone. This method is consistent with the Higgs branch constructions of non-normal Classical orbits studied in 7.2 and has been sufficient to specify candidates for the non-normal orbits of F_4. For exam-

ple, the calculation of the restriction of the non-normal $F_4[0002]$ to $\mathcal{N}$ is outlined in Appendix A.6.

Secondly, since the charged NOL formula does not generally yield an orthogonal basis, there may be alternative charged NOL formula descriptions of the non-normal orbits that give the same result.

Finally, it has only proved possible to calculate character HWGs and to use their Taylor series expansions to check the irrep inclusion relations explicitly up to the 34 dimensional nilpotent orbit; for the 36 dimensional and 38 dimensional non-normal orbits, in particular, the analysis has been largely dimensional in nature and therefore should not be taken as definitive.

It is interesting to compare the inclusion relations obtained from this analysis of moduli spaces with the standard Hasse diagrams of nilpotent orbits in the mathematical Literature [33, 70, 71], which are based on earlier work in [81]. Figure 7.2 compares the Hasse diagram defined by the inclusion relations amongst the Hilbert series of nilpotent orbits $g_{NO}^{F_4}$ to the standard Hasse diagram.

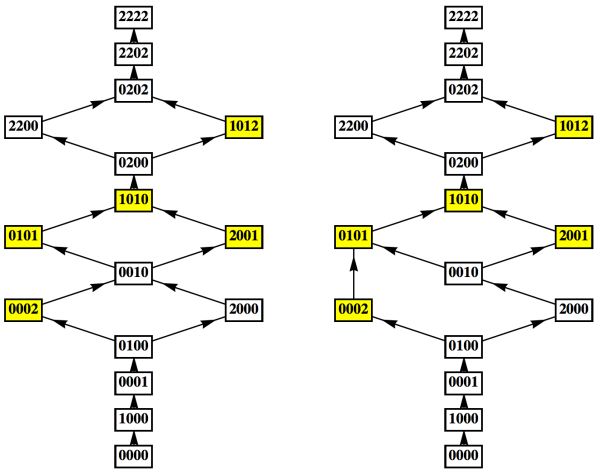

Figure 7.2.: Hasse Diagram of F_4 Nilpotent Orbits. The left hand diagram is derived from Hilbert series and HWG inclusion relations. The right hand diagram is taken from the mathematical Literature [70, 71]. Yellow nodes indicate non-normal nilpotent orbits.

Unlike the case of Classical group nilpotent orbits, where there is an

exact correspondence between the Hasse diagrams (not shown) based upon Hilbert Series inclusion relations and the standard diagrams [33, 6], there is a discrepancy involving the linking pattern between $F_4[2000]$ and $F_4[0010]$, where the restricted NOL method yields an inclusion relationship that is absent in the standard diagram. One possibility could be that the subtle distinction between normal and non-normal orbits has not been consistently treated in the analyses in the Literature upon which the standard Hasse diagrams are based. In this context, it is worth noting that $g_{NO}^{F_4[0010]}$ *does not* include $g_{NOL}^{F_4[2000]}$, which is the normalisation of $g_{NO}^{F_4[2000]}$.

The nilpotent orbits of F_4 include some special orbits, as defined in section 4.4.6. These are summarised in Table 7.4, along with their duals under the Spaltenstein map.

Spaltenstein Dual Orbits
$[0000] \Leftrightarrow [2222]$
$[0001] \Leftrightarrow [2202]$
$[0100] \Leftrightarrow [0202]$
$[0002] \Leftrightarrow [1012]$
$[2000] \Leftrightarrow [2200]$
$[0200] \Leftrightarrow [0200]$

Table 7.4.: F_4 Special Nilpotent Orbits

The special orbit [0200] is self dual. The non-normal orbits [0002] and [1012] are special and dual to each other. The other non-normal orbits [2001], [0101] and [1010] are not special. It is clear that the symmetries of the left hand Hasse diagram based on Hilbert series and HWG inclusion relations are a better fit for the symmetries of the Spaltenstein map.

Characteristic	Type	Construction	Dim.	Unrefined HS
[0000]	Even	$g_{NOL}^{F_4[0000]}(x,t)$	0	1
[1000]	Rigid	$g_{Coulomb}^{F_4[1000]}(x,t)$ or $g_{NOL}^{F_4[1000]}(x,t)$	16	$\frac{\left(\begin{array}{c}1+36t+341t^2+1208t^3+1820t^4\\+1208t^5+341t^6+36t^7+t^8\end{array}\right)}{(1-t)^{16}}$
[0001]	Rigid	$g_{Coulomb}^{F_4[0001]}(x,t)$ or $g_{NOL}^{F_4[0001]}(x,t)$	22	$\frac{\left(\begin{array}{c}1+29t+435t^2+2948t^3+8998t^4+12969t^5\\+8998t^6+2948t^7+435t^8+29t^9+t^{10}\end{array}\right)}{(1-t)^{22}(1+t)^{-1}}$
[0100]	Rigid	$g_{NOL}^{F_4[0100]}(x,t)$	28	$\frac{\left(1+9t+19t^2+9t^3+t^4\right)\times\left(\begin{array}{c}1+13t+118t^2+455t^3+716t^4\\+455t^5+118t^6+13t^7+t^8\end{array}\right)}{(1-t)^{28}(1+t)^{-2}}$
[2000]	Even	$g_{NOL}^{F_4[2000]}(x,t)$	30	$\frac{\left(\begin{array}{c}1+21t+231t^2+1498t^3+6219t^4+16834t^5\\+30420t^6+36972t^7+\ldots\,\text{palindrome}\,\ldots+t^{14}\end{array}\right)}{(1-t)^{30}(1+t)^{-1}}$
[0002]	Even Non-normal	$g_{NOL}^{F_4[0002]}(x,t)-g_{NOL}^{F_4[0100]}(x,t)\left[x_4t^2\right]$	30	$\frac{\left(\begin{array}{c}1+22t+252t^2+1729t^3+6988t^4+18300t^5\\+40835t^6+92700t^7+166252t^8+177698t^9+83654t^{10}\\-16141t^{11}-38932t^{12}-19256t^{13}-4581t^{14}-545t^{15}-26t^{16}\end{array}\right)}{(1-t)^{30}}$
[0010]	Rigid	$g_{NOL}^{F_4[0100]}(x,t)$	34	$\frac{\left(\begin{array}{c}1+17t+153t^2+969t^3+4495t^4+15022t^5\\+35477t^6+59244t^7+70204t^8+\ldots\,\text{palindrome}\,\ldots+t^{16}\end{array}\right)}{(1-t)^{34}(1+t)^{-1}}$
[2001]	Non-rigid Non-normal	$g_{NOL}^{F_4[2001]}(x,t)-g_{NOL}^{F_4[0010]}(x,t)\left[x_1t^3\right]$	36	$\frac{\left(\begin{array}{c}1+15t+120t^2+680t^3+2710t^4+7001t^5+10981t^6\\+16728t^7+51374t^8+123121t^9+151421t^{10}+76671t^{11}\\-13927t^{12}-37160t^{13}-19312t^{14}-5053t^{15}-712t^{16}-51t^{17}\end{array}\right)}{(1-t)^{36}(1+t)^{-1}}$
[0101]	Rigid Non-normal	$g_{NOL}^{F_4[0101]}(x,t)-g_{NOL}^{F_4[0010]}(x,t)\left[x_4t^2\right]$	36	$\frac{\left(\begin{array}{c}1+14t+106t^2+574t^3+2460t^4+8752t^5+25497t^6\\+57619t^7+91602t^8+93161t^9+52381t^{10}+8699t^{11}\\-7915t^{12}-5991t^{13}-1936t^{14}-324t^{15}-25t^{16}\end{array}\right)}{(1-t)^{36}(1+t)^{-2}}$

Table 7.5.: F_4 Orbit Constructions and Hilbert Series (A)

Characteristic	Type	Construction	Dim.	Unrefined HS
[1010]	Non-rigid Non-normal	$g_{NOL}^{F_4[1010]}(x,t)$ $-g_{NOL}^{F_4[0010]}(x,t)\left[x_3x_4t^6\right]$ $-g_{NOL}^{F_4[2001]}(x,t)\left[x_1t^3+x_4t^2\right]$	38	$\frac{\left(\begin{array}{c}1+13t+91t^2+455t^3+1794t^4+5824t^5\\+14859t^6+25830t^7+36686t^8+103415t^9+274079t^{10}\\+418078t^{11}+194377t^{12}-202566t^{13}-231712t^{14}\\-8813t^{15}+52245t^{16}+16746t^{17}-455t^{18}\\-92t^{19}+170t^{20}+40t^{21}-t^{22}\end{array}\right)}{(1-t)^{38}(1+t)^{-1}}$
[0200]	Distinguished	$g_{NOL}^{F_4[0200]}(x,t)$	40	$\frac{\left(\begin{array}{c}1+10t+56t^2+230t^3+745t^4+1946t^5+4112t^6\\+7028t^7+9692t^8+10782t^9+\ldots\text{palindrome}\ldots+t^{18}\end{array}\right)}{(1-t)^{40}(1+t)^{-2}}$
[2200]	Even	$g_{NOL}^{F_4[2200]}(x,t)$	42	$\frac{\left(\begin{array}{c}1+7t+29t^2+91t^3+213t^4+397t^5\\+591t^6+657t^7+\ldots\text{palindrome}\ldots+t^{14}\end{array}\right)}{(1-t)^{43}(1+t)^{-2}(1-t^6)^{-1}}$
[1012]	Richardson Non-normal	$g_{NOL}^{F_4[1012]}(x,t)$ $-g_{NOL}^{F_4[0200]}\left[x_3t^6+x_4t^2\right]$	42	$\frac{\left(\begin{array}{c}1+8t+37t^2+128t^3+367t^4+920t^5+2082t^6\\+4292t^7+8091t^8+13973t^9+21078t^{10}+26327t^{11}\\+22895t^{12}+10177t^{13}-2954t^{14}-6994t^{15}-4858t^{16}\\-1680t^{17}-291t^{18}+t^{19}\end{array}\right)}{(1-t)^{42}(1+t)^{-2}}$
[0202]	Distinguished	$g_{NOL}^{F_4[0202]}(x,t)$	44	$\frac{\left(\begin{array}{c}1+5t+16t^2+41t^3+91t^4+182t^5\\+336t^6+530t^7+723t^8+830t^9+\ldots\text{palindrome}\ldots+t^{18}\end{array}\right)}{(1-t)^{45}(1+t)^{-2}(1-t^3)^{-1}}$
[2202]	Distinguished	$g_{NOL}^{F_4[2202]}(x,t)$	46	$\frac{\left(\begin{array}{c}1+3t+6t^2+10t^3+16t^4+24t^5+34t^6+46t^7\\+\ldots\text{palindrome}\ldots+t^{14}\end{array}\right)}{(1-t)^{49}(1-t^2)^{-1}(1-t^4)^{-1}(1-t^6)^{-1}}$
[2222]	Distinguished	$g_{NOL}^{F_4[2222]}(x,t)$	46	$\frac{(1-t^2)(1-t^6)(1-t^8)(1-t^{12})}{(1-t)^{52}}$

Table 7.6.: F_4 Orbit Constructions and Hilbert Series (B)

Characteristic	Character HWG	mHL HWG
[0000]	1	$\dots$
[1000]	$\frac{1}{1-m_1t}$	$\dots$
[0001]	$\frac{1}{(1-m_1t)(1-{m_4}^2t^2)}$	$\dots$
[0100]	$\frac{1}{(1-m_1t)(1-{m_4}^2t^2)(1-m_2t^3)(1-{m_3}^2t^4)}$	$\dots$
[2000]	$\frac{1+m_1m_2t^5}{(1-m_1t)(1-{m_4}^2t^2)(1-m_2t^3)(1-{m_1}^2t^4)(1-{m_3}^2t^4)(1-{m_2}^2t^6)}$	not shown
[0002]	$\frac{\left(\begin{array}{c}1-m_4t^2-m_3t^3+{m_4}^2t^4+2m_3m_4t^5+{m_3}^2t^6\\+m_3{m_4}^2t^6+{m_3}^2m_4t^7-m_3{m_4}^2t^7-{m_3}^2m_4t^8-{m_3}^2{m_4}^2t^9\end{array}\right)}{(1-m_1t)(1-{m_4}t^2)(1-{m_4}^2t^2)(1-m_2t^3)(1-{m_3}t^3)(1-{m_3}^2t^4)}$	not shown
[0010]	not shown	$1-h_4t^4-{h_4}^2t^4-h_1t^5+h_3h_4t^6+h_2t^7+h_3t^7+$ $h_1h_4t^7+h_3h_4t^7-{h_4}^3t^7+h_3t^8-h_1h_3t^8-h_4t^8-$ $h_2h_4t^8-h_1{h_4}^2t^8+h_3t^9-2h_1h_3t^9+{h_3}^2t^9+$ ${h_1}^2h_4t^9-h_2h_4t^9-h_3h_4t^9-{h_4}^2t^9+h_3{h_4}^2t^9-$ $h_1h_3t^{10}+{h_3}^2t^{10}-h_1h_4t^{10}+{h_1}^2h_4t^{10}+h_2h_4t^{10}+$ $h_1{h_4}^2t^{10}+h_3{h_4}^2t^{10}-{h_4}^4t^{10}+h_3t^{11}-h_1h_4t^{11}+$ ${h_1}^2h_4t^{11}+h_2h_4t^{11}-h_1h_3h_4t^{11}+h_2t^{12}-h_1h_2t^{12}+$ $h_2h_4t^{12}-2h_1h_3h_4t^{12}-h_1h_2t^{13}+h_2h_3t^{13}-$ $2h_1h_3h_4t^{13}+h_2{h_4}^2t^{13}+h_1{h_4}^3t^{13}+h_2h_3t^{14}-$ ${h_3}^2h_4t^{14}$
[2001]	$\dots$	not shown
[0101]	$\dots$	$1-h_4t^4-h_1t^5-{h_1}^2t^6+h_3t^7+h_3t^8+h_1h_3t^8-$ $h_4t^8+h_1h_2t^9+h_3t^9-{h_4}^2t^9-{h_1}^3t^{10}+h_1h_2t^{10}+$ $h_1h_3t^{10}-h_1h_4t^{10}-h_2h_4t^{10}-h_1h_3h_4t^{10}+h_3t^{11}+$ ${h_3}^2t^{11}-h_1h_4t^{11}-h_2h_4t^{11}-2h_1h_3h_4t^{11}+$ $h_1{h_4}^3t^{11}+h_2t^{12}+{h_1}^2h_3t^{12}+h_2h_3t^{12}-h_1h_3h_4t^{12}+$ $h_1{h_4}^3t^{12}+h_2h_3t^{13}-h_2{h_4}^2t^{13}+{h_1}^2h_3t^{14}-$ $h_1h_2h_4t^{14}-h_2{h_4}^2t^{14}+h_1{h_3}^2t^{15}-h_1h_2h_4t^{15}$

An mHL HWG of 1 denotes $mHL^{F_4}_{[0000]}(t)$.
The character or mHL HWGs for some quivers are not shown for brevity.

Table 7.7.: F_4 Orbits and HWGs (A)

Characteristic	Character HWG	mHL HWG
[1010]	...	$1 - h_4t^4 - h_1t^5 - {h_1}^2t^6 + h_3t^7 + h_3t^8 + h_1h_3t^8 +$ $h_3{}^2t^8 - h_4t^8 + h_3t^9 - h_4{}^2t^9 - h_3h_4{}^2t^9 + h_1h_3t^{10} -$ $h_2h_3t^{10} - h_1h_4t^{10} - h_2h_4t^{10} - h_1h_3h_4t^{10} + h_3t^{11} +$ ${h_1}^2h_3t^{11} + h_3{}^2t^{11} - h_1h_4t^{11} - h_2h_4t^{11} - h_1h_3h_4t^{11} +$ $h_3{}^2h_4t^{11} + h_2h_4{}^2t^{11} + h_1h_4{}^3t^{11} + h_2t^{12} - h_2{}^2t^{12} +$ ${h_1}^2h_3t^{12} + h_2h_3t^{12} - {h_1}^2h_4{}^2t^{12} + h_2h_4{}^2t^{12} +$ $h_1h_4{}^3t^{12} - h_3h_4{}^3t^{12} + {h_1}^2h_2t^{13} + h_2h_3t^{13} -$ $h_1h_3{}^2t^{13} - h_1h_2h_4t^{13} + h_2h_3h_4t^{13} - h_3{}^2h_4t^{13} -$ ${h_1}^2h_4{}^2t^{13} - h_2h_4{}^2t^{13} + h_2{}^2t^{14} - h_3{}^3t^{14} -$ $h_1h_2h_4t^{14} - {h_1}^2h_3h_4t^{14} + h_2h_3h_4t^{14} - h_2h_4{}^2t^{14} +$ $h_1h_3h_4{}^2t^{14} - h_2h_4{}^3t^{14} + h_1h_3{}^2t^{15} - {h_1}^2h_3h_4t^{15} +$ $h_1h_3h_4{}^2t^{15} + h_3{}^2h_4{}^2t^{15} + {h_1}^2h_4{}^3t^{15} + h_1h_2h_3t^{16} -$ $h_2h_3h_4t^{16} - h_1h_2h_4{}^2t^{17}$
[0200]	...	$1 - h_4t^4 - h_1t^5 + h_3t^7 + h_3t^8 - h_4t^8 + h_3t^9 - h_4{}^2t^9 -$ $h_1h_4t^{10} + h_3t^{11} - h_1h_4t^{11} + h_2t^{12}$
[2200]	...	$1 - h_4t^4 + h_3t^8 - h_4t^8 - h_4{}^2t^9 + h_3t^{11}$
[1012]	...	$1 - h_1t^7 - h_4t^8 - {h_1}^2t^{10} + h_3t^{11} + h_1h_4{}^2t^{13} +$ $h_1h_3t^{14} - h_2h_4t^{15}$
[0202]	...	$1 - h_1t^7 - h_4t^8 + h_3t^{11}$
[2202]	...	$1 - h_4t^8$
[2222]	...	1

An mHL HWG of 1 denotes $mHL^{F_4}_{[0000]}(t)$.

Table 7.8.: F_4 Orbits and HWGs (B)

Characteristic	Type	Construction	Dim.	Unrefined HS
[0002]	Even Normalisation	$g_{NOL}^{F_4[0002]}(x,t)$	30	$\frac{\left(\begin{array}{c}1+21t+257t^2+2018t^3+9573t^4+28261t^5\\+53781t^6+66651t^7+\ldots\,\text{palindrome}\ldots+t^{14}\end{array}\right)}{(1-t)^{30}(1+t)^{-1}}$
[2001]	Non-rigid Normalisation	$g_{NOL}^{F_4[2001]}(x,t)$	36	$\frac{\left(\begin{array}{c}1+14t+106t^2+626t^3+2811t^4+9363t^5\\+21662t^6+35663t^7+41812t^8+\ldots\,\text{palindrome}\ldots+t^{16}\end{array}\right)}{(1-t)^{36}(1+t)^{-2}}$
[0101]	Rigid Normalisation	$g_{NOL}^{F_4[0101]}(x,t)$	36	$\frac{\left(\begin{array}{c}1+14t+132t^2+912t^3+4528t^4+15655t^5\\+37940t^6+64575t^7+77161t^8+\ldots\,\text{palindrome}\ldots+t^{16}\end{array}\right)}{(1-t)^{36}(1+t)^{-2}}$
[1010]	Non-rigid Normalisation	$g_{NOL}^{F_4[1010]}(x,t)$	38	$\frac{\left(\begin{array}{c}1+13t+117t^2+819t^3+4121t^4+15171t^5\\+41431t^6+84642t^7+129597t^8+149240t^9+\ldots\,\text{palindrome}\ldots+t^{18}\end{array}\right)}{(1-t)^{38}(1+t)^{-1}}$
[2002]	Even Cover	$g_{NOL}^{F_4[2002]}(x,t)$	40	$\frac{\left(\begin{array}{c}1+10t+82t^2+516t^3+2408t^4+8255t^5\\+21525t^6+42408t^7+63690t^8+72742t^9+\ldots\,\text{palindrome}\ldots+t^{18}\end{array}\right)}{(1-t)^{40}(1+t)^{-2}}$
[1012]	Richardson Normalisation	$g_{NOL}^{F_4[1012]}(x,t)$	42	$\frac{\left(\begin{array}{c}1+7t+55t^2+247t^3+811t^4+1840t^5\\+3061t^6+3556t^7+\ldots\,\text{palindrome}\ldots+t^{14}\end{array}\right)}{(1-t)^{42}(1+t)^{-3}(1-t^2)(1-t^6)^{-1}}$

In addition to the normalisations of non-normal nilpotent orbits, the extension $F_4[2002]$ is shown (see text).

Table 7.9.: F_4 Nilpotent Orbit Normalisations and Hilbert Series

Characteristic	Character HWG	mHL HWG
[0002]	$\frac{1+m_3m_4t^4}{\left(\begin{array}{c}(1-m_1t)(1-m_4t^2)(1-{m_4}^2t^2)\\ \times(1-m_2t^3)(1-m_3t^3)(1-{m_3}^2t^4)\end{array}\right)}$	not shown
[2001]	...	$1+h_1t^3-h_4t^4-{h_4}^2t^4-h_1t^5-h_3t^5+h_1h_3t^7+$ $h_1h_4t^7+h_3h_4t^7+h_3t^8-h_4t^8+h_1h_4t^8-h_2h_4t^8+$ $h_3h_4t^8-h_1{h_4}^2t^8+h_3t^9-h_1h_3t^9+h_1h_4t^9-$ $h_2h_4t^9-{h_4}^2t^9+h_3{h_4}^2t^9-{h_4}^3t^9-h_2t^{10}-$ $h_1h_3t^{10}+{h_3}^2t^{10}-h_1h_4t^{10}-h_2h_4t^{10}+h_3{h_4}^2t^{10}-$ $h_4{}^4t^{10}+h_1h_2t^{11}+h_3t^{11}-h_1h_3t^{11}+{h_3}^2t^{11}-$ $h_1h_4t^{11}+{h_1}^2h_4t^{11}+h_2t^{12}+h_2h_4t^{12}-h_1h_3h_4t^{12}+$ $h_1{h_4}^2t^{12}-h_1h_2t^{13}-h_1h_3h_4t^{13}+h_1{h_4}^3t^{13}$
[0101]	...	$1+h_4t^2-h_4t^4-{h_4}^2t^4-2h_1t^5-h_3t^5-h_1h_4t^5-$ $h_3t^6+h_3h_4t^6+2h_2t^7+h_3t^7+h_1h_4t^7+2h_3h_4t^7+$ $h_4{}^2t^7-{h_4}^3t^7+h_2t^8+h_3t^8-h_4t^8+h_1h_4t^8-$ $h_1{h_4}^2t^8-{h_1}^2t^9+h_2t^9+h_3t^9-2h_1h_3t^9+h_1h_4t^9-$ $h_2h_4t^9-h_3h_4t^9-{h_4}^2t^9-h_1{h_4}^2t^9-h_2t^{10}-$ $2h_1h_3t^{10}-h_1h_4t^{10}+{h_1}^2h_4t^{10}-h_3h_4t^{10}+$ $h_3{h_4}^2t^{10}+h_1h_2t^{11}+h_3t^{11}+{h_3}^2t^{11}-h_1h_4t^{11}+$ $h_1{}^2h_4t^{11}+h_2h_4t^{11}-h_3h_4t^{11}+h_3{h_4}^2t^{11}+h_2t^{12}+$ $2h_2h_4t^{12}-h_1h_3h_4t^{12}-h_1h_2t^{13}+h_1h_3t^{13}-$ $2h_1h_3h_4t^{13}+h_2h_3t^{14}-h_1h_3h_4t^{14}$
[1010]	...	$1+h_4t^2+h_1t^3-h_4t^4-{h_4}^2t^4-2h_1t^5-2h_3t^5-$ $h_3t^6+h_1h_4t^7+h_3h_4t^7+{h_4}^2t^7+h_2t^8+h_3t^8-$ $h_4t^8+2h_1h_4t^8+h_3h_4t^8-{h_1}^2t^9+h_2t^9+h_3t^9-$ $h_1h_3t^9+2h_1h_4t^9-{h_4}^2t^9-{h_4}^3t^9-2h_2t^{10}-$ $h_1h_3t^{10}-h_1h_4t^{10}-h_2h_4t^{10}-h_3h_4t^{10}+h_3t^{11}-$ $h_1h_3t^{11}+{h_3}^2t^{11}-h_1h_4t^{11}+{h_1}^2h_4t^{11}-h_3h_4t^{11}+$ $h_2t^{12}+h_2h_4t^{12}+h_1{h_4}^2t^{12}-h_1h_2t^{13}+h_1h_3t^{13}$
[2002]	...	$1+h_4t^2+h_1t^3-h_4t^4-2h_1t^5-2h_3t^5-h_3t^6-h_2t^7+$ $h_4{}^2t^7+h_2t^8+h_3t^8-h_4t^8+2h_1h_4t^8+h_3h_4t^8-$ $h_1{}^2t^9+h_2t^9+h_3t^9+2h_1h_4t^9+h_3h_4t^9-h_4{}^2t^9-$ $h_4{}^3t^9-2h_2t^{10}-h_1h_4t^{10}-h_3h_4t^{10}+h_3t^{11}-$ $h_1h_3t^{11}-h_1h_4t^{11}-h_3h_4t^{11}+h_2t^{12}+h_1h_4{}^2t^{12}+$ $h_1h_3t^{13}$
[1012]	...	$1+h_4t^2-h_1t^5-h_3t^5-h_1t^7+h_2t^8-$ $h_4t^8-{h_1}^2t^9+h_2t^{11}+h_3t^{11}$

In addition to the normalisations of non-normal nilpotent orbits, the extension $F_4[2002]$ is shown (see text).

Table 7.10.: F_4 Nilpotent Orbit Normalisations and HWGs

7.3.3. Orbits of E_6

The 21 nilpotent orbits of E_6 are described in Tables 7.11 to 7.13, which give their classification, constructions and unrefined HS. Table 7.14 contains the same information for the normalisations of the non-normal nilpotent orbits. Table 7.15 analyses the three extra root maps that were identified in section 4.2.1.

Unlike F_4, it has not proved practicable to resolve many Hilbert series into HWGs, other than for near minimal and maximal orbits, so much of the analysis is based upon unrefined HS. In Table 7.16, the character HWGs and mHL HWGs are given for those orbits where it has been possible to complete the calculations.

The non-normal orbits exactly match those listed in [72] (see section 4.4.7). The tables contain candidates for the constructions of the non-normal orbits. These have been obtained by restricting their normalisations to the nilpotent cone $\mathcal{N}$ through the subtraction of sub-spaces, similar to the method used for $g_{NO}^{G_2}$ and $g_{NO}^{F_4}$. Much of the analysis is, however, based on unrefined Hilbert series and should not be taken as definitive. The picture that emerges can be summarised:

[000001] and [100010]: 22 dimensional minimal and 32 dimensional next to minimal nilpotent orbits. These orbits have the invariant subgroups A_5 and D_4 respectively. The orbits can be calculated either (i) from the Coulomb branch of a quiver theory built on the affine or twisted affine Dynkin diagram, or (ii) from the NOL formula. The HS and character HWGs are palindromic, and the latter are freely generated.

[001000] and [000002]: 40 and 42 dimensional nilpotent orbits. These orbits have the invariant subgroups $A_2 \otimes A_2 \otimes A_1$ and A_5, respectively. The orbits are calculated from the NOL formula. The HS and character HWGs are palindromic, and the latter are freely generated or complete intersections.

[100011], [200020], [100012], [010101] and [200022]: 46, 48, 52, 56 and 60 dimensional nilpotent orbits. These orbits have the invariant subgroups A_3, D_4, A_3, A_1^3 and A_3 respectively. The orbits are non-normal and candidates for the orbits are found by excluding sub-spaces, as

shown in the tables, from their normalisations obtained from the NOL formula. The Hilbert series are non-palindromic.

The remaining orbits are normal, with palindromic Hilbert series. The decompositions into mHL functions are shown for the 66 dimensional orbit upwards.

The Hasse diagram based on the inclusion relationships between unrefined Hilbert series is compared in Figure 7.3 with the standard diagram in the mathematical Literature [70, 71].

The two diagrams are broadly consistent. Some of the extra links appearing in the left hand diagram might disappear if the moduli space calculations could be repeated with refined (rather than unrefined) Hilbert series, or with character HWGs. However, the left hand diagram does not have a link (i.e. inclusion relation) between the non-normal [200022] and the normal [110111]; considering that unrefined Hilbert series cannot miss an inclusion relation, this may indicate an anomaly in the standard diagram; alternatively, there may be other restrictions of the normalisation of [200022] that should be considered.

Turning to the three extra root maps, whose unrefined HS are set out in Table 7.15: two of these maps, [111110] and [020202], have identical *refined* Hilbert series to the nilpotent orbits with Characteristics [110111] and [202020], respectively; these provide examples of dualities, with different $SU(2)$ homomorphisms generating the same nilpotent orbit. The third map, [110110], is non-normal, containing elements outside the nilpotent cone; it can be restricted to the nilpotent cone, by excluding a subspace defined by the charged NOL formula, whereupon it appears to be an extension of [002000], the distinguished nilpotent orbit of the same dimension:

$$g_{NOL}^{E_6[110110]}(x,t) = g_{NOL}^{E_6[002000]}(x,t)\left[1 + x_6 t^3 + x_3 t^6\right] \tag{7.30}$$

The Weyl group of E_6 has 25 irreps and conjugacy classes. In [82], the 21 nilpotent orbits are identified as these conjugacy classes, modulo some actions of the symmetric groups S_2 or S_3. Two of the three extra root maps, [110110] and [020202], appear to correspond to other members of these conjugacy classes; however, these are identified in [82] by Bala Carter labels, so the correspondence with root maps or Characteristics is unclear.

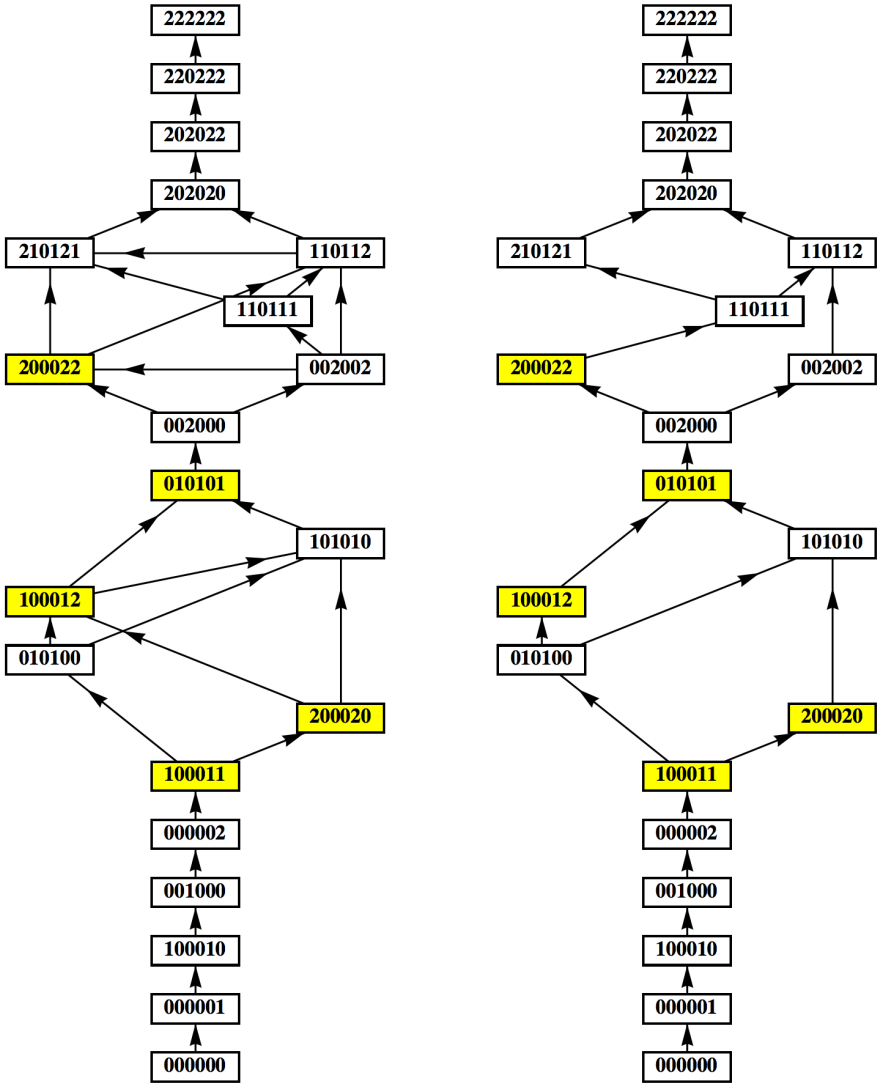

Figure 7.3.: Hasse Diagram of E_6 Nilpotent Orbits. The left hand diagram is indicative, being partly derived from *unrefined* Hilbert series, with arrows indicating inclusion relations and yellow nodes indicating non-normal nilpotent orbits. The right hand diagram is taken from the mathematical Literature.

Characteristic	Type	Construction	Dim.	Unrefined HS
[000000]	Even	$g_{NOL}^{E_6[000000]}(x,t)$	0	1
[000001]	Rigid	$g_{Coulomb}^{E_6[000001]}(x,t)$ or $g_{NOL}^{E_6[000001]}(x,t)$	22	$\frac{\left(\begin{array}{c}1+55t+890t^2+5886t^3+17929t^4+26060t^5\\+\ldots\,\text{palindrome}\,\ldots+t^{10}\end{array}\right)}{(1-t)^{22}(1+t)^{-1}}$
[100010]	Richardson	$g_{Coulomb}^{E_6[100010]}(x,t)$ or $g_{NOL}^{E_6[100010]}(x,t)$	32	$\frac{\left(\begin{array}{c}1+44t+991t^2+11649t^3+75681t^4+285009t^5\\+632941t^6+827309t^7+\ldots\,\text{palindrome}\,\ldots+t^{14}\end{array}\right)}{(1-t)^{32}(1+t)^{-2}}$
[001000]	Rigid	$g_{NOL}^{E_6[001000]}(x,t)$	40	$\frac{\left(\begin{array}{c}1+38t+740t^2+9192t^3+76974t^4+446483t^5\\+1832104t^6+5408077t^7+11624874t^8+18343974t^9+21346158t^{10}\\+\ldots\,\text{palindrome}\,\ldots+t^{20}\end{array}\right)}{(1-t)^{40}}$
[000002]	Even	$g_{NOL}^{E_6[000002]}(x,t)$	42	$\frac{\left(\begin{array}{c}1+35t+630t^2+7120t^3+54640t^4+294385t^5\\+1139307t^6+3216888t^7+6702843t^8+10382781t^9+12008160t^{10}\\+\ldots\,\text{palindrome}\,\ldots+t^{20}\end{array}\right)}{(1-t)^{42}(1+t)^{-1}}$
[100011]	Non-rigid Non-normal	$g_{NOL}^{E_6[100011]}(x,t)$ $-g_{NOL}^{E_6[000002]}(x,t)\left[x_6t^2\right]$	46	$\frac{\left(\begin{array}{c}1+31t+496t^2+5456t^3+45648t^4+303442t^5\\+1570349t^6+6114940t^7+17426810t^8+35866167t^9+53265869t^{10}\\+58043959t^{11}+48411638t^{12}+32923009t^{13}+18740108t^{14}+8202867t^{15}\\+2156737t^{16}+17233t^{17}-221603t^{18}-85366t^{19}-16244t^{20}\\-1658t^{21}-77t^{22}\end{array}\right)}{(1-t)^{46}(1+t)^{-1}}$
[200020]	Even Non-normal	$g_{NOL}^{E_6[200020]}(x,t)$ $-g_{NOL}^{E_6[000002]}(x,t)\left[x_6t^2\right]$	48	$\frac{\left(\begin{array}{c}1+29t+435t^2+4495t^3+35882t^4+232149t^5\\+1171457t^6+4383879t^7+11766232t^8+22712054t^9+33186041t^{10}\\+40726538t^{11}+44327421t^{12}+38695845t^{13}+22831110t^{14}+8234564t^{15}\\+2786494t^{16}+2013171t^{17}+1068403t^{18}+146307t^{19}-109837t^{20}\\-60051t^{21}-13489t^{22}-1532t^{23}-78t^{24}\end{array}\right)}{(1-t)^{48}(1+t)^{-1}}$
[010100]	Richardson	$g_{NOL}^{E_6[010100]}(x,t)$	50	$\frac{\left(\begin{array}{c}1+27t+378t^2+3654t^3+26677t^4+151633t^5\\+679211t^6+2411434t^7+6802614t^8+15252535t^9+27167919t^{10}\\+38421369t^{11}+43128016t^{12}+\ldots\,\text{palindrome}\,\ldots+t^{24}\end{array}\right)}{(1-t)^{50}(1+t)^{-1}}$

Table 7.11.: E_6 Orbit Constructions and Hilbert Series (A)

Characteristic	Type	Construction	Dim.	Unrefined HS
[100012]	Richardson Non-normal	$g_{NOL}^{E_6[100012]}(x,t)$ $-g_{NOL}^{E_6[000002]}(x,t)\left[x_6t^3\right]$	52	$\frac{\left(\begin{array}{c}1+25t+325t^2+2925t^3+20397t^4+116805t^5\\+562496t^6+2201433t^7+6660591t^8+15233736t^9+27936753t^{10}\\+44893175t^{11}+60568689t^{12}+56711757t^{13}+35968001t^{14}+28729791t^{15}\\+27096886t^{16}+5811534t^{17}-7028305t^{18}+1316117t^{19}+4719834t^{20}\\-231609t^{21}-1389570t^{22}-78065t^{23}+249547t^{24}+51338t^{25}\\-15378t^{26}-7854t^{27}-1221t^{28}-78t^{29}\end{array}\right)}{(1-t)^{52}(1+t)^{-1}}$
[101010]	Rigid	$g_{NOL}^{E_6[101010]}(x,t)$	54	$\frac{\left(\begin{array}{c}1+21t+233t^2+1813t^3+11013t^4+55097t^5\\+231652t^6+814942t^7+2352615t^8+5460885t^9+10045178t^{10}\\+14521163t^{11}+16426194t^{12}+\ldots\,\text{palindrome}\ldots+t^{24}\end{array}\right)}{(1-t)^{54}(1+t)^{-3}}$
[010101]	Non-rigid Non-normal	$g_{NOL}^{E_6[010101]}(x,t)$ $-g_{NOL}^{E_6[101010]}(x,t)\left[x_6t^3\right]$	56	$\frac{\left(\begin{array}{c}1+21t+231t^2+1771t^3+10548t^4+51492t^5\\+212289t^6+752158t^7+2315893t^8+6248619t^9+14884446t^{10}\\+31537643t^{11}+58591608t^{12}+91163801t^{13}+111457472t^{14}+99817922t^{15}\\+58890046t^{16}+16128539t^{17}-5514308t^{18}-7464927t^{19}-3286296t^{20}\\-760330t^{21}-172433t^{22}-120068t^{23}-76638t^{24}-30650t^{25}\\-8184t^{26}-1539t^{27}-210t^{28}-20t^{29}-t^{30}\end{array}\right)}{(1-t)^{56}(1+t)^{-1}}$
[002000]	Even	$g_{NOL}^{E_6[002000]}(x,t)$	58	$\frac{\left(\begin{array}{c}1+17t+155t^2+1003t^3+5076t^4+21012t^5\\+72753t^6+212554t^7+526005t^8+1104427t^9+1968242t^{10}\\+2976459t^{11}+3816658t^{12}+4147046t^{13}\\+3816658t^{14}+\ldots\,\text{palindrome}\ldots+t^{26}\end{array}\right)}{(1-t)^{58}(1+t)^{-3}}$
[002002]	Even	$g_{NOL}^{E_6[002002]}(x,t)$	60	$\frac{\left(\begin{array}{c}1+14t+107t^2+588t^3+2515t^4+8716t^5\\+24956t^6+58860t^7+114672t^8+184443t^9+244674t^{10}\\+269178t^{11}+\ldots\,\text{palindrome}\ldots+t^{22}\end{array}\right)}{(1-t)^{64}(1-t^2)^{-3}(1-t^6)^{-1}}$
[200022]	Even Non-normal	$g_{NOL}^{E_6[200022]}(x,t)$ $-g_{NOL}^{E_6[002000]}(x,t)\left[x_6t^3\right]$	60	$\frac{\left(\begin{array}{c}1+16t+137t^2+832t^3+4013t^4+16257t^5\\+57091t^6+180151t^7+521432t^8+1375550t^9+3229355t^{10}\\+6552743t^{11}+11221499t^{12}+15931890t^{13}+18517801t^{14}+17407937t^{15}\\+13045728t^{16}+7612781t^{17}+3291500t^{18}+911351t^{19}+42335t^{20}\\-105546t^{21}-61493t^{22}-19309t^{23}-3591t^{24}-259t^{25}\\+59t^{26}+16t^{27}+t^{28}\end{array}\right)}{(1-t)^{60}(1+t)^{-2}}$

Table 7.12.: E_6 Orbit Constructions and Hilbert Series (B)

Characteristic	Type	Construction	Dim.	Unrefined HS
[110111]	Richardson	$g_{NOL}^{E_6[110111]}(x,t)$	62	$\frac{\left(\begin{array}{c}1+12t+80t^2+389t^3+1536t^4+5133t^5\\+14863t^6+37773t^7+84597t^8+166302t^9+284667t^{10}\\+421063t^{11}+534371t^{12}+579012t^{13}+\ldots\,\text{palindrome}\ldots+t^{26}\end{array}\right)}{(1-t)^{66}(1-t^2)^{-3}(1-t^3)^{-1}}$
[210121]	Non-rigid	$g_{NOL}^{E_6[210121]}(x,t)$	64	$\frac{\left(\begin{array}{c}1+10t+56t^2+232t^3+791t^4+2343t^5\\+6228t^6+15100t^7+33650t^8+69224t^9+129347t^{10}\\+213929t^{11}+298121t^{12}+335808t^{13}+\ldots\,\text{palindrome}\ldots+t^{26}\end{array}\right)}{(1-t)^{68}(1-t^2)^{-2}(1-t^3)^{-2}}$
[110112]	Richardson	$g_{NOL}^{E_6[110112]}(x,t)$	64	$\frac{\left(\begin{array}{c}1+11t+67t^2+298t^3+1079t^4+3366t^5\\+9362t^6+23671t^7+54328t^8+112202t^9+205531t^{10}\\+330265t^{11}+463957t^{12}+568853t^{13}+608454t^{14}+568853t^{15}\\+\ldots\,\text{palindrome}\ldots+t^{28}\end{array}\right)}{(1-t)^{67}(1-t^2)^{-2}(1-t^3)^{-1}}$
[202020]	Distinguished	$g_{NOL}^{E_6[202020]}(x,t)$	66	$\frac{\left(\begin{array}{c}1+7t+30t^2+100t^3+283t^4+710t^5\\+1623t^6+3364t^7+6314t^8+10710t^9+16269t^{10}\\+22197t^{11}+26940t^{12}+28824t^{13}+\ldots\,\text{palindrome}\ldots+t^{26}\end{array}\right)}{(1-t)^{71}(1-t^2)^{-3}(1-t^3)^{-2}}$
[202022]	Even	$g_{NOL}^{E_6[202022]}(x,t)$	68	$\frac{\left(\begin{array}{c}1+6t+22t^2+62t^3+149t^4+319t^5\\+626t^6+1146t^7+1905t^8+2883t^9+3941t^{10}\\+4824t^{11}+5087t^{12}+\ldots\,\text{palindrome}\ldots+t^{24}\end{array}\right)}{(1-t)^{72}(1-t^2)^{-2}(1-t^4)^{-1}(1-t^6)^{-1}}$
[220222]	Distinguished	$g_{NOL}^{E_6[220222]}(x,t)$	70	$\frac{\left(\begin{array}{c}1+3t+6t^2+11t^3+19t^4+30t^5+45t^6+65t^7\\+90t^8+120t^9+156t^{10}+\ldots\,\text{palindrome}\ldots+t^{20}\end{array}\right)}{(1-t)^{75}(1-t^2)^{-1}(1-t^3)^{-1}(1-t^4)^{-1}(1-t^5)^{-1}(1-t^6)^{-1}}$
[222222]	Distinguished	$g_{NOL}^{E_6[222222]}(x,t)$	72	$\frac{(1-t^2)(1-t^5)(1-t^6)(1-t^8)(1-t^9)(1-t^{12})}{(1-t)^{78}}$

Table 7.13.: E_6 Orbit Constructions and Hilbert Series (C)

Characteristic	Type	Construction	Dim.	Unrefined HS
[100011]	Non-rigid Normalisation	$g_{NOL}^{E_6[100011]}(x,t)$	46	$\frac{\left(\begin{array}{c}1+31t+574t^2+7145t^3+62466t^4+395953t^5\\+1854418t^6+6493660t^7+17124491t^8+34156960t^9\\+51650252t^{10}+59277910t^{11}+\ldots\,\text{palindrome}\ldots+t^{22}\end{array}\right)}{(1-t)^{46}(1+t)^{-1}}$
[200020]	Even Normalisation	$g_{NOL}^{E_6[200020]}(x,t)$	48	$\frac{\left(\begin{array}{c}1+27t+457t^2+5059t^3+38341t^4+205456t^5\\+794669t^6+2248381t^7+4698986t^8+7296802t^9\\+8446562t^{10}+\ldots\,\text{palindrome}\ldots+t^{20}\end{array}\right)}{(1-t)^{51}(1-t^2)^{-2}(1-t^3)^{-1}}$
[100012]	Richardson Normalisation	$g_{NOL}^{E_6[100012]}(x,t)$	52	$\frac{\left(\begin{array}{c}1+24t+301t^2+2702t^3+18916t^4+105743t^5+472131t^6\\+1677965t^7+4733104t^8+10579022t^9+18750304t^{10}\\+26396098t^{11}+29577416t^{12}+\ldots\,\text{palindrome}\ldots+t^{24}\end{array}\right)}{(1-t)^{52}(1+t)^{-2}}$
[010101]	Non-rigid Normalisation	$g_{NOL}^{E_6[010101]}(x,t)$	56	$\frac{\left(\begin{array}{c}1+20t+211t^2+1638t^3+10469t^4+56733t^5+260036t^6\\+993325t^7+3125563t^8+8036658t^9+16802409t^{10}\\+28491536t^{11}+39129101t^{12}+43499048t^{13}\\+\ldots\,\text{palindrome}\ldots+t^{26}\end{array}\right)}{(1-t)^{56}(1+t)^{-2}}$
[200022]	Even Normalisation	$g_{NOL}^{E_6[200022]}(x,t)$	60	$\frac{\left(\begin{array}{c}1+16t+136t^2+894t^3+5046t^4+24136t^5\\+96384t^6+318938t^7+873668t^8+1984329t^9+3747603t^{10}\\+5898185t^{11}+7743629t^{12}+8479209t^{13}+7743629t^{14}\\+\ldots\,\text{palindrome}\ldots+t^{26}\end{array}\right)}{(1-t)^{60}(1+t)^{-2}(1+t^2)^{-1}}$

Table 7.14.: E_6 Nilpotent Orbit Normalisations and Hilbert Series

Characteristic	Type	Construction	Dim.	Unrefined HS
[110110]	Cover	$g_{NOL}^{E_6[110110]}(x,t)$	58	$\frac{\left(\begin{array}{c}1+17t+155t^2+1159t^3+7570t^4+41208t^5\\+186890t^6+699308t^7+2146085t^8+5383228t^9+11015451t^{10}\\+18374964t^{11}+24976338t^{12}+27669872t^{13}+24976338t^{14}\\+\ldots\,\text{palindrome}\ldots+t^{26}\end{array}\right)}{(1-t)^{58}(1+t)^{-3}}$
[111110]	Richardson Dual	$g_{NOL}^{E_6[111110]}(x,t)$	62	$\frac{\left(\begin{array}{c}1+12t+80t^2+389t^3+1536t^4+5133t^5\\+14863t^6+37773t^7+84597t^8+166302t^9+284667t^{10}\\+421063t^{11}+534371t^{12}+579012t^{13}+\ldots\,\text{palindrome}\ldots+t^{26}\end{array}\right)}{(1-t)^{66}(1-t^2)^{-3}(1-t^3)^{-1}}$
[020202]	Even Dual	$g_{NOL}^{E_6[020202]}(x,t)$	66	$\frac{\left(\begin{array}{c}1+7t+30t^2+100t^3+283t^4+710t^5\\+1623t^6+3364t^7+6314t^8+10710t^9+16269t^{10}\\+22197t^{11}+26940t^{12}+28824t^{13}+\ldots\,\text{palindrome}\ldots+t^{26}\end{array}\right)}{(1-t)^{71}(1-t^2)^{-3}(1-t^3)^{-2}}$

These moduli spaces are associated with SU(2) homomorphisms but do not represent additional nilpotent orbits (see text).

Table 7.15.: E_6 Extra Moduli Spaces and Hilbert Series

Characteristic	Character HWG	mHL HWG
[000000]	1	$\dots$
[000001]	$\frac{1}{1-m_6t}$	$\dots$
[100010]	$\frac{1}{(1-m_6t)(1-m_1m_5t^2)}$	$\dots$
[001000]	$\frac{1}{(1-m_6t)(1-m_1m_5t^2)(1-m_3t^3)(1-m_2m_4t^4)}$	$\dots$
[000002]	$\frac{1+m_3m_6t^5}{(1-m_6t)(1-m_1m_5t^2)(1-m_3t^3)(1-{m_6}^2t^4)(1-m_2m_4t^4)(1-m_3t^6)}$	$\dots$
$\dots$	$\dots$	$\dots$
[202020]	$\dots$	$1-h_6t^7-h_6t^8-h_6t^{11}+$ $h_1h_5t^{11}+h_1h_5t^{12}+h_1h_5t^{13}-h_3t^{16}$
[202022]	$\dots$	$1-h_6t^8-h_6t^{11}+h_1h_5t^{13}$
[220222]	$\dots$	$1-h_6t^{11}$
[222222]	$\dots$	1

An mHL HWG of 1 denotes $mHL^{E_6}_{[000000]}(t)$.
Orbits in the centre of the Hasse diagram remain to be calculated.

Table 7.16.: E_6 Orbits and HWGs

7.3.4. Orbits of E_7 and E_8

A comparable analysis for the 45 nilpotent orbits of E_7 and 70 orbits of E_8 poses computational challenges and it is only possible to present a partial picture. Tables 7.17 to 7.30 set out those Hilbert series and HWGs that have been calculated, along with details of the constructions. Unrefined HS for normal nilpotent orbits of E_7 and E_8 are shown in Tables 7.17 to 7.22 and 7.27 to 7.28; the normalisations of the 10 non-normal nilpotent orbits of E_7 are shown in Tables 7.23 and 7.24; the 8 extra root maps of E_7 are analysed in Tables 7.25 and 7.26; and the character HWGs for near minimal orbits of E_7 and E_8 are shown in Tables 7.29 and 7.30, respectively.

The pattern of results is similar to that for E_6. The near-minimal orbits are normal, with palindromic Hilbert series, and have character HWGs that are freely generated or complete intersections. All these orbits can be constructed using the NOL formula. In addition, the minimal and next to minimal orbits (and the next to next to minimal E_7 orbit), have Coulomb branch constructions. In all the cases calculated, the non-normal orbits are consistent with the established classification, described in section 4.4.7.

Turning to the 8 extra root maps of E_7. Amongst these: $E_7[2020000]$ and $E_7[0110100]$ are normal, with their unrefined HS matching $E_7[0200200]$ and $E_7[0020000]$, respectively; $E_7[2000002]$ appears to be non-normal, with its unrefined HS matching $E_7[0100011]$; of the others, four generate extensions that do not match either the orbits or their normalisations; and the unrefined HS of one remains to be calculated. Once again, these appear to provide examples of dualities, with at least three of the extra root maps from $SU(2)$ homomorphisms giving copies of nilpotent orbits.

The Weyl group of E_7 has 60 irreps and conjugacy classes. In [82], the 45 nilpotent orbits are identified as these conjugacy classes, modulo some actions of the symmetric groups S_2 or S_3. Six of the eight extra root maps, appear to correspond to other members of these conjugacy classes; however, these are identified in [82] by Bala Carter labels, so their root maps or Characteristics are not clear. The Weyl group of E_8 has 112 irreps and conjugacy classes. In [82], the 70 nilpotent orbits are identified as these conjugacy classes, modulo some actions of the symmetric groups S_2, S_3 or S_5. It can be anticipated that most of the 39 extra root maps of E_8 correspond to other members of these conjugacy classes.

Characteristic	Type	Construction	Dim.	Unrefined HS
[0000000]	Even	$g_{NOL}^{E_7[0000000]}(x,t)$	0	1
[1000000]	Rigid	$g_{Coulomb}^{E_7[1000000]}(x,t)$ or $g_{NOL}^{E_7[1000000]}(x,t)$	34	$\frac{\left(\begin{array}{c}1+98t+3312t^2+53305t^3+468612t^4\\+2421286t^5+7664780t^6+15203076t^7+19086400t^8\\+\ldots\,\text{palindrome}\,\ldots+t^{16}\end{array}\right)}{(1-t)^{34}(1+t)^{-1}}$
[0000100]	Rigid	$g_{Coulomb}^{E_7[0000100]}(x,t)$ or $g_{NOL}^{E_7[0000100]}(x,t)$	52	$\frac{\left(\begin{array}{c}1+79t+3161t^2+75291t^3+1158376t^4\\+12099785t^5+88650725t^6+465895118t^7+1783653576t^8\\+5026645901t^9+10497603729t^{10}+16309233956t^{11}+18885794304t^{12}\\+\ldots\,\text{palindrome}\,\ldots+t^{24}\end{array}\right)}{(1-t)^{52}(1+t)^{-2}}$
[0000020]	Even	$g_{Coulomb}^{E_7[0000020]}(x,t)$ or $g_{NOL}^{E_7[0000020]}(x,t)$	54	$\frac{\left(\begin{array}{c}1+76t+2928t^2+67583t^3+1012266t^4\\+10332067t^5+74214232t^6+383547072t^7+1448282149t^8\\+4037523484t^9+8366120760t^{10}+12936087566t^{11}+14955872444t^{12}\\+\ldots\,\text{palindrome}\,\ldots+t^{24}\end{array}\right)}{(1-t)^{54}(1+t)^{-3}}$
[0100000]	Rigid	$g_{NOL}^{E_7[0100000]}(x,t)$	64	$\frac{\left(\begin{array}{c}1+69t+2414t^2+55623t^3+919520t^4+11342968t^5+106958600t^6\\+784535006t^7+4537123626t^8+20910056245t^9+77451415678t^{10}\\+232139956863t^{11}+566045584244t^{12}+1127581533400t^{13}\\+1840753744695t^{14}+2467945228350t^{15}+2720953919604t^{16}\\+\ldots\,\text{palindrome}\,\ldots+t^{32}\end{array}\right)}{(1-t)^{64}}$
[2000000]	Even	$g_{NOL}^{E_7[2000000]}(x,t)$	66	$\frac{\left(\begin{array}{c}1+66t+2211t^2+48653t^3+769406t^4+9115701t^5+82935951t^6\\+589544021t^7+3317603364t^8+14933718295t^9+54217280987t^{10}\\+159809769683t^{11}+384450581989t^{12}+757911779139t^{13}\\+1228177330314t^{14}+1639405203212t^{15}+1804825398942t^{16}\\+\ldots\,\text{palindrome}\,\ldots+t^{32}\end{array}\right)}{(1-t)^{66}(1+t)^{-1}}$
[0000011]	Rigid	$g_{NOL}^{E_7[0000011]}(x,t)$	70	$\frac{\left(\begin{array}{c}1+60t+1832t^2+37940t^3+590418t^4+7183420t^5+69289970t^6\\+532384159t^7+3266437503t^8+16043947731t^9+63267289791t^{10}\\+200890430458t^{11}+515036877963t^{12}+1068616936078t^{13}\\+1797599354636t^{14}+2454711103950t^{15}+2723124368404t^{16}\\+\ldots\,\text{palindrome}\,\ldots+t^{32}\end{array}\right)}{(1-t)^{70}(1+t)^{-3}}$

Table 7.17.: E_7 Orbit Constructions and Hilbert Series (A)

Characteristic	Type	Construction	Dim.	Unrefined HS
[1000100]	Non-rigid	$g_{NOL}^{E_7[1000100]}(x,t)$	76	$\frac{\left(\begin{array}{c}1+55t+1541t^2+29315t^3+424272t^4+4952595t^5\\+47877722t^6+386190616t^7+2596530729t^8+14510866523t^9\\+67296385685t^{10}+259002809519t^{11}+828279369291t^{12}\\+2205076546265t^{13}+4896965388648t^{14}+9088788793591t^{15}\\+14120229879183t^{16}+18383918865257t^{17}+20072546522168t^{18}\\+\ldots\text{palindrome}\ldots+t^{36}\end{array}\right)}{(1-t)^{76}(1+t)^{-2}}$
[0010000]	Rigid	$g_{NOL}^{E_7[0010000]}(x,t)$	82	$\frac{\left(\begin{array}{c}1+48t+1178t^2+19696t^3+250716t^4+2565971t^5\\+21762497t^6+155518280t^7+944204003t^8+4887315987t^9\\+21592275087t^{10}+81450603000t^{11}+262392783373t^{12}\\+722133713475t^{13}+1698619550612t^{14}+3416812201696t^{15}\\+5880606714062t^{16}+8663598664204t^{17}+10929523033749t^{18}\\+11809319976778t^19+\ldots\text{palindrome}\ldots+t^38\end{array}\right)}{(1-t)^{82}(1+t)^{-3}}$
[0000002]	Even	$g_{NOL}^{E_7[0000002]}(x,t)$	84	$\frac{\left(\begin{array}{c}1+45t+1038t^2+16350t^3+196152t^4+1888083t^5+\\14993188t^6+99820004t^7+562706250t^8+2702760610t^9+\\11106249929t^{10}+39151678087t^{11}+118627422888t^{12}+\\309366846442t^{13}+695134757350t^{14}+1346841349931t^{15}+\\2251533783397t^{16}+3248988761423t^{17}+4048166195313t^{18}+\\4355986374750t^{19}+\ldots\text{palindrome}\ldots+t^{38}\end{array}\right)}{(1-t)^{84}(1+t)^{-4}}$
[0000200]	Even	$g_{NOL}^{E_7[0000200]}(x,t)$	84	$\frac{\left(\begin{array}{c}1+47t+1129t^2+18471t^3+231429t^4+2357290t^5+\\20161290t^6+147126015t^7+921831949t^8+4966553008t^9+\\23009208438t^{10}+91673050291t^{11}+314317403484t^{12}+\\928489331649t^{13}+2366228206771t^{14}+5209496539692t^{15}+\\9920162607040t^{16}+16355180626673t^{17}+23363121371124t^{18}+\\28931405790760t^{19}+31067160767506t^{20}+\ldots\text{palindrome}\ldots+t^{40}\end{array}\right)}{(1-t)^{84}(1+t)^{-2}}$
[2000100]	Non-rigid Non-normal	?	84	...
[2000020]	Even Non-normal	?	86	...

Table 7.18.: E_7 Orbit Constructions and Hilbert Series (B)

Characteristic	Type	Construction	Dim.	Unrefined HS
[0100100]	Rigid	$g_{NOL}^{E_7[0100100]}(x,t)$	90	$\frac{\left(\begin{array}{c}1+40t+822t^2+11560t^3+125053t^4+1107492t^5+\\ 8324729t^6+54205995t^7+308921360t^8+1547294387t^9+\\ 6817553073t^{10}+26416129223t^{11}+89960249299t^{12}+\\ 269160204736t^{13}+707461384957t^{14}+1633679518004t^{15}+\\ 3315057850714t^{16}+5912586107207t^{17}+9270875065762t^{18}+\\ 12781960001328t^{19}+15497517399838t^{20}+16525204589536t^{21}\\ +\ldots\text{palindrome}\ldots+t^{42}\end{array}\right)}{(1-t)^{90}(1+t)^{-3}}$
[1010000]	Rigid Non-normal	?	92	...
[0200000]	Even	$g_{NOL}^{E_7[0200000]}(x,t)$	94	$\frac{\left(\begin{array}{c}1+36t+668t^2+8508t^3+83586t^4+673392t^5+\\ 4607032t^6+27312586t^7+141941392t^8+650985986t^9+\\ 2645699417t^{10}+9554923437t^{11}+30727827270t^{12}+\\ 88136822566t^{13}+225764838482t^{14}+516956432313t^{15}+\\ 1058929210661t^{16}+1941429840126t^{17}+3186932272113t^{18}+\\ 4685112655122t^{19}+6169119469044t^{20}+7276373148733t^{21}+\\ 7687953729238t^{22}+\ldots\text{palindrome}\ldots+t^{44}\end{array}\right)}{(1-t)^{94}(1+t)^{-3}}$
[1001010]	Non-rigid Non-normal	?	94	...
[2200000]	Even	$g_{NOL}^{E_7[2200000]}(x,t)$	96	$\frac{\left(\begin{array}{c}1+33t+563t^2+6611t^3+60030t^4+447623t^5+\\ 2833362t^6+15497108t^7+73908939t^8+308781681t^9+\\ 1133005339t^{10}+3657592128t^{11}+10402882911t^{12}+\\ 26099373954t^{13}+57818269950t^{14}+113192145007t^{15}+\\ 195958590574t^{16}+300141740919t^{17}+406880376207t^{18}+\\ 488318218464t^{19}+518927857452t^{20}+\ldots\text{palindrome}\ldots+t^{40}\end{array}\right)}{(1-t)^{100}(1-t^2)^{-3}(1-t^6)^{-1}}$
[0100011]	Richardson Non-normal	?	96	...
[0010100]	Non-rigid Non-normal	?	98	...

Table 7.19.: E_7 Orbit Constructions and Hilbert Series (C)

Characteristic	Type	Construction	Dim.	Unrefined HS
[0002000]	Even	$g_{NOL}^{E_7[0002000]}(x,t)$	100	$\frac{\left(\begin{array}{c}1+29t+438t^2+4582t^3+37271t^4+250862t^5+\\ 1450141t^6+7367761t^7+33375509t^8+135968656t^9+\\ 500664993t^{10}+1670928197t^{11}+5061667873t^{12}+\\ 13926555453t^{13}+34810610044t^{14}+79050125417t^{15}+\\ 163069587001t^{16}+305534193394t^{17}+519874019101t^{18}+\\ 803213777947t^{19}+1126718360132t^{20}+1434898159505t^{21}+\\ 1658939075660t^{22}+1741143029810t^{23}+\ldots\text{palindrome}\ldots+t^{46}\end{array}\right)}{(1-t)^{100}(1+t)^{-4}}$
[2000200]	Even Non-normal	?	100	...
[2000220]	Even Non-normal	?	102	...
[2100011]	Non-rigid	$g_{NOL}^{E_7[2100011]}(x,t)$	102	$\frac{\left(\begin{array}{c}1+28t+408t^2+4116t^3+32280t^4+209580t^5+\\ 1171719t^6+5794499t^7+25834071t^8+105236571t^9+\\ 395177977t^{10}+1374921878t^{11}+4440514461t^{12}+\\ 13302464973t^{13}+36864118261t^{14}+94136235017t^{15}+\\ 220539780742t^{16}+471978064553t^{17}+919131363037t^{18}+\\ 1623431344293t^{19}+2593892844620t^{20}+3741627500468t^{21}+\\ 4865497692158t^{22}+5698077622856t^{23}+6006501802258t^{24}\\ +\ldots\text{palindrome}\ldots+t^{48}\end{array}\right)}{(1-t)^{102}(1+t)^{-3}}$
[1010100]	Richardson	$g_{NOL}^{E_7[1010100]}(x,t)$	104	$\frac{\left(\begin{array}{c}1+27t+379t^2+3681t^3+27784t^4+173459t^5+930518t^6\\ +4398690t^7+18647529t^8+71800205t^9+253451882t^{10}\\ +825944836t^{11}+2497351881t^{12}+7028854183t^{13}\\ +18440277693t^{14}+45077002396t^{15}+102476397815t^{16}\\ +216029662181t^{17}+420887182105t^{18}+755319761316t^{19}\\ +1244815205429t^{20}+1879314008730t^{21}+2593939349101t^{22}\\ +3268552500629t^{23}+3756276826771t^{24}+3934763086966t^{25}\\ +\ldots\text{palindrome}\ldots+t^{50}\end{array}\right)}{(1-t)^{104}(1+t)^{-2}}$
[0020000]	Even	$g_{NOL}^{E_7[0020000]}(x,t)$	106	$\frac{\left(\begin{array}{c}1+22t+254t^2+2048t^3+12949t^4+68223t^5+310470t^6\\ +1248798t^7+4509005t^8+14770398t^9+44209400t^{10}\\ +121447827t^{11}+306952315t^{12}+714370802t^{13}+1530391654t^{14}\\ +3014498298t^{15}+5450883816t^{16}+9031969079t^{17}\\ +13689807076t^{18}+18950786410t^{19}+23928392089t^{20}\\ +27532705839t^{21}+28852797782t^{22}+\ldots\text{palindrome}\ldots+t^{44}\end{array}\right)}{(1-t)^{111}(1-t^2)^{-2}(1-t^4)^{-1}(1-t^3)^{-2}}$

Table 7.20.: E_7 Orbit Constructions and Hilbert Series (D)

Characteristic	Type	Construction	Dim.	Unrefined HS
[2010100]	Richardson	$g_{NOL}^{E_7[2010100]}(x,t)$	106	$\frac{\left(\begin{array}{c}1+23t+278t^2+2347t^3+15528t^4+85677t^5+409818t^6\\+1744604t^7+6733298t^8+23872838t^9+78471083t^{10}\\+240598830t^{11}+690346420t^{12}+1854303338t^{13}\\+4651709274t^{14}+10851525702t^{15}+23419398905t^{16}\\+46527253037t^{17}+84742390056t^{18}+141081479581t^{19}\\+214295496214t^{20}+296699661744t^{21}+374312393511t^{22}\\+430286790879t^{23}+450739862708t^{24}+\ldots\,\text{palindrome}\,\ldots+t^{48}\end{array}\right)}{(1-t)^{110}(1-t^2)^{-3}(1-t^3)^{-1}}$
[2002000]	Even	$g_{NOL}^{E_7[2002000]}(x,t)$	108	$\frac{\left(\begin{array}{c}1+20t+213t^2+1601t^3+9511t^4+47457t^5+206535t^6\\+804110t^7+2849798t^8+9301048t^9+28157657t^{10}\\+79371845t^{11}+208613748t^{12}+511155245t^{13}+1166404057t^{14}\\+2475221676t^{15}+4877328017t^{16}+8910423434t^{17}\\+15071159308t^{18}+23570050287t^{19}+34043293243t^{20}\\+45364765295t^{21}+55726054790t^{22}+63063271014t^{23}\\+65720671708t^{24}+\ldots\,\text{palindrome}\,\ldots+t^{48}\end{array}\right)}{(1-t)^{113}(1-t^2)^{-4}(1-t^3)^{-1}}$
[1010200]	Non-rigid	$g_{NOL}^{E_7[1010200]}(x,t)$	108	$\frac{\left(\begin{array}{c}1+22t+254t^2+2047t^3+12926t^4+68080t^5+310960t^6\\+1264637t^7+4666092t^8+15835477t^9+49925712t^{10}\\+147222704t^{11}+407639569t^{12}+1061263019t^{13}\\+2596136476t^{14}+5955138398t^{15}+12772447382t^{16}\\+25532967194t^{17}+47425451135t^{18}+81608753812t^{19}\\+129761856605t^{20}+190227006014t^{21}+256633049320t^{22}\\+318159221002t^{23}+362094599888t^{24}+378074695796t^{25}\\+\ldots\,\text{palindrome}\,\ldots+t^{50}\end{array}\right)}{(1-t)^{111}(1-t^2)^{-2}(1-t^3)^{-1}}$
[1010120]	Non-rigid	$g_{NOL}^{E_7[1010120]}(x,t)$	108	...
[0200200]	Even	$g_{NOL}^{E_7[0200200]}(x,t)$	110	$\frac{\left(\begin{array}{c}1+19t+191t^2+1350t^3+7526t^4+35208t^5+143642t^6\\+524421t^7+1744507t^8+5355360t^9+15303933t^{10}\\+40934228t^{11}+102767564t^{12}+242325486t^{13}+536176791t^{14}\\+1110998287t^{15}+2150326632t^{16}+3877166750t^{17}\\+6495975323t^{18}+10090787477t^{19}+14505728258t^{20}\\+19267371072t^{21}+23618674467t^{22}+26697216460t^{23}\\+27811736966t^{24}+\ldots\,\text{palindrome}\,\ldots+t^{48}\end{array}\right)}{(1-t)^{114}(1-t^2)^{-2}(1-t^3)^{-1}(1-t^4)^{-1}}$
[0101021]	Non-rigid Non-normal	?	110	...

Some orbits in the upper Hasse diagram remain to be calculated.

Table 7.21.: E_7 Orbit Constructions and Hilbert Series (E)

Characteristic	Type	Construction	Dim.	Unrefined HS
[0020020]	Distinguished	$g_{NOL}^{E_7[0020020]}(x,t)$	112	$\frac{\left(\begin{array}{c}1+16t+138t^2+849t^3+4168t^4+17338t^5+63414t^6\\+208931t^7+630376t^8+1761854t^9+4597735t^{10}\\+11259794t^{11}+25951083t^{12}+56346651t^{13}+115226073t^{14}\\+221674893t^{15}+400557834t^{16}+678589198t^{17}+1075849008t^{18}\\+1593563475t^{19}+2202070691t^{20}+2835436943t^{21}\\+3398852391t^{22}+3790337376t^{23}+3930789260t^{24}\\+\ldots\text{palindrome}\ldots+t^{48}\end{array}\right)}{(1-t)^{117}(1-t^2)^{-3}(1-t^3)^{-1}(1-t^4)^{-1}}$
[2200200]	Even	$g_{NOL}^{E_7[2000202]}(x,t)$	112	$\frac{\left(\begin{array}{c}1+17t+154t^2+986t^3+5000t^4+21352t^5+79766t^6\\+267478t^7+820082t^8+2329206t^9+6180894t^{10}\\+15395201t^{11}+36035767t^{12}+79165241t^{13}+162774319t^{14}\\+312189809t^{15}+556698600t^{16}+920602987t^{17}+1409431708t^{18}\\+1996091906t^{19}+2614816619t^{20}+3169351708t^{21}\\+3556104836t^{22}+3695053378t^{23}+\ldots\text{palindrome}\ldots+t^{46}\end{array}\right)}{(1-t)^{116}(1-t^2)^{-2}(1-t^4)^{-1}(1-t^6)^{-1}}$
[0020200]	Even	$g_{NOL}^{E_7[0020200]}(x,t)$	114	$\frac{\left(\begin{array}{c}1+15t+120t^2+681t^3+3076t^4+11763t^5+39561t^6\\+119903t^7+332732t^8+854295t^9+2043682t^{10}+4576333t^{11}\\+9619784t^{12}+19009985t^{13}+35326464t^{14}+61701521t^{15}\\+101189577t^{16}+155639584t^{17}+224285198t^{18}+302586504t^{19}\\+382011620t^{20}+451230570t^{21}+498645737t^{22}+515532540t^{23}\\+\ldots\text{palindrome}\ldots+t^{46}\end{array}\right)}{(1-t)^{118}(1-t^2)^{-1}(1-t^3)^{-1}(1-t^4)^{-1}(1-t^6)^{-1}}$
[2101101]	Richardson	$g_{NOL}^{E_7[2101101]}(x,t)$	114	...
[2101021]	Richardson Non-normal	?	114	...
[2020020]	Even	$g_{NOL}^{E_7[2020020]}(x,t)$	116	$\frac{\left(\begin{array}{c}1+12t+80t^2+389t^3+1537t^4+5224t^5+15812t^6\\+43613t^7+111414t^8+266651t^9+602833t^{10}+1294980t^{11}\\+2653055t^{12}+5193586t^{13}+9719982t^{14}+17382620t^{15}\\+29666335t^{16}+48232766t^{17}+74551722t^{18}+109315541t^{19}\\+151747724t^{20}+199048858t^{21}+246304054t^{22}+287105977t^{23}\\+314916175t^{24}+324800118t^{25}+\ldots\text{palindrome}\ldots+t^{50}\end{array}\right)}{(1-t)^{121}(1-t^2)^{-3}(1-t^4)^{-1}(1-t^3)^{-1}}$
[2020200]	Even	$g_{NOL}^{E_7[2020200]}(x,t)$	118	$\frac{\left(\begin{array}{c}1+10t+55t^2+221t^3+726t^4+2068t^5+5291t^6\\+12441t^7+27313t^8+56496t^9+110640t^{10}+205664t^{11}\\+363299t^{12}+609916t^{13}+973433t^{14}+1477359t^{15}\\+2131586t^{16}+2921382t^{17}+3797706t^{18}+4673326t^{19}\\+5432001t^{20}+5951813t^{21}+6137514t^{22}+\ldots\text{palindrome}\ldots+t^{44}\end{array}\right)}{(1-t)^{123}(1-t^2)^{-1}(1-t^3)^{-1}(1-t^4)^{-1}(1-t^5)^{-1}(1-t^6)^{-1}}$
...	...	...	...	...
[2222222]	Distinguished	$g_{NOL}^{E_7[2222222]}(x,t)$	126	$\frac{(1-t^2)(1-t^6)(1-t^8)(1-t^{10})(1-t^{12})(1-t^{14})(1-t^{18})}{(1-t)^{133}}$

Some orbits in the upper Hasse diagram remain to be calculated.

Table 7.22.: E_7 Orbit Constructions and Hilbert Series (F)

Characteristic	Type	Construction	Dim.	Unrefined HS
[2000100]	Non-rigid Normalisation	$g_{NOL}^{E_7[2000100]}(x,t)$	84	$\frac{\left(\begin{array}{c}1+47t+1129t^2+18604t^3+236007t^4+2439134t^5+\\ 21162857t^6+156442728t^7+991136142t^8+5390236639t^9+\\ 25171607172t^{10}+100975434413t^{11}+348257944507t^{12}+\\ 1033980718497t^{13}+2646472834763t^{14}+5847508202694t^{15}+\\ 11167569105434t^{16}+18453105745417t^{17}+26401938893655t^{18}+\\ 32725550735483t^{19}+35152494567578t^{20}+\ldots\text{palindrome}\ldots+t^{40}\end{array}\right)}{(1-t)^{84}(1+t)^{-2}}$
[2000020]	Even Normalisation	$g_{NOL}^{E_7[2000020]}(x,t)$	86	$\frac{\left(\begin{array}{c}1+44t+992t^2+15401t^3+186066t^4+1858596t^5+\\ 15801050t^6+115491687t^7+726319079t^8+3923623495t^9+\\ 18189961165t^{10}+72405189290t^{11}+247811206611t^{12}+\\ 730559598720t^{13}+1858314990721t^{14}+4084659605334t^{15}+\\ 7767711560354t^{16}+12792450962244t^{17}+18258619963592t^{18}+\\ 22598363867429t^{19}+24262180770322t^{20}+\ldots\text{palindrome}\ldots+t^{40}\end{array}\right)}{(1-t)^{86}(1+t)^{-3}}$
[1010000]	Rigid Normalisation	$g_{NOL}^{E_7[1010000]}(x,t)$	92	$\frac{\left(\begin{array}{c}1+39t+781t^2+10832t^3+117764t^4+1068886t^5+\\ 8366502t^6+57321559t^7+345662862t^8+1837194990t^9+\\ 8607330680t^{10}+35546401942t^{11}+129433976719t^{12}+\\ 415755856459t^{13}+1178772756488t^{14}+2951866871355t^{15}+\\ 6532714259889t^{16}+12783348175656t^{17}+22127754013620t^{18}+\\ 33894008054339t^{19}+45953335735135t^{20}+55157071947443t^{21}+\\ 58617041465558t^{22}+\ldots\text{palindrome}\ldots+t^{44}\end{array}\right)}{(1-t)^{92}(1+t)^{-2}}$
[1001010]	Non-rigid Normalisation	$g_{NOL}^{E_7[1001010]}(x,t)$	94	$\frac{\left(\begin{array}{c}1+36t+668t^2+8641t^3+88240t^4+757413t^5+\\ 5640210t^6+36937648t^7+213664469t^8+1092448880t^9+\\ 4936955929t^{10}+19722690196t^{11}+69678831438t^{12}+\\ 217824528290t^{13}+602894508685t^{14}+1478256695785t^{15}+\\ 3212596081865t^{16}+6190973025268t^{17}+10583499697498t^{18}+\\ 16054911924583t^{19}+21617382287205t^{20}+25839887564200t^{21}+\\ 27422997701800t^{22}+\ldots\text{palindrome}\ldots+t^{44}\end{array}\right)}{(1-t)^{94}(1+t)^{-3}}$
[0100011]	Richardson Normalisation	$g_{NOL}^{E_7[0100011]}(x,t)$	96	$\frac{\left(\begin{array}{c}1+33t+564t^2+6777t^3+64849t^4+524725t^5+\\ 3696270t^6+22952836t^7+126186057t^8+614879502t^9+\\ 2656800340t^{10}+10184095054t^{11}+34652624372t^{12}+\\ 104728696487t^{13}+281292351713t^{14}+671789330508t^{15}+\\ 1427206725858t^{16}+2698313629951t^{17}+4541504048285t^{18}+\\ 6806645160112t^{19}+9086346089774t^{20}+10805286175350t^{21}+\\ 11447593810728t^{22}+\ldots\text{palindrome}\ldots+t^{44}\end{array}\right)}{(1-t)^{96}(1+t)^{-4}}$

Table 7.23.: E_7 Nilpotent Orbit Normalisations and Hilbert Series (A)

Characteristic	Type	Construction	Dim.	Unrefined HS
[0010100]	Non-rigid Normalisation	$g_{NOL}^{E_7[0010100]}(x,t)$	98	$\frac{\left(\begin{array}{c}1+32t+530t^2+6181t^3+57541t^4+453663t^5+\\ 3113473t^6+18837445t^7+101120527t^8+483453140t^9+\\ 2063999692t^{10}+7883746897t^{11}+26978747805t^{12}+\\ 82795280050t^{13}+228030235944t^{14}+563908554084t^{15}+\\ 1252637000445t^{16}+2500204122427t^{17}+4485045975803t^{18}+\\ 7232498422887t^{19}+10486086399152t^{20}+13671033536263t^{21}+\\ 16028614605883t^{22}+16901469671998t^{23}+\\ \ldots\text{palindrome}\ldots+t^{46}\end{array}\right)}{(1-t)^{98}(1+t)^{-3}}$
[2000200]	Even Normalisation	$g_{NOL}^{E_7[2000200]}(x,t)$	100	$\frac{\left(\begin{array}{c}1+31t+496t^2+5589t^3+50366t^4+384882t^5+\\ 2559623t^6+14987542t^7+77732943t^8+358507573t^9+\\ 1474780676t^{10}+5424817521t^{11}+17880645370t^{12}+\\ 52902604370t^{13}+140698668543t^{14}+336770031480t^{15}+\\ 726143059501t^{16}+1411518293411t^{17}+2475048767521t^{18}+\\ 3916605082526t^{19}+5595119586673t^{20}+7217473926998t^{21}+\\ 8408241643667t^{22}+8847237672754t^{23}+\ldots\text{palindrome}\ldots+t^{46}\end{array}\right)}{(1-t)^{100}(1+t)^{-2}(1+t^2)^{-1}}$
[2000220]	Even Normalisation	$g_{NOL}^{E_7[2000220]}(x,t)$	102	$\frac{\left(\begin{array}{c}1+28t+406t^2+4193t^3+35056t^4+250188t^5+\\ 1554077t^6+8463228t^7+40558959t^8+171532123t^9+\\ 641766636t^{10}+2128615090t^{11}+6269960410t^{12}+\\ 16425061205t^{13}+38313744215t^{14}+79664576550t^{15}+\\ 147784794213t^{16}+244777770909t^{17}+362202240175t^{18}+\\ 479033526384t^{19}+566445179272t^{20}+598980047444t^{21}\\ +\ldots\text{palindrome}\ldots+t^{42}\end{array}\right)}{(1-t)^{105}(1-t^2)^{-1}(1-t^4)^{-1}(1-t^6)^{-1}}$
[0101021]	Non-rigid Normalisation	$g_{NOL}^{E_7[0101021]}(x,t)$	110	...
[2101021]	Richardson Normalisation	$g_{NOL}^{E_7[2101021]}(x,t)$	114	...

Some orbits in the upper Hasse diagram remain to be calculated.

Table 7.24.: E_7 Nilpotent Orbit Normalisations and Hilbert Series (B)

Characteristic	Type	Construction	Dim.	Unrefined HS
[2000002]	Even Normalisation Dual	$g_{NOL}^{E_7[2000002]}(x,t)$	96	$\frac{\left(\begin{array}{c}1+33t+564t^2+6777t^3+64849t^4+524725t^5+\\ 3696270t^6+22952836t^7+126186057t^8+614879502t^9+\\ 2656800340t^{10}+10184095054t^{11}+34652624372t^{12}+\\ 104728696487t^{13}+281292351713t^{14}+671789330508t^{15}+\\ 1427206725858t^{16}+2698313629951t^{17}+4541504048285t^{18}+\\ 6806645160112t^{19}+9086346089774t^{20}+10805286175350t^{21}+\\ 11447593810728t^{22}+\ldots\,\text{palindrome}\,\ldots+t^{44}\end{array}\right)}{(1-t)^{96}(1+t)^{-4}}$
[0000202]	Even Cover	$g_{NOL}^{E_7[0000202]}(x,t)$	104	$\frac{\left(\begin{array}{c}1+27t+379t^2+3681t^3+27917t^4+176916t^5+977308t^6\\ +4835965t^7+21801267t^8+90393556t^9+346150921t^{10}\\ +1225347941t^{11}+4006584460t^{12}+12082557933t^{13}\\ +33549402062t^{14}+85635361526t^{15}+200649655775t^{16}\\ +431024819812t^{17}+847995374640t^{18}+1526658506276t^{19}\\ +2513332265924t^{20}+3781664655782t^{21}+5198296443145t^{22}\\ +6526055274327t^{23}+7481012613977t^{24}+7829538747780t^{25}\\ +\ldots\,\text{palindrome}\,\ldots+t^{50}\end{array}\right)}{(1-t)^{104}(1+t)^{-2}}$
[0200020]	Even Cover	$g_{NOL}^{E_7[0200020]}(x,t)$	104	$\frac{\left(\begin{array}{c}1+27t+379t^2+3681t^3+27917t^4+176916t^5+977308t^6\\ +4835965t^7+21801267t^8+90393556t^9+346150921t^{10}\\ +1225347941t^{11}+4006584460t^{12}+12082557933t^{13}\\ +33549402062t^{14}+85635361526t^{15}+200649655775t^{16}\\ +431024819812t^{17}+847995374640t^{18}+1526658506276t^{19}\\ +2513332265924t^{20}+3781664655782t^{21}+5198296443145t^{22}\\ +6526055274327t^{23}+7481012613977t^{24}+7829538747780t^{25}\\ +\ldots\,\text{palindrome}\,\ldots+t^{50}\end{array}\right)}{(1-t)^{104}(1+t)^{-2}}$
[2200020]	Even Cover	$g_{NOL}^{E_7[2200020]}(x,t)$	106	$\frac{\left(\begin{array}{c}1+23t+278t^2+2347t^3+15661t^4+88602t^5+443711t^6\\ +2019526t^7+8474061t^8+32964305t^9+118904753t^{10}\\ +396852983t^{11}+1222209842t^{12}+3464334539t^{13}\\ +9017094730t^{14}+21510440738t^{15}+46954294808t^{16}\\ +93667605825t^{17}+170596058804t^{18}+283478314657t^{19}\\ +429596168703t^{20}+593606736352t^{21}+747833464708t^{22}\\ +858975277303t^{23}+899574922840t^{24}+\ldots\,\text{palindrome}\,\ldots+t^{48}\end{array}\right)}{(1-t)^{110}(1-t^2)^{-3}(1-t^3)^{-1}}$

These moduli spaces are associated with SU(2) homomorphisms but do not represent additional nilpotent orbits (see text).

Table 7.25.: E_7 Extra Moduli Spaces and Hilbert Series (A)

Characteristic	Type	Construction	Dim.	Unrefined HS
[0110100]	Richardson Dual	$g_{NOL}^{E_7[0110100]}(x,t)$	106	$\frac{\left(\begin{array}{c}1+22t+254t^2+2048t^3+12949t^4+68223t^5+310470t^6\\+1248798t^7+4509005t^8+14770398t^9+44209400t^{10}\\+121447827t^{11}+306952315t^{12}+714370802t^{13}+1530391654t^{14}\\+3014498298t^{15}+5450883816t^{16}+9031969079t^{17}\\+13689807076t^{18}+18950786410t^{19}+23928392089t^{20}\\+27532705839t^{21}+28852797782t^{22}+\ldots\text{palindrome}\ldots+t^{44}\end{array}\right)}{(1-t)^{111}(1-t^2)^{-2}(1-t^3)^{-2}(1-t^4)^{-1}}$
[2020000]	Even Dual	$g_{NOL}^{E_7[2020000]}(x,t)$	110	$\frac{\left(\begin{array}{c}1+19t+191t^2+1350t^3+7526t^4+35208t^5+143642t^6\\+524421t^7+1744507t^8+5355360t^9+15303933t^{10}\\+40934228t^{11}+102767564t^{12}+242325486t^{13}+536176791t^{14}\\+1110998287t^{15}+2150326632t^{16}+3877166750t^{17}\\+6495975323t^{18}+10090787477t^{19}+14505728258t^{20}\\+19267371072t^{21}+23618674467t^{22}+26697216460t^{23}\\+27811736966t^{24}+\ldots\text{palindrome}\ldots+t^{48}\end{array}\right)}{(1-t)^{114}(1-t^2)^{-2}(1-t^3)^{-1}(1-t^4)^{-1}}$
[2000202]	Even Cover	$g_{NOL}^{E_7[2000202]}(x,t)$	112	$\frac{\left(\begin{array}{c}1+16t+138t^2+849t^3+4168t^4+17471t^5+65408t^6\\+225142t^7+724817t^8+2200974t^9+6320547t^{10}\\+17149886t^{11}+43841235t^{12}+105203348t^{13}+236137382t^{14}\\+494303171t^{15}+962735326t^{16}+1741496782t^{17}\\+2921452525t^{18}+4539095853t^{19}+6523887358t^{20}\\+8663785096t^{21}+10619676955t^{22}+12004111582t^{23}\\+12505497100t^{24}+\ldots\text{palindrome}\ldots+t^{48}\end{array}\right)}{(1-t)^{117}(1-t^2)^{-3}(1-t^3)^{-1}(1-t^4)^{-1}}$
[2011010]	Non-rigid Extra	$g_{NOL}^{E_7[2011010]}(x,t)$	112	...

These moduli spaces are associated with SU(2) homomorphisms but do not represent additional nilpotent orbits (see text).

Table 7.26.: E_7 Extra Moduli Spaces and Hilbert Series (B)

Characteristic	Type	Construction	Dim.	Unrefined HS
[00000000]	Trivial	$g_{NOL}^{E_8[00000000]}(x,t)$	0	1
[00000010]	Rigid	$g_{Coulomb}^{E_8[00000010]}(x,t)$ or $g_{NOL}^{E_8[00000010]}(x,t)$	58	$\frac{\left(\begin{array}{c}1+189t+14080t^2+562133t^3+13722599t^4+220731150t^5\\+2454952400t^6+19517762786t^7+113608689871t^8\\+492718282457t^9+1612836871168t^{10}\\+4022154098447t^{11}+7692605013883t^{12}+11332578013712t^{13}\\+12891341012848t^{14}+\ldots\,\text{palindrome}\,\ldots+t^{28}\end{array}\right)}{(1-t)^{58}(1+t)^{-1}}$
[10000000]	Rigid	$g_{Coulomb}^{E_8[10000000]}(x,t)$ or $g_{NOL}^{E_8[10000000]}(x,t)$	92	$\frac{\left(\begin{array}{c}1+154t+11936t^2+590394t^3+20506501t^4+527204320t^5\\+10378075500t^6+160202160870t^7+1974075401833t^8\\+19687582048248t^9+160663069166772t^{10}+1082397634755580t^{11}\\+6063957293140705t^{12}+28419656685639506t^{13}\\+111973818366411496t^{14}+372403620091866888t^{15}\\+1048956129150029406t^{16}+2509111945366416404t^{17}\\+5107852437413443490t^{18}+8864217905887836806t^{19}\\+13130135397834893988t^{20}+16614983532652987182t^{21}\\+17970189038072829240t^{22}+\ldots\,\text{palindrome}\,\ldots+t^{44}\end{array}\right)}{(1-t)^{92}(1+t)^{-2}}$
[00000100]	Rigid	$g_{NOL}^{E_8[00000100]}(x,t)$	112	$\frac{\left(\begin{array}{c}1+136t+9315t^2+428400t^3+14708060t^4+396277232t^5\\+8617281802t^6+154047376228t^7+2294538829234t^8\\+28778512108660t^9+306547418244756t^{10}+2793130207608416t^{11}\\+21902089359475164t^{12}+148574498522828576t^{13}\\+875844462689467918t^{14}+4504433101633914112t^{15}\\+20280338406367275682t^{16}+80174835126831444248t^{17}\\+279043709885823869536t^{18}+856992570120176226304t^{19}\\+2327140363248048742796t^{20}+5597079269967040359776t^{21}\\+11940943517987127026935t^{22}+22625554953126294656764t^{23}\\+38114904246052740864163t^{24}+57133198249164919950508t^{25}\\+76253347580416742978018t^{26}+90657328908674311746240t^{27}\\+96036853608886812320440t^{28}+\ldots\,\text{palindrome}\,\ldots+t^{56}\end{array}\right)}{(1-t)^{112}}$

Table 7.27.: E_8 Orbit Constructions and Hilbert Series (A)

Characteristic	Type	Construction	Dim.	Unrefined HS
[00000020]	Even	$g_{NOL}^{E_8[00000020]}(x,t)$	114	$\frac{\left(\begin{array}{c}1+133t+8911t^2+400995t^3+13486580t^4+356584057t^5\\+7623391966t^6+134206634140t^7+1971437827690t^8\\+24415159489727t^9+257072913186568t^{10}+2317538562914724t^{11}\\+17995649940635004t^{12}+120979229232553840t^{13}\\+707282480739436178t^{14}+3609956701308961796t^{15}\\+16140434282332124866t^{16}+63405524248622811378t^{17}\\+219417855826005179940t^{18}+670412057684945457526t^{19}\\+1812177346079591528612t^{20}+4341065907801003784365t^{21}\\+9229322963452174348555t^{22}+17436647191913535443645t^{23}\\+29303858730884657436479t^{24}+43844634221326426603948t^{25}\\+58440640016940455205864t^{26}+69425059021468796578222t^{27}\\+73525348635628936776580t^{28}+\ldots\,\text{palindrome}\,\ldots+t^{56}\end{array}\right)}{(1-t)^{114}(1+t)^{-1}}$
...	...	...	...	...
[22222222]	Distinguished	$g_{NOL}^{E_8[22222222]}(x,t)$	240	$\frac{(1-t^2)(1-t^8)(1-t^{12})(1-t^{14})(1-t^{18})(1-t^{20})(1-t^{24})(1-t^{30})}{(1-t)^{240}}$

Orbits in the centre of the Hasse diagram remain to be calculated.

Table 7.28.: E_8 Orbit Constructions and Hilbert Series (B)

Characteristic	Character HWG	mHL HWG
[0000000]	1	$\dots$
[1000000]	$\frac{1}{1-m_1t}$	$\dots$
[0000100]	$\frac{1}{(1-m_1t)(1-m_5t^2)}$	$\dots$
[0000020]	$\frac{1}{(1-m_1t)(1-m_5t^2)(1-{m_6}^2t^3)}$	$\dots$
[0100000]	$\frac{1}{(1-m_1t)(1-m_2t^3)(1-m_3t^4)(1-m_5t^2)}$	$\dots$
[2000000]	$\frac{1-{m_1}^2{m_2}^2t^{10}}{(1-m_1t)(1-{m_1}^2t^4)(1-m_2t^3)(1-{m_2}^2t^6)(1-m_3t^4)(1-m_5t^2)(1-m_1m_2t^5)}$	$\dots$
$\dots$	$\dots$	$\dots$
[2222222]	$\dots$	1

An mHL HWG of 1 denotes $mHL^{E_7}_{[0000000]}(t)$.
Orbits in the centre of the Hasse diagram are not shown.

Table 7.29.: E_7 Orbits and HWGs

Characteristic	Character HWG	mHL HWG
[00000000]	1	...
[00000010]	$\frac{1}{1-m_7t}$	...
[10000000]	$\frac{1}{(1-m_7t)(1-m_1t^2)}$	...
[00000100]	$\frac{1}{(1-m_7t)(1-m_1t^2)(1-m_6t^3)(1-m_5t^4)}$	...
[00000020]	$\frac{1-{m_6}^2{m_7}^2t^{10}}{(1-m_7t)(1-m_1t^2)(1-m_6t^3)(1-m_5t^4)(1-{m_7}^2t^4)(1-m_6m_7t^5)(1-{m_6}^2t^6)}$	...
...	...	...
[22222222]	...	1

An mHL HWG of 1 denotes $mHL^{E_8}_{[00000000]}(t)$.
Orbits in the centre of the Hasse diagram are not shown.

Table 7.30.: E_8 Orbits and HWGs

8. Deconstructions

A considerable portion of this study has been devoted to examining the relationship between the moduli spaces of quiver theories and the nilpotent orbits of G. Nilpotent orbits provide a structured context for the exploration of many relationships between quiver theories, beyond the $3d$ mirror symmetry and other dualities examined thus far. Such relationships can result from various mechanisms, including, inter alia, branchings to subgroups of G and HyperKähler quotients by gauge groups.

Under some types of branching relationship (introduced in section 2.6), a quiver theory is equivalent to a combination of *glued* quiver theories. Such branchings can be thought of as *deconstructions*, in which no information is lost and the original moduli space can be reassembled. Deconstructions are facilitated by standard building blocks and these can be provided by modified Hall Littlewood functions, which form an orthogonal basis.

Importantly, while singlet modified Hall Littlewood functions correspond to (uncharged) maximal nilpotent orbits, all A series modified Hall Littlewood functions correspond to Coulomb branches of (a class of) $T(SU(N))$ quiver theories with background flavour charges. In the brane view of $T(SU(N))$ theories [31], the $D5$ branes carry these monopole flavour charges, while the $NS5$ and $D3$ branes supply the $U(N)$ gauge group structure.

Under a HyperKähler quotient, which gauges away a subgroup, for example, after symmetry breaking through subgroup branching, a quiver theory for a nilpotent orbit of G may reduce to a quiver theory for a nilpotent orbit of a subgroup of G.

We can use the methods described in Chapter 2 to decompose the refined Hilbert series of nilpotent orbit quiver theories into representations and/or modified Hall Littlewood functions of subgroups and thereby explore such types of relationship.

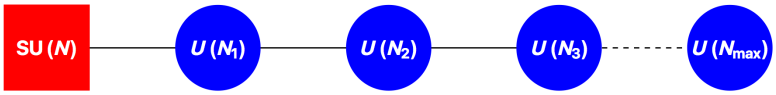

Figure 8.1.: The $T_{\hat{\rho}}(SU(N))$ quiver consists of a $SU(N)$ flavour node connected to gauge nodes $U(N_1)$ through $U(N_{\max})$, where the increments are described by the partition $\hat{\rho} = (N - N_1, \ldots, N_{\max -1} - N_{\max})$. The flavour node carries fixed monopole charges described by a second partition λ.

8.1. mHL Functions and $T(SU(N))$

One of the remarkable aspects of the A series mHL functions is that they correspond to the Coulomb branches of certain $\mathcal{N} = 4$ SUSY quiver gauge theories in $2+1$ dimensions, within the class known as $T^{\sigma}_{\hat{\rho}}(SU(N))$ [31, 55], (where $\hat{\rho}$ is used to denote the transpose of ρ).

When $\sigma = (1^N)$, the quivers take the linear form in Figure 8.1 and the Higgs branches of these theories correspond to the A series nilpotent orbits defined by ρ. The case $\hat{\rho} = (1^N) \leftrightarrow \rho = N$ gives the maximal nilpotent orbit. If these quivers are generalised, by assigning external charges λ to the flavour node, then the Coulomb branches of the family of quivers with $\hat{\rho} = (1^N)$ correspond to the mHL basis functions, defined in 2.18, with quivers carrying zero charge giving mHL singlets (i.e. maximal nilpotent orbits). These theories, in which $\sigma = \hat{\rho} = (1^N)$, are often simply referred to as $T(SU(N))$.

Following [55], the Coulomb branch formula 6.2 can be adapted to attach fixed monopole charges to the flavour node. These charges are described by a partition $\lambda \equiv (\lambda_1, \ldots, \lambda_N)$, where $\lambda_N = 0$, and the partitions map to $SU(N)$ highest weight Dynkin labels $[n] \equiv [n_1, \ldots, n_r]$ through the relationship $\lambda_j = \sum_{i=j}^{r} n_i$.

The monopole formula for $T(SU(N))$ becomes[1]:

$$T(SU(N))\,(\lambda, z, t) \equiv \sum_{q} P_q^{U(N)}\,(t)\, z_0^{-|\lambda|} z^{-q} t^{\Delta(q,\lambda)}, \tag{8.1}$$

[1]Note the signs of the exponents of the roots; these are chosen for consistency with the mHL definitions used herein.

where $|\lambda| \equiv \sum_{i=1}^{N} \lambda_i$, and z_0 can be chosen by an overall gauge invariance condition:

$$z_0^N \prod_{i=1}^{r} z_i^{N_i} = 1. \tag{8.2}$$

The Cartan matrix relationship between fugacities for $SU(N)$ weights and simple roots, $x_1^N = \prod_{i=1}^{N-1} z_i^{N-i}$, entails that $z_0^{-1} = x_1$.

With a little work, 8.1 can be rearranged into a recursive set of relations:

$$\begin{aligned} T(SU(N))(\lambda, z, t) = x_1^{|\lambda|} \sum_{q_1 \geq \cdots \geq q_{N-1} \geq -\infty}^{\infty} & P_q^{U(N-1)}(t)\, x_1^{-\frac{N}{N-1}|q|} t^{\Delta(q,\lambda)} \\ & \times\ T(SU(N-1))(q, z_2, \ldots, z_{N-1}, t), \end{aligned} \tag{8.3}$$

where $z \equiv (z_1, \ldots, z_{N-1})$, $q \equiv (q_1, \ldots, q_{N-1})$, and

$$\Delta(q, \lambda) = \frac{1}{2} \sum_{i=1}^{N} \sum_{j=1}^{N-1} |\lambda_i - q_j| - \sum_{i=1}^{N-1} \sum_{j=1}^{i-1} |q_i - q_j|. \tag{8.4}$$

The $U(N)$ Casimir symmetry factors, which depend, as before, on the partition q of monopole charges on each node, are given by:

$$P_q^{U(N)} = \prod_{i=1}^{N} \frac{1}{1 - t^{d_i(q)}}. \tag{8.5}$$

The recursion relations 8.3 assume the q form an ordered partition, but may range over both positive and negative integers. Each summation corresponds to one of the gauge nodes.

We set $T(SU(1)) = 1$ and the second member of the series follows as:

$$T(SU(2))(\lambda_1, \lambda_2, z_1, t) = x_1^{(\lambda_1+\lambda_2)} \frac{1}{(1-t)} \sum_{q_1=-\infty}^{\infty} z_1^{-q_1} t^{\frac{1}{2}|\lambda_1 - q_1| + \frac{1}{2}|\lambda_2 - q_1|}, \tag{8.6}$$

where $z_1 = x_1^2$.

As shown in [55], the $T(SU(N))$ Hilbert series correspond to modified Hall-Littlewood polynomials of $SU(N)$. The correspondence is modulated by a pre-factor in t, so that:

$$mHL_{[n]}(z,t) = t^{-\rho_w.\mathcal{G}.[n]} T(SU(N))(\lambda(n), z, t). \tag{8.7}$$

The exponent of the pre-factor equals the contraction of the Weyl vector ρ_w, which is $(1,\ldots,1)$ in a canonical basis of CSA coordinates, with the Dynkin labels of the mHL polynomial, using the group metric tensor $\mathcal{G}$.[2]

In principle, as discussed in [29], any refined Hilbert series, expressed in terms of class functions of G, can be branched to a semi-simple subgroup of G that consists solely of A series groups. It can then be decomposed into A series modified Hall Littlewood polynomials and thereby expressed as a summation over a series of $T(SU(N))$ quiver theories.

8.1.1. $T(SU(N))$ and Star Shaped Quivers

Some of these deconstructions are more elegant than others, with interesting examples being provided by families of *star-shaped* quivers. For example, the deconstructions of certain nilpotent orbits of Classical and Exceptional groups into A series mHL polynomials follow the structural relationships between their Coulomb branch quiver theories (which are based on Dynkin diagrams) and the linear quivers of $T(SU(N))$. Figure 8.2 shows the quiver diagrams involved in these family relationships; the Dynkin diagrams can be constructed by identifying the flavour nodes of the $T(SU(N))$ quivers.

The non-trivial aspect of these deconstructions is that of finding the branching coefficients into mHL functions; while these can be expected to reflect the symmetries of the diagrams, they can also incorporate non-obvious patterns, particularly for the non-simply laced diagrams.

One way of finding the branching coefficients for the simply laced $D_4 \to A_1^{\otimes 4}$ and $E_6 \to A_2^{\otimes 3}$ deconstructions is to rearrange the Coulomb branch constructions (discussed in section 6.2) for the RSIMS (or minimal nilpotent orbits), under a gauge choice that sets the lowest $U(1)$ monopole charge of the central node of the D_4 or E_6 extended Dynkin diagram to zero, such that the contributions of each leg can be separated from the residual *gluing* coefficients.

The more general method, however, for deconstructing a refined Hilbert

[2] While mHL polynomials with similar properties can be defined for other groups, the $T(G)$ quiver theories that have been proposed for these functions, other than for isomorphisms with the A series, face some critical issues.

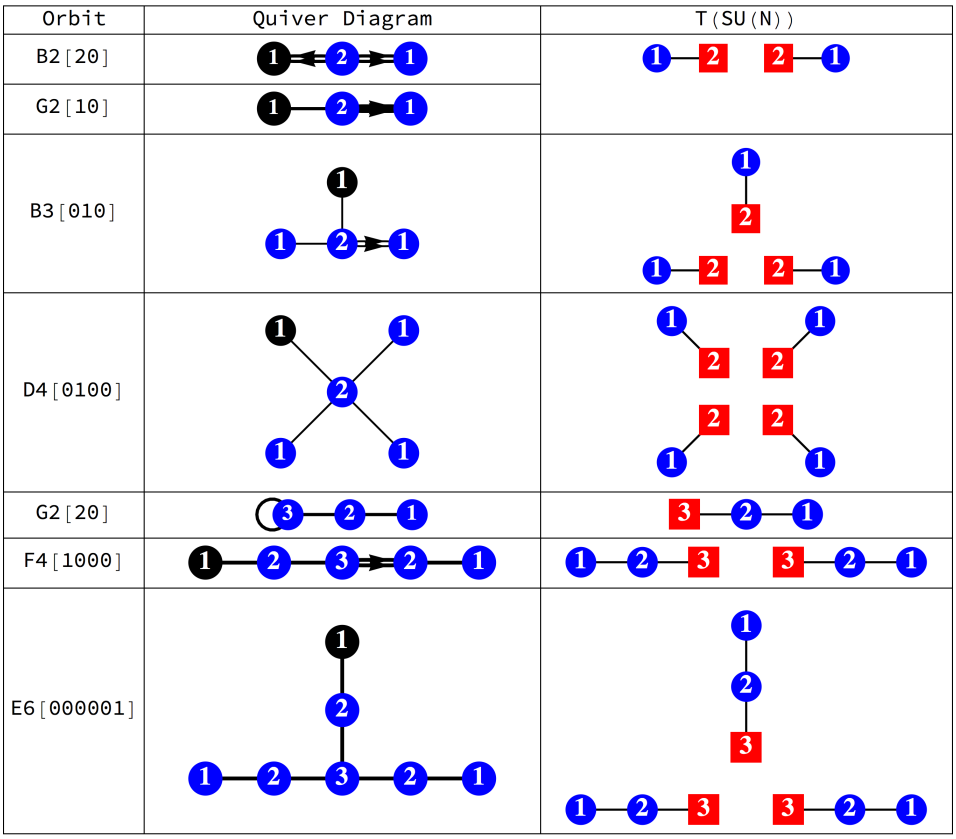

Figure 8.2.: Quivers for Nilpotent Orbit deconstructions to $T(SU(N))$. Blue nodes denote simple roots. Affine Dynkin diagrams are labelled with black nodes indicating the affine root. The dual Coxeter numbers of each node are shown. The quiver diagram for $G_2[20]$ is a hybrid in which the $SU(3)$ gauge node is self linking and contains the flavour node. $T(SU(N))$ quivers are labelled as in Figure 8.1.

series into mHL functions, is to find the $C_{[n]} \cong C_\lambda$ branching coefficients, defined as in 2.26, by using 2.27. As an example, the calculation of the $C_{[n]}$ for the deconstruction of the RSIMS of D_4 into mHL functions of the semi-simple ${A_1}^{\otimes 4} \equiv A_1 \otimes A_1 \otimes A_1 \otimes A_1$ subgroup proceeds as follows.

We wish to calculate the coefficients $C_{[n_A],[n_B],[n_C],[n_D]}(t)$ such that:

$$g^{D_4}_{HS:RSIMS}(w,x,y,z,t) = g^{A_1^{\otimes 4}}(a,b,c,d,t)\Big|_{(a,b,c,d)\to(w,x,y,z)},$$

where

$$g^{A_1^{\otimes 4}}(a,b,c,d,t) = \sum_{[n_A],[n_B],[n_C],[n_D]} C_{[n_A],[n_B],[n_C],[n_D]}(t)\ mHL^{A_1}_{[n_A]}(a,t) \times mHL^{A_1}_{[n_B]}(b,t)\ mHL^{A_1}_{[n_C]}(c,t)\ mHL^{A_1}_{[n_D]}(d,t). \tag{8.8}$$

We start with the expansion[3] for $g^{D_4}_{HS:RSIMS}(w,x,y,z,t)$, obtained by one of the methods in sections 2.2, 5.1 or 6.2, where $\{w,x,y,z,t\}$ are CSA coordinates for D_4. By eliminating the second node in the extended Cartan matrix of D_4, and using the relationships between roots and weights encoded and the Cartan matrices of A_1 and D_4, we obtain the root and CSA coordinate mappings in Table 8.1.

Table 8.1.: D_4 to ${A_1}^{\otimes 4}$ Simple Root and CSA Coordinate Mappings

D_4 roots	D_4 CSA coords	${A_1}^{\otimes 4}$ roots	${A_1}^{\otimes 4}$ CSA coords
z_1	w^2x	z_a	a^2
z_2	x^2/wyz	$-$	$-$
z_3	y^2/x	z_b	b^2
z_4	z^2/x	z_c	c^2
z_0	$1/x$	z_d	d^2

We solve the root mapping $\{z_1 \leftrightarrow z_a, z_3 \leftrightarrow z_b, z_4 \leftrightarrow z_c, z_0 \leftrightarrow z_d\}$ to obtain the CSA coordinate mapping $\{w \leftrightarrow \frac{a}{d}, x \leftrightarrow \frac{1}{d^2}, y \leftrightarrow \frac{b}{d}, z \leftrightarrow \frac{c}{d}\}$ and use this to transform $g^{D_4}_{HS:RSIMS}(w,x,y,z,t)$ to $g^{A_1^{\otimes 4}}(a,b,c,d,t)$. We then introduce generating functions for the $\overline{g_{mHL}}$ using the Dynkin label fugacities

[3]The refined Hilbert series is not shown here since it is rather lengthy.

h_A, h_B, h_C, h_D and specialise 2.27 as:

$$\begin{aligned} g_{HWG}^{A_1^{\otimes 4}}(h,t) &\equiv \sum_{[n_A],[n_B],[n_C],[n_D]=[0]}^{\infty} C_{[n_A][n_B][n_C][n_D]}(t)\ {h_A}^{n_A} {h_B}^{n_B} {h_C}^{n_C} {h_D}^{n_D} \\ &= \oint_{A_1^{\otimes 4}} d\mu_{mHL}^{A_1^{\otimes 4}}\ \overline{g_{mHL}^{A_1}}(a^*, h_A, t)\ \overline{g_{mHL}^{A_1}}(b^*, h_B, t) \\ &\quad \times\ \overline{g_{mHL}^{A_1}}(c^*, h_C, t)\ \overline{g_{mHL}^{A_1}}(d^*, h_D, t)\ g^{A_1^{\otimes 4}}(a,b,c,d,t)\,. \end{aligned} \tag{8.9}$$

The Hall-Littlewood polynomials of A_1, follow from 2.17 and can be expressed in terms of characters $[n]$ as:

$$HL_{[n]}^{A_1}(\chi, t) = \begin{cases} n = 0 : 1 + t \\ n = 1 : [1] \\ n \geq 2 : [n] - t\,[n-2] \end{cases}. \tag{8.10}$$

Their generating function follows from 2.22 and can be encoded as a highest weight generating function, using h as the HL Dynkin label fugacity:

$$g_{HL}^{A_1}(\chi, h, t)\ = (1 + t - [1]\,ht)\ PE\,[[1]\,h]\,. \tag{8.11}$$

The generating function $\overline{g_{HL}^{A_1}}$ for the conjugate orthonormal Hall-Littlewood polynomials $\overline{HL_{[n]}^{A_1}}$ differs from $g_{HL}^{A_1}$ in its numerator, as discussed in section 2.4:

$$\overline{g_{HL}^{A_1}}(\chi, h, t) = \left(1 - h^2 t\right)\ PE\,[[1]\,h]\,. \tag{8.12}$$

The modified Hall-Littlewood polynomials $mHL_{[n]}^{A_1}$, $\overline{mHL_{[n]}^{A_1}}$ and their generating functions all differ from the above by the pre-factor, $PE[[2]t - t]$:

$$\begin{aligned} g_{mHL}^{A_1}(\chi, h, t) &= PE[[2]t - t]\ g_{HL}^{A_1}(\chi, h, t)\,, \\ \overline{g_{mHL}^{A_1}}(\chi, h, t) &= PE[[2]t - t]\ \overline{g_{HL}^{A_1}}(\chi, h, t)\,. \end{aligned} \tag{8.13}$$

We evaluate 8.9, by taking the conjugate generating functions from 8.13, expanding the characters, and applying Weyl integration using the mHL Haar measure, to obtain:

$$g_{HWG}^{A_1^{\otimes 4}}(h,t) = \frac{1 - h_A^2 h_B^2 h_C^2 h_D^2 t^4}{(1-t^2)(1 - h_A h_B h_C h_D t)(1 - h_A h_B h_C h_D t^2)}. \tag{8.14}$$

Family	mHL HWG for $C_{[n]}$	
$\left.\begin{array}{r} B_2[20] \\ G_2[10] \\ B_3[010] \\ D_4[0100] \end{array}\right\} \rightarrow {A_1}^{\otimes r}$	$\frac{1-h^2t^4}{(1-t^2)(1-ht)(1-ht^2)}$	$\left\{\begin{array}{l} B_2 : h \equiv h_A h_B \\ G_2 : h \equiv h_A^3 h_B \\ B_3 : h \equiv h_A h_B^2 h_C \\ D_4 : h \equiv h_A h_B h_C h_D \end{array}\right.$
$\left.\begin{array}{r} G_2[20] \\ F_4[1000] \\ E_6[000001] \end{array}\right\} \rightarrow {A_2}^{\otimes r/2}$	$\frac{1+h_1t^2+h_2t^2+h_1t^3+h_2t^3+h_1h_2t^5}{(1-t^2)(1-t^3)(1-h_1t)(1-h_2t)}$	$\left\{\begin{array}{l} G_2 : h_i \equiv h_{Ai} \\ F_4 : h_i \equiv h_{Ai} h_{Bi}^2 \\ E_6 : h_i \equiv h_{Ai} h_{Bi} h_{Ci} \end{array}\right.$

Table 8.2.: mHL HWGs for Nilpotent Orbits of $T(SU(N))$ families

This simple HWG is of a diagonal form, in which the Dynkin label fugacities of different subgroups always appear with matching exponents. Taylor series expansion yields the explicit non-zero $C_{[n]}(t)$ coefficients:

$$C_{[n][n][n][n]}(t) = \begin{cases} n = 0 : \left(1 - t^2\right)^{-1} \\ n \geq 1 : t^n (1-t)^{-1}. \end{cases} \tag{8.15}$$

These can be checked by substitution back into 8.8 followed by Taylor expansion or gluing to recover the RSIMS for D_4. The coefficients follow a pattern related to the $SU(2)$ Casimir symmetry factors discussed in Chapter 6.

We can repeat the procedure described for D_4 for a selection of lower rank Classical and Exceptional groups. The low dimensions of the HWGs built on mHL polynomials can lead to particularly simple decompositions of RSIMS into A series subgroups. These include two families, $B_2, G_2, B_3, D_4 \rightarrow {A_1}^{\otimes r}$ and $G_2, F_4, E_6 \rightarrow {A_2}^{\otimes r/2}$ that have simple HWGs of dimension 2 and 4 respectively, as shown in Table 8.2. The A_1 family shares $D_4[0100] \cong A_1^{\otimes 4}$ and $B_2[20] \cong A_1^{\otimes 2}$ with the quivers constructed from $SU(2)$ tri-fundamental fields, against a background of $\mathcal{N} = 2$ SUSY in $(3+1)$ dimensions in [83].

As the limiting case of a star shaped quiver with a single arm, it is notable that the 10 dimensional G_2 nilpotent orbit can be deconstructed into mHL^{A_2} functions, equivalent to $T(SU(3))$ quivers. The G_2 orbit is obtained, after an elementary transformation from G_2 to A_2, by summing over the flavour nodes of the $T(SU(3))$ quiver. The $C_{[n]}$ coefficients can be found from the refined Hilbert series for $G_2[20]$ by projection methods, similar to the D_4 RSIMS example above, and turn out to complete the

$T(SU(3))$ family in Table 8.2. This nilpotent orbit can also be constructed directly, as shown in [23], on the Coulomb branch of the quiver in Figure 8.2, in which one of the gauge nodes is self-linking.

8.1.2. $T^{\sigma}_{\hat{\rho}}(SU(N))$ Theories

A more substantial class of modifications to the Hall-Littlewood polynomials is implemented in [26], where these (heavily) modified Hall-Littlewood functions are used to construct the RSIMS of E_6, E_7 and E_8. In the case of E_6, the result is equivalent to that obtained by the mHL deconstruction described above. For E_7 and E_8 RSIMS, the (heavily) modified Hall-Littlewood functions incorporate elements of the broader class of $T^{\sigma}_{\hat{\rho}}(SU(N))$ theories, introduced above. The quivers for the Coulomb branch constructions of Exceptional group nilpotent orbits in Figure 6.13 all contain linear sub-quivers, such as $[4]-(2)$, $[6]-(3)$ and $[6]-(4)-(2)$, that correspond to $T^{\sigma}_{\hat{\rho}}(SU(N))$ theories, where $\sigma=(1^N)$, and $\hat{\rho}=(2^2)$ or (3^2) or (2^3), respectively.

The (heavy) modifications involve subjecting the Hall-Littlewood polynomials to a branching map that, at the risk of introducing divergences, treats t as a unimodular $SU(2)$ fugacity; the resulting functions are prefixed by a number of factors and glued together with $C_{[n][n][n]}$ branching coefficients. The constructions are guided by a conjectured characterisation of punctures on Riemann spheres wrapped by $M5$ branes, which helps to identify those combinations of A series (heavily) modified Hall-Littlewood polynomials that yield the desired moduli spaces.

These (heavily) modified Hall-Littlewood polynomials provide alternative building blocks to the monopole formula for some Coulomb branches. Their usage presupposes that the quiver diagram symmetries are readily identifiable; they can be used on quivers that are simply laced, with a central gauge node, single flavour node, and linear arms, even if some of these do not obey $\rho=(1^N)$.

While the (heavily) modified Hall-Littlewood polynomials can facilitate Coulomb branch calculations, their drawback is that they do not form a set of orthogonal basis functions; so the resulting deconstructions do not uniquely decode the moduli spaces, and their branching coefficients cannot readily be found by the projection methods developed herein.

8.2. Subgroup Branching of Nilpotent Orbits

The nilpotent orbits of a group G have relationships with those of its subgroups; indeed this follows from the fact that orbits can be induced from subgroup orbits using the NOL formula (version 7.11). Naturally, the process can be reversed and the subgroup orbits can be recovered from the parent. The regular semi-simple branchings discussed in section 2.6 map the adjoint of G to representations of its semi-simple product groups; gauging away the unwanted members of the product group leaves a representation of a simple subgroup G_0 that includes the adjoint of G_0. Consequently, any nilpotent orbit of G maps to a representation space of G_0 that contains some nilpotent orbit of G_0, although this is quite often combined with other representations.

8.2.1. RSIMS Branching

A variety of branchings of RSIMS of Classical and Exceptional groups were investigated in [29]. Given a coordinate map $\mathcal{M}$ from a parent group G of rank r to a subgroup $G_0 \otimes \ldots \otimes G_m$ of equal rank, the refined Hilbert series $g^G_{HS:RSIMS}(x,t)$ can be expressed in terms of the CSA coordinates $\{y_1,\ldots,y_r\}$ of its subgroup. Then, following the methods laid out in Chapter 2, a character generating function $g_\chi^{G_0\otimes\ldots G_m}(y,m)$ can be used to project $g_{HS}^{G_0\ldots\otimes G_m}(y,t)$ onto the irreps of the subgroup; these are tracked using the Dynkin label fugacities $\{m_1,\ldots,m_r\}$. The projection coefficients, which are polynomials in the fugacity t, are encoded in the HWG $g_{HWG}^{G_0\ldots\otimes G_m}(m,t)$:

$$g^G_{HS:RSIMS}(x,t) \to g_{HS}^{G_0\ldots\otimes G_m}(y,t) \to g_{HWG}^{G_0\ldots\otimes G_m}(m,t) \tag{8.16}$$

Specialising to G of the type SO or USp, with branching to a product group with two constituents of the same type, the HWGs $g_{HWG}^{G_0\otimes G_1}(m,t)$ take the same form. This can be shown using notation where the highest weight fugacities for the adjoint, vector and graviton representations of the two (primed and unprimed) subgroups are replaced by $\{\theta,v,g\}$ respectively; thus, for $B/D_{r\geq 3}$: $\{m_1 \to v, m_2 \to \theta, m_1^2 \to g\}$, and for C_r : $\{m_1 \to$

$v, m_1^2 \to \theta\}$. The generalised HWGs follow the pattern:

$$\begin{aligned} g^{B/D}_{HS:RSIMS} \to g^{G_0\otimes G_1}_{HWG} &= PE\left[(\theta+\theta'+v\otimes v')\,t+(1+g+g'+v\otimes v')\,t^2-g\otimes g' t^4\right], \\ g^{C}_{HS:RSIMS} \to g^{G_0\otimes G_1}_{HWG} &= PE\left[(\theta+\theta'+v\otimes v')\,t-\theta\otimes\theta' t^2\right], \end{aligned} \tag{8.17}$$

The dimensions of these generalised HWGs vary from two in the case of the C series to six for the B/D series. The Hilbert series only contain representations whose Dynkin labels are monomials of the singlet, vector, adjoint and graviton labels. Importantly, since their form does not change for higher rank, these expressions encode such RSIMS deconstructions for any BCD group. The deconstructions contain all the information in the original RSIMS, which can be recovered by applying the inverse coordinate map $\mathcal{M}^{-1}$.

If the HWGs are gauged by selecting singlets of one of the subgroups - easily carried out by eliminating those HWG monomials that are not its singlets - then the connection from the minimal nilpotent orbit of G to the nilpotent orbits of G_0 is manifest:

$$\begin{aligned} g^{B/D}_{HS:RSIMS} \to g^{G_0}_{HWG} &= PE\left[\theta t+g t^2\right] PE\left[t^2\right] \\ g^{C}_{HS:RSIMS} \to g^{G_0}_{HWG:RSIMS} &= PE\left[\theta t\right], \end{aligned} \tag{8.18}$$

While the RSIMS of a C parent maps to the minimal nilpotent orbit of a C subgroup, the RSIMS of a B/D parent maps to the next to minimal orbit of a B/D subgroup, multiplied by a series of singlets. In order to eliminate singlets and to obtain exact B/D mappings to subgroup nilpotent orbits, it is necessary to incorporate a Hyper Kähler quotient by the gauge subgroup, similar to the procedures in Chapter 5.

8.2.2. Hyper Kähler Quotients

Hyper Kähler quotients between nilpotent orbits were treated in [7], albeit from a geometric rather than representation theoretic perspective. Table 8.3 sets out a selection of pairs of nilpotent orbits of groups that are related by Hyper Kähler quotients. The Classical cases are largely drawn from [7], with the orbits described by their Higgs branch quivers, which typically follow the subgroup branching. The logic behind the Hyper Kähler quotients follows the discussion in section 5.4.3. The Exceptional cases are drawn from the covering spaces identified in [80]; the branchings are to maximal

subgroups, based on elementary transformations or folding maps, and quiver descriptions are not available.

The relationship between each pair $\{\mathcal{O}_G \equiv g^G_{NO}, \mathcal{O}_{G_0} \equiv g^{G_0}_{NO}\}$ can be described by a character map $\chi^G \to \chi^{G_0 \otimes G_1 \otimes \ldots G_m}$, followed by a HKQ by the subgroup $H \equiv G_1 \otimes \ldots G_m$; this may include the discrete action of a finite group [6]:

$$g^{G_0}_{NO}\left(\chi^{G_0}, t\right) = \frac{1}{|\mathbb{Z}_n|} \sum_{\mathbb{Z}_n} \oint_H d\mu^H \; \frac{g^G_{NO}\left(\chi^{G_0 \otimes H}, t\right)}{\prod_{i=1}^{m} PE\left[[adj]_{G_i}, t^2\right]} \tag{8.19}$$

Table 8.3 contains only a sample of the possible HyperKähler quotients between nilpotent orbits, but these serve to exemplify particular types of relationship. These include:

1. 2-node quivers (9 examples). The fundamental of the flavour group is broken to a sum of fundamentals of groups of the same type ($O/Sp/U$). The HKQ is taken over the lower rank group, with the quotient for $B_0 \cong O(1)$ given by a $\mathbb{Z}_2$ factor. There are conditions that follow from the requirement that the new quiver should be based on a well ordered partition. Possibilities for Classical flavour groups are shown in Table 8.4. In all cases the reduction in complex dimension of the nilpotent orbit is equal to twice the dimension of the HKQ gauge group.

2. $SU(2k)$ RSIMS folding to the supra minimal nilpotent orbit of C_k (1 example). Consider the RSIMS quiver $SU(2k) - U(1)$. The complex character of the flavour group fundamental representation can be mapped to the pseudo real C_k fundamental. The gauge group maps from $U(1)$ to $O(2)$. The HKQ is a $\mathbb{Z}_2$ factor, as shown in Table 8.4.

3. The other types of Classical subgroup branching include special branchings, such as those from $SU(8)$ and $SU(10)$, in addition to regular ones. Considering that the subgroup may contain Abelian components, there are many possibilities for branching a group into its subgroups [54]; these are compounded by the alternative choices of HKQ. [4]

[4] Not all combinations lead to nilpotent orbits of the new flavour group; many lead to covering spaces.

$\mathcal{O}_G$	$\lvert\mathcal{O}_G\rvert$	$\chi^G \to \chi^{G_0 \otimes H}$	HK Quotient	$\mathcal{O}_{G_0}$	$\lvert\mathcal{O}_{G_0}\rvert$
$B_2 - C_1$	4	$[10]_B \to [11]_D \oplus 1$	$\mathbb{Z}_2$	$D_2 - C_1 - B_0$	4
$D_3 - C_1$	6	$[100]_D \to [10]_B \oplus 1$	$\mathbb{Z}_2$	$B_2 - C_1 - B_0$	6
$[4] - (2)$	8	$[100] \to [10]q \oplus \frac{1}{q^3}$	$U(1)$	$[3] - (2) - (1)$	6
$B_3 - C_1$	8	$[100]_B \to [100]_D \oplus 1$	$\mathbb{Z}_2$	$D_3 - C_1 - B_0$	8
$D_4 - C_1$	10	$[1000]_D \to [100]_D \oplus (q + \frac{1}{q})$	$O(2)$	$D_3 - C_1 - D_1$	8
$D_4 - C_1$	10	$[1000]_D \to [100]_B \oplus 1$	$\mathbb{Z}_2$	$B_3 - C_1 - B_0$	10
$[5] - (2)$	12	$[1000] \to [100]q \oplus \frac{1}{q^4}$	$U(1)$	$[4] - (2) - (1)$	10
$B_4 - C_2$	16	$[1000]_B \to [100]_B \oplus (q + \frac{1}{q})$	$O(2)$	$B_3 - C_2 - D_1$	14
$C_4 - D_2$	20	$[1000]_C \to [100]_C \oplus [1]_C$	C_1	$C_3 - D_2 - C_1$	14
$[6] - (1)$	10	$[10000] \to [100]_C$	$\mathbb{Z}_2$	$C_3 - D_1$	10
$D_4 - C_1$	10	$[1000]_D \to [10]q \oplus [01]\frac{1}{q} + (\frac{q}{q_1} + \frac{q_1}{q})$	$U(1) \otimes U(1)$	$[3] - (2) - (1)$	6
$[8] - (1)$	14	$[1000000] \to [10][1]q \oplus [1]\frac{1}{q^3}$	$SU(2) \otimes U(1)$	$[3] - (2) - (1)$	6
$[8] - (1)$	14	$[1000000] \to [100][1]$	$SU(2)$	$[4] - (2)$	8
$D_4 - C_1 - B_0$	12	$[1000]_D \to [100]q \oplus [001]\frac{1}{q}$	$U(1)$	$[4] - (2) - (1)$	10
$D_5 - C_1$	14	$[10000]_D \to [100]q \oplus [001]\frac{1}{q} + (\frac{q^4}{q_1^4} + \frac{q_1^4}{q^4})$	$U(1) \otimes U(1)$	$[4] - (2) - (1)$	10
$[10] - (1)$	18	$[100000000] \to [100][1]q + [1]\frac{1}{q^4}$	$SU(2) \otimes U(1)$	$[4] - (2) - (1)$	10
$G_2[10]$	6	$[10]_{G_2} \to [11] \oplus [10] \oplus [01]$	$\mathbb{Z}_3$	$[3] - (2) - (1)$	6
$D_4 - C_1$	10	$[0100]_{D_4} \to [10]_{G_2} \oplus 2[01]_{G_2}$	${\mathbb{Z}_2}^3/\mathbb{Z}_2$	$G_2[20]$	10
$F_4[1000]$	16	$[1000]_{F_4} \to [0100]_B \oplus [0001]_B$	$\mathbb{Z}_2$	$B_4 - C_2 - B_0$	16
$F_4[1000]$	16	$[1000]_{F_4} \to [0100]_D \oplus [1000]_D \oplus [0010]_D \oplus [0001]_D$	${\mathbb{Z}_2}^3/\mathbb{Z}_2$	$D_4 - C_2 - B_0$	16
$E_6[000001]$	22	$[000001]_{E_6} \to [1000]_{F_4} \oplus [0001]_{F_4}$	$\mathbb{Z}_2$	$F_4[0001]$	22

Dynkin labels are A series unless otherwise indicated,
B/D gauge groups in a quiver indicate the corresponding O gauge group,
$[N]$ indicates $SU(N)$ flavour and (N) indicates $U(N)$ gauge groups,
$U(1)$ or $O(2)$ fugacities in the character map are denoted by q.

Table 8.3.: HyperKähler Quotients between Nilpotent Orbits

4. The branchings from/to the nilpotent orbits of Exceptional groups require Hyper Kähler quotients by finite groups, as shown, to recover orbits of lower rank groups, rather than covering spaces. These are not discussed in [80], but can be identified from the HWGs of the various orbits and moduli spaces.

The generalisations in Table 8.4 extend the results of [7] and [80] to a wide class of relationships involving nilpotent orbits based on the Higgs branches of 2-node quivers.

Quiver $\mathcal{O}_G$	$\lvert\mathcal{O}_G\rvert$	HKQ	Quiver $\mathcal{O}_{G_0}$	$\lvert\mathcal{O}_{G_0}\rvert$	Conditions
$[n+1]-(k)$	$2k(n+1-k)$	$U(N)$	$[n+1-N]-(k)-(N)$	$2k(n+1-k)-2N^2$	$n+1 \geq 2k \geq 4N$
$SO(N)-C_k$	$2k(N-2k-1)$	$O(N')$	$SO(N-N')-C_k-O(N')$	$2k(N-2k-1)-N'(N'-1)$	$N \geq 4k \geq 4N'$
$C_k-O(N)$	$N(2k-N+1)$	$C_{k'}$	$C_{k-k'}-O(N)-C_{k'}$	$N(2k-N+1)-2k'(2k'+1)$	$k \geq N \geq 4k'$
$[2k]-(1)$	$2(2k-1)$	$\mathbb{Z}_2$	C_k-D_1	$2(2k-1)$	$k>1$

The quivers shown are for Higgs branch nilpotent orbit constructions,
B/D gauge groups indicate the corresponding O gauge group,
$[N]$ indicates $SU(N)$ flavour and (N) indicates $U(N)$ gauge groups.

Table 8.4.: Generalised HyperKähler Quotients between Orbits

9. Conclusions and Outlook

9.1. Reflections

This study set out with the aim of understanding and explicating the relationships between the structure of SUSY quiver gauge theories and symmetry groups. While much has been accomplished, the progress has been greatest with those quiver theories that possess natural decodings in terms of canonical objects from Lie groups and their representation theory. This is illustrated nicely by the symmetries of the invariant tensors of G, which manifest in flavour group representations on the Higgs branches of SQCD quiver theories; and by the (closures of) nilpotent orbits of Classical G, which appear on the Higgs branches of linear quiver chains built from G and its subgroups; and by the nilpotent orbits of Classical or Exceptional G, which appear on the Coulomb branches of quivers built from Dynkin diagrams of G.

The rationale for focusing on certain SUSY backgrounds ($\mathcal{N} = 2$ theories in the case of Higgs branch constructions and $\mathcal{N} = 4$ $3d$ theories in the case of Coulomb branch constructions) has been that these backgrounds, with 8 SUSY supercharges, support quiver theories with rich gauge group structures; the tools and methods developed in this context should, however, be equally useful in the analysis of any SUSY (or other physical) theory with a non-trivial gauge group content.

This study would claim to have made useful progress in two areas. The first is the development of the Highest Weight Generating function methodology for decoding the representation content of a refined Hilbert series. This methodology draws systematically on the group theoretic relationships between various families of generating functions, including Hilbert series, HWGs, and generating functions for characters of Lie group representations, Hall-Littlewood polynomials, modified Hall Littlewood functions and their orthonormal conjugates. The end result is a toolbox for faithfully

transforming and/or combining the Hilbert series of moduli spaces, such that their properties and relationships with other moduli spaces can be concisely and unambiguously defined and understood.

It is a central theme in this study that the systematic use of refined Hilbert series, concisely encapsulated as HWGs, provides a faithful encoding of any moduli space that can be expressed over the class functions of some symmetry group. This opens the door to identifying and analysing, in a precise and systematic manner, the structures of and relationships between a wide variety of field theories. While SUSY quiver gauge theories have formed the centre piece herein, SUSY backgrounds are not a prerequisite for the use of Hilbert series and HWGs. Indeed, the treatment in Chapter 7 of nilpotent orbits, through the refined Hilbert series and HWGs of moduli spaces generated by the background independent NOL formula, indicates that these methods should have broad physics and/or mathematical applicability.

The second area has been the application of HWG methodology, augmented by established Plethystics Program techniques, to develop an improved understanding of the moduli spaces of SUSY quiver theories, from a representation theoretical perspective; this has included systematising many of the non-trivial relationships between the Higgs and Coulomb branch vacuum moduli spaces of quiver theories for the closures of nilpotent orbits. Findings in relation to SQCD and instanton moduli spaces are given within Chapter 3. The main findings, which relate to nilpotent orbits generally, are summarised in the sections below. Findings in relation to deconstructions of nilpotent orbits are given in Chapter 8.

In the course of research, some categories of quiver theory were found to have moduli spaces that do not have simple decompositions in terms of HWGs, whether using characters, HL polynomials or mHL functions as a basis. Examples include multiple instanton moduli spaces, touched on in section 3.3, and Masterspace quiver theories [57, 56]. In the case of Masterspace theories, which deal with Calabi-Yau spaces defined by brane tilings, such as delPezzo surfaces, the multiple Abelian symmetries of the manifolds mostly preclude the description of their Hilbert series in terms of simple HWGs. In the case of multiple instanton theories, the interlacing of global $SU(2)$, instanton gauge and Yang-Mills symmetry groups also, thus far, frustrates a general description in terms of simple HWGs. These quiver theories were not explored further in this study.

When decoding recent Literature involving nilpotent orbits, it has proved invaluable to be able to draw on the seminal papers by Dynkin [61, 54], which not only introduced some powerful group theoretic tools, such as Dynkin diagrams, but also developed many of the concepts, such as Characteristics, which are essential for an effective analysis of nilpotent orbits. The interplay between recent ideas from SUSY quiver theory and foundational mathematical frameworks has played an important role in facilitating the resolution of many puzzles in the course of this study.

This study also identifies a few tensions between the theoretical narrative surrounding nilpotent orbits in the mathematical Literature and direct computations of their properties as moduli spaces. This suggests that there could be future benefits from a dialogue between the strands of mathematical and theoretical physics research in this field.

The study has made much use of *Mathematica*, supported by the LieArt add-in [84], to calculate refined Hilbert series and their HWGs. To do this, it has also proved necessary to build a number of custom algorithms to implement the often complicated and lengthy group theoretic transformations, which typically involve Weyl integration and/or Weyl group summation, between different types of generating function. While every effort has been made to describe and/or state the key formulae deployed, either in the text or in the Appendices, progress has also depended on the formulation of efficient algorithmic procedures; necessarily, these live within the *Mathematica* workbooks designed during this study rather than in this document.

9.2. Findings - Nilpotent Orbits

9.2.1. Higgs Branch

Every nilpotent orbit of a Classical group has a canonical Higgs branch quiver theory that can be identified from its Characteristic. A Higgs branch formula for A series nilpotent orbits is given by 5.4. A detailed formula, 5.23, for the closure of a BCD group nilpotent orbits was obtained in Chapter 5. This caters for the group averaging that is necessary over the components of orthogonal subgroups, to construct nilpotent orbits rather than their normalisations. Hilbert series, calculated up to rank 4, and analysed both as unrefined HS and in terms of HWGs, using both character and mHL

bases, are set out in Tables 5.4 to 5.5 and 5.12 to 5.17. A generalised analysis for certain types of orbit at any rank is given in Tables 5.6 and 5.18 to 5.20.

While all the moduli spaces are HyperKähler, not all are Calabi-Yau with palindromic Hilbert series. The Higgs branch formula precisely identifies the non-normal nilpotent orbits of the BCD series through their non-palindromic HS; and the moduli space inclusion (and union) relations between the calculated orbits are consistent with the Hasse diagrams presented in the Mathematical Literature [33, 6].

Taken together, these results, which appeared in [24], provide a systematic analysis of the Higgs branch Hilbert series of quivers for Classical group nilpotent orbits of low rank. While refined Hilbert series for some A series orbits had been obtained in [25], the prior work on BCD series had been limited to selective calculations of some unrefined Hilbert series, [31], and an identification of the representation structure of the minimal and maximal nilpotent orbits [16, 55]. The results show that a convoluted narrative, involving GNO dual groups and Spaltenstein dual orbits, whilst perhaps relevant for other purposes, is not necessary for the Higgs branch construction of the full set of BCD series nilpotent orbits.

There exist many dual quivers that have the same Higgs branch moduli spaces as the canonical quivers. For the A series, such dual quivers are provided by ordered linear quivers that are not *very unbalanced*; these can be transformed to canonical quivers by reordering partition data and/or by eliminating duplicate nodes, as elaborated in section 5.3.4. For the BCD series, dual quivers can be obtained from the canonical quivers by *dimension shifting* within the partition data and/or by extending maximal subchains, as elaborated in section 5.4.6. Many, but not all, BCD quivers can be rearranged as pure BC or DC chains, which can help avoid parity anomalies in certain field theoretic embeddings.

Higgs branch constructions are not available for Exceptional group nilpotent orbits, since the relationship between their vector and adjoint representations does not just involve bilinear invariants and singlets (which can be eliminated by a Hyper Kähler quotient) [6]. The construction of Exceptional group nilpotent orbits requires either the Coulomb branch method, which is available for near to minimal orbits, or a different plethystic approach, such as the NOL formula.

9.2.2. Coulomb Branch

The nilpotent orbits of A series groups, as well as the minimal and near to minimal nilpotent orbits of Classical and Exceptional groups, can be constructed on the Coulomb branches of quiver theories with unitary gauge nodes, using the unitary monopole formula [20, 22], as elaborated in Chapter 6. The number of flavour nodes and the dimensions of the unitary gauge groups in a quiver, as well as their linking pattern, can be determined by one or more of a variety of methods.

A quiver for the Coulomb branch construction of any A series nilpotent orbit, can be obtained from the corresponding Higgs branch quiver through brane manipulations, as described in section 6.4, according to the principles of $3d$ mirror symmetry [1].

Also, the quiver for a near to minimal nilpotent orbit can be identified from its Characteristic, as discussed in section 6.5, providing the (complex) dimension of the nilpotent orbit is equal to twice the sum of the $U(N)$ gauge node ranks in the quiver. In the case of minimal nilpotent orbits, such quivers correspond to those obtained from affine Dynkin diagrams, both for simply laced ADE groups [9] and for non simply laced $BCFG$ groups [22], with the $U(N)$ gauge node ranks being equal to the dual Coxeter numbers of G. In the case of next to minimal nilpotent orbits of BCD groups, these quivers correspond to those obtained from twisted affine Dynkin diagrams [24]. All the quivers in this category assign a Characteristic height of 2 to the highest root.

All the Coulomb branch quivers for nilpotent orbits are balanced, as discussed in section 6.1.1, and this imposes a particular form of overall gauge invariance on the gauge and flavour nodes; nevertheless, the monopole formula permits a gauge choice as to which monopole charge should be defined as zero, and this choice can simplify calculations, for example, of the Coulomb branches of star-shaped quivers and/or their deconstructions into $T(SU(N))$ quiver theories.

This gauge invariance imposes the Weyl group symmetries of G on the moduli space, by encoding the Cartan matrix into the structure of the quiver (and hence the GNO lattice of $U(N)$ topological symmetries). In the case of the RSIMS of low rank groups, these Weyl group symmetries are manifest in the measure of conformal dimension $\Delta(q)$, which serves to grade Weyl

group orbits. The unitary monopole formula collects these Weyl group orbits, which consist of sets of root space monomials z^q, into a moduli space graded by powers of t that combine conformal dimension $\Delta(q)$ with the degrees and multiplicity of the $U(N)$ Casimirs of each monopole charge configuration q.

From a SUSY perspective, the conformal dimension grading of the GNO lattice of monopole charges corresponds to R-charge, with the hypermultiplets between gauge nodes each contributing a half unit of R-charge, while the vector fields within each gauge node each contribute a negative unit of R-charge.

One of the features of these Coulomb branch moduli spaces is that they all have palindromic Hilbert series. These reconcile to non-normal BCD series nilpotent orbits, as discussed in 6.3.2: in the case of a pair of spinor orbits of D_{2r}, the Coulomb branch construction yields the palindromic spinor moduli spaces, while the Higgs branch construction yields their non-palindromic union; other BCD non-normal orbits are not near minimal, so Coulomb branch constructions are not available, and the issue does not arise.

9.2.3. NOL Formula

In the absence of a quiver theory construction for Exceptional group nilpotent orbits beyond the near to minimal category, it is a significant finding that a direct plethystic calculation of the closure of any normal nilpotent orbit is possible, by the Nilpotent Orbit Localisation formula developed in Chapter 7. One of the attractions of the NOL formula is that it explicates, in a direct manner, the relationship between an $SU(2)$ homomorphism, as defined by its Characteristic, its nilpotent element X and its nilpotent orbit (or normalisation).

Like the Coulomb branch formula, the NOL formula yields a moduli space with a palindromic Hilbert series, so the situation surrounding non-normal nilpotent orbits needs consideration; however, for normal orbits, the Higgs branch, Coulomb branch (where available) and NOL methods all construct the same canonical moduli spaces.

Turning to the established list of non-normal orbits; in all the cases calculated, the NOL formula leads to moduli spaces, with palindromic Hilbert series, containing elements outside the nilpotent cone $\mathcal{N}$.

For Classical non-normal orbits, the NOL formula either yields the normal components of those orbits that are unions, as in the case of D_{2r} spinor pairs, or it yields their normalisations. These normalisations can be restricted to equal the non-normal orbits by excluding sub-spaces described by *charged* orbits of lower dimension.

In the case of Exceptional non-normal orbits, there are no spinor pairs, and the NOL formula yields their normalisations. By conjecturing relationships, similar to those between Classical non-normal orbits and their normalisations, it has been possible to find restrictions of the normalisations in G_2, F_4 and E_6, that yield Hilbert series lying within $\mathcal{N}$, and which, subject to a more definitive analysis, can be viewed as candidates for the non-normal orbits.

9.3. Puzzles from the Mathematical Literature

By working with characters, quivers and refined Hilbert series, this study has found some precise and direct routes through a subject that can be treated in an arcane manner in the mathematical Literature.

This study has not made significant use of Bala-Carter labels. The perspective herein is that a nilpotent element X is more naturally characterised by an extension of the quotient group structure G/G_0 that applies to Richardson orbits. The NOL formula generalises this structure to non-Richardson orbits, by defining $\tilde{\Phi}_{G/G_0}$ to exclude the roots in $\Phi_G^{[1]}$ from the positive roots in Φ_{G/G_0}; this appears to be permissible due to the Weyl group invariance of $\Phi_G^{[1]}$ under the subset W_{G_0} of reflections of Φ_G.

The analysis does, however, leave a few residual puzzles in relation to the narrative in the mathematical Literature regarding the nilpotent orbits of Exceptional groups. Specifically:

1. A small number of *extra root maps*, which are not listed amongst the Characteristics in standard tables, appear to be consistent with the $SU(2)$ homomorphisms of EF groups, and also to correspond to conjugacy classes of their Weyl groups. Some of these extra root maps, such as $E_6[111110]$, $E_6[020202]$, $E_7[2020000]$, $E_7[0110100]$, $E_7[2000002]$ and $E_7[2020000]$, generate refined Hilbert series that are identical to those of the standard Characteristics; others give rise to moduli spaces,

with palindromic HS, that are extensions of nilpotent orbits outside $\mathcal{N}$. Although several cases for E_7 and E_8 remain to be calculated, no new nilpotent orbits have been identified. This appears consistent with the perspective that these extra root maps are members of Weyl group conjugacy classes that are equivalent to nilpotent orbits, modulo certain symmetric group actions [82].

Nonetheless, these extra roots maps provide examples of dualities, such that $SU(2)$ embeddings in G with different root maps or Characteristics lead to identical nilpotent orbits of G; such dualities would conflict with the standard narrative surrounding the Jacoboson-Morozov theorem in the Literature [33], which claims a bijection, not just between $SU(2)$ embeddings and nilpotent elements X, but also between $SU(2)$ embeddings and nilpotent orbits $\mathcal{O}_X$.

2. When defining the partial ordering (or topology) of nilpotent orbits within the nilpotent cone $\mathcal{N}$, it is important to deal with the orbits, rather than their normalisations. The Hasse diagrams of inclusion relations depend on whether non-normal nilpotent orbits, or their normalisations, are used. This may account for the differences in linking patterns (to or from non-normal orbits) between the F_4 and E_6 Hasse diagrams obtained from the moduli space analysis in this study and the standard diagrams in the Literature. Whereas the standard diagrams date from [81], the listing of non-normal orbits of Exceptional groups appears some years later in [72]. It would be interesting to be able to give a precise account of the source of the differences between the topologies of orbits calculated from the NOL formula and the standard diagrams.

3. It is also somewhat perplexing to note the view expressed in [78],

> "the main disadvantage of Dynkin's classification is that there is no simple algorithm to determine whether or not a given weighted Dynkin diagram [Characteristic] represents a nilpotent class."

This study of moduli spaces via Hilbert series has essentially established the contrary perspective that, subject to a limited number of complications surrounding the non-normal orbits and *extra root maps* of Exceptional

groups, (i) whether or not a given Characteristic of G represents an $SU(2)$ embedding can be determined by a simple character mapping technique, augmented by the Real and Pseudo real selection rules, and (ii) whether or not a given Characteristic of G represents a nilpotent orbit can, in principle, be determined from its Higgs branch construction (for G Classical) and/or the NOL formula.

9.4. Open Questions

The moduli space calculations for Exceptional groups, in particular, have been limited by practical computing constraints and so several tables herein are incomplete, more so in terms of HWG descriptions than unrefined HS. Given continuing developments in computing power, in terms of memory, speed and standard algorithms for polynomial algebra, it should eventually be possible to fill in the gaps in this analysis of the moduli spaces of quiver theories. This may resolve the open questions about the structures of the refined Hilbert series of SQCD theories and nilpotent orbits of Exceptional groups.

Setting aside those matters which may simply require computational advances, this study of quiver theories and nilpotent orbits also leaves open a number of questions that are more conceptual in nature.

Firstly, the only nilpotent orbits for which Coulomb branch quiver theory constructions are known, are A series or near minimal orbits, and these all use the unitary monopole formula. Is a broader class of Coulomb branch constructions of nilpotent orbits feasible? There would seem to be various avenues for further exploration.

1. Are there balanced unitary quivers (other than those defined by Characteristics), whose Coulomb branches correspond to BCD or Exceptional group nilpotent orbits beyond the near to minimal cases?

2. Can the rules of $3d$ mirror symmetry for the A series be translated to a simple rule for finding all the A series Coulomb branch quivers directly from the Characteristics of nilpotent orbits?

3. Can a modified version of the monopole formula be found that incorporates the relations necessary to restrict the Coulomb branch moduli

spaces from quivers with Characteristic height greater than 2 to their nilpotent orbits?

4. The rules of $3d$ mirror symmetry for the BCD series [31] transform Higgs branch quivers (for nilpotent orbits) of G into mirrors with alternating O/USp gauge nodes that are not equal in number to the simple roots of G. The problem in studies to date [21], has been how to map the topological symmetries of such gauge nodes to the simple roots of G. Can a modified Coulomb branch formula be found that encodes an effective mapping?

5. Both the NOL and monopole formulae work with the root system of G and encode Weyl group symmetries - albeit in very different ways. Can the NOL formula be transformed into a general Coulomb branch monopole formula, along with some family of quiver theories, for nilpotent orbits?[1]

Within the above, the task of finding a general (beyond the A series) Coulomb branch quiver theory construction for $T(G)$ theories would appear to be an interesting priority, in order to validate the conjectured equivalence between these quiver theories and mHL functions [31, 55].

Secondly, there remains the problem of how to formulate an analytic method for restricting the normalisation of a non-normal Exceptional group nilpotent orbit to the nilpotent cone $\mathcal{N}$, as required by 7.6. The analysis for Classical orbits, drawing on Higgs branch results, describes the difference between a non-normal orbit and its normalisation in terms of the charged NOL formula for orbits lower down the Hasse diagram; but what determines the particular charges and coefficients that appear? The solution may be related to the type of degeneration between adjacent orbits, where it is known from [71] that for Exceptional group orbits this is considerably more complicated than the Kraft-Procesi transitions [6] between Classical group orbits.

As discussed, it is unlikely that Higgs branch constructions for Exceptional group nilpotent orbits can be found due to the interplay between Exceptional group defining representations and their invariants.

[1] Building, for example, on the calculations for low rank RSIMS in section 6.2.

9.5. Generalised Quiver Theories

Naturally, quiver theories for the canonical Higgs branch and Coulomb branch constructions of nilpotent orbits comprise only a small subset of possible quiver theories. These canonical quivers can, however, be viewed as building blocks from which many other quiver theories can be constructed. There are many and varied composing mechanisms, including (i) background charges, (ii) quiver dualities (as discussed in sections 5.3.4 and 5.4.6), (iii) flavour node gluing of Higgs branches, as used in the recursive construction of Higgs branches in Chapter 5, (iv) flavour node gluing of Coulomb branches (as touched on in section 8.1), and/or (v) subgroup branching, with or without gauge group HyperKähler quotients (as touched on in section 8.2).

More general types of quiver that could be approached with this building block approach include linear quivers with multiple flavour nodes, star shaped quivers, quivers with internal loops, ... Studies of many different quiver types, touched on herein, have been carried out with comparable motivation, for example in [83, 26, 30, 31, 55]. However, the absence of a systematic reference to orthogonal bases has sometimes lead to a lack of clarity regarding results.

It has been helpful in this study to work with orthogonal bases, principally in the form of class functions based on Lie group characters and (modified) Hall Littlewood polynomials, to guide the systematic construction and analysis of quiver theories. The modified Hall Littlewood functions of the A series correspond to $T(SU(N))$ theories, and, indeed, in [55] it is conjectured that the Coulomb branches of $T_{\hat{\rho}}(G)$ theories correspond to mHL^G functions, with theories for $\hat{\rho} = (1, 1, \ldots, 1)$ corresponding to maximal nilpotent orbits. While the quivers for such $T_{\hat{\rho}}(G)$ theories are not known beyond the A series, the use of mHL functions may anticipate their eventual construction; in such an event, any nilpotent orbit would posses a description as some combination of (Coulomb branches of) $T(G)$ quivers in the presence of background charges, essentially as detailed in the tables herein. It may be that the eventual construction of $T(G)$ quiver theories can be guided by the NOL formula, since both types of construction work with root systems and background charges. Also, $T(G)$ quiver theories would shed light on the open Coulomb branch questions.

One useful next step in such a building block approach could be to develop a systematic account of charged nilpotent orbits, their decompositions in terms of characters and mHL bases, and their relationships, such as dualities or orthogonality.

Nilpotent orbits can be assigned background charges in various ways; directly, as in the NOL or Coulomb branch formulae, or by ungauging $U(1)$ or O nodes in Higgs branch quivers. When $U(1)$ nodes in a unitary quiver are ungauged, the mesonic moduli spaces acquire baryonic branches defined by the antisymmetric invariant tensors of the gauge group. Physically, these U(1) charges correspond to the introduction of Fayet-Iliopoulos terms into the SUSY action [56]. When O nodes in a BCD quiver are ungauged, to become SO nodes, the moduli spaces may also acquire additional branches. A systematic account could help to address open questions relating to the relationship between the NOL formula and the closures of non-normal nilpotent orbits and to the relationship between charged nilpotent orbits and $T^{\sigma}_{\hat{\rho}}(G)$ theories.

This study has made progress in bringing a systematic analysis to bear on the representation structure of the closures of nilpotent orbits, which include reduced single instanton moduli spaces; however, the preliminary work in section 3.3 indicates that the moduli spaces of multiple instanton theories are less tractable and may benefit from some basis, other than characters or mHL functions, for their efficient decomposition.

It could be interesting, therefore, to investigate other classes of orthogonal functions that incorporate Lie group symmetries. Several avenues open up. For example, both characters and Hall Littlewood polynomials are specialisations of Macdonald polynomials [60]. Also, we have also seen how orthogonal bases can be obtained as specialisations of a general localisation formula, such as 7.1. There may be other orthogonal bases, yet to be exploited, that could assist in the tasks of decoding quiver theories into their underlying representation theoretic content and unravelling their interrelationships.

Bibliography

[1] K. A. Intriligator and N. Seiberg, "Mirror symmetry in three-dimensional gauge theories," *Phys. Lett.* **B387** (1996) 513–519, arXiv:hep-th/9607207 [hep-th].

[2] A. Hanany and E. Witten, "Type IIB superstrings, BPS monopoles, and three-dimensional gauge dynamics," *Nucl. Phys.* **B492** (1997) 152–190, arXiv:hep-th/9611230 [hep-th].

[3] G. W. Moore, N. Nekrasov, and S. Shatashvili, "Integrating over Higgs branches," *Commun. Math. Phys.* **209** (2000) 97–121, arXiv:hep-th/9712241 [hep-th].

[4] N. Nekrasov and S. Shadchin, "ABCD of instantons," *Commun.Math.Phys.* **252** (2004) 359–391, arXiv:hep-th/0404225 [hep-th].

[5] N. Berkovits and N. Nekrasov, "The Character of pure spinors," *Lett. Math. Phys.* **74** (2005) 75–109, arXiv:hep-th/0503075 [hep-th].

[6] H. Kraft and C. Procesi, "On the geometry of conjugacy classes in classical groups," *Commentarii Mathematici Helvetici* **57** no. 1, (1982) 539–602.

[7] P. Z. Kobak and A. Swann, "Classical nilpotent orbits as hyperkähler quotients," *International Journal of Mathematics* **7** no. 02, (1996) 193–210.

[8] M. R. Douglas, "Branes within branes," arXiv:hep-th/9512077 [hep-th].

[9] M. R. Douglas and G. W. Moore, "D-branes, quivers, and ALE instantons," arXiv:hep-th/9603167 [hep-th].

[10] S. Benvenuti, B. Feng, A. Hanany, and Y.-H. He, "Counting BPS Operators in Gauge Theories: Quivers, Syzygies and Plethystics," *JHEP* **0711** (2007) 050, arXiv:hep-th/0608050 [hep-th].

[11] B. Feng, A. Hanany, and Y.-H. He, "Counting gauge invariants: The Plethystic program," *JHEP* **0703** (2007) 090, arXiv:hep-th/0701063 [hep-th].

[12] A. Butti, D. Forcella, A. Hanany, D. Vegh, and A. Zaffaroni, "Counting Chiral Operators in Quiver Gauge Theories," *JHEP* **11** (2007) 092, arXiv:0705.2771 [hep-th].

[13] J. Gray, A. Hanany, Y.-H. He, V. Jejjala, and N. Mekareeya, "SQCD: A Geometric Apercu," *JHEP* **0805** (2008) 099, arXiv:0803.4257 [hep-th].

[14] A. Hanany and N. Mekareeya, "Counting Gauge Invariant Operators in SQCD with Classical Gauge Groups," *JHEP* **0810** (2008) 012, arXiv:0805.3728 [hep-th].

[15] A. Hanany, N. Mekareeya, and G. Torri, "The Hilbert Series of Adjoint SQCD," *Nucl. Phys.* **B825** (2010) 52–97, arXiv:0812.2315 [hep-th].

[16] S. Benvenuti, A. Hanany, and N. Mekareeya, "The Hilbert Series of the One Instanton Moduli Space," *JHEP* **1006** (2010) 100, arXiv:1005.3026 [hep-th].

[17] C. A. Keller and J. Song, "Counting Exceptional Instantons," *JHEP* **1207** (2012) 085, arXiv:1205.4722 [hep-th].

[18] C. A. Keller, N. Mekareeya, J. Song, and Y. Tachikawa, "The ABCDEFG of Instantons and W-algebras," *JHEP* **1203** (2012) 045, arXiv:1111.5624 [hep-th].

[19] A. Hanany, N. Mekareeya, and S. S. Razamat, "Hilbert Series for Moduli Spaces of Two Instantons," *JHEP* **1301** (2013) 070, arXiv:1205.4741 [hep-th].

[20] D. Gaiotto and E. Witten, "S-Duality of Boundary Conditions In N=4 Super Yang-Mills Theory," *Adv.Theor.Math.Phys.* **13** (2009) 721, arXiv:0807.3720 [hep-th].

[21] S. Cremonesi, A. Hanany, and A. Zaffaroni, "Monopole operators and Hilbert series of Coulomb branches of $3d$ $\mathcal{N} = 4$ gauge theories," *JHEP* **1401** (2014) 005, arXiv:1309.2657 [hep-th].

[22] S. Cremonesi, G. Ferlito, A. Hanany, and N. Mekareeya, "Coulomb Branch and The Moduli Space of Instantons," *JHEP* **12** (2014) 103, arXiv:1408.6835 [hep-th].

[23] S. Cremonesi, A. Hanany, N. Mekareeya, and A. Zaffaroni, "Coulomb branch Hilbert series and Three Dimensional Sicilian Theories," *JHEP* **09** (2014) 185, arXiv:1403.2384 [hep-th].

[24] A. Hanany and R. Kalveks, "Quiver Theories for Moduli Spaces of Classical Group Nilpotent Orbits," *JHEP* **06** (2016) 130, arXiv:1601.04020 [hep-th].

[25] A. Hanany and N. Mekareeya, "Complete Intersection Moduli Spaces in N=4 Gauge Theories in Three Dimensions," *JHEP* **01** (2012) 079, arXiv:1110.6203 [hep-th].

[26] A. Gadde, L. Rastelli, S. S. Razamat, and W. Yan, "Gauge Theories and Macdonald Polynomials," *Commun.Math.Phys.* **319** (2013) 147–193, arXiv:1110.3740 [hep-th].

[27] L. Lehman and A. Martin, "Hilbert Series for Constructing Lagrangians: expanding the phenomenologist's toolbox," *Phys. Rev.* **D91** (2015) 105014, arXiv:1503.07537 [hep-ph].

[28] A. Hanany and R. Kalveks, "Highest Weight Generating Functions for Hilbert Series," *JHEP* **10** (2014) 152, arXiv:1408.4690 [hep-th].

[29] A. Hanany and R. Kalveks, "Construction and Deconstruction of Single Instanton Hilbert Series," *JHEP* **12** (2015) 118, arXiv:1509.01294 [hep-th].

[30] O. Chacaltana, J. Distler, and Y. Tachikawa, "Nilpotent orbits and codimension-two defects of 6d N=(2,0) theories," *Int. J. Mod. Phys.* **A28** (2013) 1340006, arXiv:1203.2930 [hep-th].

[31] S. Cremonesi, A. Hanany, N. Mekareeya, and A. Zaffaroni, "T_ρ^σ (G) theories and their Hilbert series," *JHEP* **01** (2015) 150, arXiv:1410.1548 [hep-th].

[32] P. Howe, K. Stelle, and P. Townsend, "Miraculous ultraviolet cancellations in supersymmetry made manifest," *Nuclear Physics B* **236** no. 1, (1984) 125–166.

[33] D. H. Collingwood and W. M. McGovern, *Nilpotent Orbits In Semisimple Lie Algebra: An Introduction.* CRC Press, 1993.

[34] S.-S. Kim, J. Lindman Hornlund, J. Palmkvist, and A. Virmani, "Extremal Solutions of the S3 Model and Nilpotent Orbits of G2(2)," *JHEP* **08** (2010) 072, arXiv:1004.5242 [hep-th].

[35] A. Bourget and J. Troost, "Counting the Massive Vacua of N=1* Super Yang-Mills Theory," *JHEP* **08** (2015) 106, arXiv:1506.03222 [hep-th].

[36] V. G. Kac and A. V. Smilga, "Normalized vacuum states in N=4 supersymmetric Yang-Mills quantum mechanics with any gauge group," *Nucl. Phys.* **B571** (2000) 515–554, arXiv:hep-th/9908096 [hep-th].

[37] F. Benini, Y. Tachikawa, and D. Xie, "Mirrors of 3d Sicilian theories," *JHEP* **09** (2010) 063, arXiv:1007.0992 [hep-th].

[38] O. Chacaltana, J. Distler, and A. Trimm, "Tinkertoys for the Twisted D-Series," *JHEP* **04** (2015) 173, arXiv:1309.2299 [hep-th].

[39] O. Chacaltana, J. Distler, and A. Trimm, "Tinkertoys for the Twisted E_6 Theory," arXiv:1501.00357 [hep-th].

[40] A. A. Belavin, A. M. Polyakov, A. S. Schwartz, and Yu. S. Tyupkin, "Pseudoparticle Solutions of the Yang-Mills Equations," *Phys. Lett.* **B59** (1975) 85–87.

[41] M. Atiyah, N. Hitchin, and I. Singer, "Self-duality in four-dimensional riemannian geometry," *Proceedings of the Royal Society of London. Series A, Mathematical and Physical Sciences* **Vol 362** no. No 1711, (1978) 425–461.

[42] T. Eguchi and A. J. Hanson, "Asymptotically Flat Selfdual Solutions to Euclidean Gravity," *Phys. Lett.* **B74** (1978) 249–251.

[43] T. Eguchi and A. J. Hanson, "Selfdual Solutions to Euclidean Gravity," *Annals Phys.* **120** (1979) 82.

[44] J. J. Oh and H. S. Yang, "Einstein Manifolds As Yang-Mills Instantons," *Mod. Phys. Lett.* **A28** (2013) 1350097, `arXiv:1101.5185 [hep-th]`.

[45] J. J. Oh, C. Park, and H. S. Yang, "Yang-Mills Instantons from Gravitational Instantons," *JHEP* **04** (2011) 087, `arXiv:1101.1357 [hep-th]`.

[46] M. F. Atiyah, N. J. Hitchin, V. G. Drinfeld, and Yu. I. Manin, "Construction of Instantons," *Phys. Lett.* **A65** (1978) 185–187.

[47] C. Soo, "Einstein manifolds, Abelian instantons, bundle reduction, and the cosmological constant," *Class. Quant. Grav.* **18** (2001) 709–718, `arXiv:gr-qc/0009007 [gr-qc]`.

[48] J. Lee, J. J. Oh, and H. S. Yang, "An Efficient Representation of Euclidean Gravity I," *JHEP* **12** (2011) 025, `arXiv:1109.6644 [hep-th]`.

[49] A. L. Besse, *Einstein Manifolds*. Springer-Verlag, Berlin Heidelberg, 1987.

[50] J. Baez and J. P. Muniain, *Gauge Fields, Knots and Gravity*. World Scientific Publishing, Singapore, 1994.

[51] M. Nakahara, *Geometry, Topology and Physics*. Taylor and Francis Group, Boca Raton, 2003.

[52] D. Tong, "TASI lectures on solitons: Instantons, monopoles, vortices and kinks," `arXiv:hep-th/0509216 [hep-th]`.

[53] P. B. Kronheimer, "Instantons and the geometry of the nilpotent variety," *J. Diff. Geom.* **32** no. 2, (1990) 473–490.

[54] E. Dynkin, "Semisimple subalgebras of semisimple Lie algebras," *Trans.Am.Math.Soc.* **6** (1957) 111.

[55] S. Cremonesi, A. Hanany, N. Mekareeya, and A. Zaffaroni, "Coulomb branch Hilbert series and Hall-Littlewood polynomials," *JHEP* **09** (2014) 178, arXiv:1403.0585 [hep-th].

[56] D. Forcella, A. Hanany, Y.-H. He, and A. Zaffaroni, "The Master Space of N=1 Gauge Theories," *JHEP* **0808** (2008) 012, arXiv:0801.1585 [hep-th].

[57] D. Forcella, A. Hanany, Y.-H. He, and A. Zaffaroni, "Mastering the Master Space," *Lett.Math.Phys.* **85** (2008) 163–171, arXiv:0801.3477 [hep-th].

[58] J. Fuchs and C. Schweigert, *Symmetries, Lie Algebras and Representations*. Cambridge University Press, Cambridge, 1997.

[59] H. F. Jones, *Groups, Representations and Physics*. Taylor and Francis Group, New York, 1998.

[60] I. Macdonald, *Symmetric Functions and Hall Polynomials*. Clarendon Press, second edition ed., 1995.

[61] E. B. Dynkin, "The maximal subgroups of the classical groups," *Trudy Moskovskogo Matematicheskogo Obshchestva* **1** (1952) 39–166.

[62] P. Cvitanovic, *Group Theory: Birdtracks, Lie Algebras and Exceptional Groups*. Princeton University Press, Princeton, 2008.

[63] J. de Azcarraga, A. Macfarlane, A. Mountain, and J. Perez Bueno, "Invariant tensors for simple groups," *Nucl.Phys.* **B510** (1998) 657–687, arXiv:physics/9706006 [physics].

[64] P. Pouliot, "Spectroscopy of gauge theories based on exceptional Lie groups," *J.Phys.* **A34** (2001) 8631–8658, arXiv:hep-th/0107151 [hep-th].

[65] J. Wess and J. Bagger, *Supersymmetry and Supergravity*. Princeton University Press, Princeton, 1992.

[66] E. Witten, "An SU(2) Anomaly," *Phys.Lett.* **B117** (1982) 324–328.

[67] H. Nakajima and K. Yoshioka, "Instanton counting on blowup. 1.," *Invent.Math.* **162** (2005) 313–355, arXiv:math/0306198 [math-ag].

[68] B. Fu, "Symplectic resolutions for nilpotent orbits," *Inventiones mathematicae* **151** no. 1, (2003) 167–186.

[69] W. H. Hesselink, "Polarizations in the classical groups.," *Math. Z.* (1978) 217–234.

[70] J. Adams, "Closure diagrams for nilpotent orbits of exceptional groups." http://www.liegroups.org/tables/unipotentOrbits/unipotentOrbits.pdf.

[71] B. Fu, D. Juteau, P. Levy, and E. Sommers, "Generic singularities of nilpotent orbit closures," *Advances in Mathematics* **305** (2017) 1–77.

[72] A. Broer, "Decomposition varieties in semisimple lie algebras.," *Can. J. Math.* **50** no. 5, (1998) 929–971.

[73] I. Yaakov, "Redeeming Bad Theories," *JHEP* **11** (2013) 189, arXiv:1303.2769 [hep-th].

[74] P. Goddard, J. Nuyts, and D. I. Olive, "Gauge Theories and Magnetic Charge," *Nucl.Phys.* **B125** (1977) 1.

[75] B. Feng and A. Hanany, "Mirror symmetry by O3 planes," *JHEP* **11** (2000) 033, arXiv:hep-th/0004092 [hep-th].

[76] D. I. Panyushev, "On spherical nilpotent orbits and beyond," *Annales de l'institut Fourier* **49** no. 5, (1999) 1453–1476.

[77] A. Hanany, S. Ramgoolam, and D. Rodriguez-Gomez, "Highest Weight Generating functions for hyperKahler T*(G/H) spaces," arXiv:1601.02531 [hep-th].

[78] P. Bala and R. W. Carter, "Classes of unipotent elements in simple algebraic groups. i," *Math. Proc. Camb. Phil. Soc. Mathematical*

Proceedings of the Cambridge Philosophical Society **79** no. 03, (1976) 401.

[79] P. Bala and R. W. Carter, "Classes of unipotent elements in simple algebraic groups. ii," *Math. Proc. Camb. Phil. Soc. Mathematical Proceedings of the Cambridge Philosophical Society* **80** no. 01, (1976) 1.

[80] R. Brylinski and B. Kostant, "Nilpotent orbits, normality, and hamiltonian group actions," *Journal of the American Mathematical Society* **7** no. 2, (1994) 269.

[81] N. Spaltenstein, "Classes unipotentes et sous-groupes de borel," *Lecture Notes in Mathematics* (1982) .

[82] W. Beynon and N. Spaltenstein, "Green functions of finite chevalley groups of type en (n = 6, 7, 8)," *Journal of Algebra* **88** no. 2, (1984) 584–614.

[83] A. Hanany and N. Mekareeya, "Tri-vertices and SU(2)'s," *JHEP* **02** (2011) 069, `arXiv:1012.2119 [hep-th]`.

[84] R. Feger and T. W. Kephart, "LieART - A Mathematica Application for Lie Algebras and Representation Theory," `arXiv:1206.6379 [math-ph]`.

[85] W. Fulton and J. Harris, *Representation Theory*. Springer, New York, 2004.

[86] C. Hughes, "Haar measure and weyl integration." 2006.

[87] G. B. Elkington, "Centralizers of unipotent elements in semisimple algebraic groups," *Journal of Algebra* **23** no. 1, (1972) 137–163.

A. Appendices

A.1. Plethystic Functions

Plethystic functions can be used to symmetrise or antisymmetrise polynomials, such as characters of representations. The Plethystic Exponential ("PE") is a symmetrising function and the Fermionic Plethystic Exponential ("PEF") is an antisymmetrising function. They have inverse functions given respectively by the Plethystic Logarithm ("PL") and the Fermionic Plethystic Logarithm ("PLF") [60, 11, 13, 28].

Consider a function in some variable t, which can be expressed as a power series:

$$f(t) \equiv \sum_{n=0}^{\infty} a_n t^n. \tag{A.1}$$

The Plethystic Exponential for such a function is defined as:

$$\begin{aligned} PE\left[f(t), t\right] &\equiv \exp\left(\sum_{k=1}^{\infty} \frac{f(t^k) - f(0)}{k}\right) \\ &= \prod_{n=1}^{\infty} \frac{1}{(1-t^n)^{a_n}}. \end{aligned} \tag{A.2}$$

The PE can be generalised for power series of more than one variable, so that for:

$$f(t_1, \ldots, t_N) \equiv \sum_{n=0}^{\infty} \sum_{i=1}^{N} a_{n_i} t_i^n, \tag{A.3}$$

we obtain the PE:

$$PE[f(t_1,\ldots,t_N),(t_1,\ldots,t_N)] \equiv \exp\left(\sum_{k=1}^{\infty}\frac{f(t_1^k,\ldots,t_N^k)-f(0,\ldots,0)}{k}\right) = \prod_{n=1}^{\infty}\prod_{i=1}^{N}\frac{1}{(1-t_i^n)^{a_{ni}}}. \tag{A.4}$$

In order to avoid ambiguities, we shall, where necessary, use the notation:

$$PE[f(t_1,\ldots,t_N),(t_1,\ldots,t_N)], \tag{A.5}$$

to distinguish the variables, with respect to which the PE is being taken, from their coefficients (and similarly for the PL); where no ambiguity arises, the notation $PE[f(t_1,\ldots,t_N)]$ may be used.

The Plethystic Logarithm makes use of the Mobius function $\mu(k)$, which is defined as $(-1)^n$ for an integer that is the product of n distinct primes other than unity, and zero otherwise, such that $\mu(1)=1,\mu(2)=\mu(3)=-1,\ldots$ etc. For the general case, the PL is defined as:

$$PL[g(t_1\ldots,t_N),(t_1\ldots,t_N)] \equiv \sum_{k=1}^{\infty}\frac{1}{k}\mu(k)\log g(t^k{}_1,\ldots,t^k{}_N). \tag{A.6}$$

If we set $g(t_1\ldots,t_N)=PE[f(t_1\ldots,t_N)]$, we then obtain $f(t_1\ldots,t_N)=PL[g(t_1,\ldots,t_N),(t_1,\ldots,t_N)]$, as required. The identity can be proved by manipulation of the various series using the properties of the Mobius function [11], which include the key simplifying identity:

$$\sum_{l=1}^{\infty}\sum_{m=1}^{\infty}\frac{\mu(l)}{lm}t^{klm} = t^k. \tag{A.7}$$

The Fermionic Plethystic Exponential is defined as:

$$PEF[f(t_1,\ldots,t_N),(t_1,\ldots,t_N)] \equiv \exp\left(\sum_{k=1}^{\infty}(-1)^{k+1}\frac{f(t_1^k,\ldots,t_N^k)-f(0,\ldots,0)}{k}\right) = \prod_{n=1}^{\infty}\prod_{i=1}^{N}(1+t_i^n)^{a_{ni}}. \tag{A.8}$$

The Fermionic Plethystic Logarithm is given by:

$$\begin{aligned} PLF[g(t_1,\ldots,t_N),(t_1,\ldots,t_N)] &= \sum_{m=0}^{\infty} PL[g(t_1^{2^m},\ldots,t_N^{2^m}),(t_1^{2^m},\ldots,t_N^{2^m})] \\ &= \sum_{m=0}^{\infty}\sum_{k=1}^{\infty}\frac{1}{k}\mu(k)\log g(t_1^{(2^m)k}\ldots,t_N^{(2^m)k}). \end{aligned} \tag{A.9}$$

The PE and PEF have the useful properties that:

$$\begin{aligned} PE[f_1+f_2] &= PE[f_1]PE[f_2] \\ PEF[f_1+f_2] &= PEF[f_1]PEF[f_2] \end{aligned} \tag{A.10}$$

and the PL and PLF have the related properties that:

$$\begin{aligned} PL[g_1 g_2] &= PL[g_1]+PL[g_2] \\ PLF[g_1 g_2] &= PLF[g_1]+PLF[g_2]. \end{aligned} \tag{A.11}$$

We can use the Plethystic Exponential to symmetrise the character of an irrep of some group G as follows. Suppose the character χ of the irrep is composed of monomials $A_i(x_1,\ldots,x_r)$, where the x_j are CSA coordinates ranging over the rank r of the group and the index i ranges over the dimension $|\chi|$ of the irrep:

$$\chi = \sum_{i=1}^{|\chi|} A_i(x_1,\ldots,x_r). \tag{A.12}$$

We form a generating function $g^G(\chi,t)$ by taking the PE of the sum of fugacities $t_i \equiv tA_i$, which are given by the products of each coordinate monomial with a fugacity t, where $0<|t|<1$:

$$\begin{aligned} g^G(\chi,t) &\equiv PE\left[\chi\ t\right] \\ &\equiv PE\left[\sum_{i=1}^{|\chi|} t_i,(t_1,\ldots,t_{|\chi|})\right] \\ &= \prod_{i=1}^{|\chi|}\frac{1}{(1-tA_i)}. \end{aligned} \tag{A.13}$$

The Taylor expansion of $g^G(\chi,t)$ generates an infinite polynomial in the

fugacity t, whose coefficients are all symmetric functions of the coordinate monomials. Importantly, the PE of a character is a class function and the Peter Weyl Theorem [58] entails that the characters of a compact group form a complete basis for its class functions, so this Taylor expansion can be decomposed as a sum of characters of irreps, identified by Dynkin labels $[n]$, each with a coefficient in the form of a series in the fugacity t:

$$PE[\chi\ t] = \sum_{[n]} a_{[n]}(t)\chi_{[n]} = \sum_{k=0}^{\infty}\sum_{[n]} t^k a_{k[n]}\chi_{[n]}. \tag{A.14}$$

We can use the PEF in a similar manner to form antisymmetric combinations of the monomials within the character χ of an irrep.

$$\begin{aligned} g^G_\Lambda(\chi, t) &\equiv PEF[\chi\ t] \\ &\equiv PEF\left[\sum_{i=1}^{|\chi|} t_i, (t_1, \ldots, t_{|\chi|})\right] \\ &= \prod_{i=1}^{|\chi|}(1 + tA_i). \end{aligned} \tag{A.15}$$

Following similar reasoning, the PEF of χ can also be expanded as a finite sum of characters:

$$PEF\left[\chi\ t\right] = \sum_{[n]} \tilde{a}_{[n]}(t)\chi_{[n]} = \sum_{k=0}^{|\chi|}\sum_{[n]} t^k \tilde{a}_{k[n]}\chi_{[n]}. \tag{A.16}$$

Collecting the above results, we obtain the key relationships for symmetrising and antisymmetrising characters and similar functions:

$$\sum_{k=0}^{\infty} t^k Sym^k\left[\chi\right] = PE\left[\chi\ t\right] = \prod_{i=1}^{|\chi|}\frac{1}{(1 - tA_i)} = \sum_{k=0}^{\infty}\sum_{[n]} t^k a_{k[n]}\chi_{[n]} \tag{A.17}$$

$$\sum_{k=0}^{|\chi|} t^k \Lambda^k\left[\chi\right] = PEF\left[\chi\ t\right] = \prod_{i=1}^{|\chi|}(1 + tA_i) = \sum_{k=0}^{|\chi|}\sum_{[n]} t^k \tilde{a}_{k[n]}\chi_{[n]} \tag{A.18}$$

A.2. Weyl Integration

Weyl integration and the Reynolds operator provide methods for obtaining invariants by taking group averages over continuous and finite groups respectively.

In the case of a finite group, invariant objects can be constructed from a function by group averaging using the Reynolds operator [10]:

$$R^G\left[f[\gamma]\right] \equiv \frac{1}{|G|}\sum_G G \cdot f[\gamma], \tag{A.19}$$

where $\gamma \in G$. This operator can be used to construct Molien sums that enumerate the invariants of finite groups [10].

In the case of continuous groups, the role of the Reynolds operator is played by Weyl integration. Any continuous group has a manifold, metric and volume form, and it is possible to integrate a function over the group volume in the usual manner [58]:

$$I = \int_G d\mu^G(\gamma) f(\gamma), \tag{A.20}$$

where $d\mu^G(\gamma)$ is the Haar measure. Normally this requires taking the integral over all the dimensions $|G|$ of the group. In Weyl integration the integral is simplified to one over the maximal torus of the group by conjugating the class function $f[\gamma]$ with other elements of the Group, such that it is always represented by an element of the maximal torus. This conjugation reduces the number of integrations required from $|G|$ to rank$[G]$. To do this consistently, the Haar measure, which is effectively a volume element, has to be modified by scaling to reflect the projection of the entire group onto its maximal torus [58, 85].

Tables of modified Haar measures for $U(r)$ and the Classical groups are given in [86]. It is convenient, however, to rewrite the Haar measures in a simple form, for use within contour integrals, that generalises to any group. This makes use of the unimodular weight space and root space coordinates, introduced in section 2.2, and the Weyl group:

$$\oint_G d\mu^G = \frac{1}{|W_G|}\oint_G \frac{dx}{x}\prod_{\alpha\in\Phi}(1-z^\alpha). \tag{A.21}$$

For brevity, a factor of $1/(2\pi i)^r$ has been omitted from the residues and the definition $\frac{dx}{x} \equiv \prod_{i=1}^{r} \frac{dx_i}{x_i}$ is used. This form of the Weyl integral lends itself to explicit evaluation using the residue theorem.

We can verify the orthonormality of characters under the Weyl integral as defined above. Consider the integral:

$$I = \oint_G d\mu^G \; \chi_{[n]}(x^*)\, \chi_{[m]}(x) \tag{A.22}$$

Inserting terms from A.21 and 2.4 into A.22, the terms involving roots cancel with the Haar measure and we obtain:

$$I = \frac{1}{|W_G|} \oint_G \frac{dx}{x} \sum_{w' \in W_G} \left|w'\right| w' \cdot \left(x^{-n} x^{-\rho}\right) \sum_{w \in W_G} |w|\, w \cdot (x^m x^\rho). \tag{A.23}$$

Considering this as a $U(1)^r$ contour integral, a non-zero contribution only arises when $w' = w$, so:

$$\begin{aligned} I &= \frac{1}{|W_G|} \oint_G \frac{dx}{x} \sum_{w \in W_G} |w|^2 w \cdot \left(x^{m-n}\right) \\ &= \delta_{[m][n]}, \end{aligned} \tag{A.24}$$

since $|w|^2 = 1$ and $w \cdot (x^{m-n}) = 1$ only if $[m] = [n]$. As a corollary, the Weyl integral of a single character is zero for any irrep other than the singlet and the Weyl integral can be used to form an inner product that projects out the singlet content of products of characters or class functions of characters.

A simpler form of the Haar measure is noted in [15], which gives the Haar measure in terms of the positive (or negative) root space only. In some circumstances this produces simpler expressions that can be evaluated more quickly:

$$\oint_G d\mu^{G+/-} \equiv \oint_G \frac{dx}{x} \prod_{\alpha \in \Phi+/-} (1 - z^\alpha). \tag{A.25}$$

The full form of the Haar measure A.21, however, has the feature of being invariant under the Weyl group and can participate in other Weyl group simplifications, unlike A.25 which transforms in the alternating representation.

Consider, for example, a typical Weyl integration to find the inner product

of two class functions, g^G_{HS1} and g^G_{HS2}, one of which has an explicit expression as a sum over the Weyl group:

$$I\left(m,n\right)=\oint\limits_G d\mu^G\ g^G_{HS1}\left(x^*,m\right)\ g^G_{HS2}\left(x,n\right), \tag{A.26}$$

where

$$g^G_{HS1}\left(x^*,m\right)=\sum_{w\in W_G} f^G_{HS1}\left(w\cdot x^*,m\right). \tag{A.27}$$

Clearly, the integrand of A.26, taken as a whole, is invariant under conjugation by the Weyl group. Moreover, the full Haar measure $d\mu^G$ in A.21 is invariant under the Weyl group, as is the class function g^G_{HS2}, so each element w of the Weyl group sum over f^G_{HS1} can be conjugated to the identity and we obtain:

$$I\left(m,n\right)=\left|W_G\right|\oint\limits_G d\mu^G\ f^G_{HS1}\left(x^*,m\right)\ g^G_{HS2}\left(x,n\right) \tag{A.28}$$

This reduces the number of terms to be evaluated by the order of the Weyl group of G. For example, a typical HWG evaluation can be rearranged:

$$\begin{aligned}
g^G_{HWG}\left(m,t\right)&\equiv\oint\limits_G d\mu^G\ g^G_\chi\left(x^*,m\right)\ g^G_{HS}\left(x,t\right)\\
&=\oint\limits_G d\mu^G\ \sum_{w\in W_G} w\cdot\left(\prod_{i=1}^{r}\frac{1}{1-m_i/x_i}\prod_{\alpha\in\Phi+}\frac{1}{1-z^\alpha}\right)g^G_{HS}\left(x,t\right)\\
&=\left|W_G\right|\oint\limits_G d\mu^G\ \prod_{i=1}^{r}\frac{1}{1-m_i/x_i}\prod_{\alpha\in\Phi+}\frac{1}{1-z^\alpha}\ g^G_{HS}\left(x,t\right)\\
&=\oint\limits_G\frac{dx}{x}\prod_{\alpha\in\Phi+}\left(1-z^{-\alpha}\right)\prod_{i=1}^{r}\frac{1}{1-m_i/x_i}\ g^G_{HS}\left(x,t\right)\\
&=\oint\limits_G d\mu^{G-}\ \prod_{i=1}^{r}\frac{1}{1-m_i/x_i}\ g^G_{HS}\left(x,t\right)
\end{aligned} \tag{A.29}$$

Further simplifications of such contour integrals can be found by exploiting any invariance subgroups of the Weyl group within $g^G_{HS}\left(x,t\right)$, as in 2.12 and 7.5, for example.

At some point, however, it is necessary to carry out explicit residue calculations to determine the integrals. In this study *Mathematica* is used to carry out the residue calculations and summations. The summation can generally be done most efficiently by first summing over any multiple poles contributed by each factor in a denominator, as indicated in Table A.1. The sum for each factor is then necessarily a real polynomial (or quotient of polynomials) in the various fugacities. This minimises the computational difficulties encountered by *Mathematica* in the simplification of sums of quotients of complex functions with fractional exponents.

Function	Order of Pole	No. of Poles	Residue
$\frac{f(x)}{(x-a)}$	1	1	$f(a)$
$\frac{f(x)}{(x-a)^n}$	n	1	$\frac{1}{(n-1)!}\frac{d^{n-1}f(x)}{dx^{n-1}}\Big\vert_{x=a}$
$\frac{f(x)}{(x^m-a)}$	1	m	$\sum_{k=1}^{m}\frac{x-a^{1/m}e^{2\pi ik/m}}{x^m-a}f(x)\Big\vert_{x=a^{1/m}e^{2\pi ik/m}}$
$\frac{f(x)}{(x^m-a)^n}$	n	m	$\frac{1}{(n-1)!}\sum_{k=1}^{m}\frac{d^{n-1}}{dx^{n-1}}\left(\frac{x-a^{1/m}e^{2\pi ik/m}}{x^m-a}\right)^n f(x)\Big\vert_{x=a^{1/m}e^{2\pi ik/m}}$

Factors of $(2\pi i)$ omitted for brevity

Table A.1.: Calculation of Residues

A.3. Affine and Twisted Affine Lie Algebras

It is useful to give a brief summary of the relationship between a simple Lie algebra and its related *untwisted affine* (or *extended*) and *twisted affine* Lie algebras. The defining feature of an affine Lie algebra is that its Cartan matrix is positive semi-definite, having a zero determinant and one zero eigenvalue. This is achieved by generalising a regular Cartan matrix A^{ij} through the addition of an extra row and column, corresponding to an extra simple root and an extra CSA operator, and equivalent to an extra node on the Dynkin diagram. The additional root and eigenvalue operators are chosen to be linear combinations of the other operators. Naturally, the rank is unchanged.

The linear relationship between the operators is encapsulated in the Coxeter labels a_j and dual Coxeter labels $\breve{a}_i$ of each node. These labels are,

respectively, the left and right eigenvectors with zero eigenvalue of an affine Cartan matrix:

$$\sum_{i=0}^{r} a_i A^{ij} = 0 = \sum_{j=0}^{r} A^{ij} \breve{a}_j. \tag{A.30}$$

The two types of Coxeter label differ according to the length of the simple root to which they refer: the ratio between the dual Coxeter and Coxeter labels of a root is equal to the ratio of its length to that of the longest root [58].

The Dynkin diagrams of affine Lie algebras are obtained by attaching a single extra node to a regular Dynkin diagram, subject to the constraints (i) that the links are of a type permitted in a regular Dynkin diagram and (ii) that the resulting Cartan matrix is positive semi-definite.

Each simple group has an untwisted affine Dynkin diagram, with the extra node attached to the adjoint node of the regular Dynkin diagram, as shown in Figures 2.1 and 2.2. The Cartan matrix A^{ij} is thus modified according to the schema:

$$A^{ij}_{extended} = \begin{pmatrix} A^{ij} & [col] \\ -[adjoint] & 2 \end{pmatrix}, \tag{A.31}$$

where the column vector $[col]$ is obtained by transposing the Dynkin labels of the adjoint representation and replacing all non-zero entries with -1 or -2, such that $A^{ij}_{extended}$ becomes degenerate. The dual Coxter labels of existing nodes are unchanged, with the new node acquiring a dual Coxeter label of 1. This follows from the dual Coxeter labels of the affine Dynkin diagram being the kernel (i.e. column eigenvector with zero eigenvalue) of the affine Cartan matrix.

In a *twisted* affine Dynkin diagram, the extra node is attached to some other node of the regular Dynkin diagram. A twisted affine Cartan matrix takes the form:

$$A^{ij}_{twisted} = \begin{pmatrix} A^{ij} & [col] \\ -[irrep] & 2 \end{pmatrix}, \tag{A.32}$$

where the column vector $[col]$ is obtained by transposing the Dynkin labels of $[irrep]$ and replacing any non-zero entries with one of $\{-1, -2, -3, -4\}$, such that $A^{ij}_{twisted}$ becomes degenerate. The dual Coxeter labels are given by the kernel of the twisted affine Cartan matrix.

There are six permissible types of twisted affine Dynkin diagram, with

three of these, $B_n^{(2)}, \tilde{B}_n^{(2)}$ and $C_n^{(2)}$, forming infinite families, plus three unique cases, $A_1^{(2)}, F_4^{(2)}$ and $G_2^{(3)}$. Figure 6.7 shows the BCF twisted affine Dynkin diagrams using the naming convention in [58].

The degeneracy of an affine Dynkin diagram permits a gauge choice to eliminate one of the nodes. The other nodes become the nodes of a regular Dynkin diagram. Correspondingly, the Cartan matrix for an affine Lie algebra can be reduced to that for a regular Lie algebra by the elimination of a row and its corresponding column. The dual Coxeter and Coxeter labels of other nodes are invariant under this addition or subtraction of affine nodes.

For further detail the reader is referred to [58].

A.4. Chevalley Serre Basis of Lie Algebra

The Lie algebra $\mathfrak{g}$ of a group G of rank r, consisting of operators $\{H_i, E_{\alpha+}, E_{\alpha-}\}$, can be expressed in terms of the basis $\{H_i, E_{i+}, E_{i-}\}$, where $i = 1, \ldots, r$, and the roots $\alpha \in \Phi$ are expressed in the basis of simple roots $(\alpha_1, \ldots, \alpha_r)$. The simple root operators $E_{i\pm}$ combine into the root operators $E_{\alpha\pm}$, in accordance with the Chevalley-Serre relations [58, 87], and the Lie algebra $\mathfrak{g}$, can be reconstructed from the Cartan matrix A:

$$\begin{aligned} [H_i, H_j] &= 0, \\ [H_i, E_{j\pm}] &= \pm A_{ji} E_{j\pm}, \\ [E_{i+}, E_{i-}] &= H_i, \\ [E_\alpha, E_\beta] &= N_{\alpha\beta} E_{\alpha+\beta}, \\ N_{\alpha\beta} &= \pm \begin{cases} \alpha + \beta \in \Phi : \pi \\ \alpha + \beta \notin \Phi : 0 \end{cases}, \end{aligned} \tag{A.33}$$

where π is the maximum integer such that $\alpha + \beta - \pi\alpha \in \Phi$, (so that π is the length of the root string starting at $\alpha + \beta$ and passing through α). A consistent conventional choice is necessary regarding the signs of $N_{\alpha\beta}$.

A.5. Bala-Carter Labels

Bala-Carter theory [33, 87, 78, 79] leads to a system of labels for nilpotent orbits ("BC labels"), that do not relate in a simple manner to the invariant subgroups of G and W_G deployed in the NOL formula; nonetheless, the labels are widely used in the Literature, in particular for Exceptional groups, and require comment.

The initial motivation for the Bala-Carter approach was [78],

> "[to] give an alternative way of describing the unipotent classes of G which, while being quite close to Dynkin's method[1], nevertheless gives a conceptually fairly simple way of describing the classes."

The selection of a Bala-Carter label for a nilpotent orbit starts from a given Characteristic and proceeds by Lie algebra and dimensional reasoning. A simplified account, drawing on [33, 54, 87, 78, 79], can be given as follows.

The aim is to classify a nilpotent element X (in a standard triple) of the algebra $\mathfrak{g}$ of G, based on the identity of the minimal regular semi-simple subalgebra $\mathfrak{l} \subseteq \mathfrak{g}$ within which X is distinguished. In [78], Bala-Carter establish a bijection between the (conjugacy classes of) distinguished nilpotent elements X^d of $\mathfrak{g}$ and the distinguished parabolic subalgebras $\mathfrak{p}^d$ of $\mathfrak{g}$. In [79], Bala-Carter seek to extend this bijection to all nilpotent elements X of $\mathfrak{g}$, by positing minimal regular semi-simple Levi subalgebras $\mathfrak{l} \subseteq \mathfrak{g}$, whose distinguished parabolic subalgebras $\mathfrak{p}^d_{\mathfrak{l}}$ *contain* X. The restriction to *distinguished* parabolic subalgebras is motivated by a group G having $2^{\mathrm{rank}[G]}$ parabolic subalgebras, which are too many for a bijective map to nilpotent elements. The reconciliation in [79] between BC labels of Levi subalgebras $\mathfrak{l}$ and Characteristics ρ^G involves reference to work on centralisers in [87], which in turn draws on a subalgebra labelling scheme introduced in [54].[2]

To examine the logic of the Bala-Carter labelling method in more detail, recall that a parabolic subalgebra $\mathfrak{p}$ of $\mathfrak{g}$ contains a Borel subalgebra $\mathfrak{b} \subseteq \mathfrak{p} \subseteq \mathfrak{g}$, where $\mathfrak{b}_{+/-} \equiv \mathfrak{h} + \mathfrak{n}_{+/-}$, the CSA of $\mathfrak{g}$ is $\mathfrak{h}$, and $\mathfrak{n}_{+/-}$ are the nilradicals of $\mathfrak{g}$.

[1] The method referred to is the labelling of Characteristics with regular and special subalgebras of G.

[2] A consistent reconciliation is not helped by Bala-Carter's caution [79] that there are errors in the tables in [54] and in [87].

Certain parabolic subalgebras $\mathfrak{p} \equiv \mathfrak{g} - \mathfrak{n}$ correspond to the nilpotent subalgebras $\mathfrak{n}$ of nilpotent orbits, with $\mathfrak{p} = \mathfrak{b}_-$ and $\mathfrak{n} = \mathfrak{n}_+$ corresponding to the maximal nilpotent orbit, and $\mathfrak{p} = \mathfrak{g}$ and $\mathfrak{n} = \emptyset$ to the trivial nilpotent orbit. A distinguished nilpotent orbit of $\mathfrak{g}$ has a parabolic subalgebra $\mathfrak{p}^d \supseteq \mathfrak{b}_-$ and $\mathfrak{n}^d \subseteq \mathfrak{n}_+$.

Now, consider the adjoint partition of G under the homomorphism ρ. This can be written as $\left(b_1^{n_{b_1}}, f_1^{n_{f_1}}, \ldots, b_k^{n_{b_k}}, f_k^{n_{f_k}}, 1^{n_0}\right)$, with integers $n_j \geq 0$, where b_i denote (dimensions of) non-singlet bosonic $SU(2)$ irreps, f_i denote (dimensions of) fermionic $SU(2)$ irreps and 1 identifies $SU(2)$ singlets.

It follows from 4.10, that the dimension of the nilpotent orbit $\mathcal{O}_{\rho^{\mathcal{G}}}$ is given by:

$$\left|\mathcal{O}_{\rho^{\mathcal{G}}}\right| = |G| - (n_2 + n_1 + n_0)\,, \tag{A.34}$$

where $n_1 = \sum_{i=1}^{k} n_{f_i}$ and $n_2 = \sum_{i=1}^{k} n_{b_i}$. In effect, each $SU(2)$ representation removes one degree of freedom from the dimension of the orbit. The nilpositive element X for ρ^G is built from $\Phi_G^{[2]}$, which contains n_2 positive roots of G, one from each non-singlet bosonic $SU(2)$ irrep in the adjoint partition.

The subalgebra $\mathfrak{c}_0$ of $\mathfrak{g}$ transforming in the singlet representation of $SU(2)$ lies within the *centralizer* $\mathfrak{c}$ of the nilpotent element X. $\mathfrak{c}_0$ has dimension n_0 and is identifiable as a subgroup C of G by dimensional arguments.

From amongst the possible branchings of G into subgroups, Bala-Carter *assume** subgroups C and L can be found, such that $\text{rank}[G] = \text{rank}[C] + \text{rank}[L]$, $|C| = n_0$, and L is a minimal (lowest dimensioned) semi-simple subgroup, whose Lie algebra $\mathfrak{l}$ *contains* the nilpotent element X.

Then, X is reasoned to be an element within the distinguished parabolic subalgebra $\mathfrak{p}_{\mathfrak{l}}^d$ since, by construction, the partition of the adjoint of L does not contain any $SU(2)$ singlets. Thus, the nilpositive element X from ρ^G is both a distinguished nilpotent element of L and a nilpotent element of G.

The Bala-Carter label $L(a_i)$ for ρ^G is given by L, augmented by labels to identify the embedding of L in G (where ambiguity would otherwise exist) and/or to specify the distinguished orbit of L; if this is less than maximal, the indices i count the number of zeros in its Characteristic and the letters $\{a, b, \ldots\}$ select amongst orbits with the same number of zeros.

By way of examples, the $SU(3)$ orbits [22] and [11], analysed in Table 4.4, map to the BC labels A_2 and A_1, respectively and BC labels for F_4 Characteristics are shown in Table A.2. There are, however, drawbacks.

1. There are often inequivalent ways of embedding subgroups into G and these need to be identified as distinct in order for the BC labels L to map to the full set of nilpotent orbit Characteristics. Thus, BC labels require additional markings to select between (i) subgroups containing long and short roots, (ii) some E_7 nilpotent orbits, (iii) spinor pair orbits arising in D_{2r} (or the triplets of orbits related by D_4 triality) and (iv) distinguished orbits (as above). In all such cases, knowledge of the Characteristic is necessary to recover a unique description of the nilpotent element X.

2. The mapping from a Characteristic to its BC label L, and its inverse, are not straightforward. While the identification of the centraliser C and the rank of L may follow easily from a Characteristic, via the adjoint partition, on dimensional considerations, the identification of L generally requires analysis of the embeddings of X in $\mathfrak{g}$ and $\mathfrak{l}$.

3. Importantly, the embedding of $SU(2)$ into G under the homomorphism ρ is special, rather than regular. This entails that the nilpotent element X is generally a linear combination of multiple roots in $\mathfrak{n}_+$ [54], which complicates the structure of its centraliser. For orbits where C and L have regular embeddings into G, the unambiguous identification of the minimal subalgebra $\mathfrak{l}$ that *contains* X as a distinguished element can often be carried out; however, for other orbits, this exercise can become problematic, as illustrated below.

4. Although standard tables exist, for example in [33], there is no guarantee that BC labels are treated consistently across the Literature.[3] Furthermore, the BC labels of orbits partially match those of the prior labelling scheme developed in [54] and it is necessary to recognise which are being used.

Considering the possible group branchings from F_4 (detailed in section 2.6), the analysis in Table A.2 shows that the Characteristics [0002], [0001], [0010], [0101] and [2200] do not have mappings to regular semi-simple subgroups of equal rank $F_4 \to C \otimes L$ that resolve the BC labels. For example, G_2 and B_3 can only be obtained from F_4 via folding maps.

[3]Indeed, the tables presented in [79] contain errors: examples include the duplicated E_6 Characteristic with BC label A_4 on p.9. and the duplicated E_7 Characteristic with BC label D_5 on p.11. These errors are corrected in [33].

Characteristic	Dimension	Adjoint Partition	C	BC label - L
[0000]	0	(1^{52})	F_4	0
[1000]	16	$(3, 2^{14}, 1^{21})$	C_3	A_1
[0001]	22	$(3^7, 2^8, 1^{15})$	A_3	$\tilde{A}_1$
[0100]	28	$(4^2, 3^6, 2^{10}, 1^6)$	$A_1 \oplus A_1$	$A_1 + \tilde{A}_1$
[2000]	30	$(5, 3^{13}, 1^8)$	A_2	A_2
[0002]	30	$(5^7, 3, 1^{14})$	G_2	$\tilde{A}_2$
[0010]	34	$(5^3, 4^2, 3^6, 2^4, 1^3)$	A_1	$A_2 + \tilde{A}_1$
[2001]	36	$(7, 5^4, 4^4, 3, 1^6)$	$A_1 \oplus A_1$	B_2
[0101]	36	$(6^2, 5^3, 4^2, 3^2, 2^4, 1^3)$	A_1	$A_1 + \tilde{A}_2$
[1010]	38	$(7, 6^2, 5, 4^4, 3^3, 1^3)$	A_1	$C_3(a_1)$
[0200]	40	$(7^2, 5^4, 3^6)$	–	$F_4(a_3)$
[2200]	42	$(11, 7^5, 3, 1^3)$	A_1	B_3
[1012]	42	$(11, 10^2, 7, 4^2, 3, 1^3)$	A_1	C_3
[0202]	44	$(11^2, 9, 7, 5, 3^3)$	–	$F_4(a_2)$
[2202]	46	$(15, 11^2, 7, 5, 3)$	–	$F_4(a_1)$
[2222]	48	$(23, 15, 11, 3)$	–	F_4

C and L are subgroups of F_4, such that $|C| = n_0$ and $\text{rank}[G] = \text{rank}[C] + \text{rank}[L]$.
Red highlighting indicates cases where there is no regular branching from F_4 to $C \otimes L$.

Table A.2.: F_4 Orbits and Bala-Carter Labels

Furthermore, the non-singlet bosonic $SU(2)$ irreps in the adjoint partitions of the F_4 orbits require mapping, at the correct multiplicities, to the bosonic $SU(2)$ irreps in the adjoint partitions of the distinguished orbits of L (as listed in Appendix B. The reconciliation is straightforward for Characteristics [0000], [1000], [1010], [0200], [1012], [0202], [2202], [2222], as can be verified by inspection of adjoint partitions; however, it is problematic in the other cases. By way of example, we can compare the regular subgroup mapping for [1010], with the problematic mapping for [2200]:

$$\begin{aligned} [1010]: \ (7, 6^2, 5, 4^2, 3^2, 1^3) &\to \underbrace{(7, 5, 3^3)}_{C_3[202]} \oplus \underbrace{(1^3)}_{A_1} \oplus \underbrace{(6^2, 4^2)}_{C_3 \otimes A_1} \\ [2200]: \ (11, 7^5, 3, 1^3) &\to \underbrace{(11, 7, 3)}_{B_3[222]} \oplus \underbrace{(1^3)}_{A_1} \oplus \underbrace{(7^4)}_{B_3 \otimes A_1} . \end{aligned} \tag{A.35}$$

The latter does not include, within the distinguished $B_3[222]$ orbit, all the non-singlet bosonic $SU(2)$ irreps that contain elements of X; some elements of X are contained within a $B_3 \otimes A_1$ subalgebra.

Whenever the multiplicities of a non-singlet bosonic $SU(2)$ irrep within

the partition $\rho^G[adjoint]$ are not replicated within the adjoint partition of a distinguished orbit of L, this indicates that the nilpotent element X must contain some roots that lie outside $\mathfrak{l}$, contrary to the Bala-Carter assumption *(*)*. This in turn undermines the significance of the BC label.

Relationship to NOL formula

In order to construct nilpotent orbits, rather than just to describe the subalgebra relations surrounding nilpotent elements, we require the nilpotent subalgebra $\mathfrak{n}$ of $\mathfrak{g}$, rather than the parabolic subalgebra $\mathfrak{p}^d_{\mathfrak{l}}$ of $\mathfrak{l}$, and there is no simple relation between the two. Fortunately, all the complications surrounding the decomposition of $G \to C \otimes L$ can be avoided, by noting:

$$\begin{aligned} |\Phi_{G_0}| = 2\left|\Phi_G^{[0]}\right| &= (n_2 + n_0 - \text{rank}[G]), \\ \left|\Phi_G^{[1]}\right| &= n_1, \end{aligned} \tag{A.36}$$

where $\Phi_G^{[k]}$ is defined in 7.7, and rearranging A.34 as:

$$\left|\mathcal{O}_{\rho^G}\right| = |\Phi_G| - |\Phi_{G_0}| - \left|\Phi_G^{[1]}\right|. \tag{A.37}$$

In this form, A.37 suggests the construction of the nilpotent subalgebra $\mathfrak{n} = \{E_\alpha : \alpha \in \tilde{\Phi}_G^+\}$ of a nilpotent orbit of $\mathfrak{g}$ using an extension of the G/G_0 coset group structure applicable to Richardson orbits:

$$\tilde{\Phi}_G^+ = \Phi_G^+ - \Phi_G^{[0]} - \Phi_G^{[1]}, \tag{A.38}$$

which is precisely the prescription used in the NOL formula 7.5.

If $\Phi_G^{[1]} = \emptyset$, the complement $\mathfrak{p}$ of $\mathfrak{n}$ is a parabolic subalgebra of $\mathfrak{g}$, corresponding to a Richardson orbit. Thus, each even Characteristic corresponds to a different parabolic subalgebra of $\mathfrak{g}$, including the distinguished orbits as a subset. If $\Phi_G^{[1]} \neq \emptyset$, then $\mathfrak{p}$ is only parabolic if the orbit is a (non-even) Richardson orbit [69].

To summarise the difference in approach, whereas the Bala-Carter decomposition $G \to C \otimes L$ aims to identify a distinguished parabolic *minimal* subalgebra $\mathfrak{p}^d_{\mathfrak{l}}$ that *contains* X, the NOL formula for Richardson nilpotent orbits uses the nilpotent subalgebra $\mathfrak{n}$, which is the complement in $\mathfrak{g}$ of the *maximal* parabolic subalgebra $\mathfrak{p}$ that does *not contain* X.

A.6. Non-normal Orbit: $F_4[0002]$

Moduli Space		Unrefined HS
$g_{NO}^{F_4[2222]}(t)$	(a)	$\frac{(1-t^2)(1-t^6)(1-t^8)(1-t^{12})}{(1-t)^{52}}$
$g_{NOL}^{F_4[0002]}(t)$	(b)	$\frac{\left(\begin{array}{c}1+21t+257t^2+2018t^3+9573t^4+28261t^5\\+53781t^6+66651t^7+\ldots\,\text{palindrome}\ldots+t^{14}\end{array}\right)}{(1-t)^{30}(1+t)^{-1}}$
$g_{NOL}^{F_4[0002]}(t)\notin\mathcal{N}$	(c)	$26t^2+1053t^3+19474t^4+205803t^5+1064233t^6$
$g_{NOL}^{F_4[0100]}(t)\left[x_4t^2\right]$	(d)	$\frac{\left(\begin{array}{c}26+598t+5773t^2+30482t^3+96398t^4+190046t^5\\+237874t^6+\ldots\,\text{palindrome}\ldots+26t^{12}\end{array}\right)}{t^{-2}(1-t)^{28}}$ $=$ $+26t^2+1326t^3+33073t^4+540474t^5+6539702t^6+\mathcal{O}(t^7)$
$g_{NO}^{F_4[0002]}(t)$	(e)=(b)-(d)	$\frac{\left(\begin{array}{c}1+22t+252t^2+1729t^3+6988t^4+18300t^5\\+40835t^6+92700t^7+166252t^8+177698t^9+83654t^{10}\\-16141t^{11}-38932t^{12}-19256t^{13}-4581t^{14}-545t^{15}-26t^{16}\end{array}\right)}{(1-t)^{30}}$
	(f)	–

(c) consists of those terms in (b)-(a) with positive coefficients
(d) is a charged orbit built on $F_4[0100]$; the charge is identified from the leading term of (c)
(e) contains no terms outside $\mathcal{N}$, as required for the $F_4[0002]$ non-normal orbit
(f) consists of those terms in (e)-(a) with positive coefficients

Table A.3.: Non-Normal Orbit Construction using HS: $F_4[0002]$

Moduli Space		HWG
$g_{NO}^{F_4[2222]}(m,t)$	(a)	$1+m_4t^4+{m_1}^5t^5+{m_1}^2m_3t^5+m_1{m_3}^2t^5+m_2m_4t^5$ $+{m_1}^3{m_4}^2t^5+m_1{m_4}^4t^5+{m_1}^6t^6+{m_1}^3m_2t^6+2{m_2}^2t^6$ $+{m_1}^3m_3t^6+m_2m_3t^6+{m_1}^2{m_3}^2t^6+{m_1}^2m_4t^6$ $+m_1m_2m_4t^6+{m_1}^2m_3m_4t^6+{m_3}^2m_4t^6+{m_1}^4{m_4}^2t^6$ $+m_1m_2{m_4}^2t^6+m_1m_3{m_4}^2t^6+{m_3}^2{m_4}^2t^6+2{m_4}^3t^6$ $+m_3{m_4}^3t^6+{m_1}^2{m_4}^4t^6+{m_4}^6t^6+m_1(t+t^5)$ $+{m_1}^3(t^3+t^5)+m_3(t^3+t^5)+{m_1}^4(t^4+t^6)+{m_4}^4(t^4+t^6)$ $+{m_1}^2m_2(t^5+t^6)+m_1m_4(t^5+t^6)$ $+m_2{m_4}^2(t^5+t^6)+m_3{m_4}^2(t^5+t^6)+m_2(t^3+t^5+t^6)$ $+m_1m_2(t^4+t^5+t^6)+m_3m_4(t^4+t^5+t^6)$ $+m_1{m_4}^2(t^3+2t^5+t^6)+m_1m_3(t^4+2t^6)$ $+{m_1}^2(t^2+t^4+2t^6)+{m_4}^2(t^2+t^4+2t^6)+m_1m_3m_4(t^5+2t^6)$ $+{m_3}^2(t^4+3t^6)+{m_1}^2{m_4}^2(t^4+3t^6)+\mathcal{O}(t^7)$
$g_{NOL}^{F_4[0002]}(m,t)$	(b)	$\frac{(1+m_3m_4t^4)}{(1-m_1t)(1-m_4t^2)(1-{m_4}^2t^2)(1-m_2t^3)(1-m_3t^3)(1-{m_3}^2t^4)}$
$g_{NOL}^{F_4[0002]}(m,t)\notin\mathcal{N}$	(c)	$m_4t^2+m_1m_4t^3+{m_1}^2m_4t^4+{m_4}^3t^4+{m_1}^3m_4t^5$ $+m_1{m_4}^3t^5+{m_1}^4m_4t^6+{m_1}^2{m_4}^3t^6+{m_4}^5t^6+\mathcal{O}(t^7)$
$g_{NOL}^{F_4[0100]}(m,t)\left[x_4t^2\right]$	(d)	$\frac{(m_4+m_3t+m_3m_4t^2)t^2}{(1-m_1t)(1-{m_4}^2t^2)(1-m_2t^3)(1-{m_3}^2t^4)}$ $=$ $m_4t^2+m_3t^3+m_1m_4t^3+m_1m_3t^4+{m_1}^2m_4t^4$ $+m_3m_4t^4+{m_4}^3t^4+{m_1}^2m_3t^5+{m_1}^3m_4t^5$ $+m_2m_4t^5+m_1m_3m_4t^5+m_3{m_4}^2t^5+m_1{m_4}^3t^5$ $+{m_1}^3m_3t^6+m_2m_3t^6+{m_1}^4m_4t^6+m_1m_2m_4t^6$ $+{m_1}^2m_3m_4t^6+{m_3}^2m_4t^6+m_1m_3{m_4}^2t^6$ $+{m_1}^2{m_4}^3t^6+m_3{m_4}^3t^6+{m_4}^5t^6+\mathcal{O}(t^7)$
$g_{NO}^{F_4[0002]}(m,t)$	(e)=(b)-(d)	$\frac{\left(\begin{array}{c}1-m_4t^2-m_3t^3+{m_4}^2t^4+2m_3m_4t^5\\+m_3{m_4}^2t^6-m_3{m_4}^2t^7+{m_3}^2t^6\\+{m_3}^2m_4t^7-{m_3}^2m_4t^8-{m_3}^2{m_4}^2t^9\end{array}\right)}{(1-m_1t)(1-m_4t^2)(1-{m_4}^2t^2)(1-m_2t^3)(1-m_3t^3)(1-{m_3}^2t^4)}$
	(f)	$\mathcal{O}(t^7)$

(a) is the series expansion of the HWG up to t^6

(c) consists of those terms in (b)-(a) with positive coefficients

(d) is a charged orbit built on $F_4[0100]$; the charge is identified from the leading term of (c)

(e) contains no terms outside $\mathcal{N}$, as required for the $F_4[0002]$ non-normal orbit

(f) consists of those terms in (e)-(a) with positive coefficients

Table A.4.: Non-Normal Orbit Construction using HWGs: $F_4[0002]$

B. $SU(2)$ Homomorphisms

B.1. A Series

Dimension	Quiver	[1]	[2]	Root Map	Weight Map
0	{A_1}	$\{1^2\}$	$\{1^3\}$	{0}	{0}
2	{A_1, U_1}	{2}	{3}	{2}	{1}

Dimension	Quiver	[1,0]	[0,1]	[1,1]	Root Map	Weight Map
0	{A_2}	$\{1^3\}$	$\{1^3\}$	$\{1^8\}$	{0, 0}	{0, 0}
4	{A_2, U_1}	{2, 1}	{2, 1}	$\{3, 2^2, 1\}$	{1, 1}	{1, 1}
6	{A_2, U_2, U_1}	{3}	{3}	{5, 3}	{2, 2}	{2, 2}

Dimension	Quiver	[1,0,0]	[0,1,0]	[0,0,1]	[1,0,1]	Root Map	Weight Map
0	{A_3}	$\{1^4\}$	$\{1^6\}$	$\{1^4\}$	$\{1^{15}\}$	{0, 0, 0}	{0, 0, 0}
6	{A_3, U_1}	$\{2, 1^2\}$	$\{2^2, 1^2\}$	$\{2, 1^2\}$	$\{3, 2^4, 1^4\}$	{1, 0, 1}	{1, 1, 1}
8	{A_3, U_2}	$\{2^2\}$	$\{3, 1^3\}$	$\{2^2\}$	$\{3^4, 1^3\}$	{0, 2, 0}	{1, 2, 1}
10	{A_3, U_2, U_1}	{3, 1}	$\{3^2\}$	{3, 1}	$\{5, 3^3, 1\}$	{2, 0, 2}	{2, 2, 2}
12	{A_3, U_3, U_2, U_1}	{4}	{5, 1}	{4}	{7, 5, 3}	{2, 2, 2}	{3, 4, 3}

Dimension	Quiver	[1,0,0,0]	[0,0,0,1]	[1,0,0,1]	Root Map	Weight Map
0	$\{A_4\}$	$\{1^5\}$	$\{1^5\}$	$\{1^{24}\}$	$\{0,0,0,0\}$	$\{0,0,0,0\}$
8	$\{A_4, U_1\}$	$\{2,1^3\}$	$\{2,1^3\}$	$\{3,2^6,1^9\}$	$\{1,0,0,1\}$	$\{1,1,1,1\}$
12	$\{A_4, U_2\}$	$\{2^2,1\}$	$\{2^2,1\}$	$\{3^4,2^4,1^4\}$	$\{0,1,1,0\}$	$\{1,2,2,1\}$
14	$\{A_4, U_2, U_1\}$	$\{3,1^2\}$	$\{3,1^2\}$	$\{5,3^5,1^4\}$	$\{2,0,0,2\}$	$\{2,2,2,2\}$
16	$\{A_4, U_3, U_1\}$	$\{3,2\}$	$\{3,2\}$	$\{5,4^2,3^2,2^2,1\}$	$\{1,1,1,1\}$	$\{2,3,3,2\}$
18	$\{A_4, U_3, U_2, U_1\}$	$\{4,1\}$	$\{4,1\}$	$\{7,5,4^2,3,1\}$	$\{2,1,1,2\}$	$\{3,4,4,3\}$
20	$\{A_4, U_4, U_3, U_2, U_1\}$	$\{5\}$	$\{5\}$	$\{9,7,5,3\}$	$\{2,2,2,2\}$	$\{4,6,6,4\}$

Dimension	Quiver	[1,0,0,0,0]	[0,0,0,0,1]	[1,0,0,0,1]	Root Map	Weight Map
0	$\{A_5\}$	$\{1^6\}$	$\{1^6\}$	$\{1^{35}\}$	$\{0,0,0,0,0\}$	$\{0,0,0,0,0\}$
10	$\{A_5, U_1\}$	$\{2,1^4\}$	$\{2,1^4\}$	$\{3,2^8,1^{16}\}$	$\{1,0,0,0,1\}$	$\{1,1,1,1,1\}$
16	$\{A_5, U_2\}$	$\{2^2,1^2\}$	$\{2^2,1^2\}$	$\{3^4,2^8,1^7\}$	$\{0,1,0,1,0\}$	$\{1,2,2,2,1\}$
18	$\{A_5, U_3\}$	$\{2^3\}$	$\{2^3\}$	$\{3^9,1^8\}$	$\{0,0,2,0,0\}$	$\{1,2,3,2,1\}$
18	$\{A_5, U_2, U_1\}$	$\{3,1^3\}$	$\{3,1^3\}$	$\{5,3^7,1^9\}$	$\{2,0,0,0,2\}$	$\{2,2,2,2,2\}$
22	$\{A_5, U_3, U_1\}$	$\{3,2,1\}$	$\{3,2,1\}$	$\{5,4^2,3^4,2^4,1^2\}$	$\{1,1,0,1,1\}$	$\{2,3,3,3,2\}$
24	$\{A_5, U_4, U_2\}$	$\{3^2\}$	$\{3^2\}$	$\{5^4,3^4,1^3\}$	$\{0,2,0,2,0\}$	$\{2,4,4,4,2\}$
24	$\{A_5, U_3, U_2, U_1\}$	$\{4,1^2\}$	$\{4,1^2\}$	$\{7,5,4^4,3,1^4\}$	$\{2,1,0,1,2\}$	$\{3,4,4,4,3\}$
26	$\{A_5, U_4, U_2, U_1\}$	$\{4,2\}$	$\{4,2\}$	$\{7,5^3,3^4,1\}$	$\{2,0,2,0,2\}$	$\{3,4,5,4,3\}$
28	$\{A_5, U_4, U_3, U_2, U_1\}$	$\{5,1\}$	$\{5,1\}$	$\{9,7,5^3,3,1\}$	$\{2,2,0,2,2\}$	$\{4,6,6,6,4\}$
30	$\{A_5, U_5, U_4, U_3, U_2, U_1\}$	$\{6\}$	$\{6\}$	$\{11,9,7,5,3\}$	$\{2,2,2,2,2\}$	$\{5,8,9,8,5\}$

Partitions are shown under each homomorphism for the fundamental, anti-fundamental and adjoint representations. For A_3, the vector representation partitions are also shown.

B.2. B Series

Dimension	Quiver	[2]	[1]	Root Map	Weight Map
0	$\{B_1\}$	$\{1^3\}$	$\{1^2\}$	$\{0\}$	$\{0\}$
2	$\{B_1, C_1, B_0\}$	$\{3\}$	$\{2\}$	$\{2\}$	$\{1\}$

Dimension	Quiver	[1,0]	[0,1]	[0,2]	Root Map	Weight Map
0	$\{B_2\}$	$\{1^5\}$	$\{1^4\}$	$\{1^{10}\}$	$\{0, 0\}$	$\{0, 0\}$
4	$\{B_2, C_1\}$	$\{2^2, 1\}$	$\{2, 1^2\}$	$\{3, 2^2, 1^3\}$	$\{0, 1\}$	$\{1, 1\}$
6	$\{B_2, C_1, B_0\}$	$\{3, 1^2\}$	$\{2^2\}$	$\{3^3, 1\}$	$\{2, 0\}$	$\{2, 1\}$
8	$\{B_2, C_2, B_1, C_1, B_0\}$	$\{5\}$	$\{4\}$	$\{7, 3\}$	$\{2, 2\}$	$\{4, 3\}$

Dimension	Quiver	[1,0,0]	[0,1,0]	[0,0,1]	Root Map	Weight Map
0	$\{B_3\}$	$\{1^7\}$	$\{1^{21}\}$	$\{1^8\}$	$\{0, 0, 0\}$	$\{0, 0, 0\}$
8	$\{B_3, C_1\}$	$\{2^2, 1^3\}$	$\{3, 2^6, 1^6\}$	$\{2^2, 1^4\}$	$\{0, 1, 0\}$	$\{1, 2, 1\}$
10	$\{B_3, C_1, B_0\}$	$\{3, 1^4\}$	$\{3^5, 1^6\}$	$\{2^4\}$	$\{2, 0, 0\}$	$\{2, 2, 1\}$
12	$\{B_3, C_2, B_0\}$	$\{3, 2^2\}$	$\{4^2, 3^2, 2^2, 1^3\}$	$\{3, 2^2, 1\}$	$\{1, 0, 1\}$	$\{2, 3, 2\}$
14	$\{B_3, C_2, D_1\}$	$\{3^2, 1\}$	$\{5, 3^5, 1\}$	$\{3^2, 1^2\}$	$\{0, 2, 0\}$	$\{2, 4, 2\}$
16	$\{B_3, C_2, B_1, C_1, B_0\}$	$\{5, 1^2\}$	$\{7, 5^2, 3, 1\}$	$\{4^2\}$	$\{2, 2, 0\}$	$\{4, 6, 3\}$
18	$\{B_3, C_3, B_2, C_2, B_1, C_1, B_0\}$	$\{7\}$	$\{11, 7, 3\}$	$\{7, 1\}$	$\{2, 2, 2\}$	$\{6, 10, 6\}$

Dimension	Quiver	[1,0,0,0]	[0,1,0,0]	[0,0,0,1]	Root Map	Weight Map
0	$\{B_4\}$	$\{1^9\}$	$\{1^{36}\}$	$\{1^{16}\}$	$\{0, 0, 0, 0\}$	$\{0, 0, 0, 0\}$
12	$\{B_4, C_1\}$	$\{2^2, 1^5\}$	$\{3, 2^{10}, 1^{13}\}$	$\{2^4, 1^8\}$	$\{0, 1, 0, 0\}$	$\{1, 2, 2, 1\}$
14	$\{B_4, C_1, B_0\}$	$\{3, 1^6\}$	$\{3^7, 1^{15}\}$	$\{2^8\}$	$\{2, 0, 0, 0\}$	$\{2, 2, 2, 1\}$
16	$\{B_4, C_2\}$	$\{2^4, 1\}$	$\{3^6, 2^4, 1^{10}\}$	$\{3, 2^4, 1^5\}$	$\{0, 0, 0, 1\}$	$\{1, 2, 3, 2\}$
20	$\{B_4, C_2, B_0\}$	$\{3, 2^2, 1^2\}$	$\{4^2, 3^4, 2^6, 1^4\}$	$\{3^2, 2^4, 1^2\}$	$\{1, 0, 1, 0\}$	$\{2, 3, 4, 2\}$
22	$\{B_4, C_2, D_1\}$	$\{3^2, 1^3\}$	$\{5, 3^9, 1^4\}$	$\{3^4, 1^4\}$	$\{0, 2, 0, 0\}$	$\{2, 4, 4, 2\}$
24	$\{B_4, C_3, B_1\}$	$\{3^3\}$	$\{5^3, 3^6, 1^3\}$	$\{4^2, 2^4\}$	$\{0, 0, 2, 0\}$	$\{2, 4, 6, 3\}$
24	$\{B_4, C_2, B_1, C_1, B_0\}$	$\{5, 1^4\}$	$\{7, 5^4, 3, 1^6\}$	$\{4^4\}$	$\{2, 2, 0, 0\}$	$\{4, 6, 6, 3\}$
26	$\{B_4, C_3, D_2, C_1\}$	$\{4^2, 1\}$	$\{7, 5^3, 4^2, 3, 1^3\}$	$\{5, 4^2, 1^3\}$	$\{0, 2, 0, 1\}$	$\{3, 6, 7, 4\}$
26	$\{B_4, C_3, B_1, C_1, B_0\}$	$\{5, 2^2\}$	$\{7, 6^2, 4^2, 3^2, 1^3\}$	$\{5, 4^2, 3\}$	$\{2, 1, 0, 1\}$	$\{4, 6, 7, 4\}$
28	$\{B_4, C_3, D_2, C_1, B_0\}$	$\{5, 3, 1\}$	$\{7^2, 5^2, 3^4\}$	$\{5^2, 3^2\}$	$\{2, 0, 2, 0\}$	$\{4, 6, 8, 4\}$
30	$\{B_4, C_3, B_2, C_2, B_1, C_1, B_0\}$	$\{7, 1^2\}$	$\{11, 7^3, 3, 1\}$	$\{7^2, 1^2\}$	$\{2, 2, 2, 0\}$	$\{6, 10, 12, 6\}$
32	$\{B_4, C_4, B_3, C_3, B_2, C_2, B_1, C_1, B_0\}$	$\{9\}$	$\{15, 11, 7, 3\}$	$\{11, 5\}$	$\{2, 2, 2, 2\}$	$\{8, 14, 18, 10\}$

Dimension	Quiver	[1,0,0,0,0]	[0,1,0,0,0]	[0,0,0,0,1]	Root Map	Weight Map
0	$\{B_5\}$	$\{1^{11}\}$	$\{1^{55}\}$	$\{1^{32}\}$	$\{0,0,0,0,0\}$	$\{0,0,0,0,0\}$
16	$\{B_5, C_1\}$	$\{2^2, 1^7\}$	$\{3, 2^{14}, 1^{24}\}$	$\{2^8, 1^{16}\}$	$\{0,1,0,0,0\}$	$\{1,2,2,2,1\}$
18	$\{B_5, C_1, B_0\}$	$\{3, 1^8\}$	$\{3^9, 1^{28}\}$	$\{2^{16}\}$	$\{2,0,0,0,0\}$	$\{2,2,2,2,1\}$
24	$\{B_5, C_2\}$	$\{2^4, 1^3\}$	$\{3^6, 2^{12}, 1^{13}\}$	$\{3^2, 2^8, 1^{10}\}$	$\{0,0,0,1,0\}$	$\{1,2,3,4,2\}$
28	$\{B_5, C_2, B_0\}$	$\{3, 2^2, 1^4\}$	$\{4^2, 3^6, 2^{10}, 1^9\}$	$\{3^4, 2^8, 1^4\}$	$\{1,0,1,0,0\}$	$\{2,3,4,4,2\}$
30	$\{B_5, C_3, B_0\}$	$\{3, 2^4\}$	$\{4^4, 3^7, 2^4, 1^{10}\}$	$\{4, 3^4, 2^6, 1^4\}$	$\{1,0,0,0,1\}$	$\{2,3,4,5,3\}$
30	$\{B_5, C_2, D_1\}$	$\{3^2, 1^5\}$	$\{5, 3^{13}, 1^{11}\}$	$\{3^8, 1^8\}$	$\{0,2,0,0,0\}$	$\{2,4,4,4,2\}$
32	$\{B_5, C_2, B_1, C_1, B_0\}$	$\{5, 1^6\}$	$\{7, 5^6, 3, 1^{15}\}$	$\{4^8\}$	$\{2,2,0,0,0\}$	$\{4,6,6,6,3\}$
34	$\{B_5, C_3, D_1\}$	$\{3^2, 2^2, 1\}$	$\{5, 4^4, 3^6, 2^6, 1^4\}$	$\{4^2, 3^4, 2^4, 1^4\}$	$\{0,1,0,1,0\}$	$\{2,4,5,6,3\}$
36	$\{B_5, C_3, B_1\}$	$\{3^3, 1^2\}$	$\{5^3, 3^{12}, 1^4\}$	$\{4^4, 2^8\}$	$\{0,0,2,0,0\}$	$\{2,4,6,6,3\}$
38	$\{B_5, C_3, D_2, C_1\}$	$\{4^2, 1^3\}$	$\{7, 5^3, 4^6, 3, 1^6\}$	$\{5^2, 4^4, 1^6\}$	$\{0,2,0,1,0\}$	$\{3,6,7,8,4\}$
38	$\{B_5, C_3, B_1, C_1, B_0\}$	$\{5, 2^2, 1^2\}$	$\{7, 6^2, 5^2, 4^2, 3^2, 2^4, 1^4\}$	$\{5^2, 4^4, 3^2\}$	$\{2,1,0,1,0\}$	$\{4,6,7,8,4\}$
40	$\{B_5, C_4, B_2, C_1\}$	$\{4^2, 3\}$	$\{7, 6^2, 5^3, 4^2, 3^2, 2^2, 1^3\}$	$\{6, 5^2, 4, 3^2, 2^3\}$	$\{0,1,1,0,1\}$	$\{3,6,8,9,5\}$
40	$\{B_5, C_3, D_2, C_1, B_0\}$	$\{5, 3, 1^3\}$	$\{7^2, 5^4, 3^6, 1^3\}$	$\{5^4, 3^4\}$	$\{2,0,2,0,0\}$	$\{4,6,8,8,4\}$
42	$\{B_5, C_4, B_2, C_1, B_0\}$	$\{5, 3^2\}$	$\{7^3, 5^3, 3^6, 1\}$	$\{6^2, 4^4, 2^2\}$	$\{2,0,0,2,0\}$	$\{4,6,8,10,5\}$
42	$\{B_5, C_3, B_2, C_2, B_1, C_1, B_0\}$	$\{7, 1^4\}$	$\{11, 7^5, 3, 1^6\}$	$\{7^4, 1^4\}$	$\{2,2,2,0,0\}$	$\{6,10,12,12,6\}$
44	$\{B_5, C_4, D_3, C_2, D_1\}$	$\{5^2, 1\}$	$\{9, 7^3, 5^3, 3^3, 1\}$	$\{7^2, 5^2, 3^2, 1^2\}$	$\{0,2,0,2,0\}$	$\{4,8,10,12,6\}$
44	$\{B_5, C_4, B_2, C_2, B_1, C_1, B_0\}$	$\{7, 2^2\}$	$\{11, 8^2, 7, 6^2, 3^2, 1^3\}$	$\{8, 7^2, 6, 2, 1^2\}$	$\{2,2,1,0,1\}$	$\{6,10,12,13,7\}$
46	$\{B_5, C_4, D_3, C_2, B_1, C_1, B_0\}$	$\{7, 3, 1\}$	$\{11, 9, 7^3, 5, 3^3\}$	$\{8^2, 6^2, 2^2\}$	$\{2,2,0,2,0\}$	$\{6,10,12,14,7\}$
48	$\{B_5, C_4, B_3, C_3, B_2, C_2, B_1, C_1, B_0\}$	$\{9, 1^2\}$	$\{15, 11, 9^2, 7, 3, 1\}$	$\{11^2, 5^2\}$	$\{2,2,2,2,0\}$	$\{8,14,18,20,10\}$
50	$\{B_5, C_5, B_4, C_4, B_3, C_3, B_2, C_2, B_1, C_1, B_0\}$	$\{11\}$	$\{19, 15, 11, 7, 3\}$	$\{16, 10, 6\}$	$\{2,2,2,2,2\}$	$\{10,18,24,28,15\}$

Partitions are shown under each homomorphism for the vector, adjoint and spinor representations.

B.3. C Series

Dimension	Quiver	[1]	[2]	Root Map	Weight Map
0	$\{C_1\}$	$\{1^2\}$	$\{1^3\}$	$\{0\}$	$\{0\}$
2	$\{C_1, B_0\}$	$\{2\}$	$\{3\}$	$\{2\}$	$\{1\}$

Dimension	Quiver	[1,0]	[0,1]	[2,0]	Root Map	Weight Map
0	$\{C_2\}$	$\{1^4\}$	$\{1^5\}$	$\{1^{10}\}$	$\{0,0\}$	$\{0,0\}$
4	$\{C_2, B_0\}$	$\{2, 1^2\}$	$\{2^2, 1\}$	$\{3, 2^2, 1^3\}$	$\{1,0\}$	$\{1,1\}$
6	$\{C_2, D_1\}$	$\{2^2\}$	$\{3, 1^2\}$	$\{3^3, 1\}$	$\{0,2\}$	$\{1,2\}$
8	$\{C_2, B_1, C_1, B_0\}$	$\{4\}$	$\{5\}$	$\{7,3\}$	$\{2,2\}$	$\{3,4\}$

Dimension	Quiver	[1,0,0]	[2,0,0]	Root Map	Weight Map
0	$\{C_3\}$	$\{1^{6}\}$	$\{1^{21}\}$	$\{0, 0, 0\}$	$\{0, 0, 0\}$
6	$\{C_3, B_0\}$	$\{2, 1^{4}\}$	$\{3, 2^{4}, 1^{10}\}$	$\{1, 0, 0\}$	$\{1, 1, 1\}$
10	$\{C_3, D_1\}$	$\{2^{2}, 1^{2}\}$	$\{3^{3}, 2^{4}, 1^{4}\}$	$\{0, 1, 0\}$	$\{1, 2, 2\}$
12	$\{C_3, B_1\}$	$\{2^{3}\}$	$\{3^{6}, 1^{3}\}$	$\{0, 0, 2\}$	$\{1, 2, 3\}$
14	$\{C_3, D_2, C_1\}$	$\{3^{2}\}$	$\{5^{3}, 3, 1^{3}\}$	$\{0, 2, 0\}$	$\{2, 4, 4\}$
14	$\{C_3, B_1, C_1, B_0\}$	$\{4, 1^{2}\}$	$\{7, 4^{2}, 3, 1^{3}\}$	$\{2, 1, 0\}$	$\{3, 4, 4\}$
16	$\{C_3, D_2, C_1, B_0\}$	$\{4, 2\}$	$\{7, 5, 3^{3}\}$	$\{2, 0, 2\}$	$\{3, 4, 5\}$
18	$\{C_3, B_2, C_2, B_1, C_1, B_0\}$	$\{6\}$	$\{11, 7, 3\}$	$\{2, 2, 2\}$	$\{5, 8, 9\}$

Dimension	Quiver	[1,0,0,0]	[2,0,0,0]	Root Map	Weight Map
0	$\{C_4\}$	$\{1^{8}\}$	$\{1^{36}\}$	$\{0, 0, 0, 0\}$	$\{0, 0, 0, 0\}$
8	$\{C_4, B_0\}$	$\{2, 1^{6}\}$	$\{3, 2^{6}, 1^{21}\}$	$\{1, 0, 0, 0\}$	$\{1, 1, 1, 1\}$
14	$\{C_4, D_1\}$	$\{2^{2}, 1^{4}\}$	$\{3^{3}, 2^{8}, 1^{11}\}$	$\{0, 1, 0, 0\}$	$\{1, 2, 2, 2\}$
18	$\{C_4, B_1\}$	$\{2^{3}, 1^{2}\}$	$\{3^{6}, 2^{6}, 1^{6}\}$	$\{0, 0, 1, 0\}$	$\{1, 2, 3, 3\}$
20	$\{C_4, D_2\}$	$\{2^{4}\}$	$\{3^{10}, 1^{6}\}$	$\{0, 0, 0, 2\}$	$\{1, 2, 3, 4\}$
20	$\{C_4, B_1, C_1, B_0\}$	$\{4, 1^{4}\}$	$\{7, 4^{4}, 3, 1^{10}\}$	$\{2, 1, 0, 0\}$	$\{3, 4, 4, 4\}$
22	$\{C_4, D_2, C_1\}$	$\{3^{2}, 1^{2}\}$	$\{5^{3}, 3^{5}, 1^{6}\}$	$\{0, 2, 0, 0\}$	$\{2, 4, 4, 4\}$
24	$\{C_4, B_2, C_1\}$	$\{3^{2}, 2\}$	$\{5^{3}, 4^{2}, 3^{2}, 2^{2}, 1^{3}\}$	$\{0, 1, 1, 0\}$	$\{2, 4, 5, 5\}$
24	$\{C_4, D_2, C_1, B_0\}$	$\{4, 2, 1^{2}\}$	$\{7, 5, 4^{2}, 3^{3}, 2^{2}, 1^{3}\}$	$\{2, 0, 1, 0\}$	$\{3, 4, 5, 5\}$
26	$\{C_4, B_2, C_1, B_0\}$	$\{4, 2^{2}\}$	$\{7, 5^{2}, 3^{6}, 1\}$	$\{2, 0, 0, 2\}$	$\{3, 4, 5, 6\}$
28	$\{C_4, D_3, C_2, D_1\}$	$\{4^{2}\}$	$\{7^{3}, 5, 3^{3}, 1\}$	$\{0, 2, 0, 2\}$	$\{3, 6, 7, 8\}$
28	$\{C_4, B_2, C_2, B_1, C_1, B_0\}$	$\{6, 1^{2}\}$	$\{11, 7, 6^{2}, 3, 1^{3}\}$	$\{2, 2, 1, 0\}$	$\{5, 8, 9, 9\}$
30	$\{C_4, D_3, C_2, B_1, C_1, B_0\}$	$\{6, 2\}$	$\{11, 7^{2}, 5, 3^{2}\}$	$\{2, 2, 0, 2\}$	$\{5, 8, 9, 10\}$
32	$\{C_4, B_3, C_3, B_2, C_2, B_1, C_1, B_0\}$	$\{8\}$	$\{15, 11, 7, 3\}$	$\{2, 2, 2, 2\}$	$\{7, 12, 15, 16\}$

Dimension	Quiver	[1,0,0,0,0]	[2,0,0,0,0]	Root Map	Weight Map
0	$\{C_5\}$	$\{1^{10}\}$	$\{1^{55}\}$	{0, 0, 0, 0, 0}	{0, 0, 0, 0, 0}
10	$\{C_5, B_0\}$	$\{2, 1^8\}$	$\{3, 2^8, 1^{36}\}$	{1, 0, 0, 0, 0}	{1, 1, 1, 1, 1}
18	$\{C_5, D_1\}$	$\{2^2, 1^6\}$	$\{3^3, 2^{12}, 1^{22}\}$	{0, 1, 0, 0, 0}	{1, 2, 2, 2, 2}
24	$\{C_5, B_1\}$	$\{2^3, 1^4\}$	$\{3^6, 2^{12}, 1^{13}\}$	{0, 0, 1, 0, 0}	{1, 2, 3, 3, 3}
26	$\{C_5, B_1, C_1, B_0\}$	$\{4, 1^6\}$	$\{7, 4^6, 3, 1^{21}\}$	{2, 1, 0, 0, 0}	{3, 4, 4, 4, 4}
28	$\{C_5, D_2\}$	$\{2^4, 1^2\}$	$\{3^{10}, 2^8, 1^9\}$	{0, 0, 0, 1, 0}	{1, 2, 3, 4, 4}
30	$\{C_5, B_2\}$	$\{2^5\}$	$\{3^{15}, 1^{10}\}$	{0, 0, 0, 0, 2}	{1, 2, 3, 4, 5}
30	$\{C_5, D_2, C_1\}$	$\{3^2, 1^4\}$	$\{5^3, 3^9, 1^{13}\}$	{0, 2, 0, 0, 0}	{2, 4, 4, 4, 4}
32	$\{C_5, D_2, C_1, B_0\}$	$\{4, 2, 1^4\}$	$\{7, 5, 4^4, 3^3, 2^4, 1^{10}\}$	{2, 0, 1, 0, 0}	{3, 4, 5, 5, 5}
34	$\{C_5, B_2, C_1\}$	$\{3^2, 2, 1^2\}$	$\{5^3, 4^2, 3^6, 2^4, 1^6\}$	{0, 1, 1, 0, 0}	{2, 4, 5, 5, 5}
36	$\{C_5, D_3, C_1\}$	$\{3^2, 2^2\}$	$\{5^3, 4^4, 3^4, 2^4, 1^4\}$	{0, 1, 0, 1, 0}	{2, 4, 5, 6, 6}
36	$\{C_5, B_2, C_1, B_0\}$	$\{4, 2^2, 1^2\}$	$\{7, 5^2, 4^2, 3^6, 2^4, 1^4\}$	{2, 0, 0, 1, 0}	{3, 4, 5, 6, 6}
38	$\{C_5, D_3, C_1, B_0\}$	$\{4, 2^3\}$	$\{7, 5^3, 3^{10}, 1^3\}$	{2, 0, 0, 0, 2}	{3, 4, 5, 6, 7}
38	$\{C_5, B_2, C_2, B_1, C_1, B_0\}$	$\{6, 1^4\}$	$\{11, 7, 6^4, 3, 1^{10}\}$	{2, 2, 1, 0, 0}	{5, 8, 9, 9, 9}
40	$\{C_5, B_3, C_2, B_0\}$	$\{4, 3^2\}$	$\{7, 6^2, 5^3, 4^2, 3^2, 2^2, 1^3\}$	{1, 0, 1, 1, 0}	{3, 5, 7, 8, 8}
40	$\{C_5, D_3, C_2, D_1\}$	$\{4^2, 1^2\}$	$\{7^3, 5, 4^4, 3^3, 1^4\}$	{0, 2, 0, 1, 0}	{3, 6, 7, 8, 8}
42	$\{C_5, B_3, C_2, D_1\}$	$\{4^2, 2\}$	$\{7^3, 5^3, 3^6, 1\}$	{0, 2, 0, 0, 2}	{3, 6, 7, 8, 9}
42	$\{C_5, D_3, C_2, B_1, C_1, B_0\}$	$\{6, 2, 1^2\}$	$\{11, 7^2, 6^2, 5, 3^2, 2^2, 1^3\}$	{2, 2, 0, 1, 0}	{5, 8, 9, 10, 10}
44	$\{C_5, D_4, C_3, D_2, C_1\}$	$\{5^2\}$	$\{9^3, 7, 5^3, 3, 1^3\}$	{0, 2, 0, 2, 0}	{4, 8, 10, 12, 12}
44	$\{C_5, B_3, C_2, B_1, C_1, B_0\}$	$\{6, 2^2\}$	$\{11, 7^3, 5^2, 3^4, 1\}$	{2, 2, 0, 0, 2}	{5, 8, 9, 10, 11}
46	$\{C_5, D_4, C_3, D_2, C_1, B_0\}$	$\{6, 4\}$	$\{11, 9, 7^3, 5, 3^3\}$	{2, 0, 2, 0, 2}	{5, 8, 11, 12, 13}
46	$\{C_5, B_3, C_3, B_2, C_2, B_1, C_1, B_0\}$	$\{8, 1^2\}$	$\{15, 11, 8^2, 7, 3, 1^3\}$	{2, 2, 2, 1, 0}	{7, 12, 15, 16, 16}
48	$\{C_5, D_4, C_3, B_2, C_2, B_1, C_1, B_0\}$	$\{8, 2\}$	$\{15, 11, 9, 7^2, 3^2\}$	{2, 2, 2, 0, 2}	{7, 12, 15, 16, 17}
50	$\{C_5, B_4, C_4, B_3, C_3, B_2, C_2, B_1, C_1, B_0\}$	{10}	{19, 15, 11, 7, 3}	{2, 2, 2, 2, 2}	{9, 16, 21, 24, 25}

Partitions are shown under each homomorphism for the symplectic vector and adjoint representations. For C_2, the partition of the $[0, 1]$ representation is also shown.

B.4. D Series

Dimension	Quiver	[1,1]	[1,0]	[0,1]	[2,0]	[0,2]	Root Map	Weight Map
0	$\{D_2\}$	$\{1^4\}$	$\{1^2\}$	$\{1^2\}$	$\{1^3\}$	$\{1^3\}$	$\{0, 0\}$	$\{0, 0\}$
2	$\{D_2, C_1\}$	$\{2^2\}$	$\{1^2\}$	$\{2\}$	$\{1^3\}$	$\{3\}$	$\{0, 2\}$	$\{0, 1\}$
2	$\{D_2, C_1\}$	$\{2^2\}$	$\{2\}$	$\{1^2\}$	$\{3\}$	$\{1^3\}$	$\{2, 0\}$	$\{1, 0\}$
4	$\{D_2, C_1, B_0\}$	$\{3, 1\}$	$\{2\}$	$\{2\}$	$\{3\}$	$\{3\}$	$\{2, 2\}$	$\{1, 1\}$

Dimension	Quiver	[1,0,0]	[0,1,0]	[0,0,1]	[0,1,1]	Root Map	Weight Map
0	$\{D_3\}$	$\{1^6\}$	$\{1^4\}$	$\{1^4\}$	$\{1^{15}\}$	$\{0, 0, 0\}$	$\{0, 0, 0\}$
6	$\{D_3, C_1\}$	$\{2^2, 1^2\}$	$\{2, 1^2\}$	$\{2, 1^2\}$	$\{3, 2^4, 1^4\}$	$\{0, 1, 1\}$	$\{1, 1, 1\}$
8	$\{D_3, C_1, B_0\}$	$\{3, 1^3\}$	$\{2^2\}$	$\{2^2\}$	$\{3^4, 1^3\}$	$\{2, 0, 0\}$	$\{2, 1, 1\}$
10	$\{D_3, C_2, D_1\}$	$\{3^2\}$	$\{3, 1\}$	$\{3, 1\}$	$\{5, 3^3, 1\}$	$\{0, 2, 2\}$	$\{2, 2, 2\}$
12	$\{D_3, C_2, B_1, C_1, B_0\}$	$\{5, 1\}$	$\{4\}$	$\{4\}$	$\{7, 5, 3\}$	$\{2, 2, 2\}$	$\{4, 3, 3\}$

Dimension	Quiver	[1,0,0,0]	[0,1,0,0]	[0,0,1,0]	[0,0,0,1]	Root Map	Weight Map
0	$\{D_4\}$	$\{1^8\}$	$\{1^{28}\}$	$\{1^8\}$	$\{1^8\}$	$\{0, 0, 0, 0\}$	$\{0, 0, 0, 0\}$
10	$\{D_4, C_1\}$	$\{2^2, 1^4\}$	$\{3, 2^8, 1^9\}$	$\{2^2, 1^4\}$	$\{2^2, 1^4\}$	$\{0, 1, 0, 0\}$	$\{1, 2, 1, 1\}$
12	$\{D_4, C_2\}$	$\{2^4\}$	$\{3^6, 1^{10}\}$	$\{2^4\}$	$\{3, 1^5\}$	$\{0, 0, 0, 2\}$	$\{1, 2, 1, 2\}$
12	$\{D_4, C_2\}$	$\{2^4\}$	$\{3^6, 1^{10}\}$	$\{3, 1^5\}$	$\{2^4\}$	$\{0, 0, 2, 0\}$	$\{1, 2, 2, 1\}$
12	$\{D_4, C_1, B_0\}$	$\{3, 1^5\}$	$\{3^6, 1^{10}\}$	$\{2^4\}$	$\{2^4\}$	$\{2, 0, 0, 0\}$	$\{2, 2, 1, 1\}$
16	$\{D_4, C_2, B_0\}$	$\{3, 2^2, 1\}$	$\{4^2, 3^3, 2^4, 1^3\}$	$\{3, 2^2, 1\}$	$\{3, 2^2, 1\}$	$\{1, 0, 1, 1\}$	$\{2, 3, 2, 2\}$
18	$\{D_4, C_2, D_1\}$	$\{3^2, 1^2\}$	$\{5, 3^7, 1^2\}$	$\{3^2, 1^2\}$	$\{3^2, 1^2\}$	$\{0, 2, 0, 0\}$	$\{2, 4, 2, 2\}$
20	$\{D_4, C_3, D_2, C_1\}$	$\{4^2\}$	$\{7, 5^3, 3, 1^3\}$	$\{4^2\}$	$\{5, 1^3\}$	$\{0, 2, 0, 2\}$	$\{3, 6, 3, 4\}$
20	$\{D_4, C_3, D_2, C_1\}$	$\{4^2\}$	$\{7, 5^3, 3, 1^3\}$	$\{5, 1^3\}$	$\{4^2\}$	$\{0, 2, 2, 0\}$	$\{3, 6, 4, 3\}$
20	$\{D_4, C_2, B_1, C_1, B_0\}$	$\{5, 1^3\}$	$\{7, 5^3, 3, 1^3\}$	$\{4^2\}$	$\{4^2\}$	$\{2, 2, 0, 0\}$	$\{4, 6, 3, 3\}$
22	$\{D_4, C_3, D_2, C_1, B_0\}$	$\{5, 3\}$	$\{7^2, 5, 3^3\}$	$\{5, 3\}$	$\{5, 3\}$	$\{2, 0, 2, 2\}$	$\{4, 6, 4, 4\}$
24	$\{D_4, C_3, B_2, C_2, B_1, C_1, B_0\}$	$\{7, 1\}$	$\{11, 7^2, 3\}$	$\{7, 1\}$	$\{7, 1\}$	$\{2, 2, 2, 2\}$	$\{6, 10, 6, 6\}$

Dimension	Quiver	[1,0,0,0,0]	[0,1,0,0,0]	[0,0,0,1,0]	[0,0,0,0,1]	Root Map	Weight Map
0	$\{D_5\}$	$\{1^{10}\}$	$\{1^{45}\}$	$\{1^{16}\}$	$\{1^{16}\}$	{0, 0, 0, 0, 0}	{0, 0, 0, 0, 0}
14	$\{D_5, C_1\}$	$\{2^2, 1^6\}$	$\{3, 2^{12}, 1^{18}\}$	$\{2^4, 1^8\}$	$\{2^4, 1^8\}$	{0, 1, 0, 0, 0}	{1, 2, 2, 1, 1}
16	$\{D_5, C_1, B_0\}$	$\{3, 1^7\}$	$\{3^8, 1^{21}\}$	$\{2^8\}$	$\{2^8\}$	{2, 0, 0, 0, 0}	{2, 2, 2, 1, 1}
20	$\{D_5, C_2\}$	$\{2^4, 1^2\}$	$\{3^6, 2^8, 1^{11}\}$	$\{3, 2^4, 1^5\}$	$\{3, 2^4, 1^5\}$	{0, 0, 0, 1, 1}	{1, 2, 3, 2, 2}
24	$\{D_5, C_2, B_0\}$	$\{3, 2^2, 1^3\}$	$\{4^2, 3^5, 2^8, 1^6\}$	$\{3^2, 2^4, 1^2\}$	$\{3^2, 2^4, 1^2\}$	{1, 0, 1, 0, 0}	{2, 3, 4, 2, 2}
26	$\{D_5, C_2, D_1\}$	$\{3^2, 1^4\}$	$\{5, 3^{11}, 1^7\}$	$\{3^4, 1^4\}$	$\{3^4, 1^4\}$	{0, 2, 0, 0, 0}	{2, 4, 4, 2, 2}
28	$\{D_5, C_3, D_1\}$	$\{3^2, 2^2\}$	$\{5, 4^4, 3^4, 2^4, 1^4\}$	$\{4, 3^2, 2^2, 1^2\}$	$\{4, 3^2, 2^2, 1^2\}$	{0, 1, 0, 1, 1}	{2, 4, 5, 3, 3}
28	$\{D_5, C_2, B_1, C_1, B_0\}$	$\{5, 1^5\}$	$\{7, 5^5, 3, 1^{10}\}$	$\{4^4\}$	$\{4^4\}$	{2, 2, 0, 0, 0}	{4, 6, 6, 3, 3}
30	$\{D_5, C_3, B_1\}$	$\{3^3, 1\}$	$\{5^3, 3^9, 1^3\}$	$\{4^2, 2^4\}$	$\{4^2, 2^4\}$	{0, 0, 2, 0, 0}	{2, 4, 6, 3, 3}
32	$\{D_5, C_3, D_2, C_1\}$	$\{4^2, 1^2\}$	$\{7, 5^3, 4^4, 3, 1^4\}$	$\{5, 4^2, 1^3\}$	$\{5, 4^2, 1^3\}$	{0, 2, 0, 1, 1}	{3, 6, 7, 4, 4}
32	$\{D_5, C_3, B_1, C_1, B_0\}$	$\{5, 2^2, 1\}$	$\{7, 6^2, 5, 4^2, 3^2, 2^2, 1^3\}$	$\{5, 4^2, 3\}$	$\{5, 4^2, 3\}$	{2, 1, 0, 1, 1}	{4, 6, 7, 4, 4}
34	$\{D_5, C_3, D_2, C_1, B_0\}$	$\{5, 3, 1^2\}$	$\{7^2, 5^3, 3^5, 1\}$	$\{5^2, 3^2\}$	$\{5^2, 3^2\}$	{2, 0, 2, 0, 0}	{4, 6, 8, 4, 4}
36	$\{D_5, C_4, D_3, C_2, D_1\}$	$\{5^2\}$	$\{9, 7^3, 5, 3^3, 1\}$	{7, 5, 3, 1}	{7, 5, 3, 1}	{0, 2, 0, 2, 2}	{4, 8, 10, 6, 6}
36	$\{D_5, C_3, B_2, C_2, B_1, C_1, B_0\}$	$\{7, 1^3\}$	$\{11, 7^4, 3, 1^3\}$	$\{7^2, 1^2\}$	$\{7^2, 1^2\}$	{2, 2, 2, 0, 0}	{6, 10, 12, 6, 6}
38	$\{D_5, C_4, D_3, C_2, B_1, C_1, B_0\}$	{7, 3}	$\{11, 9, 7^2, 5, 3^2\}$	{8, 6, 2}	{8, 6, 2}	{2, 2, 0, 2, 2}	{6, 10, 12, 7, 7}
40	$\{D_5, C_4, B_3, C_3, B_2, C_2, B_1, C_1, B_0\}$	{9, 1}	{15, 11, 9, 7, 3}	{11, 5}	{11, 5}	{2, 2, 2, 2, 2}	{8, 14, 18, 10, 10}

Partitions are shown under each homomorphism for the vector, spinor and adjoint representations.

B.5. Exceptional Groups

B.5.1. G_2

Dimension	[1,0]	[0,1]	Root Map	Weight Map
0	$\{1^{14}\}$	$\{1^{7}\}$	{0, 0}	{0, 0}
6	$\{3, 2^{4}, 1^{3}\}$	$\{2^{2}, 1^{3}\}$	{1, 0}	{2, 1}
8	$\{4^{2}, 3, 1^{3}\}$	$\{3, 2^{2}\}$	{0, 1}	{3, 2}
10	$\{5, 3^{3}\}$	$\{3^{2}, 1\}$	{2, 0}	{4, 2}
12	{11, 3}	{7}	{2, 2}	{10, 6}

B.5.2. F_4

Dimension	[1,0,0,0]	[0,0,0,1]	Root Map	Weight Map
0	$\{1^{52}\}$	$\{1^{26}\}$	{0, 0, 0, 0}	{0, 0, 0, 0}
16	$\{3, 2^{14}, 1^{21}\}$	$\{2^{6}, 1^{14}\}$	{1, 0, 0, 0}	{2, 3, 2, 1}
22	$\{3^{7}, 2^{8}, 1^{15}\}$	$\{3, 2^{8}, 1^{7}\}$	{0, 0, 0, 1}	{2, 4, 3, 2}
28	$\{4^{2}, 3^{6}, 2^{10}, 1^{6}\}$	$\{3^{3}, 2^{6}, 1^{5}\}$	{0, 1, 0, 0}	{3, 6, 4, 2}
30	$\{5, 3^{13}, 1^{8}\}$	$\{3^{6}, 1^{8}\}$	{2, 0, 0, 0}	{4, 6, 4, 2}
30	$\{5^{7}, 3, 1^{14}\}$	$\{5, 3^{7}\}$	{0, 0, 0, 2}	{4, 8, 6, 4}
34	$\{5^{3}, 4^{2}, 3^{6}, 2^{4}, 1^{3}\}$	$\{4^{2}, 3^{3}, 2^{4}, 1\}$	{0, 0, 1, 0}	{4, 8, 6, 3}
36	$\{7, 5^{4}, 4^{4}, 3, 1^{6}\}$	$\{5, 4^{4}, 1^{5}\}$	{2, 0, 0, 1}	{6, 10, 7, 4}
36	$\{6^{2}, 5^{3}, 4^{2}, 3^{2}, 2^{4}, 1^{3}\}$	$\{5, 4^{2}, 3^{3}, 2^{2}\}$	{0, 1, 0, 1}	{5, 10, 7, 4}
38	$\{7, 6^{2}, 5, 4^{4}, 3^{3}, 1^{3}\}$	$\{5^{2}, 4^{2}, 3, 2^{2}, 1\}$	{1, 0, 1, 0}	{6, 11, 8, 4}
40	$\{7^{2}, 5^{4}, 3^{6}\}$	$\{5^{3}, 3^{3}, 1^{2}\}$	{0, 2, 0, 0}	{6, 12, 8, 4}
40	$\{9, 7^{4}, 3^{4}, 1^{3}\}$	$\{7, 5^{3}, 3, 1\}$	{2, 0, 0, 2}	{8, 14, 10, 6}
42	$\{11, 7^{5}, 3, 1^{3}\}$	$\{7^{3}, 1^{5}\}$	{2, 2, 0, 0}	{10, 18, 12, 6}
42	$\{11, 10^{2}, 7, 4^{2}, 3, 1^{3}\}$	$\{9, 6^{2}, 5\}$	{1, 0, 1, 2}	{10, 19, 14, 8}
44	$\{11^{2}, 9, 7, 5, 3^{3}\}$	$\{9, 7, 5^{2}\}$	{0, 2, 0, 2}	{10, 20, 14, 8}
46	$\{15, 11^{2}, 7, 5, 3\}$	{11, 9, 5, 1}	{2, 2, 0, 2}	{14, 26, 18, 10}
48	{23, 15, 11, 3}	{17, 9}	{2, 2, 2, 2}	{22, 42, 30, 16}

Partitions are shown for the F_4 adjoint and vector representations only. Homomorphisms identified include one root map which is not a nilpotent orbit: 40: [2,0,0,2]. This is highlighted in red.

B.5.3. E_6

Dimension	[1,0,0,0,0,0]	[0,0,0,0,0,1]	Root Map	Weight Map
0	$\{1^{27}\}$	$\{1^{78}\}$	{0, 0, 0, 0, 0, 0}	{0, 0, 0, 0, 0, 0}
22	$\{2^{6}, 1^{15}\}$	$\{3, 2^{20}, 1^{35}\}$	{0, 0, 0, 0, 0, 1}	{1, 2, 3, 2, 1, 2}
32	$\{3, 2^{8}, 1^{8}\}$	$\{3^{8}, 2^{16}, 1^{22}\}$	{1, 0, 0, 0, 1, 0}	{2, 3, 4, 3, 2, 2}
40	$\{3^{3}, 2^{6}, 1^{6}\}$	$\{4^{2}, 3^{9}, 2^{16}, 1^{11}\}$	{0, 0, 1, 0, 0, 0}	{2, 4, 6, 4, 2, 3}
42	$\{3^{6}, 1^{9}\}$	$\{5, 3^{19}, 1^{16}\}$	{0, 0, 0, 0, 0, 2}	{2, 4, 6, 4, 2, 4}
46	$\{4, 3^{4}, 2^{4}, 1^{3}\}$	$\{5, 4^{6}, 3^{8}, 2^{8}, 1^{9}\}$	{1, 0, 0, 0, 1, 1}	{3, 5, 7, 5, 3, 4}
48	$\{5, 3^{7}, 1\}$	$\{5^{8}, 3^{8}, 1^{14}\}$	{2, 0, 0, 0, 2, 0}	{4, 6, 8, 6, 4, 4}
50	$\{4^{2}, 3^{3}, 2^{4}, 1^{2}\}$	$\{5^{3}, 4^{4}, 3^{9}, 2^{8}, 1^{4}\}$	{0, 1, 0, 1, 0, 0}	{3, 6, 8, 6, 3, 4}
52	$\{5, 4^{4}, 1^{6}\}$	$\{7, 5^{5}, 4^{8}, 3, 1^{11}\}$	{1, 0, 0, 0, 1, 2}	{4, 7, 10, 7, 4, 6}
54	$\{5, 4^{2}, 3^{3}, 2^{2}, 1\}$	$\{6^{2}, 5^{4}, 4^{4}, 3^{5}, 2^{6}, 1^{3}\}$	{1, 0, 1, 0, 1, 0}	{4, 7, 10, 7, 4, 5}
56	$\{5^{2}, 4^{2}, 3, 2^{2}, 1^{2}\}$	$\{7, 6^{2}, 5^{3}, 4^{6}, 3^{4}, 2^{2}, 1^{4}\}$	{0, 1, 0, 1, 0, 1}	{4, 8, 11, 8, 4, 6}
58	$\{5^{3}, 3^{3}, 1^{3}\}$	$\{7^{2}, 5^{7}, 3^{9}, 1^{2}\}$	{0, 0, 2, 0, 0, 0}	{4, 8, 12, 8, 4, 6}
58	$\{6, 5, 4^{2}, 3^{2}, 2\}$	$\{7^{3}, 6^{2}, 5^{2}, 4^{4}, 3^{4}, 2^{2}, 1^{3}\}$	{1, 1, 0, 1, 1, 0}	{5, 9, 12, 9, 5, 6}
60	$\{7^{3}, 1^{6}\}$	$\{11, 7^{8}, 3, 1^{8}\}$	{0, 0, 2, 0, 0, 2}	{6, 12, 18, 12, 6, 10}
60	$\{7, 5^{3}, 3, 1^{2}\}$	$\{9, 7^{5}, 5^{3}, 3^{5}, 1^{4}\}$	{2, 0, 0, 0, 2, 2}	{6, 10, 14, 10, 6, 8}
62	{7, 6, 5, 4, 3, 2}	$\{9, 8^{2}, 7, 6^{2}, 5^{3}, 4^{2}, 3^{2}, 2^{2}, 1\}$	{1, 1, 0, 1, 1, 1}	{6, 11, 15, 11, 6, 8}
64	$\{9, 6^{2}, 5, 1\}$	$\{11, 10^{2}, 9, 7, 6^{2}, 5, 4^{2}, 3, 1^{3}\}$	{2, 1, 0, 1, 2, 1}	{8, 14, 19, 14, 8, 10}
64	{8, 7, 5, 4, 3}	$\{10^{2}, 9, 7^{2}, 6^{2}, 5^{2}, 4^{2}, 3, 1^{2}\}$	{1, 1, 1, 1, 1, 0}	{7, 13, 18, 13, 7, 9}
64	{8, 7, 6, 3, 2, 1}	$\{11, 9, 8^{2}, 7^{2}, 6^{2}, 5, 3^{2}, 2^{2}, 1\}$	{1, 1, 0, 1, 1, 2}	{7, 13, 18, 13, 7, 10}
66	$\{9, 7, 5^{2}, 1\}$	$\{11^{2}, 9^{2}, 7^{2}, 5^{3}, 3^{3}\}$	{2, 0, 2, 0, 2, 0}	{8, 14, 20, 14, 8, 10}
66	$\{9^{2}, 5, 3, 1\}$	$\{13, 11, 9^{2}, 7^{4}, 3^{2}, 1^{2}\}$	{0, 2, 0, 2, 0, 2}	{8, 16, 22, 16, 8, 12}
68	$\{11, 9, 5, 1^{2}\}$	$\{15, 11^{3}, 9, 7, 5^{2}, 3, 1\}$	{2, 0, 2, 0, 2, 2}	{10, 18, 26, 18, 10, 14}
70	{13, 9, 5}	$\{17, 15, 11^{2}, 9, 7, 5, 3\}$	{2, 2, 0, 2, 2, 2}	{12, 22, 30, 22, 12, 16}
72	{17, 9, 1}	{23, 17, 15, 11, 9, 3}	{2, 2, 2, 2, 2, 2}	{16, 30, 42, 30, 16, 22}

Partitions are shown for the E_6 adjoint and fundamental representations only. Homomorphisms identified include three root maps which are not recognised Characteristics of nilpotent orbits: these are highlighted in red.

B.5.4. E_7

Dimension	[1,0,0,0,0,0,0]	[0,0,0,0,0,1,0]	Root Map	Weight Map
0	$\{1^{133}\}$	$\{1^{56}\}$	{0, 0, 0, 0, 0, 0, 0}	{0, 0, 0, 0, 0, 0, 0}
34	$\{3, 2^{32}, 1^{66}\}$	$\{2^{12}, 1^{32}\}$	{1, 0, 0, 0, 0, 0, 0}	{2, 3, 4, 3, 2, 1, 2}
52	$\{3^{10}, 2^{32}, 1^{39}\}$	$\{3^2, 2^{16}, 1^{18}\}$	{0, 0, 0, 0, 1, 0, 0}	{2, 4, 6, 5, 4, 2, 3}
54	$\{3^{27}, 1^{52}\}$	$\{4, 2^{26}\}$	{0, 0, 0, 0, 0, 2, 0}	{2, 4, 6, 5, 4, 3, 3}
64	$\{4^2, 3^{15}, 2^{28}, 1^{24}\}$	$\{3^6, 2^{12}, 1^{14}\}$	{0, 1, 0, 0, 0, 0, 0}	{3, 6, 8, 6, 4, 2, 4}
66	$\{5, 3^{31}, 1^{35}\}$	$\{3^{12}, 1^{20}\}$	{2, 0, 0, 0, 0, 0, 0}	{4, 6, 8, 6, 4, 2, 4}
70	$\{4^6, 3^{16}, 2^{20}, 1^{21}\}$	$\{4, 3^6, 2^{14}, 1^6\}$	{0, 0, 0, 0, 0, 1, 1}	{3, 6, 9, 7, 5, 3, 5}
76	$\{5, 4^8, 3^{16}, 2^{16}, 1^{16}\}$	$\{4^2, 3^8, 2^8, 1^8\}$	{1, 0, 0, 0, 1, 0, 0}	{4, 7, 10, 8, 6, 3, 5}
82	$\{5^3, 4^8, 3^{15}, 2^{16}, 1^9\}$	$\{4^4, 3^6, 2^8, 1^6\}$	{0, 0, 1, 0, 0, 0, 0}	{4, 8, 12, 9, 6, 3, 6}
84	$\{5^7, 3^{28}, 1^{14}\}$	$\{4^7, 2^{14}\}$	{0, 0, 0, 0, 0, 0, 2}	{4, 8, 12, 9, 6, 3, 7}
84	$\{5^{10}, 3^{22}, 1^{17}\}$	$\{5^2, 3^{14}, 1^4\}$	{0, 0, 0, 0, 2, 0, 0}	{4, 8, 12, 10, 8, 4, 6}
84	$\{7, 5^7, 4^{16}, 3, 1^{24}\}$	$\{5^2, 4^8, 1^{14}\}$	{2, 0, 0, 0, 1, 0, 0}	{6, 10, 14, 11, 8, 4, 7}
86	$\{7, 5^{15}, 3^{10}, 1^{21}\}$	$\{6, 4^9, 2^7\}$	{2, 0, 0, 0, 0, 2, 0}	{6, 10, 14, 11, 8, 5, 7}
90	$\{6^2, 5^6, 4^8, 3^{11}, 2^{10}, 1^6\}$	$\{5^2, 4^4, 3^6, 2^4, 1^4\}$	{0, 1, 0, 0, 1, 0, 0}	{5, 10, 14, 11, 8, 4, 7}
92	$\{7, 6^2, 5^7, 4^{10}, 3^6, 2^6, 1^9\}$	$\{5^4, 4^4, 3^2, 2^4, 1^6\}$	{1, 0, 1, 0, 0, 0, 0}	{6, 11, 16, 12, 8, 4, 8}
94	$\{7^2, 5^{13}, 3^{15}, 1^9\}$	$\{5^6, 3^6, 1^8\}$	{0, 2, 0, 0, 0, 0, 0}	{6, 12, 16, 12, 8, 4, 8}
94	$\{7, 6^4, 5^7, 4^6, 3^7, 2^8, 1^6\}$	$\{6, 5^2, 4^5, 3^4, 2^3, 1^2\}$	{1, 0, 0, 1, 0, 1, 0}	{6, 11, 16, 13, 9, 5, 8}
96	$\{11, 7^{14}, 3, 1^{21}\}$	$\{7^6, 1^{14}\}$	{2, 2, 0, 0, 0, 0, 0}	{10, 18, 24, 18, 12, 6, 12}
96	$\{9, 7^5, 5^{14}, 3, 1^{16}\}$	$\{6^6, 4, 2^8\}$	{2, 0, 0, 0, 0, 0, 2}	{8, 14, 20, 15, 10, 5, 11}
96	$\{7^2, 6^4, 5^5, 4^8, 3^8, 2^4, 1^6\}$	$\{6, 5^4, 4^2, 3^4, 2^5\}$	{0, 1, 0, 0, 0, 1, 1}	{6, 12, 17, 13, 9, 5, 9}
98	$\{7^3, 6^4, 5^4, 4^8, 3^8, 2^4, 1^4\}$	$\{6^2, 5^2, 4^4, 3^4, 2^2, 1^2\}$	{0, 0, 1, 0, 1, 0, 0}	{6, 12, 18, 14, 10, 5, 9}
100	$\{7^5, 5^{10}, 3^{15}, 1^3\}$	$\{6^3, 4^7, 2^5\}$	{0, 0, 0, 2, 0, 0, 0}	{6, 12, 18, 15, 10, 5, 9}
100	$\{9, 7^7, 5^9, 3^7, 1^9\}$	$\{7^2, 5^6, 3^2, 1^6\}$	{2, 0, 0, 0, 2, 0, 0}	{8, 14, 20, 16, 12, 6, 10}
102	$\{11, 9^7, 7, 5^7, 3, 1^{14}\}$	$\{10, 6^7, 4\}$	{2, 0, 0, 0, 2, 2, 0}	{10, 18, 26, 21, 16, 9, 13}
102	$\{11, 8^4, 7^6, 6^4, 3^2, 2^4, 1^{10}\}$	$\{8, 7^4, 6, 2^5, 1^4\}$	{2, 1, 0, 0, 0, 1, 1}	{10, 18, 25, 19, 13, 7, 13}
104	$\{9^5, 7^2, 5^{13}, 1^9\}$	$\{8^2, 6^3, 4^5, 2\}$	{0, 0, 0, 0, 2, 0, 2}	{8, 16, 24, 19, 14, 7, 13}
104	$\{9^2, 7^8, 5^5, 3^{10}, 1^4\}$	$\{8, 6^4, 4^5, 2^2\}$	{0, 2, 0, 0, 0, 2, 0}	{8, 16, 22, 17, 12, 7, 11}
104	$\{9, 8^2, 7^3, 6^4, 5^5, 4^4, 3^4, 2^4, 1^2\}$	$\{7^2, 6^2, 5^2, 4^2, 3^2, 2^2, 1^2\}$	{1, 0, 1, 0, 1, 0, 0}	{8, 15, 22, 17, 12, 6, 11}
106	$\{13, 9^9, 5^5, 3, 1^{11}\}$	$\{10, 8^4, 4, 2^5\}$	{2, 2, 0, 0, 0, 2, 0}	{12, 22, 30, 23, 16, 9, 15}
106	$\{9^3, 7^5, 5^{10}, 3^6, 1^3\}$	$\{7^4, 5^2, 3^6\}$	{0, 0, 2, 0, 0, 0, 0}	{8, 16, 24, 18, 12, 6, 12}

Dimension	[1,0,0,0,0,0,0]	[0,0,0,0,0,1,0]	Root Map	Weight Map
106	$\{11, 9, 8^4, 7^4, 6^4, 5, 3^4, 2^4, 1^4\}$	$\{8^2, 7^2, 6^2, 3^2, 2^2, 1^4\}$	{2, 0, 1, 0, 1, 0, 0}	{10, 18, 26, 20, 14, 7, 13}
108	$\{11, 9^3, 7^8, 5^3, 3^7, 1^3\}$	$\{8^3, 6^3, 4, 2^5\}$	{2, 0, 0, 2, 0, 0, 0}	{10, 18, 26, 21, 14, 7, 13}
108	$\{10^2, 9, 8^2, 7^4, 6^2, 5^4, 4^4, 3^3, 1^3\}$	$\{8^2, 7^2, 5^2, 4^2, 3^2, 1^2\}$	{0, 1, 1, 0, 1, 0, 0}	{9, 18, 26, 20, 14, 7, 13}
108	$\{11, 10^2, 9^3, 7, 6^6, 5^3, 4^2, 3, 1^6\}$	$\{9^2, 6^4, 5^2, 1^4\}$	{1, 0, 1, 0, 2, 0, 0}	{10, 19, 28, 22, 16, 8, 14}
108	$\{11, 10^2, 9^3, 8^2, 7, 6^2, 5^3, 4^2, 3^2, 2^4, 1^3\}$	$\{10, 7^2, 6^3, 5^2, 4\}$	{1, 0, 1, 0, 1, 2, 0}	{10, 19, 28, 22, 16, 9, 14}
110	$\{11^2, 9^4, 7^4, 5^7, 3^3, 1^3\}$	$\{9^2, 7^2, 5^4, 1^4\}$	{0, 2, 0, 0, 2, 0, 0}	{10, 20, 28, 22, 16, 8, 14}
110	$\{13, 11, 9^6, 7^4, 5^2, 3^4, 1^5\}$	$\{9^4, 5^2, 3^2, 1^4\}$	{2, 0, 2, 0, 0, 0, 0}	{12, 22, 32, 24, 16, 8, 16}
110	$\{11^2, 10^2, 9, 8^2, 7^3, 6^2, 5, 4^4, 3^3, 1^3\}$	$\{10, 8, 7^2, 6, 5^2, 4^2\}$	{0, 1, 0, 1, 0, 2, 1}	{10, 20, 29, 23, 16, 9, 15}
112	$\{11^3, 9^3, 7^5, 5^4, 3^6\}$	$\{10, 8^2, 6^3, 4^3\}$	{0, 0, 2, 0, 0, 2, 0}	{10, 20, 30, 23, 16, 9, 15}
112	$\{13, 11^3, 9^2, 7^7, 5, 3^4, 1^3\}$	$\{10^2, 8^2, 6, 4^3, 2\}$	{2, 0, 0, 0, 2, 0, 2}	{12, 22, 32, 25, 18, 9, 17}
112	$\{15, 11^5, 9^3, 7, 5^4, 3, 1^6\}$	$\{11^2, 9^2, 5^2, 1^6\}$	{2, 2, 0, 0, 2, 0, 0}	{14, 26, 36, 28, 20, 10, 18}
112	$\{13, 11, 10^2, 9^2, 8^4, 6^2, 5^2, 3^5, 1^2\}$	$\{10, 9^2, 7^2, 4^2, 2^3\}$	{2, 0, 1, 1, 0, 1, 0}	{12, 22, 32, 25, 17, 9, 16}
114	$\{13^3, 11, 9^3, 7^5, 5^3, 3, 1^3\}$	$\{11^2, 7^4, 3^2\}$	{0, 0, 2, 0, 2, 0, 0}	{12, 24, 36, 28, 20, 10, 18}
114	$\{15, 12^2, 11, 10^2, 9^3, 7, 6^2, 4^2, 3^2, 1^3\}$	$\{11^2, 10, 8, 5^2, 2^3\}$	{2, 1, 0, 1, 1, 0, 1}	{14, 26, 37, 29, 20, 10, 19}
114	$\{15, 12^2, 11^2, 10^2, 9, 7^2, 6^2, 4^2, 3^2, 1^3\}$	$\{12, 10, 9^2, 6, 4, 3^2\}$	{2, 1, 0, 1, 0, 2, 1}	{14, 26, 37, 29, 20, 11, 19}
116	$\{15, 13, 11^4, 9^2, 7^3, 5^2, 3^4\}$	$\{12, 10^2, 8, 6, 4^2, 2\}$	{2, 0, 2, 0, 0, 2, 0}	{14, 26, 38, 29, 20, 11, 19}
118	$\{17, 15, 13^2, 11^2, 9^3, 7, 5^3, 3, 1\}$	$\{13^2, 9^2, 5^2, 1^2\}$	{2, 0, 2, 0, 2, 0, 0}	{16, 30, 44, 34, 24, 12, 22}
118	$\{19, 16^2, 15, 11^2, 10^2, 7, 6^2, 3, 1^3\}$	$\{16, 11^2, 10, 6, 1^2\}$	{2, 1, 0, 1, 2, 2, 1}	{18, 34, 49, 39, 28, 15, 25}
120	$\{23, 17^3, 15, 11, 9^3, 3, 1^3\}$	$\{17^2, 9^2, 1^4\}$	{2, 2, 2, 0, 2, 0, 0}	{22, 42, 60, 46, 32, 16, 30}
120	$\{19, 17, 15^2, 11^3, 9, 7^2, 5, 3^2\}$	$\{16, 12, 10^2, 6, 2\}$	{2, 0, 2, 0, 2, 2, 0}	{18, 34, 50, 39, 28, 15, 25}
122	$\{23, 19, 17, 15^2, 11^2, 9, 7, 3^2\}$	{18, 16, 10, 8, 4}	{2, 2, 0, 2, 0, 2, 2}	{22, 42, 60, 47, 32, 17, 31}
124	$\{27, 23, 19, 17, 15, 11^2, 7, 3\}$	{22, 16, 12, 6}	{2, 2, 0, 2, 2, 2, 2}	{26, 50, 72, 57, 40, 21, 37}
126	{35, 27, 23, 19, 15, 11, 3}	{28, 18, 10}	{2, 2, 2, 2, 2, 2, 2}	{34, 66, 96, 75, 52, 27, 49}

Partitions are shown for the E_7 adjoint and vector representations only. Homomorphisms identified include eight root maps which are not recognised Characteristics of nilpotent orbits: these are highlighted in red.

B.5.5. E_8

Dimension	[0,0,0,0,0,1,0]	Root Map	Weight Map
0	$\{1^{248}\}$	{0, 0, 0, 0, 0, 0, 0, 0}	{0, 0, 0, 0, 0, 0, 0, 0}
58	$\{3, 2^{56}, 1^{133}\}$	{0, 0, 0, 0, 0, 0, 1, 0}	{2, 4, 6, 5, 4, 3, 2, 3}
92	$\{3^{14}, 2^{64}, 1^{78}\}$	{1, 0, 0, 0, 0, 0, 0, 0}	{4, 7, 10, 8, 6, 4, 2, 5}
112	$\{4^2, 3^{27}, 2^{52}, 1^{55}\}$	{0, 0, 0, 0, 0, 1, 0, 0}	{4, 8, 12, 10, 8, 6, 3, 6}
114	$\{5, 3^{55}, 1^{78}\}$	{0, 0, 0, 0, 0, 0, 2, 0}	{4, 8, 12, 10, 8, 6, 4, 6}
128	$\{4^8, 3^{28}, 2^{48}, 1^{36}\}$	{0, 0, 0, 0, 0, 0, 0, 1}	{5, 10, 15, 12, 9, 6, 3, 8}
136	$\{5, 4^{12}, 3^{32}, 2^{32}, 1^{35}\}$	{1, 0, 0, 0, 0, 0, 1, 0}	{6, 11, 16, 13, 10, 7, 4, 8}
146	$\{5^3, 4^{16}, 3^{27}, 2^{32}, 1^{24}\}$	{0, 0, 0, 0, 1, 0, 0, 0}	{6, 12, 18, 15, 12, 8, 4, 9}
148	$\{7, 5^{11}, 4^{32}, 3, 1^{55}\}$	{1, 0, 0, 0, 0, 0, 2, 0}	{8, 15, 22, 18, 14, 10, 6, 11}
154	$\{5^7, 4^{14}, 3^{28}, 2^{28}, 1^{17}\}$	{0, 1, 0, 0, 0, 0, 0, 0}	{7, 14, 20, 16, 12, 8, 4, 10}
156	$\{5^{14}, 3^{50}, 1^{28}\}$	{2, 0, 0, 0, 0, 0, 0, 0}	{8, 14, 20, 16, 12, 8, 4, 10}
162	$\{6^2, 5^{10}, 4^{16}, 3^{23}, 2^{18}, 1^{17}\}$	{1, 0, 0, 0, 0, 1, 0, 0}	{8, 15, 22, 18, 14, 10, 5, 11}
164	$\{7, 6^2, 5^{15}, 4^{18}, 3^{10}, 2^{14}, 1^{24}\}$	{0, 0, 0, 0, 1, 0, 1, 0}	{8, 16, 24, 20, 16, 11, 6, 12}
166	$\{7^2, 5^{25}, 3^{27}, 1^{28}\}$	{0, 0, 0, 0, 0, 2, 0, 0}	{8, 16, 24, 20, 16, 12, 6, 12}
168	$\{11, 7^{26}, 3, 1^{52}\}$	{0, 0, 0, 0, 0, 2, 2, 0}	{12, 24, 36, 30, 24, 18, 10, 18}
168	$\{6^4, 5^{10}, 4^{16}, 3^{20}, 2^{20}, 1^{10}\}$	{0, 0, 0, 1, 0, 0, 0, 0}	{8, 16, 24, 20, 15, 10, 5, 12}
172	$\{7, 6^6, 5^{11}, 4^{16}, 3^{15}, 2^{14}, 1^{13}\}$	{0, 1, 0, 0, 0, 0, 1, 0}	{9, 18, 26, 21, 16, 11, 6, 13}
176	$\{7^2, 6^6, 5^{13}, 4^{12}, 3^{16}, 2^{14}, 1^9\}$	{0, 0, 0, 0, 0, 1, 0, 1}	{9, 18, 27, 22, 17, 12, 6, 14}
178	$\{7^3, 6^8, 5^8, 4^{16}, 3^{16}, 2^8, 1^{11}\}$	{1, 0, 0, 0, 1, 0, 0, 0}	{10, 19, 28, 23, 18, 12, 6, 14}
178	$\{9, 7^5, 6^{12}, 5^{14}, 4^2, 3, 2^{16}, 1^{19}\}$	{0, 1, 0, 0, 0, 0, 2, 0}	{11, 22, 32, 26, 20, 14, 8, 16}
180	$\{9, 7^{11}, 5^{21}, 3^{11}, 1^{24}\}$	{2, 0, 0, 0, 0, 0, 2, 0}	{12, 22, 32, 26, 20, 14, 8, 16}
182	$\{7^5, 6^6, 5^{10}, 4^{14}, 3^{15}, 2^{10}, 1^6\}$	{0, 0, 1, 0, 0, 0, 0, 0}	{10, 20, 30, 24, 18, 12, 6, 15}
184	$\{7^8, 5^{20}, 3^{28}, 1^8\}$	{0, 0, 0, 0, 0, 0, 0, 2}	{10, 20, 30, 24, 18, 12, 6, 16}
184	$\{11, 8^6, 7^{14}, 6^6, 3^2, 2^{14}, 1^{21}\}$	{0, 0, 0, 0, 0, 1, 2, 1}	{13, 26, 39, 32, 25, 18, 10, 20}
186	$\{8^2, 7^5, 6^8, 5^9, 4^{12}, 3^{11}, 2^8, 1^7\}$	{0, 1, 0, 0, 0, 1, 0, 0}	{11, 22, 32, 26, 20, 14, 7, 16}
188	$\{8^4, 7^6, 6^4, 5^{10}, 4^{16}, 3^6, 2^4, 1^{10}\}$	{1, 0, 0, 1, 0, 0, 0, 0}	{12, 23, 34, 28, 21, 14, 7, 17}
188	$\{9, 8^2, 7^7, 6^8, 5^9, 4^8, 3^8, 2^8, 1^9\}$	{1, 0, 0, 0, 1, 0, 1, 0}	{12, 23, 34, 28, 22, 15, 8, 17}
190	$\{11, 9, 8^8, 7^8, 6^8, 5, 3^8, 2^8, 1^{15}\}$	{1, 0, 0, 0, 1, 0, 2, 0}	{14, 27, 40, 33, 26, 18, 10, 20}
192	$\{9, 8^4, 7^5, 6^8, 5^9, 4^8, 3^9, 2^8, 1^4\}$	{0, 0, 1, 0, 0, 0, 1, 0}	{12, 24, 36, 29, 22, 15, 8, 18}
192	$\{9^2, 8^2, 7^8, 6^8, 5^5, 4^{10}, 3^{10}, 2^4, 1^7\}$	{0, 0, 0, 1, 0, 1, 0, 0}	{12, 24, 36, 30, 23, 16, 8, 18}
194	$\{9^3, 7^{13}, 5^{14}, 3^{18}, 1^6\}$	{0, 0, 0, 0, 2, 0, 0, 0}	{12, 24, 36, 30, 24, 16, 8, 18}
194	$\{9^5, 8^4, 7^2, 6^6, 5^{13}, 4^{10}, 2^2, 1^{12}\}$	{1, 0, 1, 0, 0, 0, 0, 0}	{14, 27, 40, 32, 24, 16, 8, 20}
196	$\{9^7, 7^7, 5^{21}, 3^7, 1^{10}\}$	{0, 2, 0, 0, 0, 0, 0, 0}	{14, 28, 40, 32, 24, 16, 8, 20}
196	$\{10^2, 9, 8^6, 7^8, 6^2, 5^8, 4^8, 3^7, 1^{10}\}$	{1, 0, 0, 0, 1, 1, 0, 0}	{14, 27, 40, 33, 26, 18, 9, 20}
196	$\{11, 10^2, 9^7, 7, 6^{14}, 5^7, 4^2, 3, 1^{17}\}$	{2, 0, 0, 0, 1, 0, 1, 0}	{16, 30, 44, 36, 28, 19, 10, 22}
196	$\{13, 10^2, 9^9, 8^8, 5^5, 4^2, 3, 2^{10}, 1^{14}\}$	{0, 0, 0, 1, 0, 1, 2, 0}	{16, 32, 48, 40, 31, 22, 12, 24}

Dimension	[0,0,0,0,0,1,0]	Root Map	Weight Map
196	$\{9^3, 8^4, 7^5, 6^6, 5^{10}, 4^8, 3^7, 2^6, 1^3\}$	{0, 1, 0, 0, 1, 0, 0, 0}	{13, 26, 38, 31, 24, 16, 8, 19}
196	$\{11, 9^3, 8^6, 7^8, 6^6, 5^3, 4^2, 3^7, 2^{10}, 1^6\}$	{0, 0, 1, 0, 0, 0, 2, 0}	{14, 28, 42, 34, 26, 18, 10, 21}
198	$\{11, 9^6, 7^{14}, 5^7, 3^{14}, 1^8\}$	{0, 0, 0, 0, 0, 0, 2, 2}	{14, 28, 42, 34, 26, 18, 10, 22}
198	$\{11^2, 9^8, 7^8, 5^{15}, 3^3, 1^{14}\}$	{2, 0, 0, 0, 0, 2, 0, 0}	{16, 30, 44, 36, 28, 20, 10, 22}
198	$\{13, 11, 9^{14}, 7^4, 5^6, 3^8, 1^{16}\}$	{0, 0, 0, 0, 2, 0, 2, 0}	{16, 32, 48, 40, 32, 22, 12, 24}
200	$\{15, 11^9, 9^7, 7, 5^8, 3, 1^{21}\}$	{2, 0, 0, 0, 0, 2, 2, 0}	{20, 38, 56, 46, 36, 26, 14, 28}
200	$\{10^2, 9^3, 8^4, 7^6, 6^6, 5^6, 4^8, 3^6, 2^4, 1^3\}$	{0, 0, 1, 0, 0, 1, 0, 0}	{14, 28, 42, 34, 26, 18, 9, 21}
202	$\{10^4, 9^3, 8^2, 7^6, 6^6, 5^9, 4^4, 3^6, 2^2, 1^4\}$	{0, 1, 0, 1, 0, 0, 0, 0}	{15, 30, 44, 36, 27, 18, 9, 22}
202	$\{11, 10^2, 9^3, 8^6, 7^4, 6^6, 5^6, 4^4, 3^7, 2^4, 1^3\}$	{0, 1, 0, 0, 1, 0, 1, 0}	{15, 30, 44, 36, 28, 19, 10, 22}
202	$\{11, 10^4, 9^3, 8^2, 7^5, 6^8, 5^7, 4^4, 3^2, 2^4, 1^6\}$	{1, 0, 1, 0, 0, 0, 1, 0}	{16, 31, 46, 37, 28, 19, 10, 23}
204	$\{11^2, 10^4, 9, 8^4, 7^7, 6^4, 5^5, 4^8, 3^3, 1^6\}$	{0, 1, 0, 0, 0, 1, 0, 1}	{16, 32, 47, 38, 29, 20, 10, 24}
204	$\{11^2, 10^2, 9^4, 8^4, 7^4, 6^6, 5^7, 4^4, 3^4, 2^4, 1^3\}$	{1, 0, 0, 1, 0, 1, 0, 0}	{16, 31, 46, 38, 29, 20, 10, 23}
204	$\{13, 11, 10^4, 9^6, 8^4, 7^4, 6^2, 5^2, 4^4, 3^5, 2^6, 1^5\}$	{0, 1, 0, 0, 1, 0, 2, 0}	{17, 34, 50, 41, 32, 22, 12, 25}
206	$\{13, 11^2, 10^4, 9^3, 8^8, 6^4, 5^4, 3^{11}, 1^5\}$	{0, 0, 0, 1, 0, 0, 2, 1}	{17, 34, 51, 42, 32, 22, 12, 26}
206	$\{11^3, 10^2, 9^3, 8^4, 7^5, 6^6, 5^4, 4^6, 3^6, 1^3\}$	{0, 0, 1, 0, 1, 0, 0, 0}	{16, 32, 48, 39, 30, 20, 10, 24}
206	$\{13, 11^3, 10^4, 9^2, 8^4, 7^7, 6^2, 5, 4^6, 3^4, 2^2, 1^6\}$	{1, 0, 1, 0, 0, 0, 2, 0}	{18, 35, 52, 42, 32, 22, 12, 26}
208	$\{11^4, 9^6, 7^{10}, 5^{10}, 3^{10}\}$	{0, 0, 0, 2, 0, 0, 0, 0}	{16, 32, 48, 40, 30, 20, 10, 24}
208	$\{13, 11^5, 9^6, 7^{10}, 5^5, 3^9, 1^4\}$	{0, 2, 0, 0, 0, 0, 2, 0}	{18, 36, 52, 42, 32, 22, 12, 26}
208	$\{13^2, 11^4, 9^9, 7^3, 5^{13}, 3, 1^8\}$	{0, 0, 0, 0, 0, 2, 0, 2}	{18, 36, 54, 44, 34, 24, 12, 28}
208	$\{14^2, 11^6, 10^4, 9^2, 7, 6^{10}, 5^3, 3, 1^{11}\}$	{1, 0, 0, 1, 0, 2, 0, 0}	{20, 39, 58, 48, 37, 26, 13, 29}
208	$\{12^2, 11^2, 10^2, 9^4, 8^4, 7^5, 6^2, 5^6, 4^6, 3^3, 1^4\}$	{0, 0, 0, 1, 0, 1, 0, 1}	{17, 34, 51, 42, 32, 22, 11, 26}
208	$\{12^2, 11^3, 10^2, 9^2, 8^4, 7^5, 6^6, 5^5, 4^2, 3^2, 2^4, 1^3\}$	{1, 0, 1, 0, 0, 1, 0, 0}	{18, 35, 52, 42, 32, 22, 11, 26}
208	$\{15, 12^2, 11^5, 10^4, 9^3, 8^2, 7, 6^2, 5^4, 4^2, 3^2, 2^6, 1^6\}$	{1, 0, 0, 1, 0, 1, 2, 0}	{20, 39, 58, 48, 37, 26, 14, 29}
210	$\{17, 15^5, 11, 9^{14}, 3, 1^{16}\}$	{2, 2, 0, 0, 0, 0, 2, 0}	{26, 50, 72, 58, 44, 30, 16, 36}
210	$\{13^3, 11^5, 9^3, 7^{13}, 5^3, 3^5, 1^6\}$	{2, 0, 0, 0, 2, 0, 0, 0}	{20, 38, 56, 46, 36, 24, 12, 28}
210	$\{15, 13^5, 11, 9^9, 7^5, 5^6, 1^{11}\}$	{2, 0, 0, 0, 0, 0, 2, 2}	{22, 42, 62, 50, 38, 26, 14, 32}
210	$\{15, 12^4, 11^2, 10^4, 9^5, 7^2, 6^4, 4^4, 3^6, 1^6\}$	{0, 1, 0, 0, 0, 1, 2, 1}	{20, 40, 59, 48, 37, 26, 14, 30}
210	$\{13, 12^2, 11, 10^4, 9^4, 8^2, 7^5, 6^4, 5^2, 4^6, 3^4, 1^3\}$	{0, 0, 1, 0, 1, 0, 1, 0}	{18, 36, 54, 44, 34, 23, 12, 27}
212	$\{13^5, 11, 9^9, 7^5, 5^{10}, 1^6\}$	{0, 0, 2, 0, 0, 0, 0, 0}	{20, 40, 60, 48, 36, 24, 12, 30}
212	$\{13^2, 12^2, 11, 10^4, 9^2, 8^4, 7^4, 6^4, 5^4, 4^2, 3^5, 1^2\}$	{0, 1, 0, 1, 0, 1, 0, 0}	{19, 38, 56, 46, 35, 24, 12, 28}
212	$\{13^3, 12^2, 11, 10^2, 9^3, 8^4, 7^5, 6^4, 5^3, 4^2, 3^2, 2^2, 1^3\}$	{1, 0, 1, 0, 1, 0, 0, 0}	{20, 39, 58, 47, 36, 24, 12, 29}
212	$\{15, 13, 12^2, 11^4, 10^4, 9^2, 8^2, 7^3, 6^2, 5^2, 4^4, 3^4, 2^2, 1^3\}$	{0, 0, 1, 0, 1, 0, 2, 0}	{20, 40, 60, 49, 38, 26, 14, 30}
214	$\{15, 13^2, 11^7, 9^5, 7^5, 5^5, 3^8, 1\}$	{0, 0, 0, 2, 0, 0, 2, 0}	{20, 40, 60, 50, 38, 26, 14, 30}
214	$\{17, 15, 13^6, 11^2, 9^7, 7, 5^7, 3, 1^8\}$	{2, 0, 0, 0, 2, 0, 2, 0}	{24, 46, 68, 56, 44, 30, 16, 34}
214	$\{14^2, 13^3, 11, 10^4, 9^3, 8^2, 7^6, 6^2, 5^2, 4^4, 3, 1^4\}$	{0, 1, 1, 0, 0, 1, 0, 0}	{21, 42, 62, 50, 38, 26, 13, 31}
216	$\{23, 17^7, 15, 11, 9^7, 3, 1^{14}\}$	{2, 0, 0, 0, 2, 2, 2, 0}	{32, 62, 92, 76, 60, 42, 22, 46}
216	$\{15^2, 13^3, 11^5, 9^4, 7^8, 5^3, 3^5, 1^2\}$	{0, 2, 0, 0, 0, 2, 0, 0}	{22, 44, 64, 52, 40, 28, 14, 32}

Dimension	[0,0,0,0,0,1,0]	Root Map	Weight Map
216	{19, 16^4, 15, 11^6, 10^4, 7, 6^4, 3, 1^{10}}	{2, 1, 0, 0, 0, 1, 2, 1}	{28, 54, 79, 64, 49, 34, 18, 40}
216	{16^2, 13^3, 12^4, 11^2, 9^2, 8^2, 7^5, 6^2, 5^3, 3, 2^2, 1^4}	{0, 1, 0, 1, 0, 2, 0, 0}	{23, 46, 68, 56, 43, 30, 15, 34}
216	{17, 14^2, 13^2, 12^4, 11^2, 10^2, 9, 8^2, 7^2, 6^2, 5^3, 3^5, 2^2, 1^2}	{0, 1, 0, 1, 0, 1, 2, 0}	{23, 46, 68, 56, 43, 30, 16, 34}
216	{15, 14^2, 13, 12^2, 11^2, 10^2, 9^3, 8^4, 7^3, 6^2, 5^3, 4^2, 3^2, 2^2, 1}	{1, 0, 1, 0, 1, 0, 1, 0}	{22, 43, 64, 52, 40, 27, 14, 32}
218	{17^2, 15^3, 13, 11^6, 9^3, 7^7, 3^3, 1^5}	{2, 0, 0, 0, 0, 2, 0, 2}	{26, 50, 74, 60, 46, 32, 16, 38}
218	{19, 15^4, 13^5, 11^2, 9^2, 7^6, 3^6, 1^4}	{0, 2, 0, 0, 0, 2, 2, 0}	{26, 52, 76, 62, 48, 34, 18, 38}
218	{16^2, 15^2, 13, 12^2, 11^2, 10^4, 9^2, 7^4, 6^4, 5, 4^2, 1^4}	{0, 1, 0, 1, 0, 1, 0, 1}	{24, 48, 71, 58, 44, 30, 15, 36}
218	{16^2, 15, 13^3, 12^2, 11, 10^2, 9^3, 8^4, 7, 6^2, 5^3, 4^2, 3, 1^3}	{1, 0, 1, 0, 1, 1, 0, 0}	{24, 47, 70, 57, 44, 30, 15, 35}
218	{17, 15, 14^2, 13^2, 12^2, 11^2, 10^2, 9^3, 8^2, 7, 6^2, 5^3, 4^2, 3^2, 2^2, 1}	{1, 0, 1, 0, 1, 0, 2, 0}	{24, 47, 70, 57, 44, 30, 16, 35}
220	{17, 15^3, 13^2, 11^6, 9^3, 7^5, 5^4, 3^4}	{0, 0, 2, 0, 0, 0, 2, 0}	{24, 48, 72, 58, 44, 30, 16, 36}
220	{21, 17^4, 15, 13^5, 9^5, 7, 5^4, 1^7}	{2, 0, 0, 0, 0, 2, 2, 2}	{30, 58, 86, 70, 54, 38, 20, 44}
220	{18^2, 15, 14^4, 13^2, 11, 10^2, 9^3, 7^5, 5^3, 3, 1^4}	{0, 0, 1, 1, 0, 2, 0, 0}	{26, 52, 78, 64, 49, 34, 17, 39}
220	{19, 17, 16^2, 15^2, 12^2, 11^3, 10^4, 9, 7^2, 6^2, 5, 3^2, 2^2, 1^3}	{2, 0, 1, 0, 1, 0, 2, 0}	{28, 54, 80, 65, 50, 34, 18, 40}
220	{17, 16^2, 15, 13^2, 12^2, 11^2, 10^2, 9^3, 8^2, 7^2, 6^2, 5^2, 4^2, 3, 1^2}	{0, 1, 1, 0, 1, 0, 1, 0}	{25, 50, 74, 60, 46, 31, 16, 37}
222	{19, 17^2, 15^3, 13, 11^6, 9^3, 7^3, 5^2, 3^4, 1}	{2, 0, 0, 2, 0, 0, 2, 0}	{28, 54, 80, 66, 50, 34, 18, 40}
222	{23, 18^2, 17^3, 16^2, 15, 11, 10^2, 9^3, 8^2, 3^2, 2^4, 1^3}	{1, 0, 1, 0, 1, 2, 2, 0}	{32, 63, 94, 77, 60, 42, 22, 47}
222	{18^2, 17, 15, 14^2, 13^2, 11^3, 10^2, 9^2, 8^2, 7, 6^2, 5^3, 3, 1^2}	{0, 1, 1, 0, 1, 1, 0, 0}	{27, 54, 80, 65, 50, 34, 17, 40}
224	{19^2, 17, 15^3, 13^3, 11^3, 9^3, 7^5, 5, 3^3}	{0, 0, 2, 0, 0, 2, 0, 0}	{28, 56, 84, 68, 52, 36, 18, 42}
224	{21, 19, 17^2, 15^4, 11^6, 7^4, 5^3, 3, 1^2}	{0, 2, 0, 0, 2, 0, 2, 0}	{30, 60, 88, 72, 56, 38, 20, 44}
224	{21, 19^3, 15^2, 13^3, 11^5, 9^2, 7^2, 3^4, 1^2}	{2, 0, 2, 0, 0, 0, 2, 0}	{32, 62, 92, 74, 56, 38, 20, 46}
224	{20^2, 17, 16^2, 15^2, 13, 12^2, 11^2, 9^3, 8^2, 7, 5^3, 3, 1^2}	{1, 0, 1, 1, 0, 2, 0, 0}	{30, 59, 88, 72, 55, 38, 19, 44}
224	{23, 19, 18^2, 17, 16^2, 15^2, 11^2, 10^2, 9, 8^2, 7, 4^2, 3^2, 1^3}	{0, 1, 0, 1, 0, 2, 2, 1}	{32, 64, 95, 78, 60, 42, 22, 48}
226	{23, 19^2, 17^3, 15^3, 11^3, 9^3, 7^2, 5, 3^4}	{0, 0, 2, 0, 0, 2, 2, 0}	{32, 64, 96, 78, 60, 42, 22, 48}
226	{25, 21, 19^4, 15^3, 11^4, 9, 7^2, 5, 3^2, 1^3}	{2, 0, 0, 2, 0, 2, 2, 0}	{36, 70, 104, 86, 66, 46, 24, 52}
226	{23, 21, 19^2, 17, 15^3, 13^2, 11^3, 9, 7^4, 3^2, 1^2}	{2, 0, 0, 0, 2, 0, 2, 2}	{34, 66, 98, 80, 62, 42, 22, 50}
226	{23, 22^2, 19, 16^2, 15, 13^3, 12^2, 11, 10^2, 7, 4^2, 3, 1^3}	{2, 1, 0, 1, 1, 0, 1, 1}	{36, 70, 103, 84, 64, 43, 22, 52}
228	{23^2, 21, 19, 17, 15^3, 13^2, 11^4, 9, 7, 5, 3^3}	{2, 0, 2, 0, 0, 2, 0, 0}	{36, 70, 104, 84, 64, 44, 22, 52}
228	{27, 23, 22^2, 19, 17, 16^2, 15, 12^2, 11^2, 7, 6^2, 3, 1^3}	{2, 1, 0, 1, 0, 2, 2, 1}	{40, 78, 115, 94, 72, 50, 26, 58}
230	{27, 23^2, 21, 19, 17^2, 15^2, 13, 11^3, 7^2, 5, 3^2}	{2, 0, 2, 0, 0, 2, 2, 0}	{40, 78, 116, 94, 72, 50, 26, 58}
232	{29, 27, 23^2, 19^2, 17, 15^3, 11^2, 9, 7, 5, 3}	{2, 0, 2, 0, 2, 0, 2, 0}	{44, 86, 128, 104, 80, 54, 28, 64}
232	{35, 28^2, 27, 23, 19, 18^2, 15, 11, 10^2, 3, 1^3}	{2, 1, 0, 1, 2, 2, 2, 1}	{52, 102, 151, 124, 96, 66, 34, 76}
232	{31, 27, 25, 23, 21, 19^2, 15^2, 13, 11^2, 7^2, 3, 1}	{2, 0, 0, 2, 0, 2, 2, 2}	{46, 90, 134, 110, 84, 58, 30, 68}
234	{35, 29, 27^2, 23, 19^2, 17, 15, 11^2, 9, 3^2}	{2, 0, 2, 0, 2, 2, 2, 0}	{52, 102, 152, 124, 96, 66, 34, 76}
236	{39, 35, 29, 27, 23^2, 19, 17, 15, 11, 7, 3}	{2, 2, 0, 2, 0, 2, 2, 2}	{60, 118, 174, 142, 108, 74, 38, 88}
238	{47, 39, 35, 29, 27, 23, 19, 15, 11, 3}	{2, 2, 0, 2, 2, 2, 2, 2}	{72, 142, 210, 172, 132, 90, 46, 106}
240	{59, 47, 39, 35, 27, 23, 15, 3}	{2, 2, 2, 2, 2, 2, 2, 2}	{92, 182, 270, 220, 168, 114, 58, 136}

Partitions are shown for the adjoint representation only. Homomorphisms identified include 39 root maps which are not recognised Characteristics of nilpotent orbits: these are highlighted in red.